The Rapid Detection of Drug Resistant Mycobacteria

By

Evans Kwame Ahortor

A thesis submitted for the degree of

Doctor of Philosophy (PhD)

July 2019

School of Pharmacy and Pharmaceutical Science

Cardiff University

Declaration

This thesis is the result of my own independent work, except where otherwise stated, and the views expressed are my own. Other sources are acknowledged by explicit references. The thesis has not been edited by a third party beyond what is permitted by Cardiff University's Use of Third-Party Editors by Research Degree Students Procedure.

Signed……(candidate) Date …22/11/2019……

STATEMENT 1

This thesis is being submitted in partial fulfilment of the requirements for the degree of PhD

Signed……(candidate) Date …22/11/2019…….

STATEMENT 2

This work has not been submitted in substance for any other degree or award at this or any other university or place of learning, nor is it being submitted concurrently for any other degree or award (outside of any formal collaboration agreement between the University and a partner organisation)

Signed …… (candidate) Date …22/11/2019..…

STATEMENT 3

I hereby give consent for my thesis, if accepted, to be available in the University's Open Access repository (or, where approved, to be available in the University's library and for inter-library loan), and for the title and summary to be made available to outside organisations, subject to the expiry of a University-approved bar on access if applicable

Signed …… (candidate) Date …22/11/2019……

Summary

Mycobacterium abscessus is a multidrug resistant pathogen commonly isolated from patients with cystic fibrosis. Currently, there is no rapid diagnostic tool to detect the presence of *M. abscessus*. Rapid diagnosis followed by appropriate, prompt treatment remains the best curative approach to mitigate disease burden and halt transmission. A major bottle neck in developing a rapid diagnostic assay is DNA extraction. Mycobacterial cells are very difficult to lyse, the existing methods are time consuming resulting in long turnaround time to detect the pathogen.

This study employed the use of microwave energy to rapidly release nucleic acids from microorganisms and test the ability to detect the released nucleic acids in a magnetic-bead-based sandwich hybridisation assay using specific DNA probes. Based on published genome sequences, probes targeting the *rpoB* and *erm-41* genes of *M. abscessus* and *M. smegmatis* were designed. In a magnetic-bead-based sandwich hybridisation assay using these specific probes, *M. abscessus* and *M. smegmatis* were distinguished from non-specific isolates within 70 mins with a lower detection limit of 1 pg/µL.

The disruptive effects of microwaves on biological structures has been attributed to the local generation of heat. The contribution, if any, of non-thermal factors is yet to be determined. To study the interaction of microwaves with cell membranes, the structure which represents the major barrier to DNA release, fluorescent microscopy was employed to examine the passage of different sized fluorescent dextran particles into bacterial and yeast cells following microwave exposure. The results show a transient membrane disruption, size dependent permeabilization of dextran particles into cells.

In conclusion, a prototype hybridisation assay capable of detecting *M. abscessus* and *M. smegmatis* has been developed. The application of microwaves to cells induced membrane disruption allowing internalisation of varying sizes of fluorescent dextran particles and the release of intact DNA for detection in hybridisation assay.

Acknowledgment

I thank my God for the strength, wisdom and knowledge and above all His Grace to complete this study.

I would like to express my sincere gratitude to Professor Les Baillie and Professor Adrian Porch for their supervision that has contributed to the success of this thesis. I will like to thank Les Baillie for securing funds to make this study and my stay in Cardiff possible. I thank Dr. Jonathan Lees, Dr. Catrin Williams, Dr. Heungjae Choi, Dr. Tina Joshi and Dr. Dmitry Malyshev for their training on the use of microwave device and Dr. James Arthur Blaxland for his support and encouragement in the lab 1.11. My appreciation also goes to Professor Arwyn Tomos Jones and Dr. Edward Sayers for their assistance with the use of confocal microscopy.

Finally, my gratitude goes to my parents Vida and Emmanuel Ahortor, siblings and family members for their encouragement and support in diverse ways.

Publications and Communications

Published work

H. Hamzah, **E. Ahortor**, D. Malyshev, H. Choi, J. Lees, L. Baillie and A. Porch. A Compact Microwave Applicator for the Rapid Detection of *Clostridium difficile*. IEE MTT-S International Microwave Biomedical Conference (IMBioC2019)

Submitted for publication

Evans K. Ahortor, Dmitry Malyshev, Catrin F. Williams, Heungjae Choi, Adrian Porch, Leslie Baillie. The biological effect of 2.45 GHz microwaves on the viability and permeability of bacterial and yeast cells

Conferences and Communications

Oral Presentation: The biological effect of 2.45 GHz microwaves on bacterial and yeast cells. Presented at Progress in Electromagnetic Research Symposium (PIERS), 31st July-4th August 2018 Toyama, Japan.

Poster presentation: Development of microwave accelerated real-time potentiometric assay for rapid detection of *Mycobacterium abscessus*. Edinburgh International Conference Center (3-5th April 2017), Edinburgh, UK

Tables of Contents

List of Abbreviations

Acquired Immune Deficiency Syndrome (AIDS)

Acyl Carrier Protein (ACP)

American Thoracic Society (ATS)

American Type Culture Collections (ATCC)

American Type Culture Collections (ATCC)

Analysis of Variance (ANOVA)

Bacilli Calmette-Guerin (BCG)

Bacillus stearothermophilus (*Bst*) *polymerase*

Biosafety Level 3 (BSL 3)

Bovine serum albumin (BSA)

Bovine tuberculosis (B. tb)

Central Nervous System (CNS)

Clinical and Laboratory Standard Institute (CLSI)

Colony Forming Unit per millilitre (CFU/mL)

Computer Tomography (CT)

Culture Filtrate Protein (CFP-10)

Cystic Fibrosis (CF)

Diacylglycerol (DAG)

Directly Observed Treatment Short-Course (DOTS)

Double stranded DNA (dsDNA)

Early secreted antigen 6 kilodaltons (ESAT-6)

Early Secretory Antigenic Target (ESAT-6)

Electric field (E field)

Electromagnetic (EM)

Enzyme Linked Oligonucleotide Sandwich Hybridisation Assay (ELOSHA)

Erythromycin ribose methylase-41 (*erm*-41)

Ethambutol (ETMB)

ethylenediaminetetraacetic acid (EDTA)

Extensive Drug Resistance (XDR)

Gas chromatography - mass spectrometry (GC-MS)

Gentamicin (Gen)

Glycopeptidolipid (GPL)

Green fluorescent protein (GFP)

Gyrase B (gyrB)

High Performance Liquid Chromatography (HPLC)

Horse radish peroxidase (HRP)

Human Immune Deficiency Virus (HIV)

Hydrochloric acid (HCl)

Insertion Sequence (IS)

Interferon Gamma (INF-γ)

Interferon Gamma (INF-γ)

Internal Transcribed Spacer (ITS) region

Isocitrate Lyase (*icl*)

Isoniazid (INH)

Isonicotinic Acid Hydrazide A (*inh*A)

Lateral flow assays (LFA)

Lipoarabinomannan (LAM)

Loop Mediated Isothermal Amplification (LAMP)

Lowenstein-Jensen (LJ)

Luria-Bertani agar (LBA)

Luria-Bertani broth (LBB)

M. tuberculosis (M. tb)

Magnetic Field (H field)

magnetic particles (MP's)

Magnetic Resonance Imaging (MRI)

Methyl tert-butyl ether (mTBE).

Microwave (MW)

Minimum Inhibition concentration (MIC)

Multi Drug Resistant TB (MDR-TB)

Multidrug Resistant TB (MDR-TB)

Multilocus Sequence Typing (MLST)

Multiplicity of Infection (MOI)

Multispacer Sequence Typing (MST)

Mycobacterium abscessus (*M. abscessus*)

Mycobacterium bovis (*M. bovis*)

Mycobacterium smegmatis (*M. smegmatis*)

Mycobacterium tuberculosis complex (MTBC)

Mycobacterium Tuberculosis Complex (MTBC).

Mycolic Acids (MA)

National collection of Pathogenic Fungi (NCPF)

National Collection of Type Cultures (NCTC)

National Tuberculosis Control Programme (NTP)

No Template Control (NTC)

Non-tuberculous mycobacteria (NTM)

Optical Density (OD)

Penicillin-streptomycin (Pen-Strep)

Peptidoglycan (PG)

Phithiocerol Dimycocerate (PDM)

Phosphate Buffered Saline

Phosphate Buffered Saline (PBS)

Phosphatidyl Ethanolamine (PE)

Phosphatidyl Glycerol (PG)

Phosphatidylinositol 3-phosphate (PIP3)

Phospholipase C (PLC)

Point-of-care (POC)

Polymerase Chain Reaction (PCR)

Polymerase Chain Reaction (PCR)

Protein Kinase C

protein kinase G (PknG)

Protein Phosphatase A/B (PtpA and PtpB)

Pulsed Field Gel Electrophoresis (PFGE)

Purified Protein Derivative (PPD)

Pyrazinamidase (PZase)

Pyrazinamide (PZ)

QuantiFERON-TB Gold-In-Tube (QFT-GIT)

Radio frequency (RF)

Region of Difference 1 (RD1)

Repetitive Sequence-Based (Rep)-PCR

RIF resistance determining region (RRDR)

RIF Resistance Determining Region (RRDR)

Rifampicin (RIF)

RNA polymerase (*rpoB*)

Rough form (R form)

Secretory Acid Phosphatase (SapM)

Single Nucleotide Polymorphisms (SNPs)

Single stranded DNA (ssDNA)

Smooth form (S form)

Sodium dodecyl sulphate (SDS)

Statistical Package for the Social Sciences (SPSS)

Total Drug Resistance (TDR)

Transcription Mediated Amplification (TMA)

Trehalose 6, 6-Dimycolate (TDM)

Tris acetate EDTA (TAE)

Tuberculin Skin Test (TST)

Tuberculosis (TB)

Tumour Necrosis Factor- alpha (TNF- α)

University Hospital of Wales (UHW)

Variable Number of Tandem Repeat (VNTR)

Whole Genome Sequencing (WGS)

World Health Organisation (WHO)

Ziehl-Neelsen (ZN)

β-subunit of the RNA polymerase (*rpoB*)

List of Figures

List of Tables

Chapter 1

General Introduction, Aims and Objectives

1.0 Mycobacteria

Mycobacteria species are a worrying problem consistently generating research interest due to their pathogenicity for humans and animals (Han *et al.* 2007). They are a diverse species reported to number over 100 members ranging from harmless saprophytes to pathogenic organisms (Ripoll *et al.* 2009). They are grouped as slow or rapid growing, pigmented or non-pigmented and tuberculous or nontuberculous (Adekambi and Drancourt 2004). They are characterised by the unique composition of their cell wall structure and high mycolic acid content comprising mainly of alkyl and long β-hydroxyl fatty acids (Hett and Rubin 2008). This enhances cell wall rigidity and enables the bacteria to survive in the presence of antibiotics which target cell wall structures common to other classes of bacteria. A typical mycobacteria specie is considered as Gram-positive, non-motile, non-spore forming and rod-shaped bacilli with size ranging between 0.3 to 0.5 μm in diameter and length between 1.5 μm and 4.0 μm (Cook *et al.* 2009). The cell wall structure and membrane compositions of mycobacteria in comparison to other groups of bacteria e.g. Gram-negative, Gram-positive and yeast cells differ significantly, and these are discussed below.

1.1 Cell wall differences of mycobacteria and other cell types

Structurally, Gram positives e.g. *S. aureus* and Gram-negatives e.g. *E. coli* are differentiated based on the composition of peptidoglycan in their cell wall. *E. coli* has a thin peptidoglycan (PG) layer that is a few nanometres thick, representing one to a few layers while in *S. aureus*, the PG is between 30–100 nm thick and contains many layers (Fig. 1.1) (Huanga *et al.* 2008). Peptidoglycan is not present in yeast cells (*C. albicans*) but the outer core consist of intricate network of polysaccharide fibrils composed of β-(1,3)-glucan which is linked covalently to β-(1,6)-glucan and chitin- a β-(1,4)-linked polymer of *N*-acetylglucosamine (Ruiz-Herrera *et al.* 2006). This organised core structure acts as a scaffold for the external layer which consist of highly glycosylated mannoproteins (McKenzie *et al.* 2010). The cell wall characteristics of mycobacteria lie between that of Gram-positive and Gram-negative bacteria. Mycobacteria have a complex cell envelope consisting of a PG containing arabinogalactan that is covalently attached to mycolic acids (Fig 1.1). Mycolic acids are characterised by intricate long chain alkyl groups with a maximum length of about 90 carbons. This intricate network of alkyl chains give the bacteria a waxy appearance and become resistant to lyse and for exogenous substances to penetrate (Silhavy *et al.* 2010).

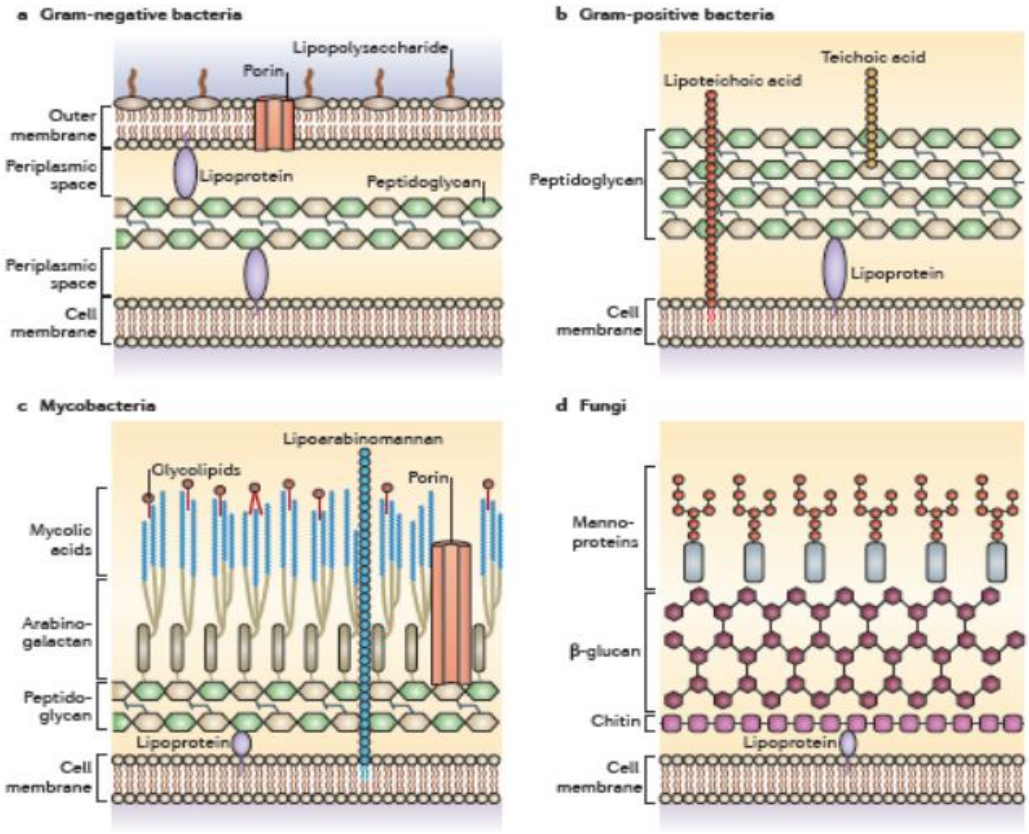

Figure 1.1. Comparison of cell wall composition between Mycobacteria (A), Gram-positive (B), Gram-negative (C) and yeast cells (D). Picture adapted from (Brown *et al.* 2015)

Tuberculous mycobacteria (slow growers) are those that cause tuberculosis and is comprised of six members known as the *Mycobacterium tuberculosis* complex (MTBC). These include; *M. tuberculosis* (M. tb), the causative agent for tuberculosis in man, *Mycobacterium africanum*, *Mycobacterium bovis*, *Mycobacterium canettii*, *Mycobacterium pinnipedii* and *Mycobacterium microti*. Although this group (MTBC) are genetically similar, they affect a diverse range of hosts. For instance, *M. africanum* and *M. canettii* are the closest relative to M. tb both causing tuberculosis (TB) but are

restricted to the equatorial regions of Africa. *M. bovis*, the causative agent of bovine tuberculosis is the only member of the complex capable of infecting a diverse range of animals including wild and domestic species (Mostowy *et al.* 2005). *M. pinnipedii* and *M. microti* infect seals and wolves respectively (Cousins *et al.* 2003; Mostowy et al. 2005). Although mycobacteria species are known primarily for their pathogenicity, some possess unique characteristics which are being exploited for industrial applications. For example, *Mycobacterium austroafricanuum* has the unique ability to degrade methyl tert-butyl ether and is being explored as a potential decontaminant of contaminated ground water (Maciel *et al.* 2008). Of species in the MTBC, M. tb and *M. bovis* are the most common and are described below.

1.2 Bovine tuberculosis (B. Tb)

Mycobacterium bovis (*M. bovis*) is the causative agent of B. tb, which mostly occurs in domestic and wild animals. *M. bovis* can be shared between humans and animals (zoonotic transmission) (Mostowy *et al.* 2004; Mostowy et al. 2005; Schiller *et al.* 2010). Zoonotic transmission occurs through the consumption of unpasteurised cow milk or meat infected with the bacilli (de la Rua-Domenech *et al.* 2006; Torres-Gonzalez *et al.* 2013). There is undisputable scientific evidence from badgers acting as reservoirs for *M. bovis* and are actively involved in transmission to cattle (Bhuachalla *et al.* 2015). Clinical evidence of human to human transmission has also been documented (Sunder *et al.* 2009). Infection with *M. bovis* is characterised by the formation of granuloma lesions with different degrees of calcification, necrosis and encapsulation in the lung tissues and other organs (Michel *et al.* 2010). B. tb remains a major public health concern in developing countries

and developed countries such as the UK. Identifying the presence of the pathogen in a single animal often results in the slaughter of the entire herd. Between 2008 and 2015, a total of 68, 630 cattle were slaughtered in the UK due to B. tb with 11.8% of these cases occurring in 2015 alone (fig 1.2) (Carl 2015). Such losses can have a huge financial impact on farm output and a subsequent decline in business. Between 2008 and 2009, Britain spent approximately £100 million on the management of B. tb (Schiller *et al.* 2010) and the Welsh government spends about £5 million a year on vaccination research.

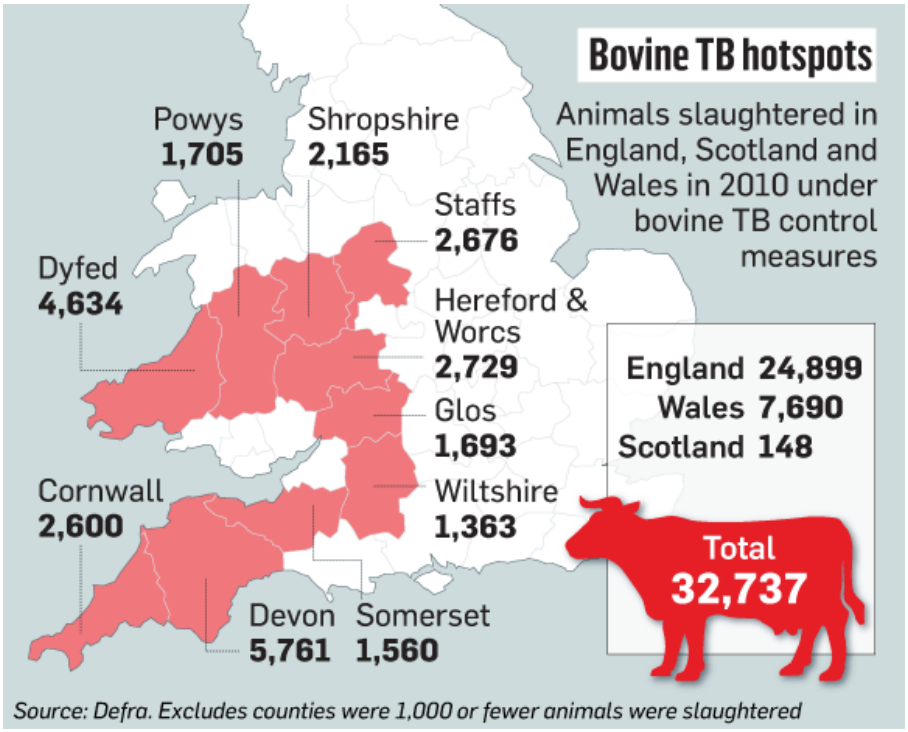

Figure 1.2 The scale of Bovine tuberculosis in UK. The total number of animals slaughtered in regions of Wales, Scotland and England. Picture adapted from https://www.thetimes.co.uk/article/shoot-the-badgers-ql67nxgjdf9. Date accessed 18/11/2018

On the global scale, an estimated US$3 billion is lost annually due to B. tb (Schiller *et al.* 2010). These are huge expenditures which are very costly and presents a major problem. The above challenges can be attributed in part to the absence of effective diagnostic tools capable of delivering patients results within a short time frame. The most widely used screening tool is the tuberculin skin test (TST). This test is discussed in detail in section 1.9.4.1. Unfortunately, TST is prone to false-positive results due to exposure of cattle to other environmental mycobacteria species (Katial *et al.* 2001; Buddle *et al.* 2009). Also, the test can generate a false-negative result due to immunosuppression, desensitization towards tuberculin and the use of less potent tuberculin (Wadhwa *et al.* 2012). Measuring humoral antibody following injection of a mycobacterial purified protein derivative (PPD) is as an alternative method to detect *M. bovis* infection. Unfortunately, this test lacks specificity due to cross reactivity with other pathogens (Lilenmaum *et al.* 1999; Molicotti *et al.* 2014). Accessing sensitive, specific point-of-care (POC) assay capable of determining whether an animal is infected will have a significant effect on disease control and prevent the needless slaughter of farm animals.

1.3 Human tuberculosis (M. tb)

TB is the number one cause of mycobacteriosis worldwide. It is transmitted through inhalation of respiratory droplet containing viable bacteria which can be produced by sneezing or coughing. Such respiratory droplets are usually 1-5 µm in diameter and contain between 1-10 bacilli (Lee 2016a). TB is reported in over 205 countries and territories which consists about 99% of the world's population (WHO 2015). The reported disease burden is low in developed countries such as Canada, New Zealand and Australia

but considerably higher in countries such as Brazil, China, Namibia and some parts of the African continent (McNerney *et al.* 2012). This is mainly attributed to factors such as HIV/AIDS co-infection, the emergence of multidrug resistant isolates, the absence of rapid and efficient diagnostic tools and the deterioration of public health systems (Weyer *et al.* 2011; Forrellad *et al.* 2013; WHO 2015). For instance, HIV/AIDS patients suffer a weakening of the immune system and as a result become susceptible to M. tb (Kasprowicz *et al.* 2011; Venturini *et al.* 2014). Disturbingly, TB has become incessantly resistant to antibiotics. In 2014, the global estimate of new multidrug resistant TB (MDR-TB) was 480, 000 with half of these cases occurring in China, India and the Russian federation (WHO 2015). TB drug resistance is difficult to treat (Kamphee *et al.* 2015).

Currently, only a small number of drug resistant TB cases are detected and appropriately treated since the tools for providing accurate and rapid diagnosis at the time of the initial patient consultation are unavailable (Ormerod 2005). A reported 32% of HIV related deaths are associated with TB, with over 650,000 cases due to MDR-TB (Moreno-Altamirano *et al.* 2012). Out of the total number of individuals infected with TB in 2014, 12% (1.2 million) were living with HIV and 0.4 million subsequently died (WHO 2015) and in 2015, an estimated 10.4 million people were reported to have suffered from TB which resulted in a total of 1.8 million deaths (WHO 2015).

TB transmission and its ability to establish lifelong infections depends on the bacterial load at the time of infection, the immune status of the individual, virulent state of the bacilli, environmental stress and biosocial factors (Lee 2016b). TB mainly presents in two

different states namely; active and latent forms. Latent TB is when an individual is infected with the TB bacilli but does not present with any clinical symptoms, with a negative chest X-ray and no microbiological evidence. Latent TB is not transmitted (Lee 2016a) since the bacilli has reduced metabolic activity and remains dormant for decades unless the host immune response is compromised then the bacterium is reactivated (fig 1.3a).

Upon infection, TB bacilli are engulfed by antigen presenting cells (alveolar macrophages or dendritic cells) to form a solid granuloma. Inside the granuloma, the bacilli are contained so that they do not develop into active forms (Fig 1.3a) (Pai *et al.* 2016). Latent TB is reported in about 2 billion individuals (Kaufmann *et al.* 2017). Solid granulomas can lose their ability to contain the bacterium through cell death and necrosis releasing dormant bacteria which are subsequently activated and go on to cause clinical symptoms (active TB) (Fig 1.3b). Apart from the lungs which TB primarily infects (pulmonary TB), M. tb also infect the lymph nodes, pleura, skin, joints, central nervous system (CNS), gastrointestinal tract, abdomen (extrapulmonary TB). Miliary TB is a hematogenous form of TB which is characterised by tiny lesions on multiple organs involving the lungs, spleen, CNS and liver (Nachiappan *et al.* 2017).

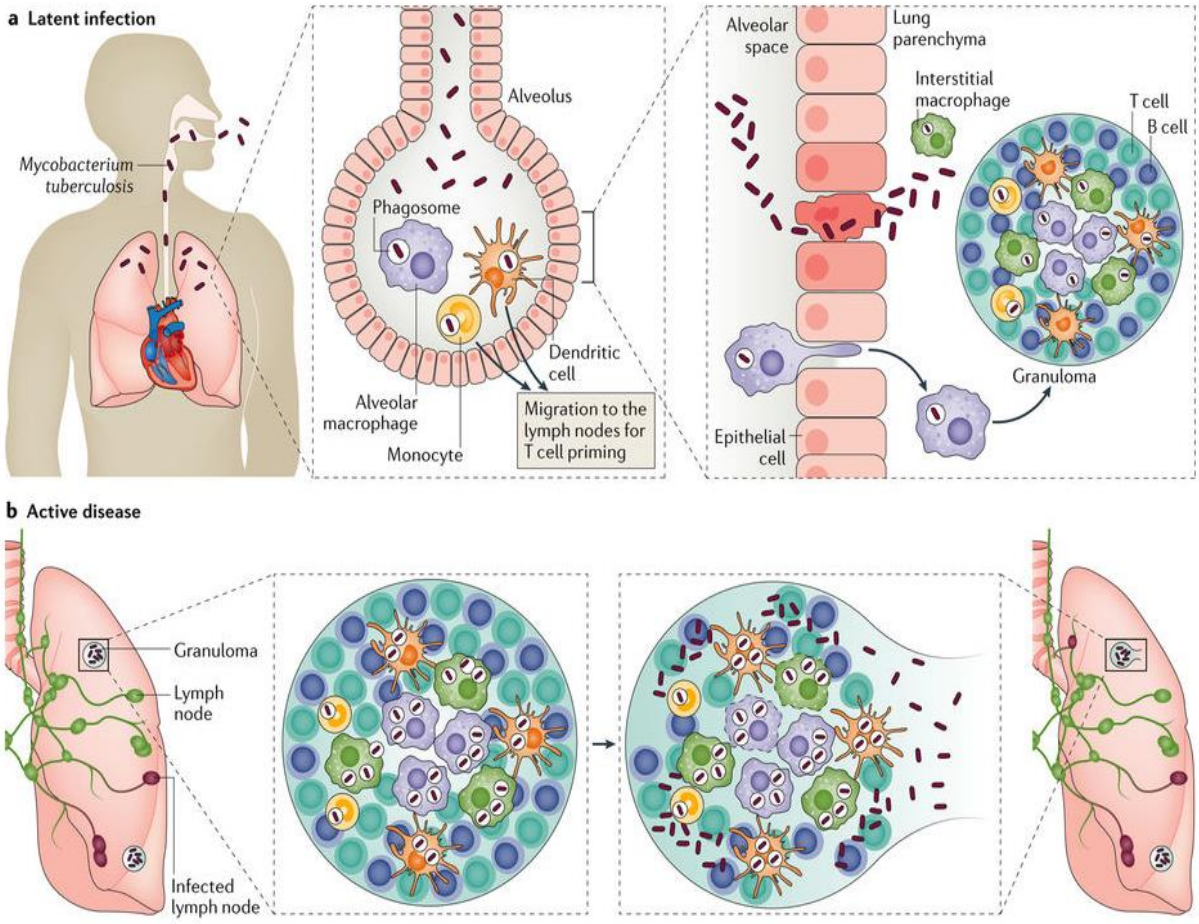

Figure 1.3. Infection stages of (a) latent and (b) active TB. **(a)** Latent TB – M. tb bacilli enters the lungs and reaches the alveoli space where it is phagocytosed by the alveolar macrophages. When this defence mechanism fails, M. tb progresses to infect the interstitial tissues of the alveolar epithelium or the infected alveolar, macrophages migrating to the lung parenchyma. This event is followed by the action of dendritic cells or inflammatory cells transporting M. tb to the pulmonary lymph nodes for T cells to be primed. T and B cells are then recruited to the lung parenchyma to form granuloma. **(b)** Active TB - The active stage develops at the stage of granuloma formation. When the bacilli load is too large for the granuloma to contain, or necrosis of the granuloma occurs, it ruptures and leads to the active and symptomatic TB. Picture adapted from (Pai *et al*. 2016).

1.4 Virulence factors of M. tb

Unlike other bacteria (e.g. *Clostridium difficle*) that produce toxins, mycobacteria lacks classical virulent factors (Forrellad *et al.* 2013). Complete sequencing of the M. tb genome reveals about 4,000 genes, of which 91 (2.3%) have been associated with virulence. Genes required for lipid metabolism, cell wall function and regulatory proteins synthesis accounts for approximately 5.7%, 13% and 4.7% respectively. These genes are needed for bacterial survival and thus could be considered as factors contributing to M. tb virulence (Smith 2003). Additionally, genes that are essential for signal transduction pathways and cell surface proteins have all been implicated as virulent factors (Smith 2003). To this end, a classical definition of M. tb virulence factors is yet to be determined. According to Dubnau, M. tb virulent factors includes elements that are required for pathogenicity and bacterial survival inside a host while excluding those that are required for bacterial growth in culture medium (Dubnau 2002). Some of the key elements considered as M. tb virulent factors (i.e. controlling the interaction of the pathogen with host phagosomes and lysosomes) are discussed in more detail below.

1.4.1 Interaction with phagosome and Lysosome

As a well-known fact, TB infection begins with the inhalation of aerosols from the environment containing viable M. tb bacilli. Upon entering the lung, the bacillus is internalised by host activated macrophages and are taken up into the acidic compartment of the lysosomes. The mechanism is demonstrated with the use of nanoparticles (fig. 1.4) (Kaufmann 2001). Bacilli which are able to evade delivery to the lysosome and survive go onto cause an infection (Kaufmann 2001; Russell 2001). The bacterium possesses a

molecule called lipoarabinomannan (LAM) in its cell wall which prevents the formation of phosphatidylinositol 3-phosphate (PIP3) on the surface of endosomal and phagosomal membranes and regulates the transfer of phagocytosed M. tb bacilli to lysosomes. (Vergne *et al.* 2003). In addition, M. tb also produces a lipid phosphatase (SapM) and a protein phosphatase (PtpA and PtpB) which are released into the cytosol for specific functions upon entry into the host. SapM hydrolyses PIP3 on the phagosomal membrane while Protein tyrosine phosphatase (A/B) interferes with trafficking processes via dephosphorylation mechanisms (Saleh and Belisle 2000; Bach *et al.* 2008).

Another mechanism by which M. tb outwits lysosomal degradation is by producing a signalling molecule that prevents fusion of the phagosome to the lysosome. Increased synthesis of protein kinase G (PknG) in the phagosome of infected macrophages has been reported in a study by Walburger and colleagues. It was discovered that PknG prevents fusion of phagosomes and lysosomes. To confirm this observation mutants lacking the ability to synthesise PknG were unable to prevent phagosome / lysosome fusion resulting the death of the bacterium (Walburger *et al.* 2004).

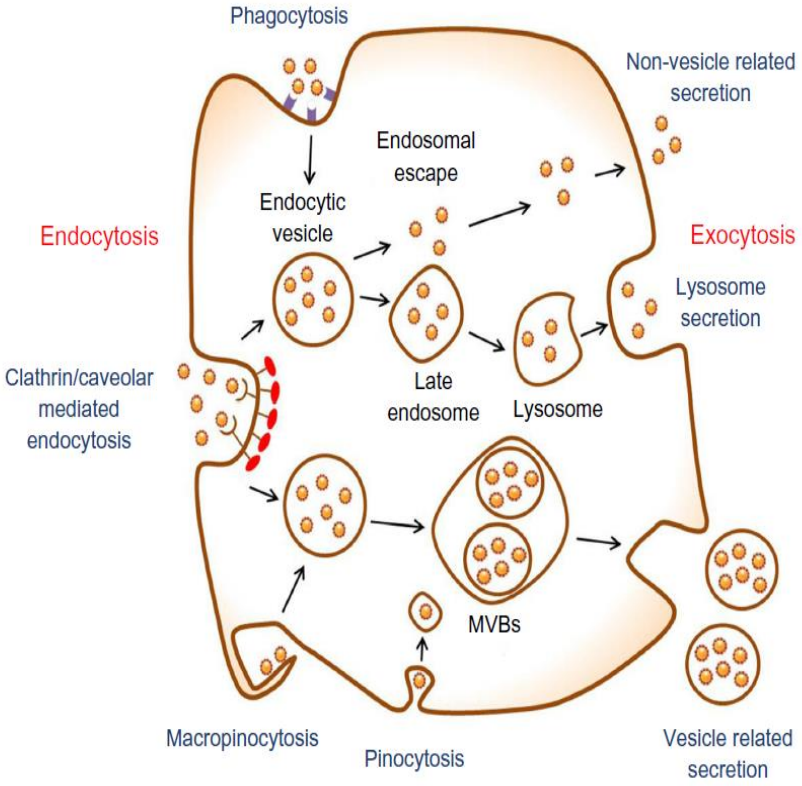

Figure 1.4. The process of macrophage mediated phagocytosis and lysosome degradation of bacteria in infected host. Nanoparticles enter the cell via four major pathways, namely; clathrin/caveolar-mediated, phagocytosis, micropinocytosis and pinocytosis. Upon entry into the cell, nanoparticles exit via lysozyme secretion, vesicle related secretion and non-vesicle related secretion. MVBs means multivesicular bodies. Picture adapted from Oh and Park 2014.

1.4.2 Cell envelope virulent factors

The outer membrane of M. tb is of interest as it interacts with macrophages. The mycobacterial cell wall consists of glycolipids such as LAM - as mentioned above, trehalose 6, 6´- di-mycolate (TDM) also known as cord factor and phithiocerol dimycocerate (PDM). All these glycolipids have been implicated in M. tb virulence (Meena and Rajni 2010). LAM stimulates the release of tumour necrosis factor (TNF- α), a major cytokine released in response to M. tb infection. TNF- α is over produced in TB infected individuals which leads to the notable Tb-like symptoms such as weight loss, fever and cytokine-mediated necrosis (Rajini *et al*., 2011). LAM also acts as a virulent factor by inhibiting the activity of protein kinase C, an enzyme required for macrophage activation (Chan *et al.* 1991). While macrophages are required to engulf (phagocytose) M. tb bacilli, their reduced activation implies a deficiency in phagocytic process, allowing M. tb to be viable and become virulent (Rajini *et al*., 2011).

When M. tb is phagocytosed, the bacilli contained in the phagosome fuses with the lysosome (acidic environment) to form the phagolysosome for intracellular destruction of the pathogen. PDM and TDM demonstrate similar virulence characteristics by preventing the formation of the phagolysosome. PDM which is present on the plasma membrane of M. tb participates in a receptor dependent phagocytosis of M. tb. This process involves modifying the plasma membrane of the host cells which eventually affects its biophysical property. One way the bacteria benefits from this is to regulate phagosomal pH, thereby creating a protective niche for the bacteria to survive (Astarie-Dequeker *et al.* 2009).

Similarly, TDM is required to inhibit fusion of phospholipid vesicles between phagosome and lysosome. This is achieved by increasing the stearic hindrance and increasing the force of hydration atb their surfaces to hinder their fusion (Rajini *et al*., 2011).

1.4.3 Metabolic adaption of gene expression

Metabolic adaptation is very important for any pathogen to survive in its host and results in the activation of specific genes are to enable the bacterium to employ an alternate biosynthetic pathway for nutrient metabolism. Studies have found that, M. tb switches from a preference for carbohydrate as main source of carbon to fatty acids after infecting its host (Segal and Hubert 1955). A key enzyme which the bacteria needs to continually metabolise fatty acids is isocitrate lyase produced by the isocitrate lyase (*icl*) gene. For M. tb to be able to thrive on fatty acids as the sole carbon source, the fatty acid is first converted into acetyl coA which can be channelled into the Kreb's cycle via the glyoxylate cycle. In this cycle, M. tb utilises isocitrate lyase to metabolise isocitrate to succinate. Mutant strains lacking *icl* cannot synthesis isocitrate lyase, hence are unable to metabolise fatty acids leading to reduced bacterial growth. This has been experimented in the lungs and extra-pulmonary organs of infected mice (McKinney *et al.* 2000; Shi *et al.* 2003). Also, the *igr* operon in M. tb contains virulent genes such as cytochrome 125, *fadE28/29* and lipid transfer protein (*lpl*2) that are required for cholesterol metabolism (Joshi *et al.* 2006). Mutant M. tb (i.e. lacking igr operon) replicate at a lesser rate in mouse models (Chang *et al.* 2009).

1.5 Treatment of M. tb and multi-drug resistant (MDR) burden

Drug resistance is a major challenge in TB treatment. Drugs commonly used include rifampicin (RIF), ethambutol (ETMB), pyrazinamide (PZ) and isoniazid (INH). These are considered the first line of drugs for TB treatment. The nature of M. tb to demonstrate varying level of resistance to antibiotics i.e. intrinsic and passive mechanisms renders monotherapy noneffective. By applying multitherapy, other resistant mechanism which normally would have escaped single antibiotic treatment can be averted. Various forms of resistance have been encountered in TB therapy, namely; multi-drug resistance (MDR), extensive drug resistance (XDR) and total drug resistance (TDR). MDR refers to high level resistance to rifampicin and isoniazid (Ormerod 2005). An MDR strain that has additional resistance to any of the fluoroquinolone antibiotics (ofloxacin, levofloxacin and moxifloxacin) and to any of the second line injectable antibiotics (amikacin, kanamycin and capreomycin) is considered an XDR (Shah *et al.* 2007). XDR TB has been detected in 92 countries and 9.6% of MDR-TB cases progress to XDR-TB (Blaas *et al.* 2008; Velayati *et al.* 2009). TDR refers to M. tb that is insensitive to all forms of anti-TB drugs. TDR M. tb have been identified in India, Italy and Iran (Migliori *et al.* 2007; Udwadia *et al.* 2012).

To enable accurate reporting of TB and drug resistant cases, the WHO collaborates with and request data from the national tuberculosis control programme (NTP) or relevant public health authorities within the 203 countries and territories that are engaged in TB surveillance. These data are collated following standard procedures and further forms the basis of annual TB reports. In 2013, less than 25% of MDR cases were detected resulting in 170, 000 deaths (WHO 2013; Günther 2014). A careful examination of this problem

could be attributed to patient-clinician inadequacies. The administration of wrong antibiotics, inappropriate treatment regimens and non-adherence to treatment plan by the patient are all contributing factors. TB treatment can be improved by following and adhering to the treatment regimen lasting between 6-9 months. Patients unable to adhere to this treatment regimen create the opportunity for selecting resistant strains. Another major contributing factor is the lack of rapid diagnostic procedures. Diagnosis remains a corner stone in TB treatment and drug resistance monitoring. Studies to underpin the development of effective POC diagnosis is lacking and there is no doubt that these tools are much needed for TB management.

1.6 Drug resistance mechanisms

Resistance due to the acquisition of transferable DNA elements has yet to be reported in TB therapy. Gene mutations at drug binding targets, or a modification of specific enzyme required to convert a pro-drug into an active drug are the main factors contributing to resistance in M. tb. Four main drugs are considered as the first line of anti-TB drugs. Their mechanism of action and resistance are discussed below.

1.6.1 Rifampicin (RIF)

RIF is a lipophilic drug which targets and binds to the β-subunit of the RNA polymerase (*rpoB*). Upon binding, rifampicin inhibits the elongation of mRNA, a key transcriptional process required for bacterial growth (fig. 1.5). Resistance to RIF arises when its binding target (an 81 base pair region of the *rpoB* gene) is mutated (El-Hajj *et al.* 2001). This region is also referred to as RIF resistance determining region (RRDR) and approximately

95% of RIF resistant strains harbour this mutated gene (Zaczek *et al.* 2009). Almost all RIF resistant strains demonstrate isoniazid resistance, hence detection of RIF resistant isolate is usually classified as MDR (Qazi *et al.* 2014).

1.6.2 Isoniazid (INH)

INH is only active against actively replicating M. tb (Palomino and Martin 2014). The drug is designed as a pro-drug that requires activation by an enzyme produced by the bacterium called catalase-peroxidase enzyme, *kat*G, which is encoded by *kat*G gene (Konno *et al.* 1967; Scorpio and Zhang 1996). Activated INH in the form of isonicotinoyl acyl radical complexes with NAD^+/NADH to form an INH-NADH adduct which inhibits an enoyl-acyl carrier protein (ACP) reductase encoded by isonicotinic acid hydrazide A (*inh*A*)* which plays a critical role in mycolic acid synthesis a key component for cell wall biosynthesis (Cade *et al.* 2010).

Resistance to INH is mainly attributed to mutations occurring in *katG*, *inhA*, *kasA* and *ndh* genes which reduce the binding affinity of the resulting proteins for INH. These genes also perform specific functions aiding M. tb survival. For instance, *KasA* encodes β-ketoacyl-ACP involved in the synthesis of mycolic acid, *KatG* catabolises catalase and peroxidases generated within macrophages to aid bacterial survival (Ng *et al.* 2015), *inhA* encodes NADH-specific enoyl-ACP reductase required for mycolic acid biosynthesis (Vilcheze *et al.* 2000) and *ndh* is involved in ATP generation (Awasthy *et al.* 2014). Mutations in *KasA* has been detected in INH resistant and susceptible isolates, hence their role in INH resistance may be of less significance (Larsen *et al.* 2002; Almeida Da Silva and Palomino 2011).

1.6.3 Ethambutol (ETMB)

ETMB is a bacteriostatic drug which interferes with the biosynthesis of arabinogalactan in the bacterial cell wall (fig 1.5). It targets the *embB* gene at position 306, although other studies have shown that mutation in this region does not necessarily lead to drug resistance but predisposes to other resistance mechanisms (Sreevatsan *et al.* 1997). As this gene is not a clear indicator of ETMB resistance, there is the need to identify other genes that can accurately predict ETMB resistance.

1.6.4 Pyrazinamide (PZ)

This is also another prodrug which is converted to its active form (pyrazinoic acid) by pyrazinamidase (PZase). The exact mechanism of PZ action is not fully known. One mechanism suggests that in acidic conditions, pyrazinoic acid disrupts bacterial membrane energetics via depletion of membrane potential and inhibits membrane transport (fig. 1.5) (Whitfield *et al.* 2015). A second mechanism suggests pyrazinoic acid inhibits fatty acid synthase type I in actively replicating M. tb bacilli (Ramaswamy and Musser 1998; Almeida Da Silva and Palomino 2011). Mutations occurring within *pncA* gene (encoding PZase) is the chief mechanism of PZ resistance. However, some pyrazinamide resistant isolates have been found not to harbour *pncA* mutations, suggesting resistance occurring through other genes such as *panD*. It is believed that *pan*D is a target for pyrazinoic acid which inhibits panthoenate and co-enzyme A synthesis which are essential for energy production and fatty acid metabolism (Zhang *et al.* 2013).

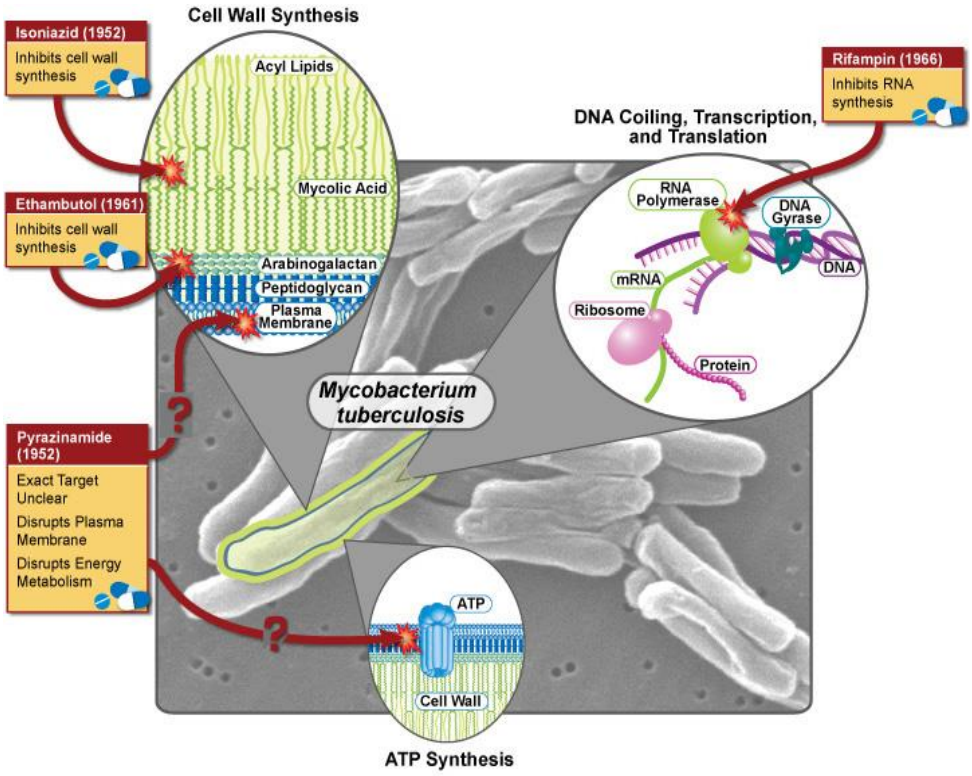

Figure 1.5 Schematic representation of the mechanism of action of the first-line anti-TB drugs. Picture adapted from (National Institute of Allergy and Infectious Diseases 2016).

1.7 Policies and strategies to prevent TB infection

The WHO has set itself the goal of a world free of TB by 2035. This can only be realised if there is a concerted effort from governments, non-governmental organisations and all other relevant bodies in countries where TB burden is high to support and implement policies developed by WHO. Two of the major policies implemented by the WHO will be discussed here i.e. The STOP TB strategy and the Directly Observed Treatment Short-Course (DOTS) program. The former was built on the success of the latter to address unmet needs. The DOTS control program was established in 1994 when the WHO declared TB a disease of public health concern. This policy has 5 main components which

requires; (1) Government bodies to be committed to and to sustain TB control activities, (2) Identification of TB by sputum smear microscopy in symptomatic patients, (3) A supervised treatment regimen in patients between 6 to 8 months of therapy, (4) A constant and uninterrupted supply of all essential TB drugs and (5) A detailed recording and reporting system that easily allows assessment to treatment (Enarsona and Billo 2007).

After 10 years of successful DOTS implementation, 20 million people have been treated and more than 16 million have been cured (Otu 2013). The implementation of DOTS also ensured that patients who do not adhere to rigorous requirement of TB medication were monitored. Also, the right drug dosage was given to patient to swallow under direct supervision from a health worker (Otu 2013). To address the unmet needs in the DOTS program, the STOP TB strategy was implemented which further focuses on addressing TB/HIV, MDR-TB, promoting research with the aim to developing vaccines, produce new drugs and diagnostic tools (The Stop TB Strategy 2018)

1.8 TB Prevention Challenges

The goal of the WHO to reduce TB mortality to 95% by 2035 can be realised by intensifying research into the development of new drugs, vaccines and rapid diagnostic tools. Vaccination is an effective method for the control of most infectious disease. Bacilli Calmette-Guerin (BCG), an attenuated strain of *M. bovis* is the first TB vaccine to be introduced in 1921 and while this vaccine shows efficacy against TB in children, it offers little or no protection in adults with pulmonary TB (Kaufmann *et al*. 2017). The inability of this vaccine in preventing pulmonary TB in adults could be due to immunogenetic

differences in adults and children. Exposure to environmental mycobacteria which is likely to be high in adults could explain the observed differences. Due to these challenges, a more efficacious form of the vaccine capable of being used to protect against all forms of TB must be developed. Having TB vaccine is also of great importance to reduce the increasing cases of MDR-TB. Currently, there are approximately 13 vaccines in clinical development. These vaccines fall under 3 categories namely; viral vectored subunit, adjuvanted protein subunit and whole cell-derived vaccines (Fletcher and Schrager 2016). These are discussed below.

1.8.1 Subunit vaccine

Subunit vaccines contain one or more antigens in the form of protein, peptides or DNA (Franco-Paredes *et al.* 2006). Out of the 13 vaccines currently being studied 8 are subunit vaccines. Six contain or express either Ag85A or Ag85B. Ag85A is an enzyme required for mycolic acid biosynthesis during M. tb dormancy. Ag85A is required for lipid accumulation and lipid storage in M. tb. To boost the protectivity of this vaccine type, antigens can be formulated with an adjuvant or expressed by a recombinant viral vector (Kaufmann *et al*. 2017).

1.8.2 Viral vectored vaccines

The immune markers produced in TB patients are very diverse. For a vaccine to be effective, it needs to identify all the immune markers produced by an individual. Subunit vaccines can only elicit an immune response in a specific subpopulation of CD4+ T- cells which may not provide complete protection against TB in humans. To increase the

efficacy and protectivity of TB vaccines, antigens can be expressed from a recombinant viral vector e.g. adenovirus or vaccinia vectors. The choice of these vectors for vaccine development stems from a number of advantages, namely (1) they are respiratory viruses and can be targeted to the lungs where M. tb resides, (2) they can express multiple antigens at the same time, (3) they possess intrinsic adjuvant property and (4) have an acceptable safety profile (da Costa *et al.* 2015). Unfortunately problems have also been encountered with an adenovirus type 5 HIV-1 vaccine trial being discontinued due to the occurrence of HIV infection in vaccine recipients (da Costa *et al*. 2015).

1.8.3 Whole Cell-derived vaccines

The challenge of identifying a single universal antigen suitable to be incorporated into a TB vaccine remains a challenge and an area of increased research. In contrast whole cells are polyantigenic and thus have the potential to stimulate a more comprehensive spectrum of protection than subunit vaccines. Vaccae^{TM} is a whole cell heat-inactivated vaccine generated from a non-tuberculous mycobacterium (*M. vaccae*) and is currently the only vaccine candidate that has reached the most advanced stage of clinical trials. In China it is currently being administered as an adjunctive treatment to M. tb (Frick 2015; Kaufmann *et al*. 2017).

1.9 Methods of TB diagnostics

Diagnosis is a key and fundamental component in the fight against TB (WHO 2015). In the absence of effective preventative methods, it is estimated that 200 million individuals

will develop active TB of which 35 million will die between 2000 and 2020 (Meena and Rajni 2010). The current control strategy for TB management requires effective diagnosis, followed by treatment at an early stage and extensive patient follow-up (Battaglioli1 *et al.* 2013). Diagnosis is estimated to have saved about 43 million lives between 2000 and 2014 (WHO 2015). Unfortunately, these requirements are not easily met especially in low resource settings such as Asia and Africa where rapid and simple diagnostic tools are not widely available. The diagnostic methods which are currently available lack specificity, sensitivity, are time consuming, requires access to sophisticated equipment and the need for highly trained technical staff (Maiga *et al.* 2012). Diagnostic tools capable of detecting the presence of M. tb in a clinical sample and at the same time determining its antibiotic sensitivity would be helpful in the effective management and control of TB. The methods that have been developed for TB diagnosis are discussed below.

1.9.1 Microscopy

Microscopy is the cheapest and fastest means of detecting pulmonary TB (WHO 2013). The characteristic cell wall composition of these species enables easy detection using the Ziehl-Neelsen (ZN) staining method which is a common staining method for mycobacteria species. After staining, bacilli appear as pink or red rods under light microscope (Perkins *et al.* 2006). This method suffers from sensitivity and is unreliable. Sensitivity ranges between 22-43% with a lower limit of detection between 10^3-10^4 bacilli per ml (Singh and Kashyap 2012; Singhal and Myneedu 2015). Sensitivity can be improved using fluorescent microscopy. While this approach makes it easier to visualise the bacterium, it is unable to determine antibiotic susceptibility and identify resistant

isolates (Ryu 2015). It is also unable to distinguish between virulent and non- virulent mycobacteria species.

Also, the cost of operation, the frequent need to replace the expensive mercury vapour lamps, the need for a continuous power supply and the need for a dark room restricts its use in less resourced communities. Light emitting diode (LED)-based fluorescent microscope have been developed and while they deliver readings three times faster than ZN, they currently lack sensitivity and specificity (Bhalla *et al.* 2013).

1.9.2 Chest X-ray

Chest X-ray has been used for more than 100 years for TB diagnosis. In a typical Tb patient, chest X-rays depict miliary nodules, lymphadenopathy, pleural effusion, cavitation and consolidation (fig. 1.6) (Nachiappan *et al*. 2017). An abnormal X- ray data is not an absolute confirmation of TB infection as other diseases such as sarcoidosis and neoplasma present with similar radiologic evidence (Mortaz *et al.* 2013) and requires further clinical testing to ascertain the diagnostic status of the patient. Chest X-ray also suffers interobserver variability and specificity. A sensitivity range between 73-79% and a specificity of 60-63% has been reported (Piccazzo *et al.* 2014). To improve on the specificity of TB radiology, more powerful and sensitive imaging tools such as magnetic resonance imaging (MRI) and computer tomography (CT) scan are currently being used (Skoura *et al.* 2015). A CT scan is twice as sensitive in the detection of TB lung cavities compared to chest X-ray (Nachiappan *et al*. 2017). Clearly given the reported level of sensitivities and specificities, chest X-ray results need to be confirmed with an additional

confirmatory test. The cost of operating such equipment, the need to train radiologists and the health hazards associated with exposures to radiations require much simpler and less expensive methods.

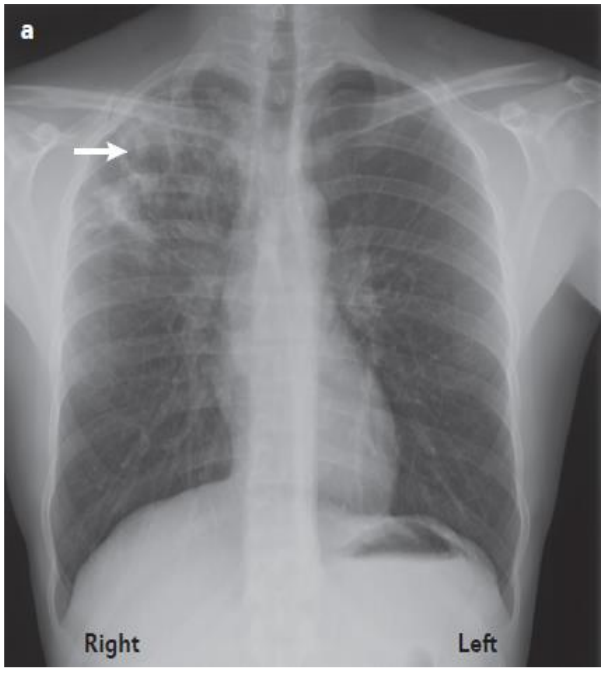

Figure 1.6 Conventional X-ray of a TB patient. The right upper lope indicates a large cavity in the lung surrounded by consolidation and infiltrates. Picture adapted from (Pai *et al*. 2016).

1.9.3 Mycobacterial culture

Sputum culture remains the gold standard for TB diagnosis (Ryu 2015). Before culturing on specialised medium (Lowenstein-Jensen), sputum samples must first be decontaminated to reduce the number of other bacteria present. Although an important procedure, decontamination reduces the number of viable bacilli in the sputum samples thus compromises sensitivity (Grandjean *et al.* 2008). The specificity and sensitivity of

this method is reported to be 98% and between 26-42% respectively (Wadhwa *et al*. 2012). Traditional M. tb culture require 4-6 weeks of incubation on solid media (fig. 1.7), but this can be reduced to 10 days using a highly enriched liquid culture (Murray *et al.* 2003; Ryu 2015). This method has some limiting factors, such as the need for biosafety level 3 (BSL 3) containment and time for pathogen detection as M. tb grows slowly (Grandjean *et al*. 2008). A tool capable of the real-time detection of the pathogen would have a significant impact on TB control.

Figure 1.7. Growth of M. tb on Lowenstein-Jensen (LJ) agar. Yellow colonies of M. tb are seen growing on LJ agar after 6-8 weeks post culture. Picture adapted from (Castellana *et al.* 2016).

1.9.4 Immunological methods

Direct detection of M. tb bacilli from sputum samples can be challenging especially in children below the age of 12 and in severely compromised individuals such as those infected with HIV and in those who are unable to produce quality sputum samples

(Shingadia and Novelli 2003). Serological based methods come in handy when blood and urine are sample targets, as any patient would be able to provide these specimens without any difficulty. Immunological assays can be categorised into (1) direct assays which target the bacterium and (2) indirect assays which detect the body's immune response to the pathogen.

1.9.4.1 Indirect assay - Tuberculin skin test (TST)

In TST, a cocktail of mycobacterial proteins containing purified peptide protein (PPD) prepared from heat killed cultures of M. tb is injected intradermally (Trajman *et al.* 2013). This induces a delayed-type hypersensitivity reaction due to the release of interferon gamma (INF-γ) at the site of injection (Huebner *et al.* 1993) and causes skin induration. The size (diameter) of induration measured on the skin is compared to a cut-off to determine whether a person is infected with TB. Although TST has been used extensively to diagnose active and latent TB (Trajman *et al.* 2013), the test lacks specificity. The components of PPD are found in other species of mycobacteria such as *M. bovis* and non-tuberculous mycobacteria. Secondly, individuals vaccinated with Bacillus Calmette-Guérin (BCG)- an attenuated strain of *M. bovis*, also respond positively to TST. The assay takes between 2-3 days for an induration to form on the skin (Pouchot *et al.* 1997). The protracted waiting period to determine ones TB status may lead to loss of active TB as patients at remote testing centres as they may fail to return to the health facility.

1.9.4.2 Direct assay - Antigen based test

The low specificity of PPD necessitates the use of more specific pathogen derived antigens. ESAT-6 and culture filtrate protein (CFP-10) are major antigenic proteins associated with M. tb and can trigger the release of INF-γ in TB infected patients (Xu *et al.* 2012). The genes encoding these antigens are located in the region of difference 1 (RD1) in the mycobacteria genome. RD1 is not present in *M. bovis* and other non-tuberculous mycobacteria species hence, it is expected to be more specific in TB diagnostic assays than TST (Trajman *et al*. 2013). The combined use of these antigens specifically selects for M. tb hence a potential to be an effective diagnostic marker (Ravn *et al.* 2000). Two commercially available test kits; QuantiFERON-TB Gold-In-Tube (QFT-GIT) assay and T-SPOT.TB have been developed to measure the amount of INF-γ released in response to ESAT-6 and CFP-10 in sputum samples (Ahmad 2010).

Unfortunately, the cost of these tests (QFT-GIT and T-SPOT.TB) limits their use in low resource settings (Lalvani and Pareek 2010; WHO 2010). Secondly, the production of antibodies in TB patients are not homogenous as they vary from patient to patient. Thus, designing a diagnostic tool based on these two antigenic proteins is likely to suffer sensitivity towards M. tb detection in a larger population set.

The nature of antigen and antigen stability in clinical specimen are very important factors to be considered in the design of an antigen based detection kit (Cho 2007). LAM, a 17KDa lipopolysaccharide is another M. tb antigen released into the urine of active TB patients (Achkar and Ziegenbalg 2012; Gomez *et al.* 2012). The sensitivity and specificity

of diagnostic assays based on this antigen ranges from 59-67% and 80-94% respectively (Peter *et al.* 2012).

1.9.5 DNA based methods

DNA diagnostic tests have proven in identifying bacteria and determining their antibiotic sensitivity within a short time frame as compared to sputum culture (Craw and Balachandran 2012). Several DNA based methods for M. tb detection have been developed and are currently in use, these are discussed below.

1.9.5.1 Xpert MTB/RIF assay

Xpert MTB/RIF is an automated real time nucleic acid assay developed for the identification of both M. tb and rifampicin resistance (Theron *et al.* 2014). This is the only rapid test approved by the WHO for the detection of TB and rifampicin resistance in symptomatic TB patients (Horne *et al*., 2019). This assay requires an extensive DNA preparation step for DNA release and to remove PCR inhibitors. This is followed by DNA amplification which takes approximately 120 minutes. In smear positive TB specimens, this assay has a sensitivity of approximately 98% while in smear negative but culture-positive specimens, the sensitivity of the assay is reduced to between 60-80% (Boehme *et al.* 2010). Although the Xpert MTB/RIF assay is an improvement over immunological tests, its low sensitivity in smear negative but culture positive samples makes it unreliable for TB diagnosis especially in patients with very low bacilli levels.

Currently, the assay is designed to detect rifampicin resistance only, which limits its application for other resistance detection. The cost in obtaining a single cartridge ($10) is

also a limitation (Engstrom *et al.* 2012). Performing this assay requires a computer, a constant supply of electrical power and requires routine maintenance to operate efficiently. All these contribute to financial burdens and makes it unattractive to use especially in resource deprived areas (Kamphee et al. 2015). Other assays such as MTBDR*plus* and MTBDRs*l* are approved by the WHO. MTBDR*plus* is developed for the detection of RIF and INH resistance. RIF resistance is associated with mutations in the *rpo*B gene while INH resistance involves multiple genes such as the *katG*, *inhA*, and *kasA* genes and the intergenic region of the *oxyR-ahpC* complex (Lacoma *et al*., 2008). MTBDRs*l* targets mutations in the *gyr*A and *rrs* genes and are associated with XDR-TB (Viveiros *et al.* 2005; Barnard *et al.* 2008; Jacobson *et al.* 2013; Kipiani *et al.* 2014; Theron *et al*. 2014). Similarly, these tests are limited by factors akin to the Xpert MTB/RIF assay (Yadav *et al.* 2013).

1.9.5.2 Isothermal nucleic acid amplification tests

PCR based diagnosis of M. tb involves long and repetitive cycles of template denaturation, annealing and strand extension of specific target region using a thermocycler. The amplicons generated can only be visualised with a specialised equipment via electrophoresis. Isothermal amplification tests rely on the generation of DNA amplicons by autocycling and strand displacement process under a constant temperature (Iwamoto *et al.* 2003). The process is mediated by a specialised polymerase (*Bst*) and is faster (60 minutes) than traditional PCR (2-3 hours). Also, the amplicons can be visual observed by a colour change in the reaction assay. Some examples of isothermal detection include Loop mediated isothermal amplification (LAMP) (Iwamoto *et al*. 2003; Ou *et al.* 2014) and transcription mediated amplification (TMA) (Shenai *et al.* 2001). LAMP and TMA

have been developed to detect TB, mainly targeting the *rrs, gyrB* gene and the insertion sequence (IS *6110*). The performance of LAMP assays targeting these gene sequences have been evaluated.

TB-LAMP targeting the *rrs* gene has sensitivity and specificity of 100% and 94.2% respectively (Pandey *et al.* 2008) while targeting *gyrB* gene yielded about 97% sensitivity in smear-positive, culture positive specimens and 48.8% in smear negative but culture positive specimens respectively (Boehme *et al.* 2007). TB-LAMP targeting the IS*6110* also has the highest sensitivity (100%) but was less specific in detecting other members of the MTB complex (Aryan *et al.* 2010). While these test shorten the time to detection in comparison to traditional PCR, they still require purified DNA from clinical samples (Shah *et al*. 2007). These assays also need costly and cold storage to guarantee assay reproducibility.

1.9.6 High performance liquid chromatography (HPLC)

HPLC is mainly used for the analysis of different compounds in samples at microliter volumes. Samples are injected into a stream of liquid (mobile phase) which passes through a column (stationary phase). The efficiency of separation is dependent on the degree of sample retention in the column (Butler *et al.* 1991). HPLC is further equipped with detectors that can identify different components present in a sample. The difference in sample composition generates a distinct chromatograph which is unique to the sample (fig 1.8) (Floyd *et al.* 1992). With the aid of an appropriate standard, the chromatograph generated can be identified. In mycobacteria species, the distributions of mycolic acids

(2-alkyl, 3-hydroxy fatty acids) are unique and has been the basis of bacteria identification via HPLC technique (Duffey *et al.* 1996). To determine this, mycolic acid is first extracted from pure cultures of mycobacteria and then analysed. This method has 100% sensitivity (Thibert and Lapierre 1993) and takes about 2 hours with the exception of the added time required to culture the pathogen (7-21 days) and extract mycolic acid from the bacteria (Duffey *et al*. 1996). HPLC is sophisticated and requires trained personnel which comes at a cost. Studies show that, growing the bacteria on solid media as compared to liquid media boosts the specificity of the assay since liquid media are likely to contain chemicals acting as contaminants (Duffey *et al*. 1996).

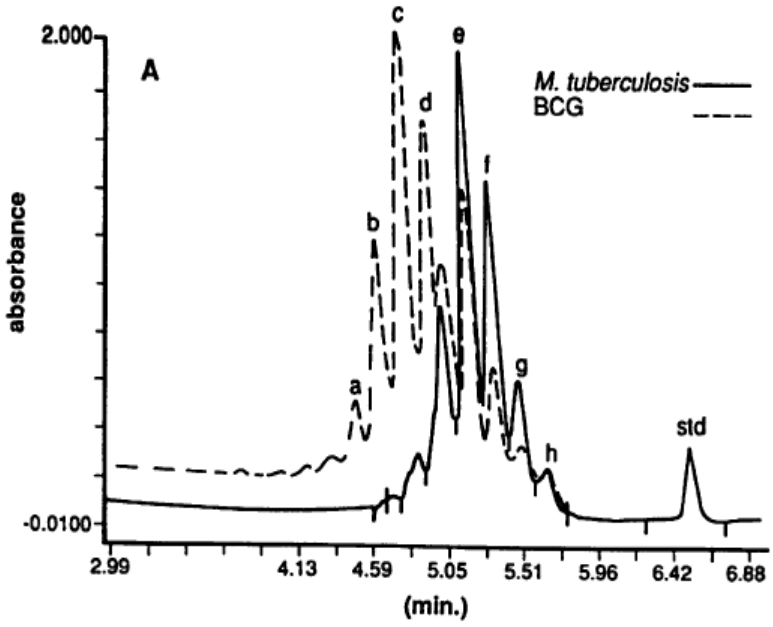

Figure 1. 8 Superimposed chromatographs of M. tuberculosis and M. bovis (BCG) determined using HPLC. The unique chromatographs from BCG and M. tb are clearly separated based on their mycolic acid composition. Picture adapted from (Floyd *et al.* 1992).

1.10 Surrogate model for TB diagnosis

Owing to the challenges associated with working with M. tb, i.e. its slow growth requiring 6-8 weeks and the need to handle the bacterium in biosafety level 3 facilities, many researchers employ faster growing and less virulent member of the mycobacterial group. These group of mycobacteria shares with M. tb the ability to develop broad spectrum antibiotic resistance, to undertake preliminary research to develop new diagnostics for M. tb. Commonly used bacteria as models for M. tb studies include *M. smegmatis* and *M. abscessus* (Cortes *et al.* 2010). These two species fall under the umbrella of nontuberculous mycobacteria (NTM) and are described below.

1.11 Non-tuberculous mycobacteria (NTM)

Non-tuberculous mycobacteria (NTM) refers to all other mycobacteria except those belonging to MTBC and *Mycobacterium leprae* (the causative agents for leprosy) (Lee *et al.* 2014). NTM are common environmental pathogens causing significant morbidity and mortality in both immunocompetent and immunosuppressed individuals (Döffinger *et al.* 2000; Nessar *et al.* 2012). Currently, species of NTM are estimated at more than 150 (Johnson and Odell 2014) with major infections occurring in HIV/AIDS patients (fig 1.9). There is a correlation between NTM infections and HIV/AIDS patients, claiming the lives of millions every year. This could be attributed to the weakening of the immune system in HIV patients. Treatment is also a major challenge due to the complex pharmacological interactions between antiretroviral and anti-mycobacterial drugs (Abston and Farber 2018; AIDSinfo. 2018).

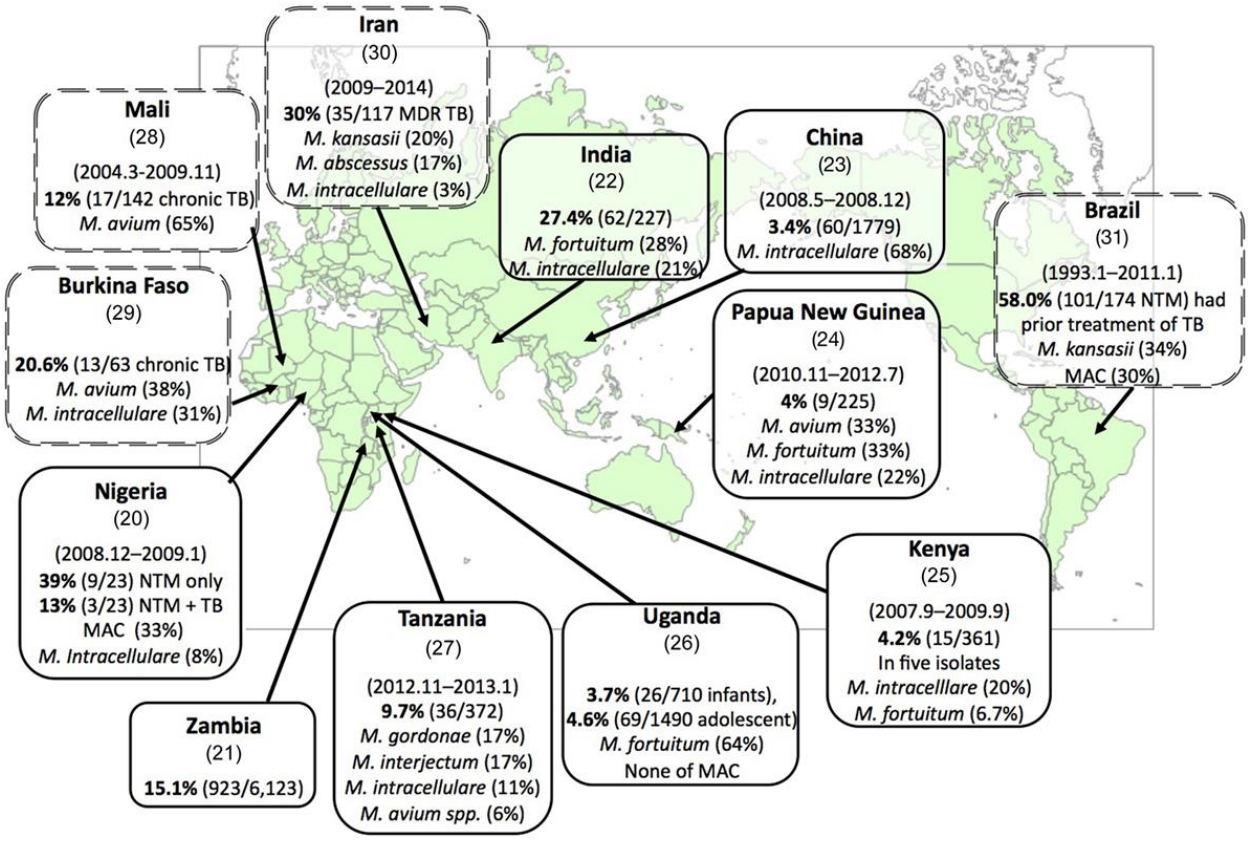

Figure 1.9 Global distribution of NTM isolated from various parts of the continent. The picture above depicts NTM surveillance among HIV/TB patients across the continent. Picture adapted from (Nishiuchi *et al.* 2017).

Other diseases that predisposes an individual to NTM infections include cystic fibrosis (CF), hematopoietic stem cell transplant, hematologic malignancies and hairy cell leukaemia (Henkle and Winthrop 2014). Based on their growth rate NTMs can be divided into two groups, namely; rapid growing (e.g. *M. abscessus, M. smegmatis, M. chelonae*) and slow growing (e.g. *M. kansasii, M. avium*). The rapid growers require 2-3 days to grow on artificial media while the slow growers take more than 7 days (Esteban and Ortiz-

Pe´rez 2009). The phylogeny of mycobacterial species showing the fast growing and slow growing NTM are indicated in figure 1.10. The most common and frequent in clinical infections (*M. abscessus*) is described below.

Figure 1.10. Phylogenetic tree of Mycobacteria. Mycobacterial species categorised as rapid or slow growers and are represented with thin or thick lines respectively. Picture adapted from https://ars.els-cdn.com/content/image/1-s2.0-S1567134817303519-gr1_lrg.jpg. Date accessed: 28/09/2019.

1.12 *Mycobacterium smegmatis* (*M. smegmatis*)

M. smegmatis is an aerobic fast-growing bacterium, commonly used as a surrogate model in TB research (Chaturvedi *et al.* 2007). *M. smegmatis* was first isolated from the human smegma in 1885. Smegma is a natural liquid produced under the foreskin of the human penis (Bohsali *et al.* 2010). This bacterium is considered non-pathogenic and uncapable of eliciting immune response even in immunocompromised individuals. A study by Best and Best contradicts the above claim, where *M. smegmatis* was implicated in the formation of granuloma on the hand of a 67-year old Caucasian (Best and Best 2009). Treatment of this condition required the combination of antibiotic (doxycycline) and surgical therapy. The gene sequence of this pathogen was not provided by the authors to ascertain whether a mutation or acquisition of a foreign gene has occurred, as is the predominant modes of resistance with bacteria. *M. smegmatis* has a generation time of between 3-4 hours as compared to M. tb 24 hours. The short generation time and safe working with a biosafety level 2 cabinet makes it a good choice as a surrogate bacterium.

1.13 *Mycobacterium abscessus* (*M. abscessus*)

M. abscessus were previously considered as an environmental pathogen inhabiting soil, biofilms and tap water systems (Honda *et al.* 2016), it is now known as the most pathogenic and multi-drug resistant opportunistic pathogen currently infecting patients with CF (Nessar *et al*. 2012). Infection with *M. abscessus* leads to TB-like symptoms in the lungs of CF patients causing lung dysfunction (Floto *et al.* 2016). The nomenclature of *M. abscessus* has undergone frequent revisions, hence the classification in the literature

is not uniform (Brown-Elliott and Wallace 2002; Adekambi and Drancourt 2004; Adekambi *et al.* 2006; Leão *et al.* 2010 ; Leao *et al.* 2011).

To enhance clarity and to facilitate reference to recent publications, the following three subspecies names is adopted in this work, i.e. *M. abscessus* subspecie *abscessus*, *M. abscessus* subspecie *bolletii* and *M. abscessus* subspecie *massiliense*, all three referred to as the *M. abscessus* complex (Lee *et al.* 2015). Of these three species, *M. bolletii* is very rare while *M. abscessus* and *M. massiliens*e occur in similar numbers (Koh *et al.* 2010). Global estimate of *M. abscessus* infection may be under reported as guidelines for the reporting and diagnosing of *M. abscessus* and NTM do not exist (Johnson and Odell 2014). Countries such as United States (Esther *et al.* 2010), Brazil (Duarte *et al.* 2009), Korea (Kwon *et al.* 2009), China (Nie *et al.* 2014) and countries in Western Europe (Roux *et al.* 2009) have documented numerous cases of *M. abscessus* infections (Tettelin *et al.* 2014).

1.14 Pathogenicity

As the name suggest, *M. abscessus* is responsible for causing an abscess in soft tissues and on the skin, characterised by a red-pink swelling filled with pus (fig. 1.11) (Kwon *et al*. 2009). *M. abscessus* infections can also occur in causing acute and chronic meningitis, neutrophilic pleocytosis and meningoencephalitis (Talati *et al.* 2008; Medjahed *et al.* 2010). *M. abscessus* contributes to about 65-80% of pulmonary disease caused by rapidly growing mycobacterium (Lee *et al*. 2014). It is the most frequent mycobacteria pathogen

isolated from patients with cystic fibrosis (Fletcher *et al.* 2016). Approximately, 3-10% of cystic fibrosis patients living in the UK and the USA are infected with *M. abscessus* (Bryant *et al.* 2013).

The lung microbiome of CF patients is very complex. While *M. abscesssus* represent the dominant mycobacterial pathogen, *Pseudomonas aeruginosa* followed by *Burkholderia cepacia* complex are the most common opportunistic bacterial pathogen isolated in these patients (Birmes *et al.* 2017). Recent studies suggest that, *M. abscessus* can inhibit quorum sensing thus preventing the growth of *Pseudomonas aeruginosa* (Birmes *et al*. 2017). This finding could suggest other multifaceted interaction occurring within the microbiome of CF patients which are yet to be investigated.

Figure 1.11 *M. abscessus* infection on the left forearm of a patient characterised by red-pink nodules filled with pus. Picture adapted from (Kwon *et al*. 2009).

1.15 *M. abscessus* virulence factors

Similar to other pathogens, *M. abscessus* is able to evade the host immune response. This suggests that the organism possesses certain virulent factors that enhances its ability to outwit host immune mechanisms and promote survival. Based on the growth morphology of *M. abscessus* on solid agar plates, two major forms (rough and smooth) have been identified (fig. 1.12). The rough (R) form lacking glycopeptidolipid (GPL) are more pathogenic, can persist and multiply in the host macrophages upon infection. The smooth (S) forms are characterised by the presence of GPL, present in their cell membrane and they tend to succumb easily to the host immune machinery (Ruger *et al.* 2014).

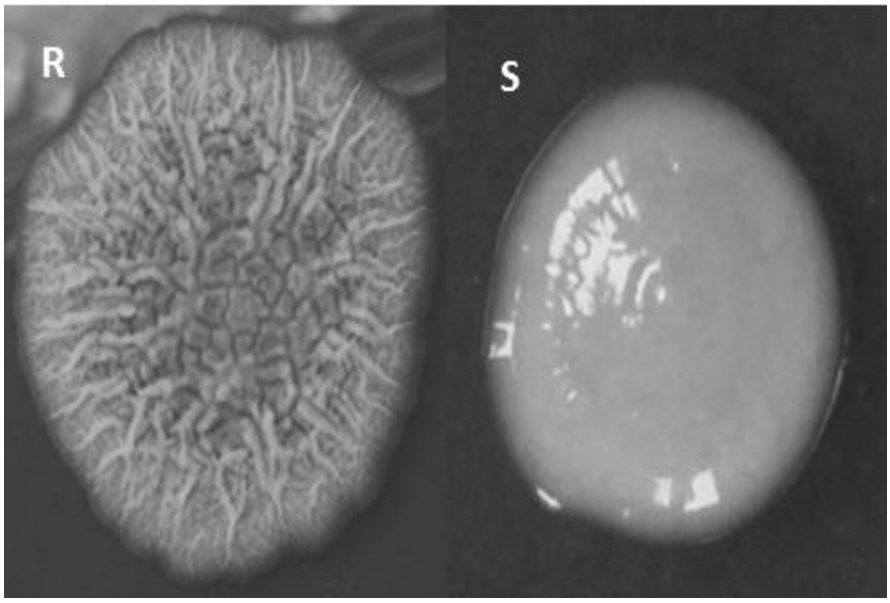

Figure 1.12 Morphology of rough (left) and smooth (right) forms of *M. abscessus* cultured on 7H11 agar. Picture adapted from (Ruger *et al.* 2014).

The chemical structure of GPL is depicted in Fig 1.13 below. Upon entry into the host cells, *M. abscessus* (R form, wild type) become tightly attached to the phagosomal

membrane while the S forms are unable to attach but resides loosely in the phagosome (Byrd and Lyons 1999). *M. abscessus* attachment to the phagosome is dependent on the absence of GPL in R (Howard *et al.* 2006). The S morphotype exhibit sliding motility and have the capacity to form biofilms (Schorey and Sweet 2008).

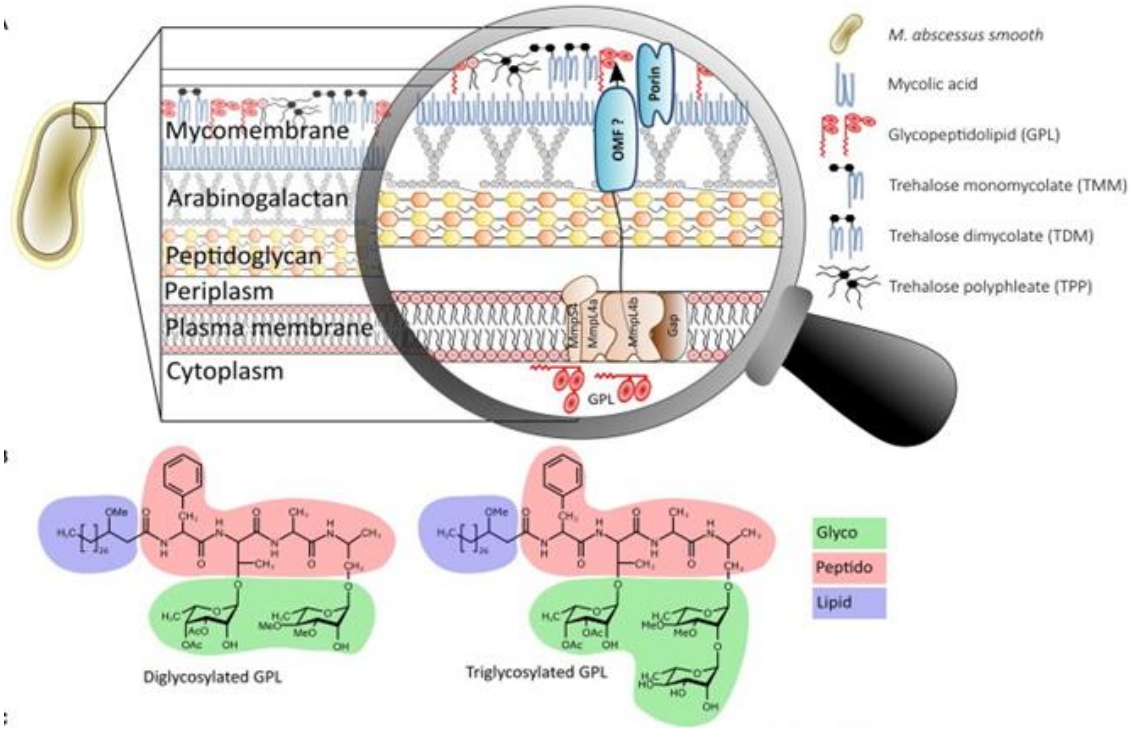

Figure 1.13. Schematic diagram of mycobacterium cell envelope. The magnified cell membrane envelope shows the different layers biomolecule arrangement and lipids present. The membrane also depicts the presence of GPL responsible for producing smooth colonies of *M. abscessus*. Picture adapted from Gutiérrez *et al*., 2018.

GPL mutants (R morphotype) are non-motile, lack the ability to form biofilms and are cord forming. Cord formation is the ability of bacteria to align end to end and side to side as compared to forming clumps (aggregates of bacteria in random orientation). Cord formation is a property of bacterial virulence associated with M. tb and NTM (Sa´nchez-

Chardi *et al.* 2011). Cord formation is enhanced by the production of trehalose 6, 6'-dimycolate (TDM) - a known virulent factor in M. tb (Behling *et al.* 1993). The mechanism of R morphotype virulence has been demonstrated using a zebrafish model. It was found that, the R morphotype inhibits macrophage and neutrophil mediated phagocytosis, partly aided by their ability to attach (Bernut *et al.* 2014). Further studies have also shown that, spontaneous conversion of the S to R form does occur after several passages (Howard *et al*. 2006). This is believed to occur due to the insertion or deletion of nucleotide bases in the *mps*1 gene required for GPL synthesis or the *mmpL4b* gene which is responsible for the translocation of GPL into the cell surface (Fig. 1.14) (Pawlik *et al.* 2013; Ridell 2015).

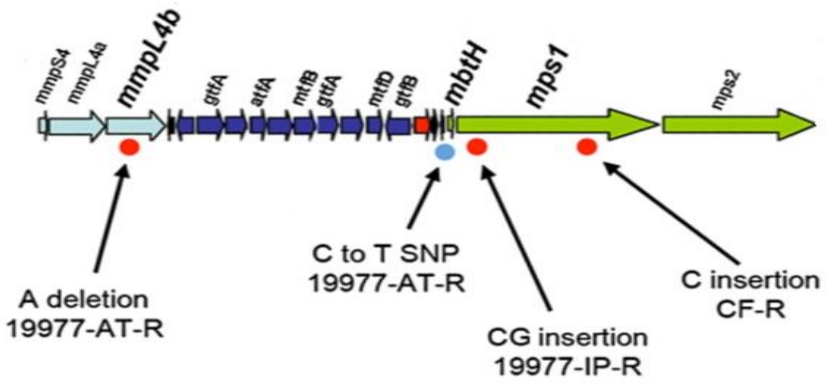

Figure 1.14 Schematic representation of the *M. abscessus* GPL genes associated with the synthesis and transport of GPL. Picture adapted from (Pawlik *et al*. 2013)

M. abscessus also harbours other genes that are linked to virulence. For instance, MAB_O55 which encodes phospholipase C (PLC), an enzyme which is absent in most rapidly growing mycobacteria. PLC mediates hydrolysis of host phospholipids to

produces diacylglycerol (DAG) which activates protein kinase C, resulting in the unregulated activation of neutrophils and macrophages which results in the inflammation observed in the lungs of CF patients (N'Goma *et al.* 2015).

1.16 Transmission of *M. abscessus*

The primary environment of *M. abscessus* includes fresh water and soil (Honda *et al*., 2016). Transmission from the environment to an individual could occur when there is close contact. Some healthy fish farmers have been reported to be infected with *M. abscessus* through contact with fish possibly contaminated with the bacterium. This is possible to the extent that, *M. abscessus* shares the same ecological niche with the fish pathogen *M. marinum*. It has been reported that *M. abscessus* harbours a mercury resistant plasmid with about 99% of its nucleotide sequence identical to an episome of *M. marinum* (Bernut *et al*. 2014).

Nosocomial transmission of NTM is also very common in haemodialysis, dental and surgery departments. Portable and treated water from hospital taps have been found to be contaminated with NTM (Phillipsa and von Reyn 2001). Recent studies have also suggested that person-to-person through the generation of aerosols particularly among CF patients is possible (Bryant *et al*. 2013; Birmes *et al*. 2017), although this observation contradicts other studies (Harris and Kenna 2014). Aerosols generated by CF patients contain significant concentrations of viable bacteria of a respirable size range which could be responsible for air borne transmission (Birmes *et al*. 2017). Additionally, the ability

of *M. abscessus* to withstand desiccation in arid environment could also suggest transmission via air (Wallace *et al.* 1997; Bryant *et al*. 2013).

Transmission via fomite formation is also another possibility, owing to *M. abscessus* resistance to disinfectants and chlorination (Koh *et al*. 2010). To prevent this form of transmission, surgical wounds, intravenous catheters and injection sites should be shielded from environmental contamination. Also, surgical apparatus (e.g. endoscope, catheters) must be well sterilised after use.

1.17 *M. abscessus* treatment and resistance mechanisms

Clarithromycin, a macrolide antibiotic is the current drug of choice for the treatment of *M. abscessus* infections (Petrini 2006). The mechanism of action of action is similar to other macrolide antibiotics in that it binds to 23S rRNA and subsequently inhibit protein synthesis (Stout and Floto 2012). Resistance to clarithromycin is a major concern and occurs in two forms, acquired and inducible. The former results from a mutation in the drug binding pocket at position 2057 or 2058 of the *rrl* gene which encodes 23S rRNA (Bastian *et al.* 2011), while the latter is associated with the presence of a complete, functional and active *erm*-41 gene. In the presence of clarithromycin, the *erm*-41 gene is activated and encodes a methylase enzyme (erythromycin methylase). This enzyme adds a methyl group to adenine at position 2057 or 2058 in the 23S rRNA, thereby inhibiting clarithromycin binding (Mougaria *et al.* 2017).

All three subspecies of *M. abscessus* have varying treatment responses to clarithromycin. *M. abscessus* and *M. bolletii* have full length copies of the *erm*-41 gene and hence are

resistant to clarithromycin. *M. massiliense* have a 274 bp deletion in the *erm*-41 gene, making it non-functional and rendering it susceptible to clarithromycin (Kim *et al.* 2010; Yoshida *et al.* 2014). Other features also contribute to the functionality of the *erm*-41 gene. The presence of thymine (T) or cytosine (C) at position 28 of *erm-41* gene confers either resistance or susceptibility to clarithromycin respectively (Mougaria *et al*. 2017).

Amikacin, an aminoglycoside antibiotic is another drug frequently used for the treatment of *M. abscessus* (Nessar *et al*. 2012). Amikacin like other aminoglycosides (kanamycin, tobramycin) inhibits protein synthesis by binding to the *rrs* gene of the 16S rRNA. Since *M. abscessus* possess a single copy of the rRNA operon which is a target for binding, a single point mutation occurring within this operon can result in resistance (Cortes *et al*. 2010). A point mutation is a single base change from A to G at position 1408 and is a well-known mutation site in the *M. abscessus rrs* gene (Nessar *et al*. 2012).

Azithromycin an anti-inflammatory drug has also been used to treat *M. abscessus* infections. However, its use has been reported to increase patient's susceptibility to *M. abscessus* and NTM in general (Renna *et al.* 2011). In a study by Renna and colleagues, azithromycin terminates autophagosome process and lysosomal acidification and degradation of pathogens in macrophages. As a result, engulfed bacteria continue to proliferate increasing pathogen survival (Renna *et al*. 2011).

M. abscessus is resistant to several anti-TB drugs including rifampicin and ethambutol making it a good surrogate bacterium for M. tb (Nessar *et al*. 2012). The antibiotic

resistance could be due to the uniqueness and diversity that exist within its genome. Among the species of mycobacteria, certain virulent genes have been identified to exist only in *M. abscessus* (Nunes-Costa *et al.* 2016). Furthermore, it has also been shown that, *M. abscessus* has undergone frequent evolutionary changes, progressing from an environmental organism to a successful human virulent lung pathogen (Birmes *et al*. 2017), during which it is likely to have acquired unique genes which encode antibiotic resistance. One of the unique enzymes produced by *M. abscesssu*s i.e. 2-N-acytyltransferase and aminoglycoside phosphotransferase have been found to degrade aminoglycoside antibiotics and promote resistance (Ripoll *et al*. 2009).

The nature of *M. abscessus* resistance demands urgent therapeutic procedures i.e. multi therapy as opposed to monotherapy. The latter is no longer recommended for *M. abscessus* treatment. The American Thoracic Society (ATS) recommends a combinatorial approach based on an oral macrolide and intravenous administration of either amikacin, cefoxitin or imipenem (Griffith *et al.* 2007). In extremely difficult to manage cases removal of affected body parts by surgery is required to enhance treatment success and this has been applied in many conditions (Jarand *et al.* 2011).

1.18 Diagnosis of *M. abscessus*

Many of the traditional approaches for M. tb diagnosis can also be applied to the detection of *M. abscessus*. Microscopy and culturing on 7H10, 7H11 agar and in 7H9 broth or Luria-Bertani broth or on agar are commonly applied (Ryu 2015). Growth appears as yellow or cream colonies after 3 days of culture (Cortes *et al*. 2010). Previously, *M.*

abscessus and *M. chelonae* were considered as same species. Biochemical tests such as sodium chloride tolerance and citrate uptake can be used to distinguish between *M. abscessus* and *M. chelonae* (Conville and Witebsky 1998). Also, growth on MacConkey agar without crystal violet, aryl sulphatase and nitrate reductase tests are used for identification (Silcox *et al.* 1981). These biochemical tests are not always reliable, giving overlapping phenotypic patterns and are time consuming and labour intensive (Conville and Witebsky 1998; Kulandai *et al.* 2014). Other innovative methods (e.g. HPLC) for *M. abscessus* detection have also been developed. HPLC is limited in the sense that it is not able to discriminate between *M. chelonae* and *M. abscessus* (Jeong *et al.* 2011). Also, in terms of simplicity, cost and portability, HPLC cannot match the requirements of a rapid diagnostic tool.

The optimal treatment regimen for *M. abscessus* is specie specific, necessitating accurate speciation followed by treatment. Thus, the diagnostic tool must be developed to be very specific and sensitive. The INNO-LiPA is an example of a molecular based commercial kit developed for the identification of M. tb complex and 8 other NTM species including *M. abscessus* (Miller *et al.* 2000; Padilla *et al.* 2004). This kit requires DNA extraction followed by DNA amplification with probes targeting the 16S-23S rRNA internal transcribed spacer region (ITS). The ITS region is selected because it is predicted to have more discriminatory power in distinguishing closely related mycobacteria species. Evaluation of the INNO-LiPA kit shows that it has specificity (87%) as compared to culture (96.3%) (García-Agudo *et al.* 2011). The reduced level of specificity could be attributed to cross reactivity with other mycobacteria species (Tortoli *et al.* 2010).

Performing this assay takes about 3 hours in addition to a DNA extraction and amplification step, defeating the purpose of POC developments.

PCR, targeting multiple gene sequences (*rpoB*, 16s rRNA, *erm*-41, *gyrB*) has also been developed for detection of *M. abscessus* (Matsumoto *et al.* 2011). The performance of PCR based assays are comparable to culture in terms of specificity and sensitivity (Kim *et al.* 2015). The disadvantage to using PCR over culture is the time to detection and the need for costly reagents and equipment. While PCR may take about 2-3 hours, culture may require about 48-72 hours. Regarding the challenges with the current detection methods as described above, they do not present as attractive tools for rapid detection of *M. abscessus*, hence the need for rapid detection tools to meet POC needs.

1.19 Point-of-care (POC) diagnostics

POC testing refers to the use of diagnostic tools to generate patient results at the point where patient consultation and presentation takes place or within the perimeter of the health care facility (Dheda *et al.* 2013). Failure to produce diagnostic results on same day has been a major challenge for disease control (Rossato Silva *et al.* 2012). By generating timely results, treatment can begin immediately and prevent adverse case of the disease (Dheda *et al*. 2013). A POC diagnostic tool must be designed to meet the ASSURED guidelines. ASSURED is an acronym meaning the diagnostic tool should be Affordable, Sensitive, Specific, User-friendly, Rapid, Equipment-free and Deliverable (Urdea *et al.* 2006). In addition, the PC tool must be portable for easy transport (fig 1.15). An ideal POC test should be able to identify the biological marker in a clinical specimen that is

predictive of a disease state. In addition, the biomarker should be specific to the pathogen causing the disease and not cross react with other pathogens. This is a challenge encountered using serological based assays.

DNA based detection methods offer superior advantage over serological tests and could be a promising option for the development of a POC testing. Identifying the specific nucleic acid sequence in M. tb as well as *M. abscessus* could serve as an important biological marker for specific and sensitive detection and monitoring of treatments. The development of a rapid assay with the potential of miniaturisation into a portable device to be used at the POC will alleviate the burden of mycobacteria related disease and other diseases of public health importance.

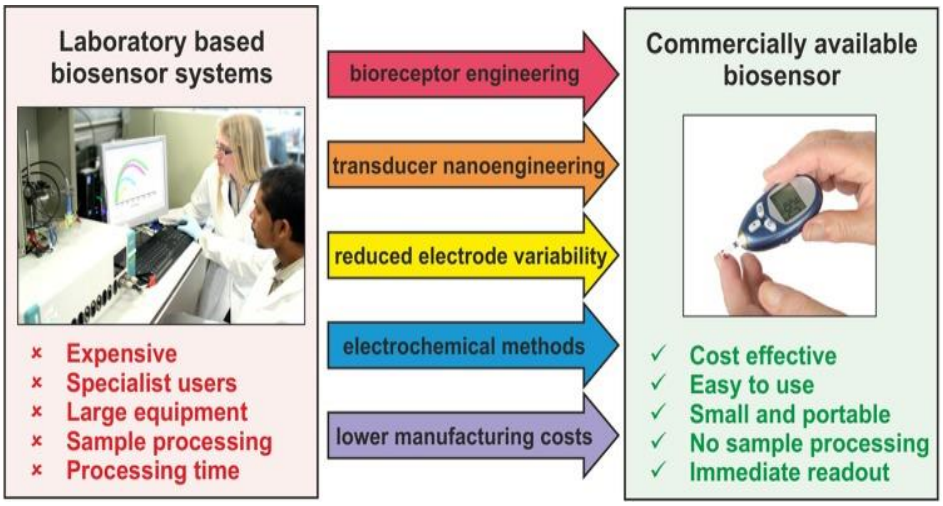

Fig 1.15 Innovative technologies for the development of miniaturised biosensors. Complex and large laboratory equipment for diagnostic purposes translated into miniaturised format biosensors. Picture adapted from (Ahmed *et al.* 2014)

1.20 Techniques for bacteria cell wall lysis

The sensitivity of any DNA based detection assay is dependent on the ability to access the target (DNA) from the specimen. This requires the release of the target DNA from the organism in sufficient quantities to allow their detection. In the case of bacteria, the DNA is locked within the bacterium necessitating the use of some form of lysis method. Also, the nature of the clinical sample in which the bacterium is present may require the use of complex purification procedures to remove inhibitory factors such (e.g. proteins) which could inhibit detection of targets. Thus, the initial processing of the clinical sample is an important consideration when attempting to develop a rapid POC. Mycobacteria species have a rigid cell wall composed of mycolic acid which make it more resistant to disruption than other types of bacteria. Currently, there lacks an efficient and rapid method for lysing mycobacterial cells and it is a bottleneck in the development of rapid DNA based detection tools.

1.20.1 Boiling and sonication

Boiling is one of the simplest methods to break open bacterial cells. This usually involves heating the bacterial suspension at boiling temperature (100˚C) in Tris acetate EDTA (TAE) buffered solution (Odumeru *et al.* 2001). Typically for mycobacterial cells that have rigid cell walls, this temperature is necessitated to permeabilise cell wall and to release intracellular DNA. Although simple to perform the purity of the DNA yield is usually low due to the presence of contaminants such as proteins and carbohydrates. Lysis protocols have been developed that employ mechanical methods such as sonication and bead beating. In sonication, a bacterial suspension is exposed to sound waves generated by an oscillating transducer which causes the bacterial cells to agitate and subsequently

leads to cell lysis. This method involves high frequency oscillation of bacterial cells in an enclosed tube containing beads (Vandeventer *et al.* 2011). These procedures also cause DNA shearing which compromise the integrity of the DNA. Rapid testing of nucleic acids in resource deprived areas require novel tools that are less sophisticated and can perform cell lysis in microliter quantities. The use of microwave energy is one such approach currently being considered (Vaid and Bishop 1998).

1.20.2 Microwave (MW) mediated cell lysis

Microwave (MW) is the second component of the electromagnetic spectrum after radio waves having a low frequency but longer wavelengths. Bacterial cells exposed to MWs results in cell lysis and the release of DNA (Jankovic *et al.* 2014). Joshi *et al*. demonstrated the use of microwave energy as a means of disrupting the vegetative and sporulating *C. difficile*. Additionally, the MW induced cell lysis, resulting in the release of sufficient single stranded DNA to enable detection of *C. difficle* toxin genes using specific DNA probes. A similar approach has also been used to recover DNA from *Bacillus anthracis* spores (Aslan *et al*. 2008) and *Chlamydia trachomatis* (Zhang *et al*. 2010). In this research, the optimum microwave condition for the release of ssDNA and dsDNA from *M. abscessus* will be determined. The released nucleic acid will then be detected in an enzyme linked oligonucleotide sandwich hybridisation assay (ELOSHA).

1.21 Factors modulating MWs effect in biological membranes

As MWs will be considered as a fast DNA release tool from cells, it is worth noting that cells have significant differences in their cell wall and membrane composition (discussed in section 1.1). The type and composition of membrane phospholipids and fatty acids in cell membranes are reported to influence cells susceptibility to MWs (Unsay *et al.* 2013a; Oncul *et al.* 2016). Fatty acids and phospholipids components in their membranes are present in diverse proportions, the reason being that the environmental conditions to which cells are cultivated or exposed in the natural are different (Sohlenkamp and Geiger 2016). The membranes of *E. coli* are composed of three major phospholipids: phosphatidyl ethanolamine (PE), phosphatidyl glycerol (PG) and cardiolipin (Raetz and Dowhan 1990; Raetz and Whitfield 2002). *S aureus* is also mainly composed of phosphatidyl glycerol, lysyl phosphatidyl glycerol and wall teichoic acids (Haest *et al.* 1972; Atilano *et al.* 2011; Piggot *et al.* 2011). Teichoic acids play a key role in concealing PG at the bacterial surface, and could contribute to membrane rigidity (Brown *et al.* 2013). Phosphatidyl choline, phosphatidyl inositol and phosphatidyl ethanolamine are the major phospholipids in *C. albicans* (Haest *et al.* 1969; Georgopapadakou *et al.* 1987). Cardiolipin (1,3-diphosphatidyl-sn-glycerol) is present in all the four types of cell membranes and has four acyl chains (Crellin *et al.* 2013). It plays a key role in maintaining membrane integrity in response to stress. Its presence of cardiolipin induces bilayer structure remodelling, deformation of the membrane and enhancing permeabilization (Unsay *et al.* 2013b).

Generally, saturated fatty acids tend to increase membrane fluidity unlike unsaturated fatty acids (Marrink *et al.* 2009). The composition of saturated FA in *E. coli* and *C.*

albicans are below 50% (Haest *et al*. 1969; Georgopapadakou *et al*. 1987) suggesting a less compact membrane. In the case of *M. smegmatis*, mycolic acid is the major fatty acid constituting about 30-60% and are predominantly saturated (Taneja *et al.* 1979). Cardiolipin is composed of about 95% unsaturated fatty acids (Unsay *et al*. 2013b). The presence of cholesterol and membrane proteins (constituting about 50% of weight in cell membrane) reduces membrane fluidity, increases stability and could also pose resistance to an external MW E fields (Israelachvili and Mitchell 1975; Cullis and De Kruijff 1979; Smaby *et al.* 1994; Veatch and Keller 2005; van Uitert *et al.* 2010a; van Uitert *et al.* 2010b).

1.22 Thesis Aim

The principal aim of this study is to develop a colorimetric oligonucleotide hybridisation assay (COHA) capable of detecting the presence of *M. abscessus* within a short time frame. The rapidity and sensitivity of the COHA would be aided using microwaves for fast DNA release and magnetite particles to trap and enrich target molecules. The development of this assay will serve as a proof-of-concept that can be used for the detection of M. tb and other pathogenic bacteria of clinical importance.

1.23 Thesis Objectives

The specific objectives of this thesis were;

1. To develop an optimised method for the extraction of DNA from *M. abscessus*
2. To design DNA probes using bioinformatic approach for the detection of *M. abscessus* and *M. smegmatis*

3. To characterise the biological effect of microwaves on micro-organisms of structural diversity
4. To identify the optimum microwave conditions for the release of DNA from *M. abscessus*
5. To develop a sandwich hybridisation assay on a magnetite bead support for the detection of *M. abscessus*
6. To develop *M. smegmatis*-macrophage infection model and detect the presence of intracellular *M. smegmatis* using the hybridisation assay.

Chapter 2

General materials and methodology

2.0 General Materials

The following methods were general throughout the study. Specific methods are described in their respective chapters (3,4,5 and 6).

2.1 Materials

The following bacterial culture media were purchased and used in the study: Luria-Bertani (LB) broth and LB agar were purchased from Thermo Fisher Scientific Ltd, UK. Yeast extract, Low-Dusting (LD) was purchased from Becton Dickinson (BD, Difco). Biological media was prepared according to manufacturer's protocol and sterilised for 15 minutes at 121°C and 100 kPa using a bench top autoclave (CertoClav EL sterilizer, Austria). Deionised water was obtained from an ELGA pure lab option BP15 dispenser (ELGA lab water, UK).

2.2 General Instruments

Nanodrop (ND 1000 spectrophotometer, LabTech), Qubit 3.0 Fluorometer (Life Technologies), Orbital incubator shaker (MaxQ^{TM} 440, Thermo Scientific), Eppendorf AG Centrifuge 5417R (Hamburg, Germany), Heat Block (DRI-Block® DB.3D, Techne), UV/Vis spectrophotometer (Ultrospec 2100 pro, Biochrom, USA), T100 Thermo cycler (Bio-Rad, UK).

2.3 General Methods

2.3.1 Revival of isolates and culture from Microbank^{TM} cryo-protective beads

Cryo-protective beads containing bacteria were stored in vials at freezing conditions (-80 ºC). Beads were thawed and kept in ice. A single bead was inoculated in 20 ml LB broth

using a 10 µl sterile loop. Broth containing bead was incubated at 37°C for 72 hours under constant shaking at 200 rpm.

2.3.2 Culture of bacterial and yeast cells

The following micro-organisms were used in this study: *Escherichia coli* (NCTC 1093) and *Staphylococcus aureus* (NCTC 13373) were purchased from the HPA culture collections service (Public Health England, Porton Down, UK). *Mycobacterium abscessus* (ATCC 19977^{T}) was purchased from American Type Culture Collection (ATCC), UK. *Candida albicans* (NCPF 3179) was purchased from the National collection of pathogenic fungi (NCPF), England, UK. *Mycobacterium smegmatis* (NCTC 8159) is an archived clinical isolate used in a previous study and was included in this study. All micro-organisms were cultured in their respective media. *M. abscessus*, *M. kansasii*, *E. coli* and *S. aureus* were cultured in 20 ml of LB broth and incubated at 37°C. Mycobacteria cells were cultured between 48 - 72 hours, whiles *E. coli* and *S. aureus* were cultured overnight under constant shaking in an orbital incubator shaker at 200 rpm. *C. albicans* were cultured in yeast extract broth at 30 °C overnight with constant shaking in an orbital incubator shaker at 200 rpm. Cells were harvested (centrifugation at 4, 000 rpm for 10 min) and resuspended in phosphate buffered saline (PBS).

2.3.3 Determining the purity of cell cultures

The following methods were performed to determine whether all bacterial and yeast cells were pure and not contaminated with other bacteria.

2.3.3.1 Streak plate method

Cell suspensions were streaked on their respective agar plate to identify single colonies (pure bacterial cultures) or mixed colonies suggesting the presence of other bacterial contaminants. With the aid of a sterile inoculating loop, 10 µL of cells suspension were transferred onto either LB agar (to identify *M. abscessus*, *M. kansasii*, *M. smegmatis*, *E. coli* and *S. aureus*) or yeast extract agar (to identify *C. albicans*) and incubated at 37°C for 48 - 72 hours in the case of *M. abscessus* and overnight for the remaining cells. Single colonies were observed for uniformity. The colonies were also stained using Ziehl Neelson and Gram staining procedures. Ziehl Neelson stain was performed to identify acid-fast bacilli (mycobacteria) and Gram staining to identify Gram-negative (*E. coli*) and Gram-positive (*S. aureus*) isolates. The methods for staining are described below.

2.3.3.2 Bacterial staining methods to determine bacterial purity

2.3.3.2.1 Acid fast staining [Ziehl Neelsen stain (ZN)]

Acid fast staining also known as ZN stain was developed specifically to identify mycobacteria species. A single colony of bacteria growing on agar and suspension prepared in PBS. Ten microliters of the stock suspension was diluted (1/100) and 10 µL spotted and smeared on microscope slide, dried in a biosafety cabinet and heat fixed for staining. The staining procedures are as follows; bacterial smear on slides were flooded with carbol fuchsin, warmed over a flame of fire and allowed to stand for 5 minutes. This is to allow carbol fuchsin to penetrate the thick cell wall of mycobacteria. Bacteria were then washed under a gentle flowing water to remove excess carbol fuchsin, decolourized with 95% ethanol containing 5% HCl for 5 minutes and washed again under tap water to

remove excess decolorizing solution. Finally, bacteria were counter stained with methylene blue for 1 minute and washed with gentle flowing tap water. The procedure for the ZN stain is depicted in Fig 2.1 below. The slide was then dried under room temperature and observed with light microscope under oil immersion using X100 objective lens.

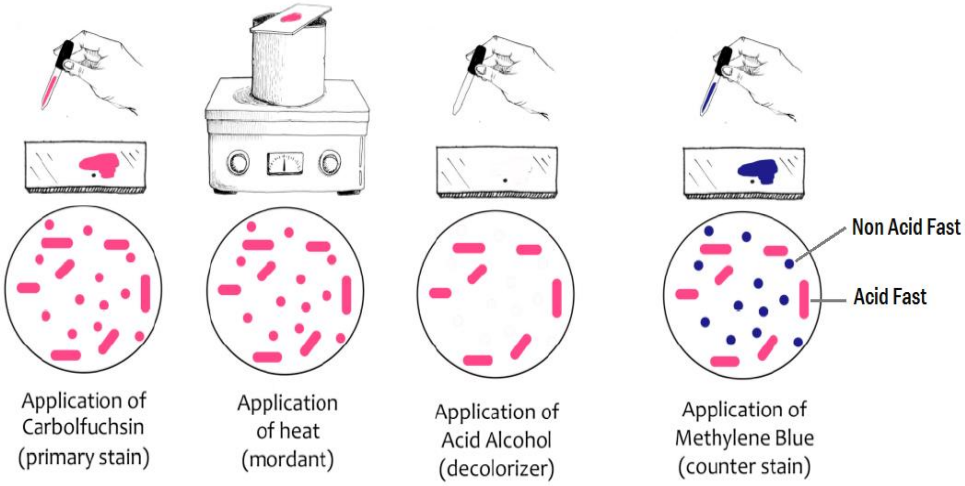

Fig 2.1. Ziehl-Neelsen Stain (ZN-Stain): principle, procedure, reporting and modifications (Laboratory Info 2018). Adapted from https://laboratoryinfo.com/zn-stain/. Date accessed 02.10.2018

2.3.2.2 Gram staining

This method was developed by Hans Christian Gram for the differentiation of bacteria based on their cell wall composition. This method can distinguish bacteria with (Gram-positive) or without (Gram-negative) peptidoglycan in their cell wall. Prior to staining, 10 µL of diluted bacteria (section 2.3.3.2.1) was spotted on microscope slides and heat fixed. Heat fixed slides were flooded with 2% crystal violet solution for 1 minute and washed using gentle flowing tap water. Slides were flooded with iodine solution for 1 minute and

rinsed with water to remove excess iodine. Slide was decolorized by dropwise addition of 95% HCl for 5 seconds while washing gently with tap water. Finally, bacteria were stained with safranin for 1 minute and the excess safranin washed with water, dried under room temperature and observed with light microscope under oil immersion using X100 objective lens.

2.3.4 Standardization of cells concentration

Suspension of *M. avium* at optical density of 1.0 corresponds to approximately 2 x 10^8 CFU/mL (Radomski *et al.* 2013). Cell density indirectly measures the turbidity of the cells solution. This parameter is largely dependent on the cells number, size and the nutritional requirement (Stevenson *et al.* 2016). Since all cells differ in relation to these parameters, the cells used in this study were standardised to determine their concentration to be used in subsequent assays. A calibration curve was generated to determine cells concentration at varying optical density (OD). Prior to standardisation, cells were cultured as described above (section 2.3.2), pelleted (centrifugation at 4,000 g for 10 min) and washed twice with sterile 1X PBS solution. This referred to as the stock bacterial concentration). Stock concentration of cells (*M. abscessus*, *E. coli*, *S. aureus* and *C. albicans*) were serially diluted ((1/10) in PBS solution to bacterial suspensions at varying OD (measured at 600 nm) ranging from 1.3 to 0.05.

The concentration of cells in CFU/mL were determined in each dilution using the method described by Miles and Misra (Miles and Misra, 1938) and is described below. Cell suspensions at their respective optical densities were further diluted (1/10), 8 times. Twenty microliters of each dilution was plated on either LB agar (*M. abscessus*, *E. coli*,

S. aureus) or Yeast extract agar (*C. albicans*) in triplicate and incubated at 37°C overnight, except for *M. abscessus* which was incubated for 72 hours. The dilution resulting in countable cell colonies between 30-100 was used to determine cell concentration and expressed as CFU/mL. The experiment was repeated twice and the mean colony forming unit was determined using the formula below.

$$\text{Colony forming unit per millilitre (CFU/mL)} = \frac{\text{Mean colony count x dilution factor}}{\text{Volume inoculated (mL)}}$$

The mean number of colonies forming unit per millilitre (y-axis) was plotted against the optical densities on the x-axis. The line of best fit and the equation of the line was generated. The estimated concentration of cells was calculated from the equation of the graph with known optical density values (Appendix 1).

2.4 Statistical Analysis

All experiments were performed at least two times under independent conditions. Statistical analysis of data was performed using the Statistical Package for the Social Sciences (SPSS) version 25 or Microsoft excel 2013 analysis tool pack. Independent sample t-Test was performed to determine statistical significance between two groups. Data was considered significant when the p-value < 0.05. Analysis of Variance (ANOVA) was performed to determine the difference among group means. To determine the difference within groups, post-hoc analysis was performed using Bonferroni and Tukey tests. p-values less than 0.05 were considered as significant.

Chapter 3

Molecular and antibiotic based characterization of *Mycobacterium abscessus* isolates

3.0 Introduction

3.1 Identification and typing methods for bacteria

Bacterial typing/characterisation systems are important scientific tools frequently used to study and understand disease epidemiology, clinical outbreaks and disease relapse (Iakhiaeva *et al.* 2012; Wong *et al.* 2012). Non-tuberculous mycobacteria (NTM) are oligotrophs, commonly inhabits the environments e.g. soil and water distribution systems and are likely to be frequently associated with humans through inhalation and soil bioaerosols (Honda *et al*. 2016). The transmission of *M. abscessus* has been hypothesised to occur via aerosol generation (Bryant *et al*. 2013; Trovato *et al.* 2017). For this reason, it is possible for frequent outbreaks of and this would require bacterial typing tools to identify and characterise them. Various techniques for typing micro-organisms have been developed and these vary widely with respect to cost, specificity, sensitivity, simplicity and the time required to perform the assay. Commonly used typing methods can be broadly divided into phenotypic and molecular approaches and are discussed in more detail below.

3.2 Phenotypic typing of *M. abscessus*

Phenotypic methods represent the traditional approach for the identification of bacteria for which other identification strategies are based on. The approach generally consists of (1) collection of a sample which is representative of the site of bacterial infection, (2) the application of various staining methods and an examination of colonial morphology and (3) response to biochemical and serological tests, susceptibility to phages and antimicrobial agents such as bacteriocins (Castro-Escarpulli *et al.* 2015). Examples of

clinical samples which are routinely screened for the presence of the pathogen include urine, semen, blood, faeces, vaginal fluid and cerebrospinal fluid. These methods albeit being cheap and simple to perform have several limitations. For instance, the presence of bacteria which are not the target organism can result in misinterpretation of clinical results. They also suffer from a lack of specificity in that they are unable to discriminate between closely related species (Suffys *et al.* 2001). To improve on specificity, it is recommended that the sample is obtained directly from the site of bacterial infection and kept under proper storage conditions (Suffys *et al*. 2001).

Clarithromycin is the drug of choice for treatment of *M. abscessus*, but treatment success is severely hampered due to inducible resistance. This mode of resistance is expressed in *M. abscessus* when full length of *erm*-41 gene is present (Ruger *et al*. 2014). While the *erm*-41 gene has phenotypic consequence, it is not definitive in *M. abscessus* characterisation. Its polymorphic nature was genotypically explored for precise detection of *M. abscessus* (discussed in chapter 4).

The full length of this gene is present in *M. abscessus* subsp *abscessus* and *M. bolletii* but truncated in *M. massiliense*. Variants of this gene are present in M. tb (*erm*-37), *M. fortuitum* (*erm-39*) and *M. smegmatis* (*erm-38*). The *erm* gene is believed to have originated from Streptomyces, a specie which synthesises macrolides (Nash *et al.* 2005) and also demonstrate inducible resistant to macrolides but they carry subtle differences in their individual nucleotide sequences which can serve as a basis for genotypic characterisation.

3.3 Molecular typing techniques

Molecular typing offers a number of advantages over phenotypic methods with regards to precision and accuracy as well as the ability to distinguish between closely related species and to detect antibiotic susceptible strains (Harris and Kenna 2014). Some of the methods currently used include DNA hybridisation, plasmid profiling, PCR, ribotyping, spoligotyping and mycobacterial interspersed repetitive unit variable number tandem repeat (MIRUS-VNTR) (Castro-Escarpulli *et al*. 2015). The massive expansion in the use of these techniques has been made possible by the proliferation of low-cost whole genome sequencing systems and the availability of open source bioinformatic tools.

3.4 Techniques for the isolation of DNA from *M. abscessus*

DNA based molecular typing methods are dependent on the ability to access high quality DNA locked inside the cell. Mycobacteria species possess a thick, waxy cell wall, which makes them difficult to lyse compared to Gram-negative and Gram-positive bacteria. Commercial DNA extraction kits are designed to lyse Gram-positive and negative bacteria and thus are relatively inefficient when applied to a mycobacteria (Kaser *et al.* 2009). In addition to affecting the overall DNA yield, the purity can also be compromised by the presence of bacterial contaminants such as carbohydrates, lipids and proteins (Timms *et al.* 2015). To increase DNA yields additional approaches such as mechanical disruption (the use of glass beads), sonication (subjecting cells to high frequency vibration) and enzymatic cell disruption have been employed (Granger *et al.* 2004; Radomski *et al*. 2013; Park *et al.* 2014). Mechanical cell disruption of mycobacteria cells has been reported to cause a 10-fold increase in DNA concentration (Granger *et al*. 2004; Radomski *et al*. 2013; Park *et al*. 2014). In-house DNA extraction methods developed by

Timms and colleagues improves yield but do not produce better DNA purity than commercial kits (Timms *et al*. 2015). This challenge needs to be addressed as any molecular based detection assay (e.g. VNTR), which would be used in this study would require purified and high yield DNA.

3.5 Molecular typing of *M. abscessus*

In the context of the molecular typing of *M. abscessus* isolates, the following methods have been employed; pulsed field gel electrophoresis (PFGE), repetitive sequence-based (Rep)-PCR, multilocus sequence typing (MLST), multispacer sequence typing (MST), variable number of tandem repeat (VNTR) and whole-genome sequencing (Harris and Kenna 2014). The usefulness and advantages of these methods over other methods are described below.

3.5.1 Pulsed field gel electrophoresis (PFGE)

PFGE is considered the gold standard for bacterial typing and is performed when a bacteria-specific typing method is not available (Machado *et al.* 2014). This technique requires careful isolation of genomic DNA, followed by restriction enzyme digest before pulsed electrophoresis. PFGE can be used to separate large size DNA (10 Mb) on an agarose gel using pulsed or alternating voltage gradients to produce high resolution DNA patterns (Jagielski *et al.* 2014). PFGE has been developed for the differentiation of the *M. abscessus* complex (Wallace *et al.* 1993; Matsumoto *et al*. 2011). Although it is considered reproducible, it requires careful isolation of DNA to avoid shearing and damage due to the rigidity of the mycobacteria cell wall as this has been observed in *M. abscessus* isolates (Machado *et al*. 2014). The procedure is also expensive to perform,

requiring high level expertise and thus is confined to highly resourced laboratories. While no standard protocol for PFGE has been approved, the existing protocols require about one week to complete (Jagielski *et al.* 2014). PFGE can only discriminate bacteria to the strain level (Quainoo *et al.* 2017).

3.5.2 Repetitive sequence-based PCR

Rep-PCR amplifies repetitive elements within the bacterial genome. The amplified fragments once separated on a gel produce a band pattern corresponding to the length and the size of the amplified region. While commercial Rep-PCR systems (e.g. DiversiLab System, bioMerieux, France) has been develop for the identification of *M. abscessus*, concerns have been expressed as to the specificity of this approach (Zelazny *et al.* 2009; Harris *et al.* 2012). It remains unclear whether the DNA profile generated represent same strain or related strains of a genotype (Harris and Kenna 2014).

3.5.3 Multilocus sequence typing (MLST) and multispacer sequence typing (MST)

MLST amplifies nucleotide sequences that are conserved in housekeeping genes (Eisenberg and Levanon 2013). Usually, about 8 housekeeping genes are targeted (Macheras *et al.* 2011). In other instances, MLST can be performed by sequencing a single copy of a gene in combination with different gene alleles to generate an allelic profile. This allele profile serves as a fingerprint to differentiate other isolate and develop an evolutionary relationship (Macheras *et al*. 2011). MLST compared to PFGE is less discriminative in identifying *M. abscessus* (Machado *et al*. 2014). It does not provide

discrimination between variants of a single clone (Machado *et al*., 2014). In organisms that have undergone high levels of recombination, MLST may not provide detail biological diversity, hence results may be misleading (Quainoo *et al*. 2017). While MLST targets housekeeping genes, MST amplifies sequences in the spacer region located between the 16S rRNA and 23S rRNA genes. These regions are less exposed to evolutionary pressures and are well conserved, hence can be informative of *M. abscessus* identity (Sassi *et al.* 2013).

3.5.4 Variable number of tandem Repeats (VNTR)

Short repeated DNA sequences adjacent to each other (tandem repeat) are useful bacterial fingerprints. The frequency with which these DNA repeats occur within the genome can vary between isolates of the same species and is referred to as VNTR. Using bioinformatic tools, VNTRs can be identified and amplified by PCR using specific DNA primers. The approach is relatively simple, rapid to perform and comparable in sensitivity to PFGE (Harris and Kenna 2014; Chen *et al.* 2017a). Several studies have reported the usefulness, efficiency and reliability of VNTR in typing *M. abscessus* isolates (Choi *et al.* 2011; Harris *et al*. 2012; Wong *et al*. 2012; Davidson *et al.* 2013; Trovato *et al*. 2017). A duplex, low cost PCR assay based on targeting a VNTR region of *M. abscessus* has been developed and proves to be efficient in differentiating *M. abscessus* group *(Choi et al*. 2011). This method is also simple, reliable and accurate. The accuracy of this method was confirmed by subjecting same bacterial isolates to multiple sequence analysis (Choi *et al*. 2011).

3.5.5 Whole Genome Sequencing (WGS)

Whole-genome sequencing is a popular and easy tool for genotyping. With the use of the tool the entire genome of a bacterial pathogen can be determined at high resolution and distinguish highly related lineages. The genomic data obtained can also detect antimicrobial resistant genes which can improve treatment outcome. Additionally, WGS can identify single nucleotide polymorphisms (SNPs), which are impossible to detect with PFGE. SNPs refer to nucleotide differences that occur at a specific location within the genome. Usually, such nucleotide differences have phenotypic outcomes and are additional source of information for differentiating closely related bacterial species. Recently, WGS has been used to predict possible person-to-person transmission of *M. abscessus* among CF patients confined in a particular hospital (Bryant *et al*. 2013). The ability of this tool to identify individual nucleotide base differences makes it valuable to support transmission dynamics and epidemiological studies. Despite carrying lots of advantages, it presents with high costs. The interpretation of genomic data also requires specific algorithms which will demand expertise.

Based on the advantages of VNTR typing (as discussed above), this tool was used for the characterisation of suspected clinical isolates of *M. abscessus* that were received from the University Hospital of Wales (UHW). VNTR typing was further supported with phenotypic testing (antibiotic susceptibility to clarithromycin).

3.6 Aims and objectives

The **aim** of this chapter is to characterise and confirm the identity of a collection of clinical isolates of *M. abscessus* provided by Public Health Wales

The **objectives** are to;

1. determine their antibiotic susceptibility to clarithromycin.
2. develop an efficient cell lysis method which maximise the release of DNA from *M. abscessus* to support VNTR based characterisation.
3. employ a VNTR assay to determine the genetic identify of each clinical isolate

3.7 Materials

3.7.1 Chemicals

Clarithromycin (Cat. No.: C9742), Tween 20, Triton X-100, acid washed diatomaceous earth, ethylenediaminetetraacetic acid (EDTA) and GenElute bacterial genomic DNA isolation kit were all purchased from Sigma Aldrich, UK. Sodium dodecyl sulphate (SDS), urea, lysozyme and Tris base were purchased from Fisher Scientific, UK. Taq PCR core kit (250U) and DNeasy blood & tissue kit were purchased from Qiagen, UK. Zirconia beads (0.1 mm) was also purchased from (BioSpec, USA). 96-well microtiter plate (Life Science, USA). All reagents were purchased as molecular grade.

3.7.2 Preparation of diatomaceous earth solution

Diatomaceous earth powder (10 g) was mixed with 50 ml of sterile milli-Q water and 500 uL of 37% HCl. The mixture was mixed and stored at 4 °C for further use.

3.7.3 Instruments

Nanodrop (ND 1000 spectrophotometer, LabTech), spectrophotometer (Ultrospec 2100 pro, USA), UV transilluminator (ChemiDoc, Bio-Rad laboratories, UK), Thermal cycler (T100, Bio-Rad).

3.7.4 Bacterial isolates

3.7.4.1 *M. abscessus* (ATCC 19977^{T})

The type strain of *M. abscessus* (ATCC 19977^{T}) is a biosafety level 2 pathogen and was purchased from the American type culture collections (ATCC), UK. This isolate demonstrates intrinsic resistance to clarithromycin due to the presence of a complete and functional *erm*-41 gene (Bryant *et al*. 2013).

3.7.4.2 *M. kansasii* (ATCC 12478)

The type strain of *M. kansasii* (ATCC 12478^{T}) is a biosafety level 2 pathogen which was first isolated from human pulmonary secretions and lesions. This bacterium was included as a negative control in the MIC assay as it lacks the *erm*-41 gene making it susceptible to clarithromycin (Biehle and Cavalieri 1992).

3.7.4.3 *E. coli* (NCTC 1093)

E. coli (NCTC 1093) is a biosafety level 2 pathogen was originally isolated from human faeces. This bacterium being Gram-negative and having a less rigid cell wall as compared to mycobacteria was used as a negative control in the DNA extraction.

3.7.4.4 *M. abscessus* clinical isolates

Eight suspected clinical isolates of *M. abscessus* were obtained from the UHW with unique identity numbers (9723, 11490, 10006, 10332, 11365, 8899, 9568, 9495) assigned by the hospital. The isolates were collected from patients in July 2012 and their corresponding antibiotic resistance profiles shown in Table 3.1

Table 3.1 The clinical isolates of suspected *M. abscessus* used in this study

Unique strain Number	Antibiotic resistance (MIC > 128 µg/mL) determined by UHW	Collection date
8899	Imipenem, Rifampicin	11/07/2012
10006	Rifampicin, ciprofloxacin, Imipenem	12/07/2012
10332	Rifampicin	22/07/2012
11365	Rifampicin, ciprofloxacin, Imipenem	23/07/2012
9495	Rifampicin, Imipenem	11/07/2012
9723	Rifampicin, ciprofloxacin	12/07/2012
11490	Rifampicin	24/07/2012
9568	Rifampicin	12/07/2012

3.8.1 Lysis buffers for DNA extraction

Genomic DNA from *M. abscessus* (ATCC 19977^{T}) was performed using three different lysis buffers (A, B and C) (Boom *et al.* 1990; Kotlowski *et al.* 2004; Kaser *et al*. 2009; Omar *et al.* 2014). The composition of the lysis buffers is shown in Table 3.2 below. *E. coli* (NCTC 1093) a common Gram-negative bacterium having a less rigid cell wall was included as a control.

Table 3.2 Lysis buffers developed to enhance mycobacteria cell wall lysis and the subsequent recovery of DNA

Lysis Buffer	Buffer Composition
Buffer A	8M urea, 60 mM Tris-HCl, 1% Triton X-100, 10% Tween-20, 3mg/mL proteinase K
Buffer B	2 mM EDTA, 10 mM Tris-HCl, 0.6% SDS, 400 mM NaCl, 3mg/mL proteinase K
Buffer C	60 mM Tris-HCl, lysozyme (50 mg/mL), 3% SDS

3.8.2 Sample processing

Stationary phase cultures of *M. abscessus* and *E. coli* grown in their respective media (described in section 2.3.2) were pelleted (centrifugation at 4, 000g for 10 min at 4 °C). Bacterial pellets were resuspended in 500 µL of PBS to a final concentration of 1 x 10^{8}

CFU/mL. Bacterial concentration was determined by comparing the optical density against that of a previously constructed calibration curve (Appendix 1). One hundred microliter of this bacterial suspension was used for DNA extraction using either a commercial kit or an in-house method as described below.

3.8.3 In-house method

To isolate DNA from highly rigid mycobacterial cell walls and support molecular characterisation of isolates by VNTR, an in-house DNA extraction protocol was developed. The in-house method was evaluated alongside commercial DNA extraction methods (section 3.8.4) with cells of *E. coli* and *M. abscessus*. One hundred microliters of bacterial suspension (*E. coli* or *M. abscessus*) were lysed with 250 µL of one of the following lysis buffers (A, B or C) (Table 3.2) and 500 µL zirconia beads. Cells were lysed overnight at 60^0C with constant shaking at 200 rpm. To capture the released DNA, 40 µL of diatomaceous earth solution was added to the lysed sample and incubated at 37^0C for 60 mins. DNA bound to diatomaceous earth was pelleted by centrifugation at 10,000 rpm for 60 seconds and the supernatant discarded. Bound DNA was washed twice with 900 µL of ice cold 70% alcohol and 900 µL of absolute acetone. After the wash step, DNA bound to diatomaceous earth was dried at 50^0C for 20 min using a heat block to evaporate any excess acetone that might be present. To elute DNA from the diatomaceous earth, 100 µL of 1x TE buffer was added and incubated at 55^0C for 20 min with intermittent vortexing. The mixture was then centrifuged (10, 000 rpm for 2 min) and the supernatant containing DNA extract was aliquoted into a new microcentrifuge tube and quantified using a Nanodrop. DNA purity was determined by measuring the 260/280 nm

absorbance ratio. The lysis buffer which resulted in the highest DNA yield was used to extract DNA from the remaining *M. abscessus* isolates (Table 3.1).

3.8.4 DNA extraction using commercial DNA extraction kits

Using the same bacterial suspension as stated in section 3.6.3, DNA was extracted using two commercial DNA kits namely (1) GenElute bacterial genomic DNA kit (Sigma Aldrich) and (2) DNeasy Blood & Tissue Kit (Qiagen) following the respective manufacture's protocol. The purity and yield of the extracted DNA obtained from both methods were quantified using a Nanodrop.

3.8.5 Characterization of *M. abscessus* isolates

The identity of the 8 clinical isolates (Table 3.1) were determined using a VNTR assay and by determining their susceptibility to clarithromycin.

3.8.5.1 VNTR assay

All *M. abscessus* DNA extracts obtained were subject to VNTR analysis. The VNTR assay is a duplex PCR based on the amplification of two VNTR targets (11 and 23). PCR was performed in 20 µL reaction containing 1 µL each of 20 nmoL of VNTR primers (Appendix 2.1), 4 µL of 5X Q-solution, 2 µL of 10X PCR buffer, 0.4 µL of 25mM $MgCl_2$, 0.4 µL of 10mM dNTP mix, 1µM each of primer, 0.2 µL of Taq DNA polymerase and 1 µL of extracted DNA. PCR was performed in a 200 µL PCR tube in a thermal cycler with the following thermocycling profile; denaturation at 95^0C for 10 min, followed by 35

cycles of 95^{0}C for 30s, 63^{0}C for 30s, 72^{0}C for 45s and a final extension at 72^{0}C for 10 min. PCR products were electrophoresed on a 2% agarose gel stained with 4 µL of Safeview^{TM}. Electrophoresis was performed in 1X TAE buffer at 100V for 30 min and visualised in UV transilluminator.

3.8.5.2 Detection of non-*M. abscessus* isolates by PCR

A conventional PCR using specific probes was performed to determine the identity of isolates which were not *M. abscessus* using primers targeting the 50 bp region of the *erm*-38 gene of *M. smegmatis*. Extracted DNA (5 µL) from isolates were amplified in a total reaction volume of 20 µL containing 0.2 µM of forward, 0.2 µM of reverse primers (Appendix 2.2), 4 µL of 5X Q-solution, 2 µL of 10X PCR buffer, 0.4 µL of 25mM $MgCl_2$, 0.4 µL of 10mM dNTP mix, 0.2 µL of Taq DNA polymerase and 1 µL of extracted DNA. DNA was first denatured at 95^{0}C for 10 min, followed by 35 cycles of 95^{0}C for 30s, 56^{0}C for 30s, 72^{0}C for 30s and a final extension at 72^{0}C for 10 min. PCR products were viewed as described above (Section 3.6.5.1).

3.8.6 Preparation of clarithromycin stock

Clarithromycin (30,000 ug/mL) was prepared in acetone and then diluted in LB broth to a stock concentration of 1000 µg/mL. The antibiotic solution was sterilised using a 0.2 µm millipore filter (Minisart syringe filter, Germany). Two-fold serial dilution of the working concentrations of the antibiotic (10, 20, 40, 80, 160, 320 and 640) µg/mL was prepared in fresh LB broth. The final antibiotic concentrations tested in each assay was reduced by 10-fold to give a final concentration range of 0, 1, 2, 4, 8, 16, 32 and 64 µg/mL.

3.8.7 Determining MIC using broth microdilution method

Bacterial suspensions to be tested (1 x 10^6 CFU/mL) as determined in section 2.2.4 were tested in the MIC assay. MIC of the bacterial isolates (Table 3.1) were determined using the broth microdilution method in a 96-well plate (CLSI 2012). In a typical experiment, the MIC assay consisted of the following; bacterial suspension (25 µL), LB broth (200 µL) and varying concentrations of clarithromycin solution (25 µL) incubated in a 96-well plate. Two standard mycobacteria strains; *M. kansasii* ATCC 12478 (clarithromycin sensitive < 1 ug/ml) and *M. abscessus* ATCC 19977^T (clarithromycin resistant > 64 ug/ml) were included in the assay. Broth solutions without clarithromycin were included to determine whether acetone had an inhibitory effect on the growth of bacterial cultures. In addition, broth alone was also included as a control to ensure that there was no bacterial contamination. The plates were incubated at 37°C and observed visually for growth on days 3, 5, 7, 9, 11, 13 and 14. Each assay was performed in triplicates and repeated twice.

3.9 Statistics

Statistical analysis of data was performed using Microsoft excel 2013 analysis tool pack. A two-tailed independent sample t-test was performed to determine statistical significance between the extraction methods.

3.10 Results

3.10.1 Determination of the clarithromycin sensitivity of *M. abscessus* isolates

The MIC of *M. abscessus* isolates was determined against clarithromycin at varying concentrations of 1, 2, 4, 8, 16, 32 and 64 µg/mL. *M. abscessus* demonstrates inducible resistance after 3 days when cultured with clarithromycin. To determine this, the MIC of each isolate was monitored on days 3, 5, 7, 9, 11, 13 and 14. The following antibiotic susceptibility breakpoints were applied based on CLSI guidelines (CLSI 2012). Isolates were determined to be susceptible, intermediate and resistant if the MIC < 2 µg/mL, MIC = 4 µg/mL and MIC ≥ 8 µg/mL respectively (Brown-Elliott *et al.* 2012). Following 14 days of incubation, isolates 10332 and 11365 were found to be sensitive and intermediate sensitive respectively. The remaining 6 isolates (9495, 8899, 10006, 9723, 11490 and 9568) were sensitive on day 3 (MIC <2 µg/mL) but had MIC values ≥ 8 µg/mL on day 14 indicating inducible resistance (fig 3.1A, B). As expected, the control isolates ATCC 19977^{T} and ATCC 12478 remained resistant and sensitive respectively 14 days post culture. There was no growth in the broth only samples or in the broth with antibiotic controls after 14 days of incubation (fig 3.1A, B).

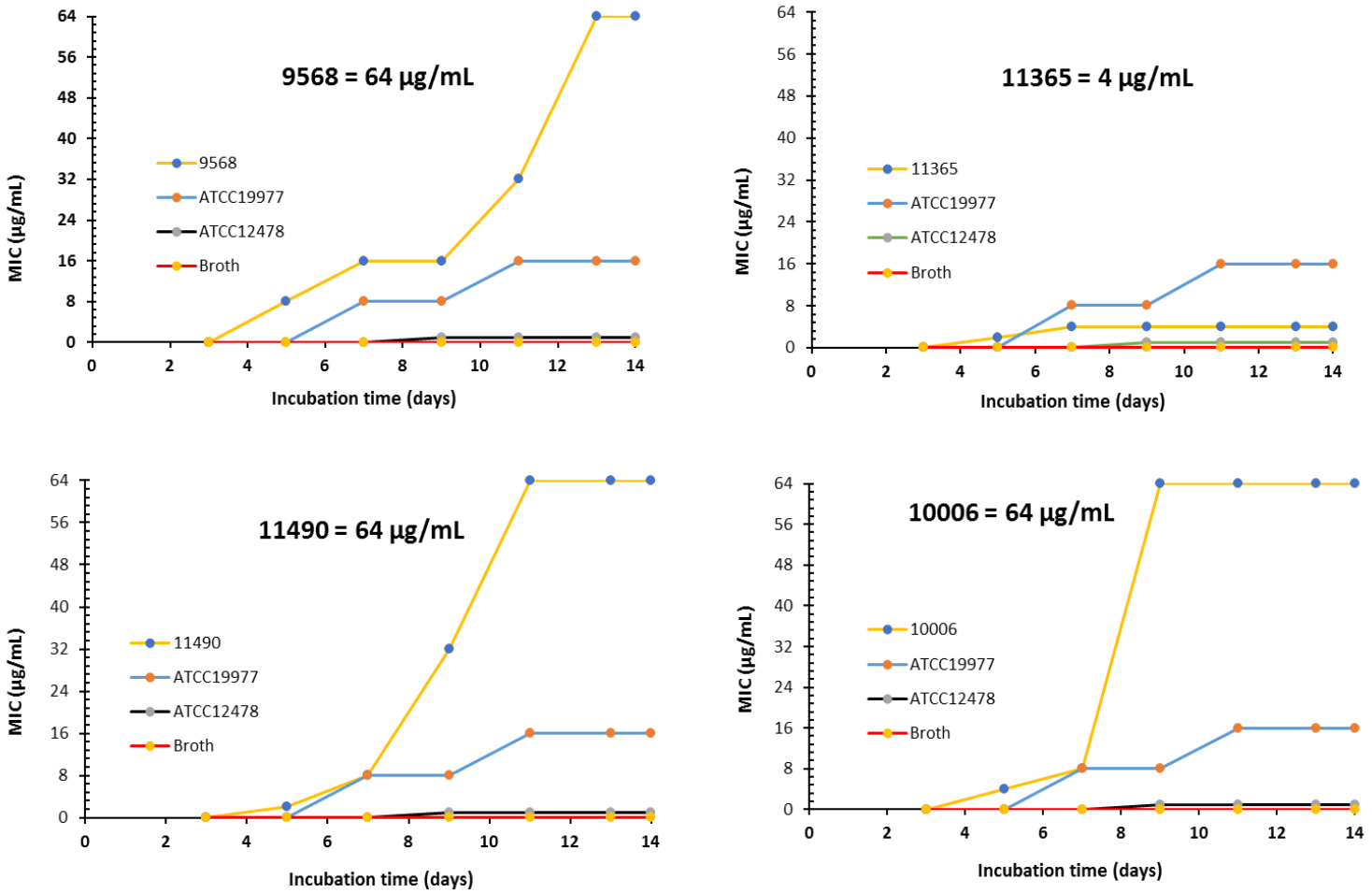

Figure 3.1A MIC of bacterial isolates against clarithromycin. *M. abscessus* isolates (9568, 11365, 11490, and 10006) at 1 x 10^6 CFU/mL were tested against varying concentrations of clarithromycin (1, 2, 4, 8, 16, 32 and 64 µg/mL) and incubated for 14 days. The MIC of each isolate was determined on days 3, 5, 7, 9, 11 and 14. Each experiment included a positive (*M. abscessus* ATCC 19977; blue line) and a negative control (*M. Kansasii* ATCC 12478; black line) isolate. Data represents MIC of triplicate experiments.

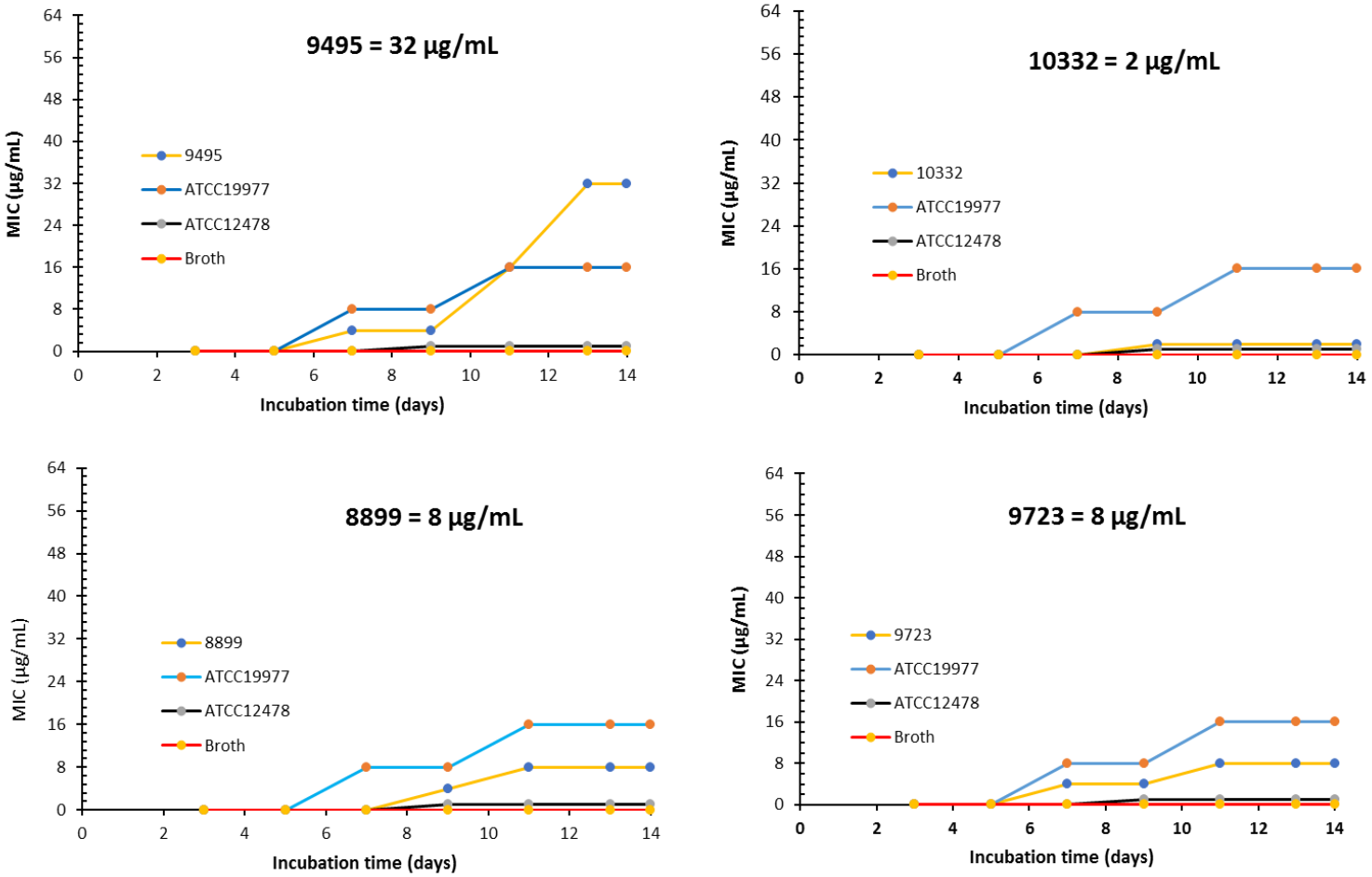

Figure 3.1B MIC of bacterial isolates against clarithromycin. *M. abscessus* isolates (9495, 10332, 8899 and 9723) at 1 x 10^6 CFU/mL were tested against varying concentrations of clarithromycin (1, 2, 4, 8, 16, 32 and 64 µg/mL) and incubated for 14 days. The MIC of each isolate was determined on days 3, 5, 7, 9, 11 and 14. Each experiment included a positive (*M. abscessus* ATCC 19977; blue line) and a negative control (*M. Kansasii* ATCC; black line) isolate. Data represents MIC of triplicate experiments.

3.10.2 Developing DNA extraction for mycobacterial cells

Three different buffer formulations (buffer A, B and C) (Table 3.1) were investigated for their ability to efficiently lyse mycobacterial cells to release DNA. Two commercial DNA extraction kits [GenElute bacterial genomic DNA kit (Sigma Aldrich) and DNeasy Blood & Tissue Kit (Qiagen)] were also included for comparison. Also, *E. coli* was included in the extraction protocol to investigate the effect of the different cell lysis compositions on different cell wall structures. The concentrations of the DNA extracts and purity obtained by the commercial kits and in-house methods were compared (fig. 3.2). The two commercial kits were effective in recovering DNA from *E. coli* but not from *M. abscessus* as the DNA yields were significantly lower than that obtained for *E. coli* ($p<0.05$). All buffer formulations investigated resulted in a significant recovery of DNA from *M. abscessus* and *E. coli* as compared to the commercial kits ($p <0.05$). Comparing the three lysis buffer formulations, buffer A was the most efficient as it resulted in a significant release of DNA ($p<0.05$) from *M. abscessus* and *E. coli* (fig. 3.2). There was no significant difference in DNA purity as determined by the 260/280 ratio when both methods i.e. commercial and in-house methods were compared ($p > 0.05$).

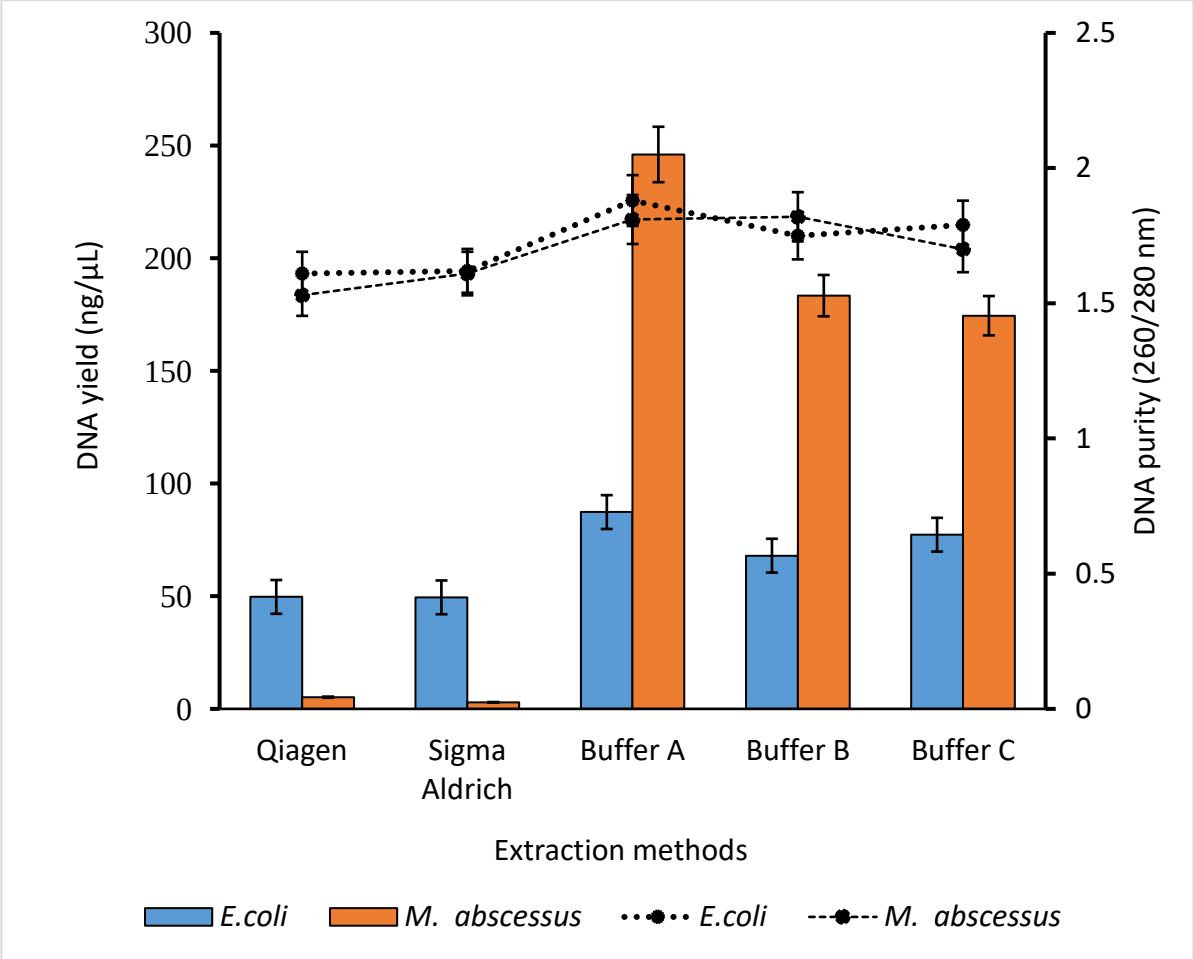

Figure 3.2 Comparison of DNA yield and purity using different extraction methods. Pairwise DNA extraction was performed on suspensions of *E. coli* and *M. abscessus* (1.0 x 10^8 CFU/mL) using two commercial kits (Qiagen and Sigma Aldrich) and an in-house method. DNA yield (bar) and purity (dotted lines) were compared from all methods. Data represents mean of 2 replicates ± standard error (SE).

Following the optimisation of the lysis buffer, DNA extraction was performed using buffer A on all of the bacterial isolates (Table 3.1). The DNA yield and purity were quantified, and the result displayed in fig 3.3. The concentration of DNA recovered varied markedly with the highest yield being obtained from isolate 8899 which was significantly higher than that obtained for isolate 11490 ($p < 0.05$).

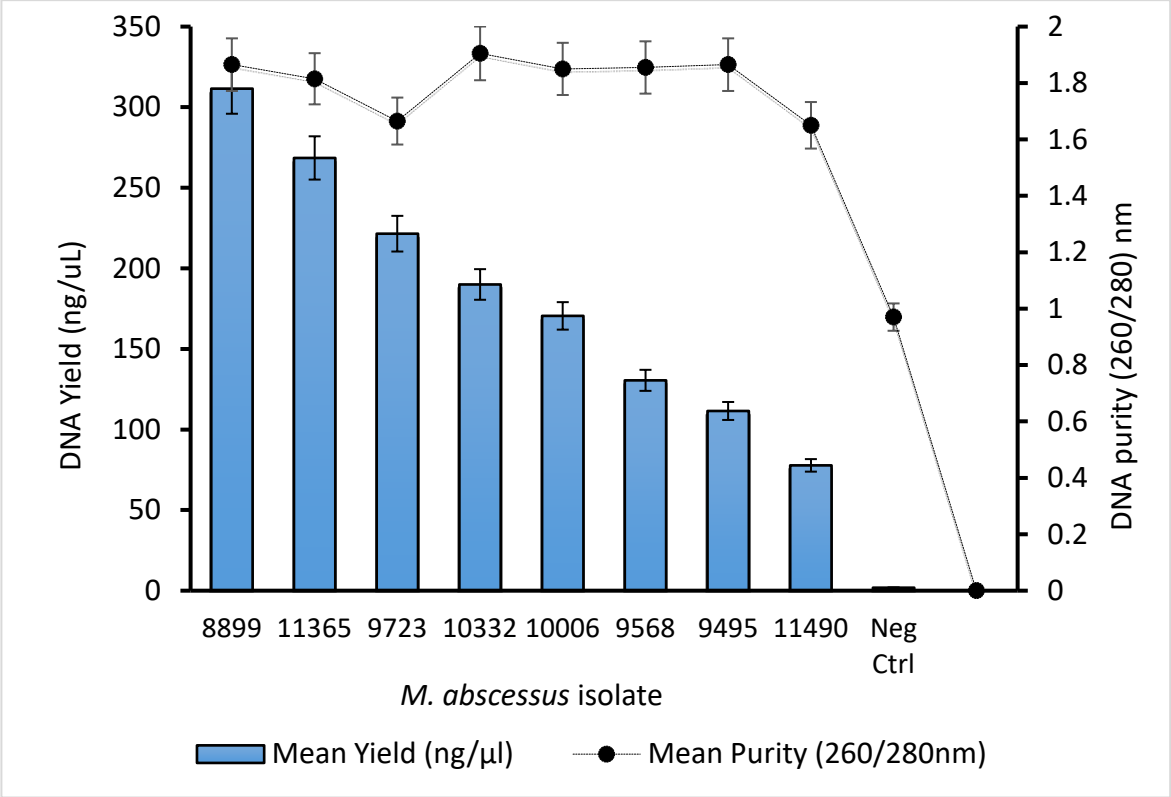

Figure 3.3. Mean concentration (bar) and purity (line) of *M. abscessus* DNA extracts. DNA was extracted from all clinical isolates using lysis buffer A. DNA concentration (bar) and purity (dotted lines) were measured using the Nanodrop. Neg ctrl represents a DNA extraction mixture where bacteria were not added. Data represents mean of 2 replicates ± standard Error (SE).

3.10.3 VNTR characterization of *M. abscessus* isolates

To confirm the identity of the clinical isolates provided by the UHW, a VNTR assay was performed targeting loci 11 and 23 of the *M. abscessus* genome. A typical *M. abscessus* with both loci present will generate two distinct bands with estimated band sizes of between 393-492 bp and 196-238 bp. Bands of the expected sizes were observed for isolates (11365, 10332, 9568, 10006, 11490, 8899 and 9495) and the positive control isolate ATCC 19977^{T}. No bands were seen for isolate 9723 (lane 8), suggesting the absence of the VNTR targets that characterise *M. abscessus* (fig 3.4). Subsequent PCR analysis using primers designed to identify the *rpo*B gene of *M. smegmatis* revealed the presence of a band of the expected size (200 bp) for the *M. smegmatis* control and sample 9723 but was absent from *M. abscessus* the ATCC 19977^{T} (fig. 3.5). These results suggest that 9723 is an isolate of *M. smegmatis*. The results for the VNTR and antibiotic susceptibility testing for each isolate are summarised in Table 3.3

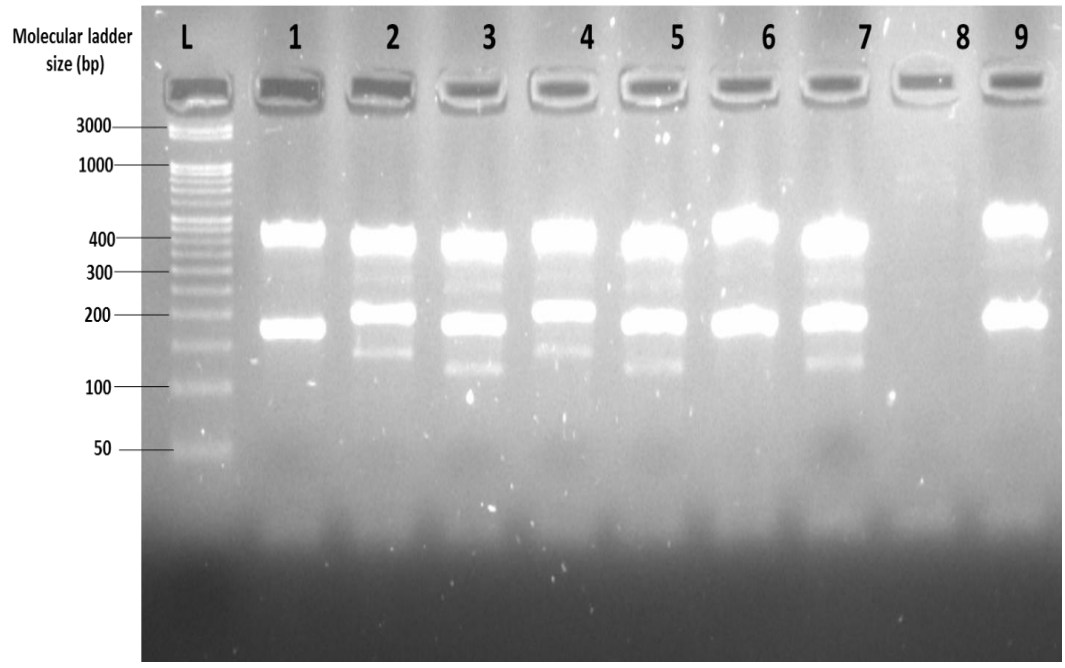

Figure 3.4. VNTR characterization of *M. abscessus* isolate. Two VNTR loci (11 and 23) were amplified in a duplex PCR. PCR amplicons (5 µL) were electrophoresed on 2% agarose gel stained with Safeview^{TM} in a 1X TAE buffer. Lane L= 50 bp molecular weight marker; lane 1= 11365, lane 2= 10332, lane 3= 9568, lane 4= 10006, lane 5= 11490, lane 6= 8899, lane 7= 9495, lane 8= 9723 (*M. smegmatis*) and lane 9= ATCC 19977^{T} (*M. abscessus*).

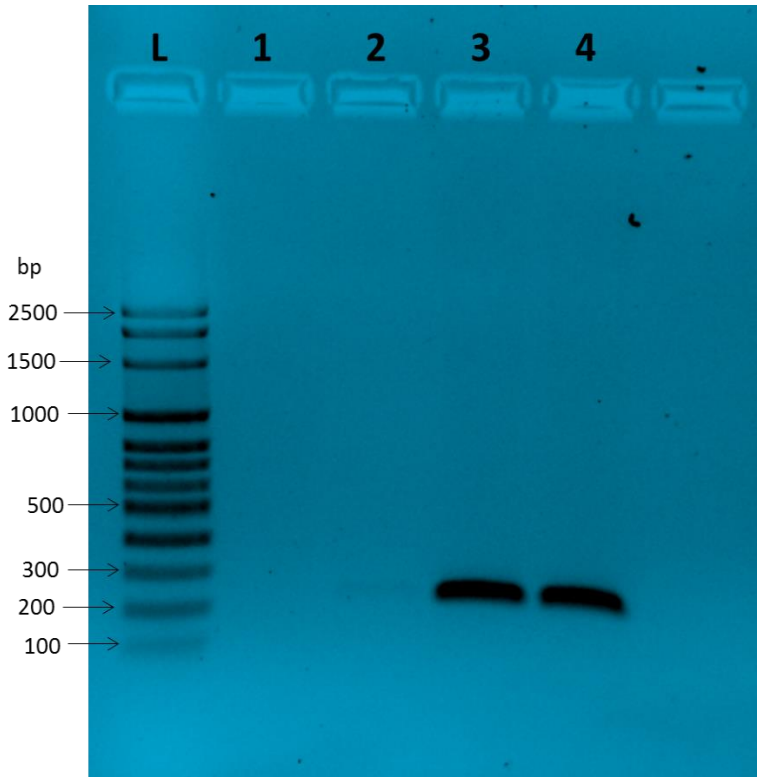

Figure 3.5 PCR identification of isolate 9723. *M. smegmatis* specific primer targeting *rpoB* gene was synthesised and the identity of isolate 9723 determined in a conventional PCR assay. PCR amplicons (5 µL) were electrophoresed on 1.5% agarose gel stained with Safeview™ in a 1X TBE electrophoresis buffer. Lane L= 100 bp molecular weight marker; lane 1= no template control, lane 2= ATCC 19977^{T} (*M. abscessus*), lane 3= 9723 (*M. smegmatis*), lane 4= *M. smegmatis* (NCTC 8159).

Table 3. 3 Summary of antibiotic and VNTR characterizations of UHW test isolates

Bacterial isolate	MIC	VNTR (loci 11 and 23)	Bacterial isolate
9568	Ind. Resistant	Present	*M. abscessus*
11365	Mod Resistant	Present	*M. abscessus*
11490	Ind. Resistant	Present	*M. abscessus*
10006	Ind. Resistant	Present	*M. abscessus*
9495	Ind. Resistant	Present	*M. abscessus*
10332	Sensitive	Present	*M. abscessus*
8899	Ind. Resistant	Present	*M. abscessus*
9723	Ind. Resistant	Absent	*M. smegmatis*
ATCC 19977	Resistant	Present	*M. abscessus*
ATCC 12478	Sensitive	ND	-

Key

Ind. Resistant = inducible resistant; Mod. Sensitivity = Moderate sensitivity; ND = Not detected.

3.11 Discussion

Identification of bacteria using phenotypic methods is not always accurate and reliable (Harris and Kenna 2014). For this reason, VNTR typing was performed in addition to clarithromycin susceptibility testing to comprehensively characterise the bacterial isolates used in this study. Based on the VNTR data, all the isolates with the exception of 9723 produced a VNTR profile indicative of *M. abscessus.* Further analysis of isolate 9723 using a PCR assay targeting the *erm*-38 gene confirmed and identified this isolate as *M. smegmatis.*

Subsequently, the susceptibility profile of the isolates to clarithromycin, which is the drug of choice for *M. abscessus* treatment was determined. Their susceptibility to clarithromycin is dependent on the presence and functionality of the *erm*-41 gene which is present in all isolates of *M. abscessus*. Of the eight isolates tested, 10332 and 11365 were susceptible and moderately susceptible respectively to clarithromycin after 14 days of incubation. Since this test is not decisive, it is not possible to assign these isolates as *M. abscessus* as these could be susceptible *M. abscessus* isolates, *M. massiliense* or any of the rapid growing NTM species harbouring the inducible *erm* gene.

While a strain may have an MIC value below 2 (susceptible) on day 3 of incubation, it could become resistant to clarithromycin with MIC greater than 8 on day 14 of incubation (Bastian et al. 2011). This mode of resistance which is described as inducible requires the presence of a complete and functional *erm*-41 gene. Full length *erm*-41 gene is present in *M. abscessus* and *M. bolletii* and confers resistance to clarithromycin but when truncated/incomplete it renders the isolate sensitive and this is usually seen in *M.*

massiliense (Sapriel *et al.* 2016). Inducible resistance was observed in 9495, 8899, 10006, 11490, 9568 and 9723 having MIC lower than 2 on day 3 but greater than 8 after 14 days post culture.

Although isolate 9723 was identified as *M. smegmatis* by PCR, it demonstrated inducible resistance to clarithromycin similar to the *M. abscessus* isolates. Inducible resistance to macrolides does not only occur in *M. abscessus* but in all mycobacteria species harbouring the *erm* gene (Nash 2003; El Helou *et al.* 2013). Variants of the *erm* gene have been identified in *M. smegmatis,* M. tb complex, *M. fortuitum* and *M. mageritense* and harbours the *erm*-38, *erm*-37, *erm*-39 and *erm*-40 genes respectively (Nash *et al.* 2009).

While the antibiotic testing of the isolates informs of inducible resistance instigated by the *erm* gene, the VNTR is more decisive in characterising *M. abscessus* isolates. This further highlight the advantage of using VNTR over clarithromycin susceptibility testing as without the former, isolate 9723 would have been characterised as *M. abscessus*. The uniqueness of the *erm*-41 gene as it is only present in *M. abscessus* serves as a useful molecular target to be used in molecular based detection assays, and this will be discussed in the next chapter.

Isolation of DNA from mycobacterium species is complicated by the presence of mycolic acids (MA) which contribute to the creation of thick and rigid cell walls which are difficult to lyse. MA is not a component of Gram-negative bacterial cell walls, and this partly explains why bacterial cells belonging to this group are easier to disrupt using

commercially available methods (Mitchell *et al.* 2012). DNA extraction from mycobacterial cells have been a major bottleneck to PCR and other DNA dependent typing and identification methods. It becomes a research priority to develop an effective cell lysis procedure to augment DNA yield and purity. To achieve this, we compared the efficiency of three different lysis buffers in combination with zirconia beads to that of two commercially available methods.

It was evident from the study that the in-house method was effective in releasing DNA from mycobacterial cells and *E. coli* compared to the two commercial DNA extraction methods. The latter was only effective against *E. coli*. DNA release from bacterial cells is enhanced in the presence of chaotropic agents, detergents, enzymes and mechanical disruption (Belisle and Sonnenberg 1998).

Urea is a chaotropic agent and detergents such as Triton X-100, SDS and Tween-20 are able to denature proteins and disrupt membrane integrity (Belisle and Sonnenberg 1998; Danilevich *et al.* 2008). These chemicals in combination with zirconia beads (mechanical lysis) maximised the recovery of DNA from the bacteria used in this study. The highest yield of DNA was achieved using buffer formulation A compared to the commercial kits. The significant release of DNA is an indicator of severe membrane damage (Zhen *et al.* 2013).

It was observed that, the three lysis buffer formulations resulted in varying DNA yield. As shown in Table 3.1, buffer A contained two main detergents (Tween 20 and Triton X-

100) and proteinase K while buffers B and C contained SDS and lysozyme. Lysozymes are known to have a disruptive and lytic activity against mycobacterial cell walls (Salton 1958) but appeared to have been inhibited in this study. Lysozyme degrades cell wall by disrupting N-acetyl-glucosamine and N-acetylmuramic acid bonds in murein. This enzyme is stabilized by four disulphide bonds which keeps it stable and active (Chamani *et al.* 2010). Lysozyme are inactivated in the presence of surfactants and detergents such as SDS (Chamani *et al*. 2010). It is likely that the lytic activity of lysozyme may have been inhibited in buffers B and C due to the presence of SDS, and resulting in the lesser DNA yield than that of buffer A (Koga and Kramer 1983). The optimal lysis buffer (A), was applied for DNA extraction from the remaining *M. abscessus* isolates. The lysis buffer components of the commercial kits were not disclosed for commercial reason and thus it was impossible to draw any conclusion as to the relative contribution of the any of the individual elements to the differences in DNA yield which was observed.

Differences in the incubation periods employed in the various lysis approaches may have also contributed to the observed differences in DNA yield (Lever *et al.* 2015). The in-house methods included an overnight (18 hours) lysis step compared to the commercial kits where the incubation period was 2 hours. Thus, the markedly longer incubation time for the in-house methods may have been a contributing factor for DNA release.

The yield of DNA recovered from the 7 *M. abscessus* isolates using lysis buffer A method differed significantly and this could be influenced by a number of factors. Mechanical and chemical cell lysis could interact with and cause degradation of nucleic acids (Islam *et al.*

2017). Another factor worthy of consideration is the technicalities of the DNA extraction procedure i.e. binding of the DNA and subsequent elution form the diatomaceous earth as this was key to maximise DNA recovery. Diatomaceous earth consists of positively charged silica matrix that attract and selectively binding to negatively charged DNA. The challenge with this technique is the inability to recover small fragments of DNA as these types of DNA bind tightly to the silica matrix (Koo *et al*., 1998) and could affect the overall DNA recovery.

On the basis of a comparison of the 260/280 ratio of the isolated DNA, the in-house method had the same level of DNA purity as that of the commercial DNA extracts, suggesting an efficient removal of DNA contaminants such as proteins and carbohydrates. The commercial kits required spin columns containing silica for DNA purification. The use of diatomaceous earth in this study proved to be efficient as that of spin columns, yielding comparable DNA purity.

Overall, the in-house method was time consuming, but economically more viable (£0.34 per sample) than the commercial kits (£3.32 per sample) and allows for the control of other parameters i.e. buffer concentrations to applied on other sample types. The method developed in this study demonstrates the ability to produce relatively high DNA yields without compromising on purity and can serve as an excellent alternative to the commercial kits. A major selling point of commercial kits is the fact that they are less time consuming. The reason we did this was to optimise DNA release from these bacteria

so that can support our subsequent probe detector work and to have a base line method against which we could compare our microwave-based lysis method.

In conclusion, the identity of the bacterial isolates obtained from the UHW have been confirmed using a combination of genetic and phenotypic methods. An efficient DNA extraction method has been developed for *M. abscessus* which would be employed in this study to isolate high quality DNA. The challenge in isolating purified DNA from mycobacterial cells that has been a frequent challenge and a bottleneck in major studies can be surmounted by employing the bacterial cell lysis procedure developed in this study.

Chapter 4

The design of DNA probes for the detection of *Mycobacterium abscessus* and *Mycobacterium smegmatis*

4.0 Introduction

The success of any molecular based identification method relies on the identification of specific nucleotide sequences which are only found in a bacterial genome. This is particularly important in the case of the non-tuberculous mycobacteria (NTM) as the taxonomy of *M. abscessus* group remains complex and debatable due to the lack of individual gene targets with sufficient specificity to support species level discrimination (Wertz *et al.* 2003; Zeigler 2003; Johnson and Odell 2014; Rubio *et al*. 2015). In chapter 3, VNTR typing was used as a tool to distinguish individual *M. abscessus* isolates. VNTR relies on the amplification of repeats of short nucleotide sequence at different loci across the genome. Thus, while an effective typing tool, it is not suitable for the development of a rapid detection system. Individual gene targets such as the *rpoB* gene have been proposed as a diagnostic marker for the identification of rapid growing mycobacteria (de Zwaan *et al.* 2014; Nasiri *et al.* 2017), but others have questioned its sensitivity reporting that it is unable to distinguish *M. abscessus* from *M. avium* (Adekambi and Drancourt 2004).

In some clinical laboratory, *M. abscessus* isolates are not routinely distinguished from *M. chelonae* and are report as *M. abscessus-M. chelonae* complex (Griffith *et al.* 2015). The distinction between these two isolates is relevant for their effective treatment. The absence of *erm*-41 gene in *M. chelonae* could be used as the basis for distinction between these two bacterial species. As discussed in section 3.2, the *erm* gene (*erm*-41) represents a potentially unique target for *M. abscessus* identification (Brown-Elliott *et al.* 2015) and the *rpoB* gene being polymorphic in nature could be exploited for specific bacterial identification (ref).

In this study we employed a bioinformatic based approach to identify unique target sequences within the *erm*-41 and *rpoB* gene sequences of *M. abscessus* and *M. smegmatis* (*rpo*B only). This approach is discussed below.

4.1 Bioinformatic probe design

When designing probes for bacterial identification, it is important to target conserved regions of the bacterial genome, as these regions are unlikely to be affected by evolution and/or environmental cues (Guerrero *et al.* 2010). An efficient method of achieving this is to employ a bioinformatic based approach (Luo *et al.* 2015). Bioinformatics refers to the application of computational algorithms to study biological information e.g. protein or DNA sequences for evidences relating to their function, identifying homologs, sequence patterns and evolutionary relatedness (Xiong 2006). The potential of this approach is based on the ability to access sequencing data from open source databases such as the National Centre for Bioinformatics Information (NCBI). In addition to providing access to genomic data, the NCBI database provides researchers with the ability to identify unknown nucleotide or protein sequences by comparing their homology to known sequences stored in its database. This homolog search is performed using a software tool called Basic Local Alignment Search Tool (BLAST) (Altschul *et al.* 1990; Pearson and Lipman 1998). BLAST can also be used to determine the specificity of short stretches of DNA probes.

4.2 Basic Local Alignment Search Tool (BLAST)

Various BLAST formats have been developed, and these include MegaBLAST, BLAST URL API, BLAST standalone applications, BLAST+ remote service, C++ Application programming interface (API) and NCBI BLAST. All except NCBI BLAST require much stricter settings (Madden 2013). The NCBI BLAST algorithm is the easiest to access and is much simpler, quick to use, requires only a web browser and set-up requires no registration (Madden 2013). In addition to its diverse formats, BLAST is designed to support more detailed data analysis. For instance, MegaBLAST performs nucleotide search by considering the first 28 nucleotides of the query sequence and then proceeds to align the remaining nucleotides. This approach is different to that of BLASTN which considers more than 28 nucleotides of the query sequence (Madden 2013).

BLASTP (searches for protein sequences and compares to other protein sequences), BLASTX (searches for nucleotide sequences and compares to protein database), TBLASTN (searches for protein sequences and compares to nucleotide database) (Morgulis *et al.* 2008; Pearson 2013). In this study, BLASTN was used to retrieve nucleotide sequences from the NCBI database.

4.3 Statistical analysis of BLAST output

To perform a similarity search, the query sequence (DNA or protein) is compared against the NCBI database of sequences (subject sequences), to generate a number of sequence output called 'matched sequence' (Pearson and Lipman 1998). While a database search will always turn out with a 'match sequence', this will require further analysis using specific statistical scoring matrices to ascertain the significance of the 'matched sequence' (Karlin *et al.* 1991). Scoring matrices such as the E- value, maximum score, total score, query coverage and maximum identity are mostly used. The E-value is the traditional statistic test used to score 'matched sequences.' The E-value is the probability of the match and the query sequence being identical. The lower the E-value, or the closer it is to zero, the more significant is the alignment between the query and the matched sequence. Shorter query sequences will produce high E-value and vice versa. This is because, the probability of finding another short sequence in the database is very high (Pearson 2013). An E-value of 10^{-3} and below is indicative of statistical significance, however, it is not uncommon for a BLAST search to produce a match with an E-value of 10^{-50} (Nagar and Hahsler 2013), indicating a very strong relationship between the query and the 'matched sequence'. The maximum score generates similar output to that of the E-value. It determines the highest scoring between a set of aligned segments from the same subject sequence. It also considers the sum of the matches, mismatches, gap openings for each segment. Gap openings usually occur because of genetic mutations from nucleotide deletions or insertions (Krane and Raymer 2002). The maximum identity is the highest percentage similarity between the query and the subject sequence over the length of the coverage area. The query coverage refers to the percentage of the length of

query sequence covered and included in the aligned sequence. The total score is also determined by the sum of the alignment scores of all segments from the same subject sequence (Madden 2013).

4.4 Multiple Sequence Alignment (MSA)

MSA is an important technique in probe design. After the BLAST search, several matched sequences are identified and the homology between these matched sequences can be retrieved and if there is any region of homology, this can be determined by performing a sequence alignment. Two types of alignment can be performed i.e. pairwise and multiple sequence alignment. The former is the alignment between two sequences and the latter is more than two nucleotide sequences using bioinformatics tools such as CLUSTAL W and T-coffee (Thompson *et al.* 1994; Notredame *et al.* 2000 ; Larkin *et al.* 2007). The regions showing homology after sequence alignment is usually chosen for the probe/ primer design. Also, when homology is identified between multiple sequences, there is the likelihood that, this region of comparison has similar function and could be structurally related and have biochemical functions (Karlin and Altschul 1990; Altschul *et al.* 1997). This can be confirmed by determined using specific tools to predict the presence of any protein secondary structures (discussed in section 4.5 below). The design of probes using bioinformatic tools are discussed in this chapter using two genes of *M. abscessus* (*erm*-41 and *rpoB*) were selected to be tested as for specific identification.

4.5 Predicting protein structure

One approach to confirm whether the nucleotide region against which our probes were designed are conserved is to determine in the gene sequence encodes for secondary structures, which serves as a starting point for determining tertiary and quaternary structures of the protein (Deng and Cheng 2011). In that case, the corresponding amino acid sequence would be the required template for secondary structure prediction. Predicting the secondary structure provides clues for

functional sites, conserved regions and protein stability (Zhou and Zhou 2005; Godzik *et al.* 2007; Deng and Cheng 2011). Additionally, the secondary structure also determines how the proteins fold (Hol *et al.* 1981).

Proteins are polymers of amino acids linked by a polypeptide bond. Four types of protein structures are formed in living tissues, namely; primary, secondary, tertiary and quaternary structures. Primary structures are the simplest, made of linear chains of amino acids. Secondary structures are composed of the α-helix and β sheet. The α-helix resembles spiral staircases while β sheets are formed when β strands self-assemble and both are stabilized by hydrogen bonding (Deng and Cheng 2011).

The initial steps in predicting secondary structure follows the same principle as determining conserved nucleotide regions. First, the query protein sequence is used to identify similar protein sequences using BLASTP, followed by sequence alignment with CLUSTAL Omega to identify domains and predict their secondary structures using a specific bioinformatic tools. A myriad of such tools is available e.g. JPRED, PHD, 3D-PSSM, GenThreader, Meta Server CBS and Phyre^2 (Edwards and Cottage 2003).

4.6 Aims and objectives

The **aim** of this chapter is to design DNA probes capable of distinguishing *M. abscessus* from other mycobacteria.

The **objectives** are to;

1. employ a bioinformatic approach to identify unique nucleotide regions within the *rpoB* and the *erm*-41 genes of *M. abscessus*

2. predict the secondary structures of the conserved regions from their corresponding protein sequences
3. design DNA specific probes capable of binding to these unique regions
4. determine the ability of the candidate probes to differentiate *M. abscessus* from other mycobacteria

4.7 Materials

4.7.1 Chemicals

Qiagen PCR core kit (Qiagen, UK), 100 bp Hyper ladder (Bioline, UK)

4.7.2 Bioinformatic tools

The following bioinformatic tools were used in this study;

1. National Center for Bioinformatic Information (NCBI). Accessed from https://www.ncbi.nlm.nih.gov/. Date accessed: November 2015.
2. NCBI-BLAST. (https://blast.ncbi.nlm.nih.gov/Blast.cgi?PROGRAM=blastn&PAGE_TYPE=BlastSearch&LINK_LOC=blasthome). (Date accessed: December 2015)
3. CLUSTAL W (http://www.ebi.ac.uk/Tools/msa/clustalw/) (Accessed on November 2015).
4. Oligo integrated DNA technologies (IDT) analyser (https://www.idtdna.com/calc/analyzer) (Accessed on December 2015).
5. Reverse complement. https://www.bioinformatics.org/sms/rev_comp.html (Date accessed: December 2015)

6. Probe check. http://131.130.66.200/cgi-bin/probecheck/probecheck.pl (Date accessed: December 2015)
7. Phyre[2]. Accessed from http://www.sbg.bio.ic.ac.uk/phyre2/phyre2_output/4dfba067a02da9d8/summary.html. (Date accessed: 29.01.2019)
8. Thermo scientific Tm calculator. Accessed from (https://www.thermofisher.com/uk/en/home/brands/thermo-scientific/molecular-biology/molecular-biology-learning-center/molecular-biology-resource-library/thermo-scientific-web-tools/tm-calculator.html) (Date accessed January 2016)

4.8 Methodology

4.8.1 Bioinformatic identification of target gene and multiple sequence alignment

The full and complete nucleotide sequences of the *erm*-41 and *rpoB* genes of *M. abscessus* (*M. abscessus;* ATCC 19977^{T}) and the *rpoB* gene sequence of *M. smegmatis* (MC2 155) were downloaded in FASTA format from NCBI. Using the BLAST tool, a similarity search was performed against the NCBI nucleotide database to obtain sequences that matched the query sequence. A major challenge encountered in post BLAST analysis was the availability of the full and complete coding sequences of the *erm*-41 and *rpoB* genes that matched the query sequence. For this reason, the number of the matched sequences that were complete were used. A total of ten, eight and three complete matched sequences out of the possible 100 for the *erm*-41 (*M. abscessus;* ATCC 19977^{T}), *rpoB* (*M. abscessus;* ATCC 19977^{T}) and *rpoB* (*M. smegmatis;* MC2 155) genes respectively were retrieved from NCBI, as these sequences showed 100% homology to the query sequence. A multiple sequence alignment was then performed using CLUSTAL W to identify conserved regions showing 100% nucleotide alignment and numbering more than 50 nucleotides in length. This region was considered suitable for probe design. Phylogenetic trees

based on each target gene (*erm*-41 and *rpo*B) were constructed with CLUSTAL W using the neighbour-joining methods. The default setting of CLUSTAL W for constructing the phylogenetic tree was applied.

4.8.2 Predicting secondary structure of conserved regions

The amino acid sequence of the *erm*-41 and *rpoB* gene (*M. abscessus*; ATCC 19977^{T}) and the rpoB of *M. smegmatis* (MC^{2} 155) was retrieved from NCBI and imported to Phyre^{2} software to determine if the conserved regions from which the probes were designed bears any secondary structures. The Phyre^{2} data output were then compared to the *erm*-41 nucleotide sequence to determine regions of secondary structure formation.

4.8.3 *In silico* analysis of designed probes

In silico analysis of potential probes (anchor and detector) were performed to determine if they were capable of forming hairpin, self- and hetero dimerization using the oligo IDT analyser tool. This tool predicts hairpin oligo secondary structure using a multiple fold (mfold) algorithm (Zuker 2003). Probes capable of forming secondary structures were discarded based on their Gibbs free energy (ΔG) values. Self-dimerization and hetero dimerization were also computed using the same software. The percentage of G-C in the probe was also determined and if more than 70%, those probes were excluded. The specificity of the probes was also determined using BLAST. Probes that were found to have nucleotide similarity with non-*M. abscessus* species were rejected. An overview of the bioinformatic probe design and analysis is shown if figure 4.1 below.

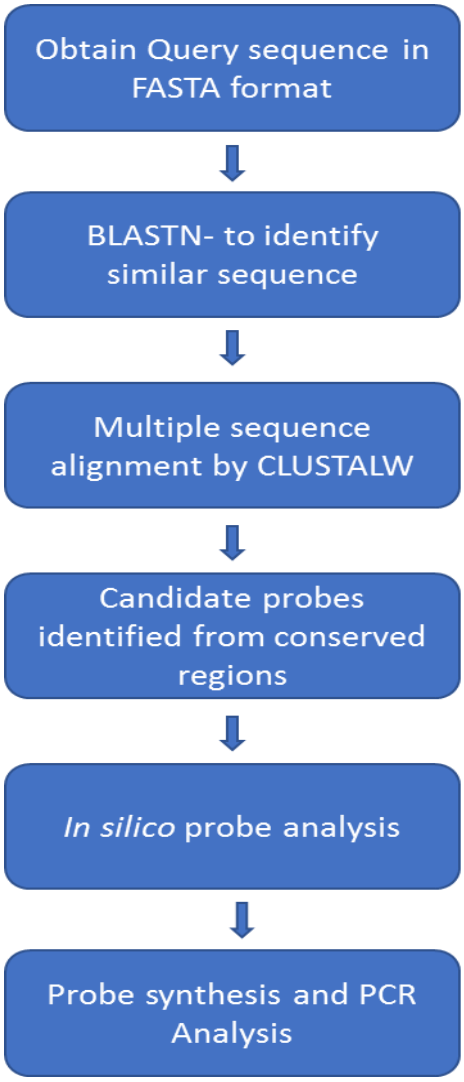

Figure 4.1. Overview of the workflow for bioinformatic probe design and in silico analysis. The first step is to load the query sequences to NCBI then the tool searches for similar sequences. Conserved regions are then located from the similarity search and the probes designed form the conserved regions.

4.8.4 Probe synthesis and modification

A pair of probes (anchor and detector) were synthesized for each conserved region that showed 100% homology. The anchor and detector probe were designed to have 17 and 22 nucleotides respectively with 5'-biotin and 3'-HRP modifications. To allow flexibility between the anchor probe and the magnetite beads, 5 thymine residues were inserted to the anchor probe sequence between the biotin and the 17-nucleotide sequence. These probes were designed to facilitate the development of the hybridization assay which will be discussed in Chapter 6. The same probes without biotin or HRP modifications at 5' (anchor probe) or 3' (detector probe) ends were synthesized so that they could be used in a PCR assay with the anchor probe serving as the forward primer and the reverse complement of the detector probe functioning as the reverse primer (Fig 4.2).

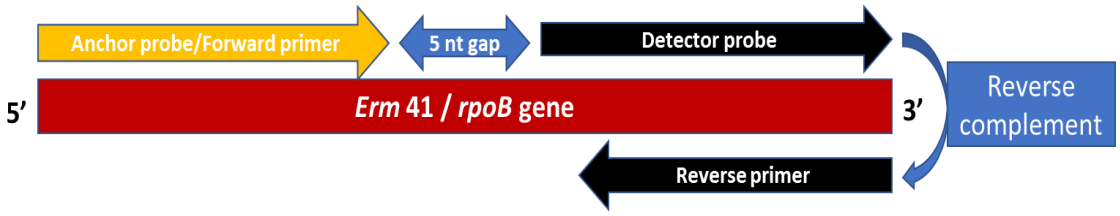

Figure 4.2 Schematic representation of probe design. The anchor (17 nucleotide) and detector probe (22 nucleotide) were designed to target same strand of bacterial gene. The reverse complement of the detector probe was obtained using Oligo IDT analyser. Between the anchor and the detector probe is a 5-nucleotide gap.

4.8.5 Determination of probe specificity via PCR assay

Following probe design and *in silico* analysis, probes were synthesized and subjected to specificity testing in a PCR assay using DNA extracts obtained from *M. abscessus* isolates (Chapter 3, Table 3.3) and non-*M. abscessus* isolates (*E. coli*, *S. aureus*, *M. smegmatis* and *M. kansasii*). DNA were amplified using the Taq PCR core kit (Qiagen, UK). The synthesized probes (forward and reverse

primer without biotin and HRP modification) were used for the PCR assay. In a typical experiment, PCR was performed in a total reaction volume of 20 µl reaction containing 10.7 µl of nuclease free water, 0.1 µM of anchor and detector probe, 4 µl of 5X Q-solution, 2 µl of 10X PCR buffer, 0.6 µl of 25mM $MgCl_2$, 0.4 µl of 10mM dNTP mix, 0.2 µl of Taq DNA polymerase and 2 µl of DNA extract. Amplification was performed in a 200 µl PCR tube using a thermal cycler (T100, Bio-Rad) with the following thermocycling profile; initial denaturation at 95^0C for 5 min, followed by 35 cycles of denaturation at 95^0C for 30s, annealing at the probe respective temperature as determined by thermo scientific Tm calculator (Table 4.5) for 60 s, 72^0C for 20s and a final extension at 72^0C for 10 min. PCR products were electrophoresed on 2% agarose gel stained with 4 µl of Safeview™. Electrophoresis was performed in 1X TBE buffer at 100 Volts for 30 min and visualized in UV transilluminator (ChemiDoc, Bio-Rad laboratories, UK).

4.8.6 Determining the sensitivity of the probes by PCR

M. abscessus (ATCC 19977^T) DNA was serially diluted in nuclease free water to the following concentrations; 10 ng/µL, 2 ng/µL, 0.4 ng/µL, 80 pg/µL, 16 pg/ µL and 3.2 pg/ µL. Serially diluted DNA was then used in a PCR reaction using each candidate probe and the amplified DNA if any, was electrophoresed and visualized as described in section 4.7.4 above.

4.9 Results

4.9.1 Multiple sequence alignment (MSA) of *M. abscessus* genes

The nucleotide sequences of the *erm-41* of *M. abscessus* were retrieved from NCBI and imported into CLUSTAL W for alignment to identify conserved regions. Probes (E1, E2 and E3) were designed to target the conserved regions of the *erm*-41 gene. These regions are highlighted in red as shown in fig. 4.3A-C. The probe targeting the *rpo*B gene of *M. abscessus* and *M. smegmatis* are displayed in fig 4.3 D and E respectively. Similarly, the probe binding regions are highlighted in red. The probe for *M. smegmatis* was also designed and used for the identification of *M. smegmatis* and isolate 9723 (discussed in chapter 3). The anchor and detector probes numbered 17 and 22 nucleotides respectively. The *erm* sequences of *S. aureus* (*erm*A, *erm*B and *erm*C), and *E. coli* and the *rpo*B sequences of *S. aureus* and *E. coli* were added to determine the specificity of the selected region. The aligned sequence showed that the region selected for probe binding did not have any similarity with the *erm* sequences of *E. coli* or *S. aureus*. Similarly, the selected region for the *rpo*B probe did not have any similarity with the *rpo*B sequences of *E. coli* or *S. aureus*. The phylogenetic analysis of the 17 sequences of *erm*-41 did not show any similarity with the *erm* genes of *E. coli* and *S. aureus* (fig. 4.4). Similarly, that of the *rpo*B gene sequences of *M. abscessus* and *M. smegmatis* did not show any similarity with those of *E. coli* or *S. aureus* as shown in figures 4.5 and 4.6 respectively.

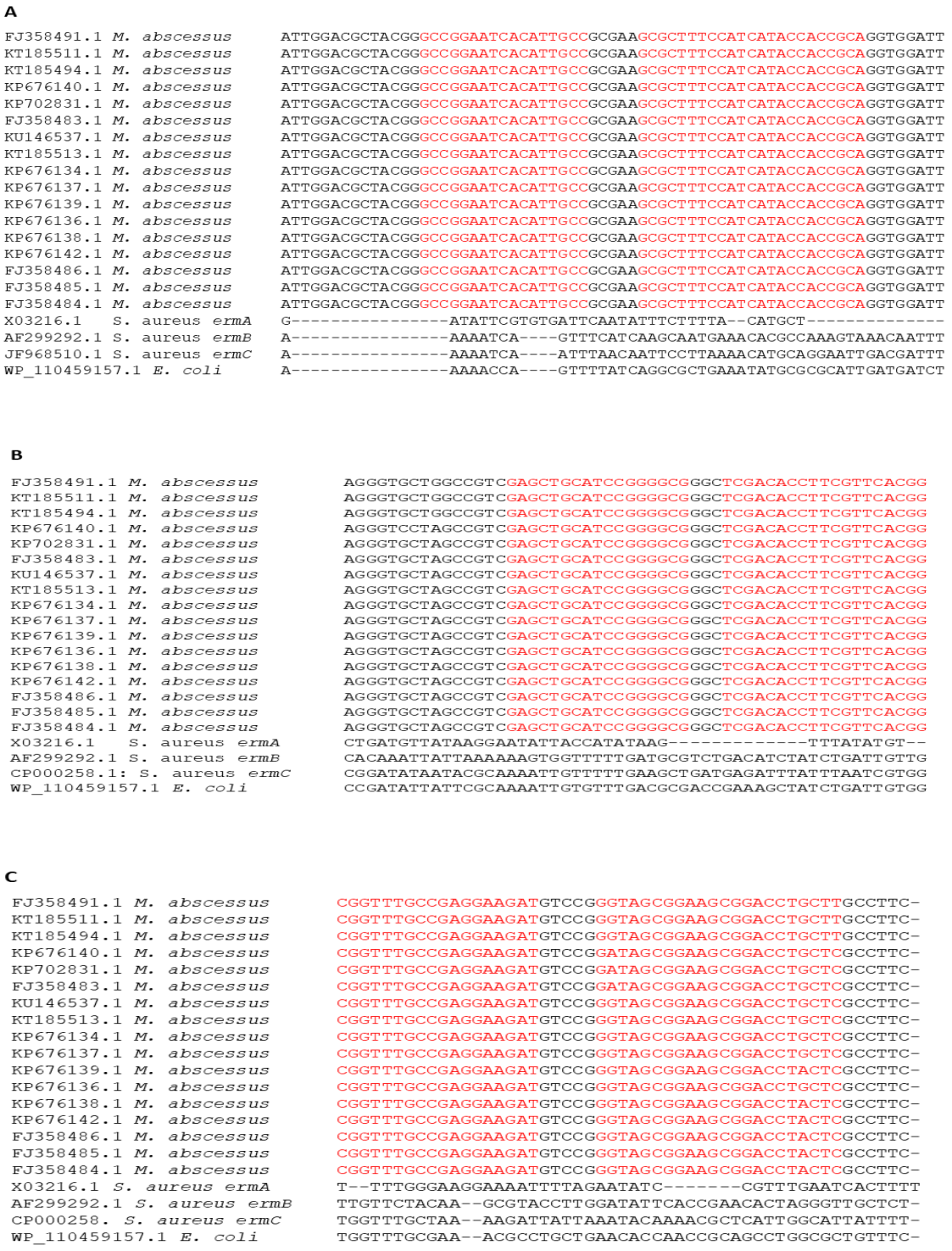

Figure 4.3A-C. Sequence alignment of conserved regions of the *erm*-41 probe. Probe binding regions for E1, E2 and E3 are shown in A, B and C respectively. DNA sequences with their respective accession numbers were retrieved from NCBI database in FASTA format. Seventeen sequences for the *M. abscessus* targeting the *erm*-41 gene were downloaded in FASTA format and aligned using CLUSTAL W to identify conserved regions (highlighted in red). The *erm* genes of *S. aureus* and *E. coli* were also included.

D

```
NC_007795. S aureus      TACACTTAGG---------TATGGCTG----------------------------------------
NC_000913. E. coli       CCCACCTGGGTATGGCTGCCAAGATCAGCTGAAACAGCAGCAAGAAGTCCCAGCGTGCGTACGATCTG
KU362972.1 M. abscessus  CCCACCTCGGGTGGATTGCCAAGACCGGCTGGAACATCGAGGGTGAGCCCGAGTGGGCGGCCAATCTG
KT185557.1 M. abscessus  CCCACCTCGGGTGGATTGCCAAGACCGGCTGGAACATCGAGGGTGAGCCCGAGTGGGCGGCCAATCTG
KT185553.1 M. abscessus  CCCACCTCGGGTGGATTGCCAAGACCGGCTGGAACATCGAGGGTGAGCCCGAGTGGGCGGCCAATCTG
KT185544.1 M. abscessus  CCCACCTCGGGTGGATTGCCAAGACCGGCTGGAACATCGAGGGTGAGCCCGAGTGGGCGGCCAATCTG
KT185554.1 M. abscessus  CCCACCTCGGGTGGATTGCCAAGACCGGCTGGAACATCGAGGGTGAGCCCGAGTGGGCGGCCAATCTG
KT185556.1 M. abscessus  CCCACCTCGGGTGGATTGCCAAGACCGGCTGGAACATCGAGGGTGAGCCCGAGTGGGCGGCCAATCTG
KT185545.1 M. abscessus  CCCACCTCGGGTGGATTGCCAAGACCGGCTGGAACATCGAGGGTGAGCCCGAGTGGGCGGCCAATCTG
JF346872.1 M. abscessus  CCCACCTCGGGTGGATTGCCAAGACCGGCTGGAACATCGAGGGTGAGCCCGAGTGGGCGGCCAATCTG
AY262741.1 M. abscessus  CCCACCTCGGGTGGATTGCCAAGACCGGCTGGAACATCGAGGGTGAGCCCGAGTGGGCGGCCAATCTG
EU109292.1 M. abscessus  CCCACCTCGGGTGGATTGCCAAGACCGGCTGGAACATCGAGGGTGAGCCCGAGTGGGCGGCCAATCTG
```

E

```
NC_000913.    E. coli           ------------------------------ATGGTT-------TACTCCTATAC------
YP_499096.2   S. aureus         ------------------------------ATGGCCGGCCAGGTGGTGCAGTACGG----
AY262741.1    M. abscessus      GCCACGACGGTGTTGTTTTGTTGTGATCGATCGGGTGTGTGTTTGGTCGTTTGCTTGCG-
U24494.1    M. smegmatis        TACCTGACACCGTGGTCCTAGCCTGAGTAGTTTGCTCAGTACCTGGTCCTGTGTCGTTGC
AJ605718.1 M. smegmatis         ----------CGTGGTCCTAGCCTGAGTAGTTTGCTCAGTACCTGGTCCTGTGTCGTTGC
AY262735.1 M. smegmatis         TACCTGACACCGTGGTCCTAGCCTGAGTAGTTTGCTCAGTACCTGGTCCTGTGTCGTTGC
```

Figure 4.3D-E. Sequence alignment of conserved regions of the *rpoB* probe for *M. abscessus* (D) and *M. smegmatis* (E). DNA sequences with their respective accession numbers were retrieved from NCBI database in FASTA format. Ten and three sequences of rpoB for *M. abscessus* and *M. smegmatis* were downloaded in FASTA format and aligned using CLUSTAL W to identify conserved regions. The probe sequences are highlighted in red in the aligned sequence. The *rpo*B sequence for *E. coli* and *S. aureus* were also retrieved from NCBI and imputed into CLUSTLAL W.

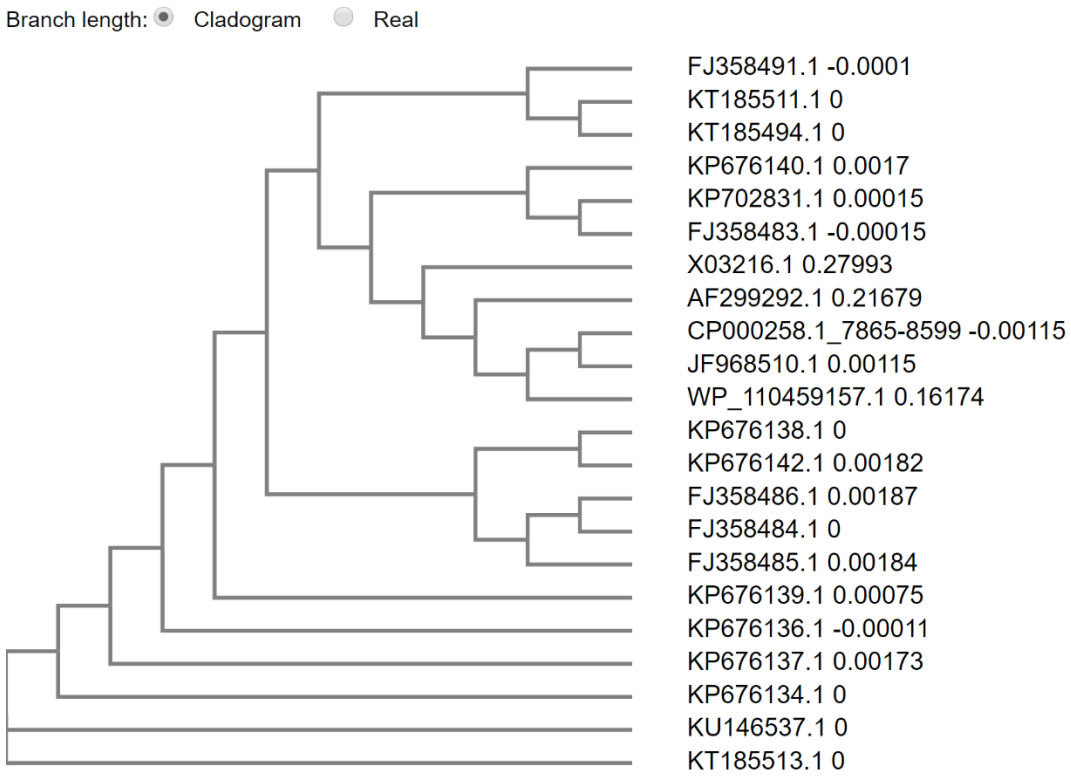

Figure 4.4. Phylogenetic tree based on the complete gene sequence of the erm-41 gene of *M. abscessus*. The *erm* genes of *E. co*li (WP_110459157.1) and *S. aureus* (CP000258.1_7865-8599-0.00115, JF968510.1, AF299292.1, X03216.1) were included to identify sequence similarity. The phylogenetic tree was constructed using the neighbour joining model in the CLUSTALW program.

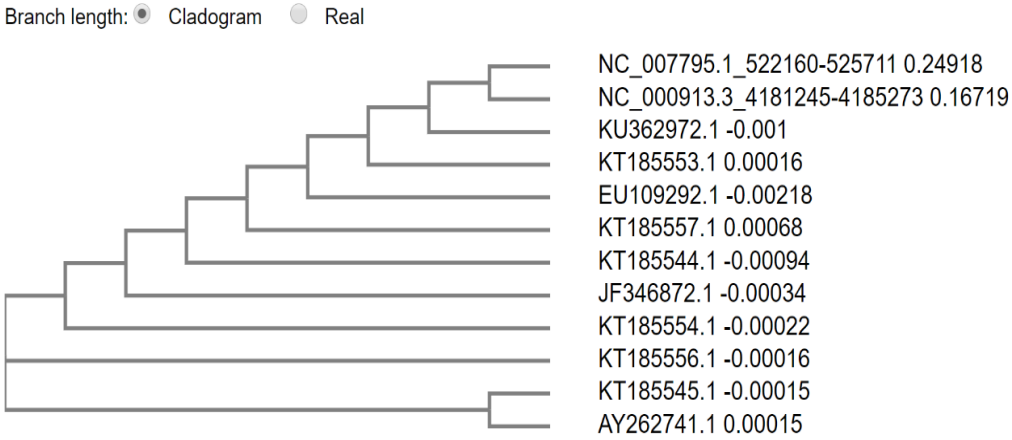

Figure 4.5. Phylogenetic tree based on the partial gene sequence of the rpoB gene of *M. abscessus*. The *rpoB* genes of *E. co*li (NC_000913.3:4181245-4185273) and *S. aureus* (NC_007795.1:522160-525711) were included to identify sequence similarity. The phylogenetic tree was constructed using the neighbour joining model in the CLUSTALW program.

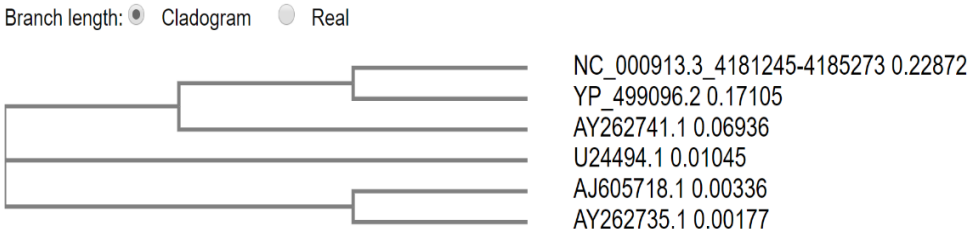

Figure 4.6. Phylogenetic tree based on the partial gene sequence of the rpoB gene of *M. smegmatis*. The *rpoB* genes of *E. co*li (NC_000913.3:4181245-4185273) and *S. aureus* (YP_499096.2) were included to identify sequence similarity. The phylogenetic tree was constructed using the neighbour joining model in the CLUSTALW2 program.

4.9.2 Determining the secondary structures of the conserved regions

To determine if the unique nucleotide regions from which the probes were designed were conserved due to an essential biological role their corresponding amino acid sequences were obtained from NCBI and modelled with Phyre[2] to determine the presence of any secondary structures i.e. α-helix and β-strand. Analysis of the *erm*-41 gene, constituting 173 amino acids showed regions of α-helix (31%) and β-strand (28%), and 98% of the total amino acid sequence were modelled with 100% confidence. Positions 57-86 and 147-162 of the amino acid sequences, the regions from which the probes were designed, contained a three α-helix and β-strands (fig 4.7).

Similarly, for the *rpoB* gene of *M. abscessus* gene, 91% of the total amino acid residues (1128) were modelled with 100% confidence. The total percentage of α-helix and β-strand formed were 28% and 26% respectively. The amino acid region where the probe was designed i.e. between positions 910 and 957 (indicated in a box in fig 4.8) had 3 α-helix and 1 β-sheet strand. Finally, the *rpoB* gene of *M. smegmatis* was modelled with a total of 1138 amino acid residues. Again, 92% of the amino acids were modelled with 100% confidence which resulted in α-helix (28%) and β-strand (26%). The probe position was identified between amino acid positions 20 to 34, which shows α-helix formation and the appeared of disordered amino acids (fig. 4.9).

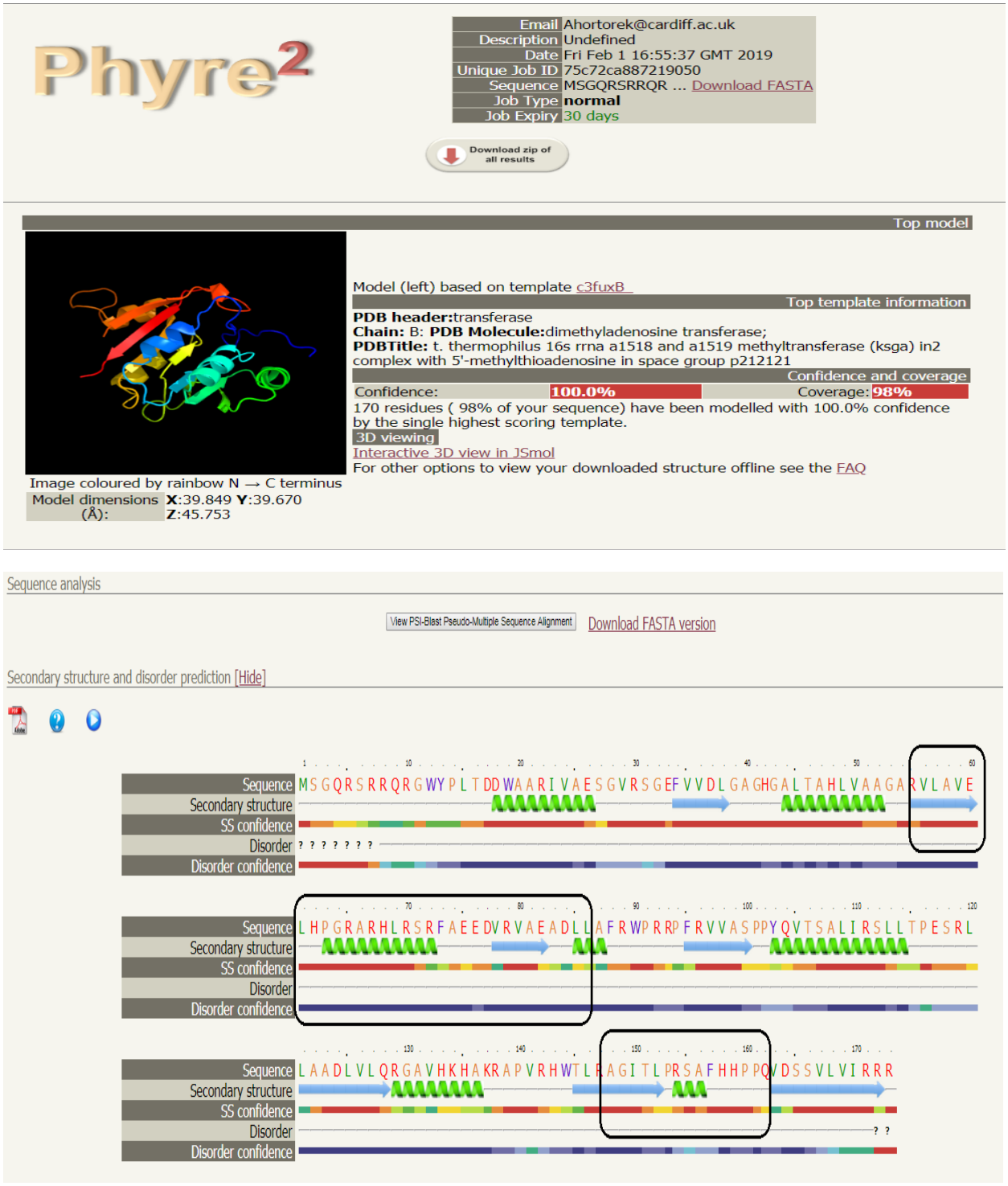

Figure 4.7 Secondary structure prediction of *M abscessus erm*-41 gene. The corresponding amino acid sequence of the *erm*-41 gene of *M. abscessus* was retrieved from NCBI and modelled in Phyre^2 to reveal any α-helix and β-strand. The regions where probes were designed (in rectangle) showed the presence of α-helix (violet) and β strands (light blue arrow).

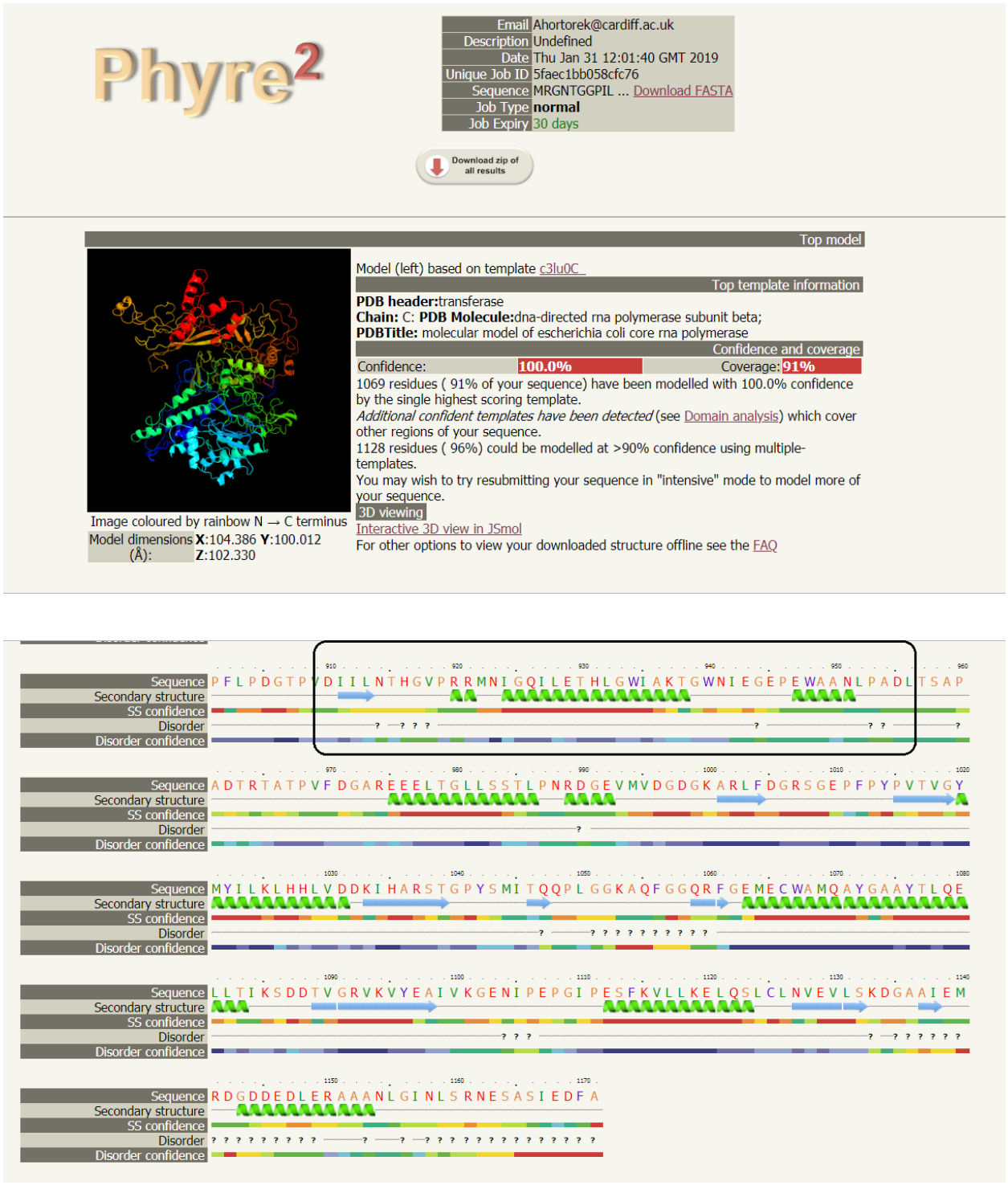

Figure 4.8 Secondary structure prediction of *M abscessus rpo*B gene. The corresponding amino acid sequence of the nucleotide sequence of the *rpoB* gene of *M. abscessus* was retrieved from NCBI and modelled in Phyre^2 to reveal any α-helix and β-strands. The regions where the probe was designed (in rectangle shape) showed α-helix and β strand formation. Amino acid positions 1 to 900 have been truncated from the figure and only shows regions of interest.

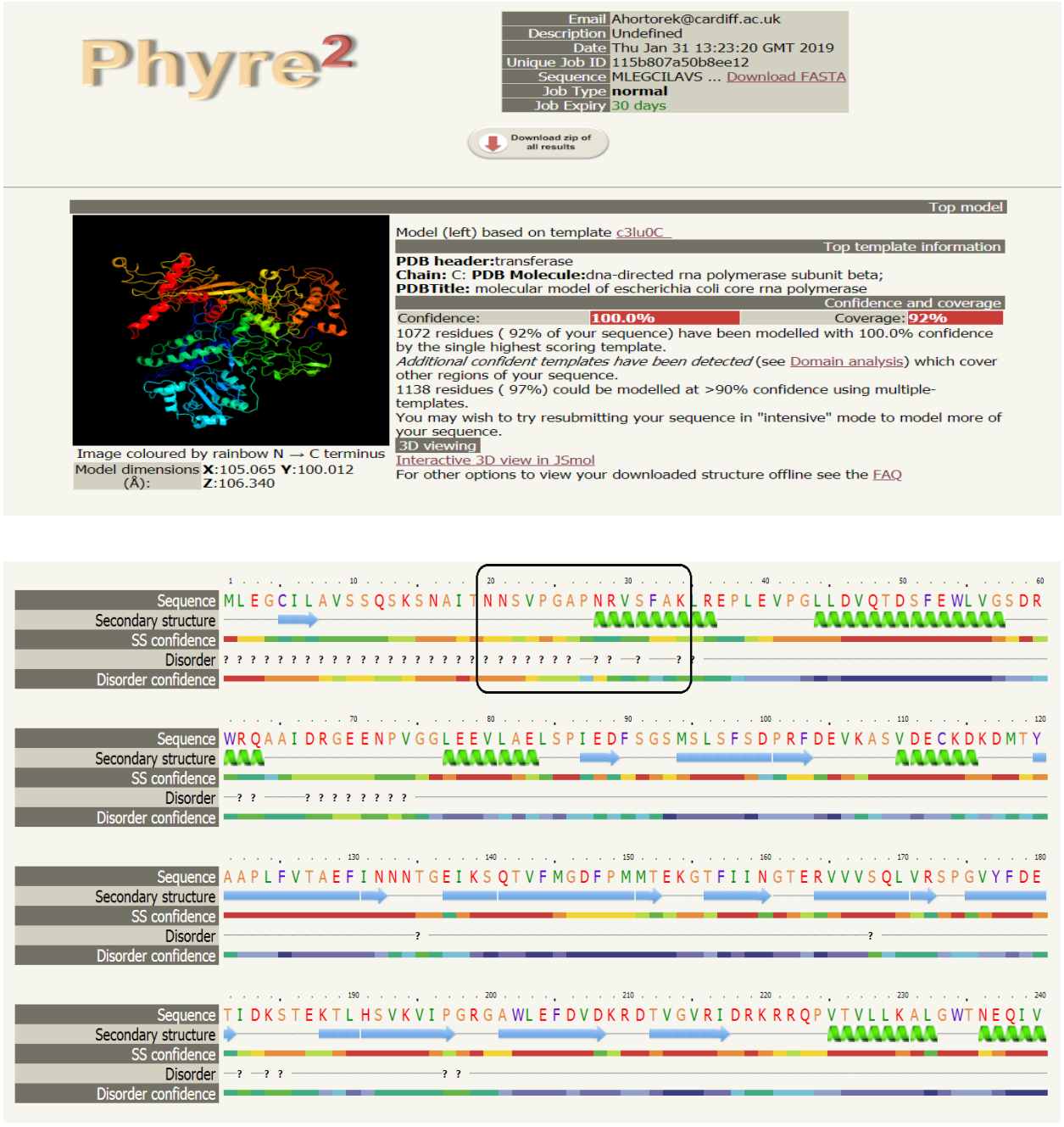

Figure 4.9 Secondary structure prediction of *M smegmatis rpo*B gene. The corresponding amino acid sequence of the nucleotide sequence of the *rpoB* gene of *M. smegmatis* was retrieved from NCBI and modelled in Phyre^2 to reveal any α-helix and β-strands. The regions where the probe was designed (in rectangle shape) showed α-helix and β strand formation.

4.9.3 *In silico* analysis of candidate probes

In silico analysis of candidate probes in terms of their potential to self and hetero-dimerize was determined. The thermodynamic stabilities of the probes, expressed as ΔG was computed by taking into consideration the probe length and concentration of Mg^{2+}, Na^{+} and dNTP used in the PCR assay. The ΔG values for probe-target was approximately four times higher than in probe-probe hybrid (Table 4.1), suggesting that hybrid formation between the probe and target is thermodynamically favourable. The specificity of the candidate probes was subjected to similarity check using BLAST. Probes that had similarity with any non-mycobacteria and any gut bacteria were rejected and considered non-specific (Appendix 3). Candidate probes with G-C content exceeding 70% were rejected as this will increase the annealing temperature substantially. The final probes for synthesis and to be used in the PCR and hybridization assays are shown in Table 4.2 and 4.3 respectively.

Table 4.1 Thermodynamic stabilities (ΔG) of probes as determine using the Oligo IDT Analyzer

The thermodynamic stability (ΔG) of the probes (anchor and detector) for each gene target forming self- or hetero dimers were determined using the Oligo IDT.

Hybrid complex	Duplex formation (ΔG) kcal/mole	Probe type
anchor-anchor	-9.75	E1
detector-detector	-9.89	E1
anchor-detector	-6.68	E1
anchor-target	-36.29	E1
detector-target	-48.17	E1
anchor-anchor	-9.75	E2
detector-detector	-4.95	E2
anchor-detector	-6.68	E2
anchor-target	-40.65	E2
detector-target	-43.17	E2
anchor-anchor	-3.61	E3
detector-detector	-4.74	E3
anchor-detector	-6.68	E3
anchor-target	-34.48	E3
detector-target	--47.58	E3
anchor-anchor	-5.02	*rpoB-M. abscessus*
detector-detector	-6.76	*rpoB-M. abscessus*
anchor-detector	-6.78	*rpoB-M. abscessus*
anchor-target	-36.34	*rpoB-M. abscessus*
detector-target	-45.23	*rpoB-M. abscessus*
anchor-anchor	-7.58	*rpoB-M. smegmatis*
detector-detector	-4.41	*rpoB-M. smegmatis*
anchor-detector	-7.58	*rpoB-M. smegmatis*
anchor-target	-32.21	*rpoB-M. smegmatis*
detector-target	-37.58	*rpoB-M. smegmatis*

*ND = Not determined.

4.9.4 Probes used in the PCR and hybridization assay

Probes targeting different conserved regions of the *erm*-41 gene (E1, E2 and E3), and rpoB of *M. abscessus* and *M. smegmatis* are presented in the Table 4.2 below. Their G-C content were also determined and those that exceed 70% were excluded. The anchor and detector probes were modified with biotin and HRP at their 5' and 3' ends respectively for the hybridization assay (Table 4.3).

Table 4.2 Probes sequences synthesized for PCR assay

Probe type	Anchor probe (5'-3') / G-C content (%)	Detection probe (5'-3') (Reverse complement) / G-C content (%)
E1	GCCGGAATCACATTGCC 58.8 %	TGCGGTGGATGATGGAAAGCGC 59.1 %
E2	GAGCTGCATCCGGGGCG 62.5 ºC	AAACCGTGAACGAAGGTGTCGA 50 %
E3	GGTTTGCCGAGGAAGAT 52.9 %	GAGCAGGTCCGCTTCCGCTACC 68.2 %
***rpo*B (*M. smegmatis*)**	GTCCTAGCCTGAGTAGTTT 47.4 %	AACGACACAGGACCAGGTAC 52.4 %
rpoB (*M. abscessus*)	CTCGGGTGGATTGCCAA 58.8 %	GGCTCACCCTCGATGTTCCAGC 63.6 %

Table 4.3 Probes sequences synthesized for DNA hybridization studies

Probe type	Anchor probe (5'-3')	Detector probe (5'-3')
E1	tttttGCCGGAATCACATTGCC	GCGCTTTCCATCATCCACCGCA-**HRP**
rpoB (*M. smegmatis*)	tttttGTCCTAGCCTGAGTAGTTT	AGTACCTGGTCCTGTGTCGTT-**HRP**
*rpo*B (*M. smegmatis*)	GTCCTAGCCTGAGTAGTTT	GTACCTGGTCCTGTGTCGTT-HRP
rpoB (*M. abscessus*)	tttttCTCGGGTGGATTGCCAA	GCTGGAACATCGAGGGTGAGCC-**HRP**

4.9.5 Determination of the specificity of candidate probes using PCR

Prior to the PCR assay, the annealing temperatures for the candidate probes were determined using the Tm calculator algorithm (Thermos fisher Scientific), based on the primer pair sequence, primer concentration and DNA polymerase used in the PCR assay. The results are shown in Table 4.4. The specificity of the probes was tested against 7 *M. abscessus* isolates (as identified in Chapter 3) and a collection of non-*M. abscessus* isolates (*E. coli*, *S. aureus* and *M. kansasii*) in a PCR assay. The anchor and detector probe pairs were designed to amplify a 50 bp region, hence an amplicon of the same size was expected. DNA amplicons estimated at 50 bp were identified for *M. abscessus* isolates 11365, 10332, 9568, 10006, 11490, 8899, 9495 (lane 1-7) and the positive

control isolate, ATCC19977^{T} (lane P) (fig 4.10). A PCR master mix control (lane M) was also included to monitor PCR contamination. The non-*M. abscessus* isolates (lane 8-12) did not generate a 50 bp amplicon indicating that the specificity of the candidate probes except for the E2 probe which produced DNA amplicons greater than 50 bp was non-specific (fig. 4.10B).

Table 4.4 The annealing temperature of the candidate probes

Bacterial target	Probe type	Annealing temperature (ºC)
M. abscessus	E 1	54.2
M. abscessus	E 2	52.4
M. abscessus	E 3	52.4
M. abscessus	*rpoB*	55.0
M. smegmatis	*rpoB*	56.0

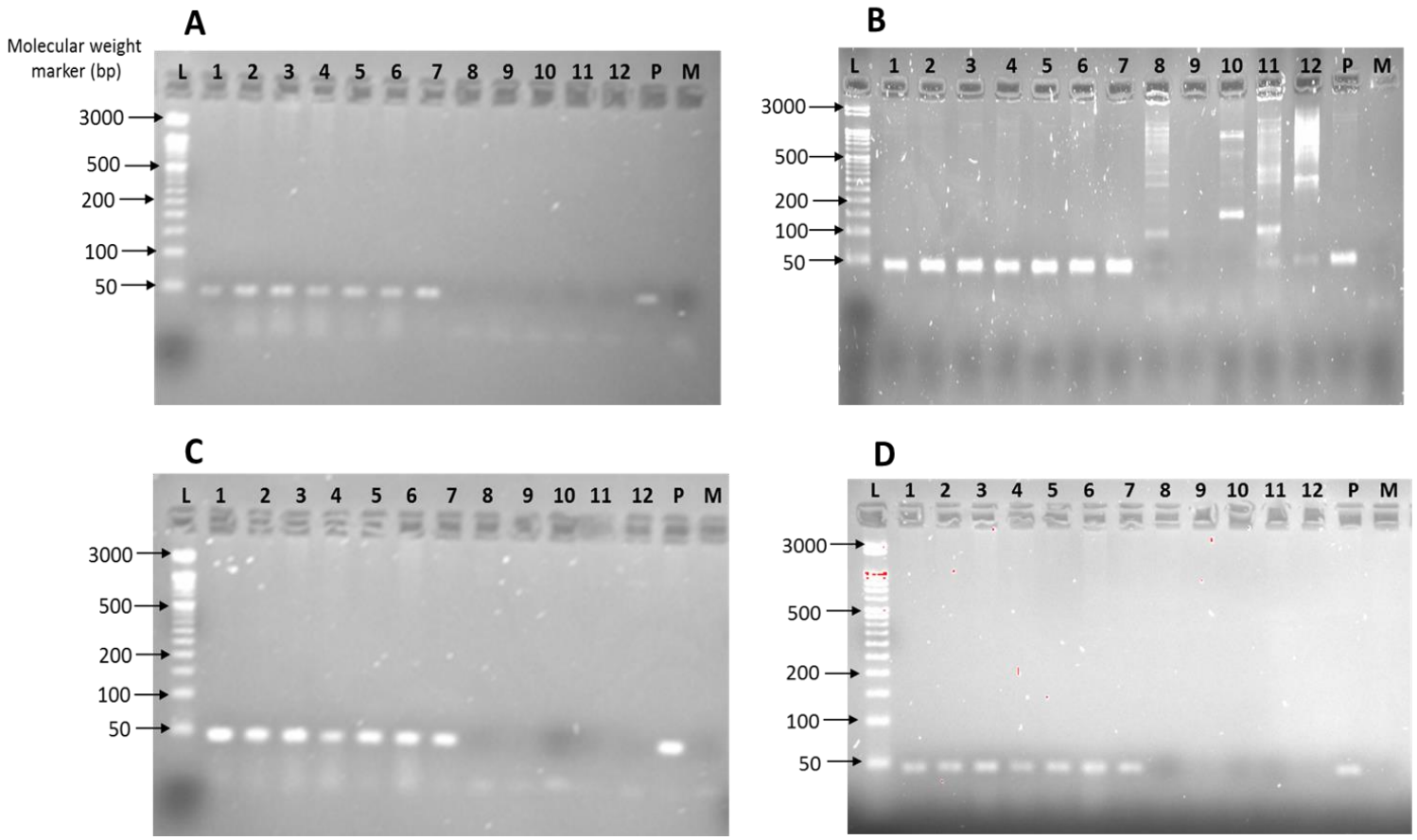

Figure 4.10 Determining the specificity of the designed probe. PCR was performed using the designed probes (A) E1 (B) E2 (C) E3 and (D) *rpoB* and amplified at their respective annealing temperatures (Table 3.2). The anchor and detector probes (reverse complement) were used as forward and reverse primer respectively against a panel of *M. abscessus* and non-*M. abscessus* DNA extracts. PCR amplicons (5 µl) was electrophoresed in 1% agarose gel stained with Safeview^{TM} in a 1X TBE electrophoresis buffer. Lane L= 50bp molecular weight marker; lane 1= 11365, lane 2= 10332, lane 3= 9568, lane 4= 10006, lane 5= 11490, lane 6= 8899, lane 7= 9495, lane 8= 9723 (*M. smegmatis*), lane 9= *S. aureus*, lane 10=*E. coli*, lane 11=*M. smegmatis*, lane 12=*M. kansasii*, lane M= PCR master mix control and lane P= *M. abscessus* type strain (ATCC 19977^{T}).

4.9.6 Determination of probe sensitivity to *M. abscessus*

Serial dilutions of *M. abscessus* DNA (ATCC 19977^T) were performed and amplified with primers specific for E1, E2, E3, and *rpoB*. Lanes 1, 2, 3, 4, 5 and 6 represent DNA concentrations 10 ng/µL, 2 ng/µL, 0.4 ng/µL, 80 pg/µL, 16 pg/ µL and 3.2 pg/ µL respectively. The limit of detection for primers E1 (A) and *rpoB* (D) was 80 pg/µL while that for E2 (B) and E3 (C) was 0.4 ng/µL and 2 ng/µL respectively (fig.4.11). E1 and *rpoB* probes were selected as the most sensitive and specific probes for detection of *M. abscessus* DNA in the hybridization studies.

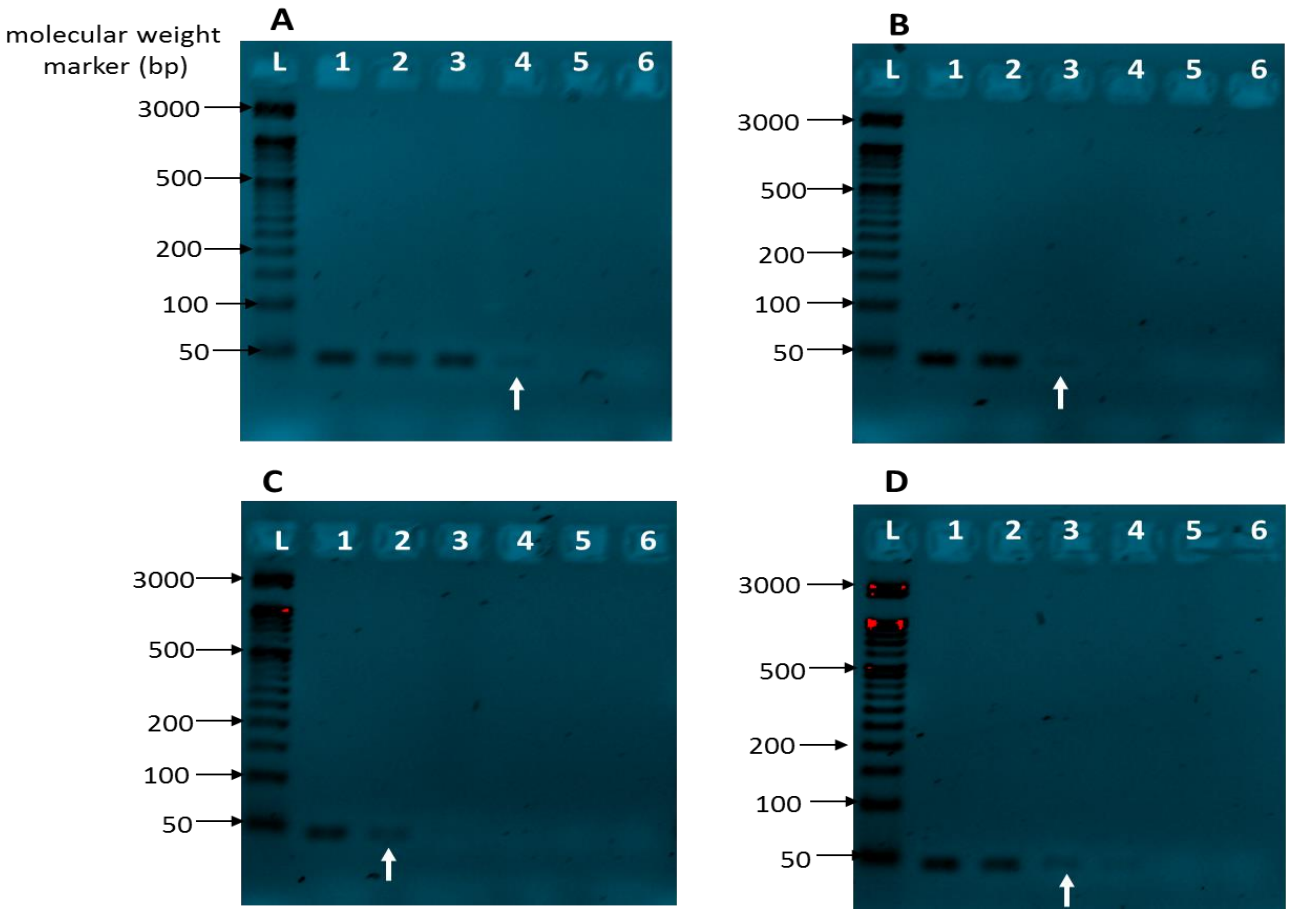

Figure 4.11 Determining the sensitivity of candidate probes (E1, E2, E3 and *rpo*B). Serially diluted *M. abscessus* DNA (10 ng/µL, 2 ng/µL, 0.4 ng/µL, 80 pg/µL, 16 pg/ µL and 3.2 pg/ µL was amplified in a PCR reaction and electrophoresed in 2% agarose gel stained with Safeview™ in a 1X TAE electrophoresis buffer. Gel electrogram results with the E1, E2, E3 and *rpo*B probes are shown in A, B, C and D respectively. Lane L= 50bp molecular weight marker; lane 1= 10 ng/µL, lane 2= 2 ng/µL, lane 3= 0.4 ng/µL, lane 4= 80 pg/µL, lane 5= 16 pg/ µL and lane 6= 3.2 pg/ µL. Arrows indicate the least concentration of DNA detected with respective primers. PCR was repeated twice ensure consistency of the amplified region.

4.10 Discussion

Conserved regions within bacterial genome are vital for the normal function of the organism and thus they represent useful identification targets (Luo *et al*. 2015). Indeed, this might be the case for the *erm*-41 gene as its maintenance is required for *M. abscessus* survival in presence of clarithromycin and other macrolide antibiotics. Also, the *rpoB* gene encode the β subunit of RNA polymerase where transcription events occur (Macheras *et al*. 2011). Additionally, this is a single copy gene (Adékambi *et al.* 2003), hence a highly important gene for bacterial survival and is not likely to undergo frequent mutation. Genomic regions conserved between related species are commonly detected by performing sequence alignment studies and as such represents the key first step in probe design (Hysom *et al.* 2012; Sobhy and Colson 2012; Nagar and Hahsler 2013).

In this study, CLUSTAL W was employed to identify conserved regions of the *erm*-41 and *rpoB* genes of *M. abscessus* and *M. smegmatis*. The accuracy and speed of this tool makes it most preferred means of performing a MSA (Daugelaite *et al.* 2013). The number of sequences aligned was determined by their availability in the database and only complete coding sequences of each gene was included in the analysis. As a result, 10 separate sequences for the E1 and E2, 8 for E3, 8 for *rpoB* gene of *M. abscessus* and 3 for *rpoB* gene of *M. smegmatis* were assessed.

The presence of any secondary structures confirms that the regions are conserved and required for biological function. Analysis of the amino acid sequences encoded by these nucleotide regions indicated they were involved in the formation of α-helix and β-strands structures. These secondary structures are often essential to biological activity and as a consequence tend to be conserved (Yang *et al.* 2016) making the nucleotide regions good targets for detection probes.

The efficiency and specificity of any probe based molecular assay is strongly connected to the accuracy, efficiency and the physicochemical characteristics of the probes. *In silico* analysis of the-candidate probes against the DNA sequences currently deposited in the NCBI database found not matches to any known mycobacteria or gut related bacteria, indicating that the probes may be well matched to their respective genes.

The thermodynamics of the probe-target hybrid must be favourable for a successful hybridization assay. While the following thermodynamic properties; Gibbs free energy (ΔG) and Enthalpy (ΔH) can be determined the former is considered a more reliable indicator (Lomzov *et al.* 2015). Based on the algorithm of this tool, the ΔG value of a probe pair must not be more negative than -9 kcal/mol (IDT 2011). Certainly, this was realized in the probe-probe hybrid complex, while that of the probe-target was approximately four times more negative. Furthermore, mycobacteria DNA have a high G-C content (Kumar and Kaur 2014). G-C formation in duplex oligonucleotides are energetically more favourable and gives maximum thermodynamic stability in DNA duplexes than A-T hybrids (Lomzov *et al.* 2015).

Although published nucleotide sequences are very informative, they do not represent a holistic collection of diversity found in nature and thus require experimental testing to confirm the predicted results. Post PCR analysis of the candidate probes against the *M. abscessus* and non-*M. abscessus* isolates used in this study found the *erm*-41 (E1) and *rpoB* probes to be the most specific and sensitive for *M. abscessus* detection. The E2 and E3 probes generated amplification products in the presence of DNA from *E. coli*, *M. smegmatis* and *M. kansasii* indicating that they lacked specificity. An explanation for this lack of specificity could be due to the fact that bioinformatic tools such as BLAST and CLUSTAL W employ heuristic approaches which provide an estimate

of the actual binding and discriminatory performances of the probe (Kalendar *et al.* 2017). Also, BLAST performs local rather than a global alignment which could limit the coverage area between the query and subject sequences. These limitations highlight the need for experimental testing using target and non-target DNA (Loy *et al.* 2008).

In conclusion, by using a bioinformatic based approach, probes which bind to the conserved regions of the *erm-41* and *rpoB* genes of *M. abscessus* have been identified. Probes E1 and *rpoB* performed similarly in the PCR assays and were modified with biotin and HRP for use in the hybridization assays. These probes were designed based on the most recent nucleotides sequences of *M. abscessus* available in the database. The ability of these probes to correctly identify all 7 *M. abscessus* isolates suggest that these probes have the potential to be employed in the hybridization assay (discussed in chapter 6).

CHAPTER 5

A study of the interaction between low power 2.45 GHz microwaves and the cell walls of structurally diverse microorganisms

5.0 Introduction

5.1 Electromagnetic (EM) spectrum

The electromagnetic spectrum is composed of seven waves, namely; Gamma (γ) rays, X-rays, ultraviolet, visible light, infrared, microwaves (MW's) and radio waves. These waves are defined by the wavelengths (λ), frequency (*f*) and photon energy (*E*), and are related by Planck's equation as shown in Eqn. 1 below,

$$\text{Energy } (E) = h f = \frac{h\,c}{\lambda} \quad \ldots\ldots\ldots\ldots\ldots\ldots\ldots\ldots \quad (5.1)$$

where c is the speed of light in meters/second (m/s) and *h* is the Plank's constant in electron volts (eV). In Eqn. 5.1, it can be deduced that, the energy of an EM wave is inversely related to the wavelength. The EM energy increases from radio waves to γ-rays and the wavelength increases from γ-rays to radio waves. The energy transmitted by γ-rays are ionising while that of MW's and radio waves are non-ionising. Ionising radiations have the capacity to break the chemical or molecular bond present in a molecule while non-ionising radiations do not have such sufficient enough energy (Beavers 2001). The frequencies of EM waves range from 1 Hz to 10^{25} Hz, with a corresponding wavelength from thousands of kilometres to the size of the nucleus of an atom (Fig 5.1) (Beavers 2001).

The EM field is a combination of both the electric (E) and magnetic (H) fields, and both are measured in volts per meter and Tesla respectively (Vorst *et al.* 2006). MWs are a component of the EM spectrum and their applications have been studied extensively and will be discussed in this chapter.

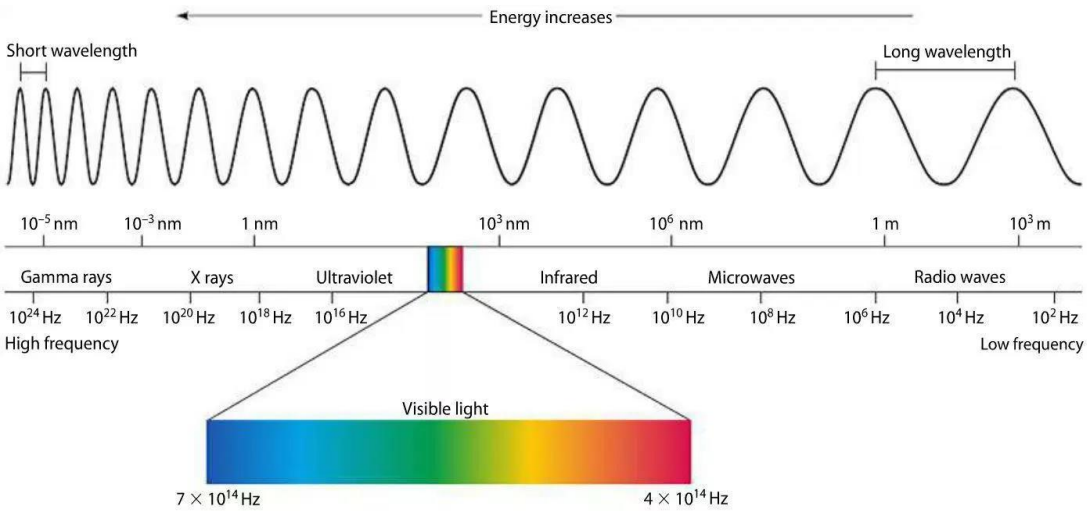

Fig 5.1 The Electromagnetic (EM) spectrum. Adapted from (Mini Physics 2018)

5.2 Microwaves (MW's) and applications

MWs originate from two sources, namely artificially and from cosmic regions. Artificial MWs are generated from the electronic oscillations of humanly crafted devices whose frequencies ranges between 300 MHz to 300 GHz with wavelengths corresponding to 1 m and 1 mm respectively (Banik *et al.* 2003; Geddes *et al.* 2017). Natural MWs are mainly those from the cosmic MW background which peaks at around 160 GHz. Other cosmic forms come from electronic transitions in hydrogen, the most common element in the universe, which emits at 1.4 GHz and correspond to a wavelength of about 21 cm (Hill *et al.* 2018). These two types of MWs differ in the sense that, natural MW's (also non-ionising) are not polarised and not biologically active while those generated artificially are polarised and have the capacity to cause biological effects (Panagopoulos *et al.* 2015). Polarisation refers to the ability of MWs to travel in a transverse manner such that the two main components i.e. the E and H fields are perpendicular to the direction of their travels

(Sun *et al*., 2016). The applications of polarised MW are numerous encompassing health, telecommunications, food industry and other industrial applications (Celandroni *et al.* 2004; Shahin *et al.* 2013). In the food industry, MWs are employed to sterilise food items to prolong their storage times (Woo *et al.* 2000). They are also used in the medical field to treat various malignant diseases such as cancer in a procedure called diathermy. This is a surgical technique which uses high frequency EM waves to generate heat directly in cancer cells to induce killing, and thereby accelerate treatment (Yang and Wang 1979). Surgical tools are also sterilised with MWs to halt transmission of nosocomial and other pathogenic diseases (Celandroni *et al*. 2004). A growing field of MW application is the isolation of DNA from microbial cells for downstream application such as PCR and hybridisation assays (Vaid and Bishop 1998; Melendez *et al.* 2016). The ability of our prototype MW device to release nucleic acids from microbial cells is explored in this chapter while the subsequent detection of the liberated nucleic acids is discussed in chapter 6.

Mobile phones, computers and several wireless devices have been built to operate at the MW frequency range. Other ISM frequency bands at 2.4 GHz, 5.7 GHz and 900 MHz also support Bluetooth applicators, RF heating and microwave heating respectively (Kumbhar 2017). The increase in demand for communication and wireless devices operating at such frequencies suggest that mankind is likely to be frequently exposed to MW radiations. This has been an area of concern and has obtained research attention. The next generation (5G) of mobile communication devices demands a high frequency to operate. The physiological effect of electromagnetic radiation changes with frequency and

as the frequency increases, the depth of penetration into biological tissues deepens. Biological organs such as eyes and skin could potential be at risk (Nature Research, 2019).

The relationship between MW frequency and their penetration depth into materials is inversely correlated. MW frequency greater than 10 GHz have low penetration depth and only induce skin surface heating while those with frequency less than 150 MHz penetrate deep into the body without loss of energy (McRee 1974; Wu *et al.* 2015). Materials (e.g. biological tissues) with high moisture content efficiently absorb MWs and the effect is pronounced, while those materials without moisture content have diminished MW effect or rather require longer exposure times (Dawkins *et al.* 1979a). Although this is an increasing area of study, the exact mechanism MW action remains elusive and has been debated between thermal and non-thermal mechanisms.

5.3 MW thermal and nonthermal bioeffect

MW induced thermal effects have been widely reported and the mechanism of action is well explained compared to its nonthermal counterpart (Rougier *et al.* 2014). Heat generation is an inevitable process during MW excitation especially in materials with high moisture content and absorb MWs effectively. These water molecules interact with the high frequency alternating electric (E) fields, rotating at about 2.4×10^9 times per oscillation. The rapid motion of water molecules induces friction, leading to the loss of energy which is dissipated in the form of heat (Kim *et al.* 2014). MW heating is different from that of conventional heating in that, the former produces a rapid intense heating while the latter is relatively slow (de la Hoz *et al.* 2007).

Nonthermal MW effect is believed to occur via direct interaction of MWs (E and or H field) with a biological material without the concomitant increase in temperature. Its existence is doubted mainly because the mechanism of action remains speculative and not well understood. Also, experiments reporting nonthermal effect are sometimes not reproducible (Pall 2013). Albeit these hindrances, several studies have reported the existence of nonthermal MW effect at a range of frequencies in biological membranes, mammalian organs (e.g. kidney, heart, brain), and their disruptive effect on purified DNA (Pall 2014; Nguyen *et al.* 2015; Pall 2015; Nguyen *et al.* 2016; Geddes *et al*. 2017).

Several mechanisms have been proposed to support the nonthermal effect and these vary with regards to the material under study. For instance, it is believed that MWs produce reactive oxygen species (ROS) that are responsible for dsDNA and ssDNA breaks (Scholes *et al.* 1960; Buxton *et al.* 1988; von sonntag 2007), Although this has been reported, the mechanism for ROS production still remain elusive (Wang and Zhang, 2017). ROS are normally generated from the mitochondria in the electron transport chain and damage to this cell machinery could lead to unregulated ROS production, hence it could be that MW induced damage to the mitochondria is responsible for the increased levels of ROS. Pore formation in biological membranes have also been reported in a phenomenon akin to electroporation (Nguyen *et al*. 2015). In electroporation, an external E field just above the membrane potential of the cell causes membrane distortion and induces pores within the membrane (Nguyen *et al*., 2016). Although such pores have been reported, they are yet to be visualised under any experimental setting.

MW parameters are key factors that determine their effect on biological cells. Also, the complexity/ composition of cells also impacts on their susceptibility to MWs, and both are discussed below specifically in their application towards biological membrane disruption

5.4 Factors modulating membrane disruption

Pulse MW are about twice more effective than continuous waves (CW) applied at same power levels (Watchtel *et al*., 1989). The former is believed to generate energetic electrons at the pulse peaks and have the capability to penetrate easily into biological cells than the latter. The peak power is expressed as the ratio of the average power to the duty cycle, hence is twice higher than CW (Ando *et al.* 2011). Repetitive short pulses have also been reported to induce stress in membranes of cells leading to membrane disruption (Nguyen *et al*. 2015). The success of electroporation/ membrane disruption can be modulated by the following MW E field parameters i.e. pulse amplitude, duration, number, shape and the repetition frequency. For instance, increasing the pulse duration and pulse number could result in joule heating and result in irreversible electroporation (Pliquett *et al.* 2007). Near optimal conditions favouring electroporation/ membrane disruption would require an increase in the amplitude, pulse number and duration (Rols 2006). The MW parameters required for the influx of small molecules such as fluorescent particles (3-2000 kDa) differs from that of larger molecules such as DNA (Batista Napotnik and Miklavcic 2018).

While the influx of small particles is easy, that of DNA is challenging and requires specialised conditions. This is because DNA molecules are negatively charged and are repelled by the cumulative negative charge on the membrane surface. While the influx of small molecules requires pulse duration between 10 to 100 μs, the influx of larger molecules require longer pulse durations lasting for a few milliseconds or a high voltage and short length pulses (Klenchin *et al.* 1991; Sukharev *et al.* 1992; Wolf *et al.* 1994; Satkauskas *et al.* 2002)

Cellular factors usually include the membrane composition and cell walls. Significant cell wall difference exists in Gram-negative, Gram-positive, Mycobacteria and yeast cells and these have been discussed in section 1.20 The shape of the cell also affects the success of electroporation/ membrane disruption (Canatella *et al.* 2001; Maček-Lebar and Miklavčič 2001; Pavlin *et al.* 2005). Cell membranes are composed of fatty acids (FA), cholesterol and membrane proteins (constituting about 50% of weight in cell membrane). These biomolecules contain ions that contribute to the transmembrane potential across the cell. The presence of the transmembrane potential does influence any external electric fields and could pose resistance to them. This interaction has the capacity to affect membrane fluidity and stability (Israelachvili and Mitchell 1975; Cullis and De Kruijff 1979; Smaby *et al*. 1994; Veatch and Keller 2005). The proportion of cells in suspension are also critical for electroporation/ membrane disruption. Dense cell suspensions tend to electrically shade other cells from E field radiation, thereby reducing the amount of E field exposures to such cells and reduce resealing process. In a low cell densities where single cells are

dominant, the fraction of cells with the membrane disrupted is significant and the resealing process is not hindered (Pavlin *et al.* 2002; Pucihar *et al.* 2006).

5.5 Challenges with MWs studies

A critical review of the literature reveals that, there is no accepted mechanism to explain MW mediated nonthermal effect. There is also a significant challenge in comparing data across studies as there are inconsistencies in the MW parameters applied. For instance, the magnitude of the E and H fields and the MW power varies in many published studies. In some studies, a conventional MW oven is used which cannot generate a constant MW E field energy. To effectively investigate nonthermal MW bioeffect, parameters such as MW power, E and H field intensities and the sample volume need to be standardised.

Controlling the temperature generated during MW exposure at a level that has no lethal effect on cells has been the common way to determine the existence of nonthermal MW effect. Major studies have focussed on the effect of 2.45 GHz MWs on mammalian cells, tissues and organs (Geddes *et al*. 2017) under nonthermal conditions, while those on bacterial and yeast cells are scarce. The most recent study shows the ability of 2.45 GHz MWs to alter cell membranes of *E. coli* (Rougier *et al*., 2014) under nonthermal conditions. In a similar study, membrane permeability was observed in a range of structurally diverse microorganisms but at a much higher frequency of 18 GHz (Shamis *et al.* 2011; Nguyen *et al*. 2015; Nguyen *et al*. 2016). Thus, there is a gap in knowledge with regards how MWs at 2.45 GHz interact with microorganisms under nonthermal conditions. Considering the significant difference in membrane composition that exist across microorganisms belonging to different taxa, there is the likelihood that they could

demonstrate varying responses following MW exposure. Also, 2.45 GHz is the designated bandwidth for the operation of common applicators such as computers, mobile phones and also in industrial and medical applications. Since mankind is frequently exposed to these devices, their possible effect on humans is an area of concern and continuous to attract research interest.

5.6 Aim

In light of the paucity of knowledge and the challenges in MW studies, the **aim** of this chapter was to investigate

1. the biological effects of 2.45 GHz MWs on biological materials using a defined MW applicator that allows the control of MW power and delivers pulses into a fixed sample volume and minimising bulk sample heating.
2. the ability of MWs to release nucleic acids from *M. smegmatis* as a model for *M. abscessus*.

5.7 Specific objectives

The specific objectives were to;

1. characterise the E, E+H and H field intensities within the sample tube and MW cavity
2. examine the effect of individual MW components (E, H and E+H) fields on the viability, morphology and membrane permeability of structurally diverse microorganisms to fluorescent dextran particles of various sizes (3, 10 and 70 kDa) following exposure to MW E. H and E+H fields.

3. determine if present, the half-life of MW mediated membrane disruption
4. examine the ability of MW components to induce DNA release from *M. smegmatis* and to characterise their disruptive effect on nucleic acids.

5.8 Materials

5.8.1 Description of MW system

As shown in the schematic diagram in Figure 5.2, the bench-top MW application system used in this study consists of the following elements: a MW signal generator (TEG-4000-1, Telemakus), a MW switch (TES-7000-50, Telemakus), 20 dB directional couplers 1 and 2 (ZABDC20-322H-S+, Mini-Circuits), MW power amplifier (ZHL-30W-252-S+), MW circulator (NG-3548, Racal-MESL), MW power sensor 1 (ZRP-Z51, Rhode & Schwarz), and power sensors 2 and 3 (TED-8000-40, Telemakus). Synchronized signal generation, switching on/off, and data acquisition from three power sensors are controlled by LabVIEW user interface. The combination of switch, attenuator and the directional coupler 1 produce microwave pulse with high on/off isolation (>50 dB) without turning on and off the MW signal generator. This also minimizes unwanted heating at the pulse OFF state due to leakage power. Power sensors 2 and 3 monitor the incident and the reflected power, respectively. Power sensor 1 also monitors the reflected power, which is technically redundant but was included as a safety measure in case the low-cost power sensors 2 and 3 fail. A cylindrical cavity resonator designed at 2.45 GHz when empty, reducing to about 2.45 GHz when sample-loaded (i.e. internal radius = 46 mm, internal height = 40 mm) is used as a MW applicator. This was made from Aluminium metal and operates in the TM_{010} mode. The cavity was critically coupled with a loop-terminated N-

type connector, which couples to the MW H field around the cavity's inner circumference. The maximum power delivered to the cavity was limited to 12 W (41 dBm). When excited in its TM_{010} mode, the cavity produces distinct E and H fields with the maximal E field obtained axially while maximal H field is obtained just inside the circumference, as shown in Figure 5.3. Each sample was contained in a 0.2 mL mini-micro tube (Alpha laboratories, UK) and was inserted into the cavity, one at a time, to allow samples to be exposed to the E field (position A), H field (position C) and E+H fields (position B), respectively.

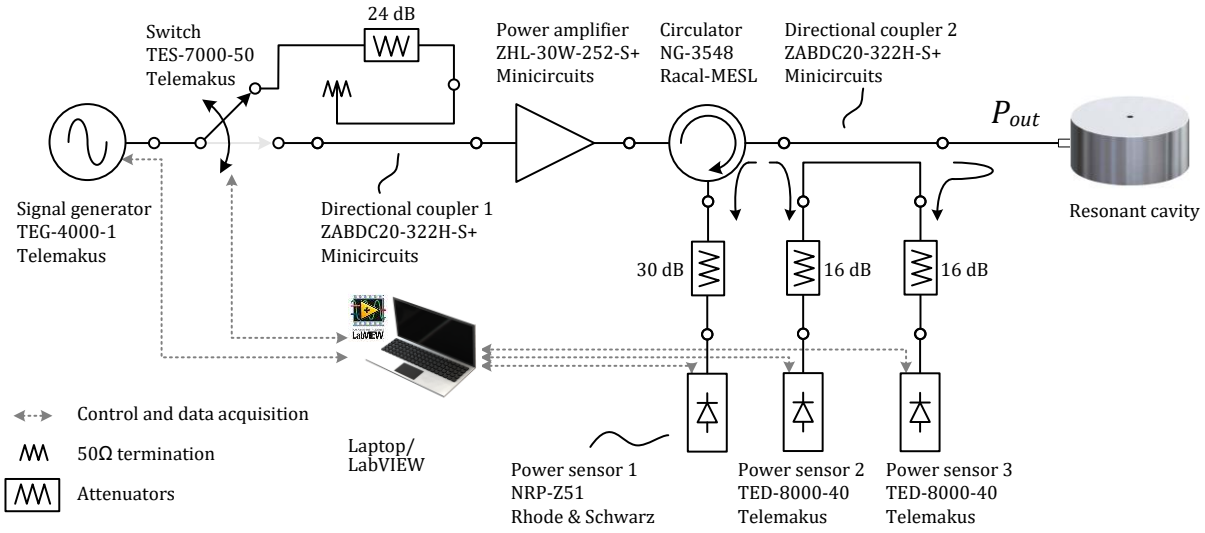

Figure 5.2. Schematic diagram of the bench-top microwave application system. Reproduced and modified with permission from (Williams *et al.* 2016)

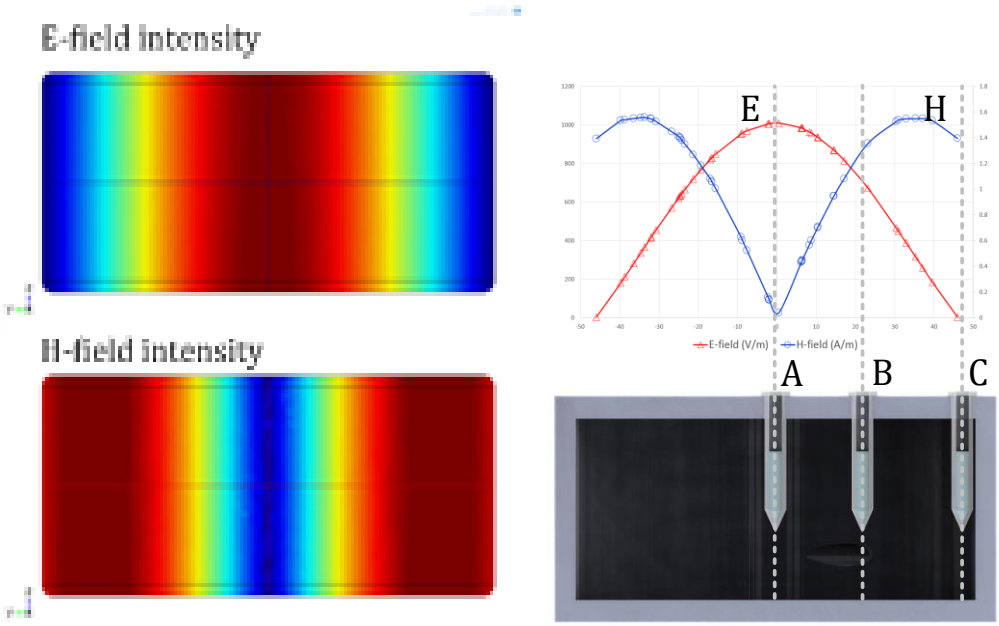

Figure 5.3. (Left) Modelling (COMSOL) of E and H field distribution inside the cavity. (Right) An illustration showing all sample tube positions (A, B, and C) inside the cavity aligned with E field maximum (A), mixed E+H field (B), and H-field maximum (C), respectively. In the experiment only one tube was inserted at a time. The distances between A-B and A-C are 27 mm and 42 mm, respectively. This cavity was designed to study the separate effect of MW E, H and E+H fields.

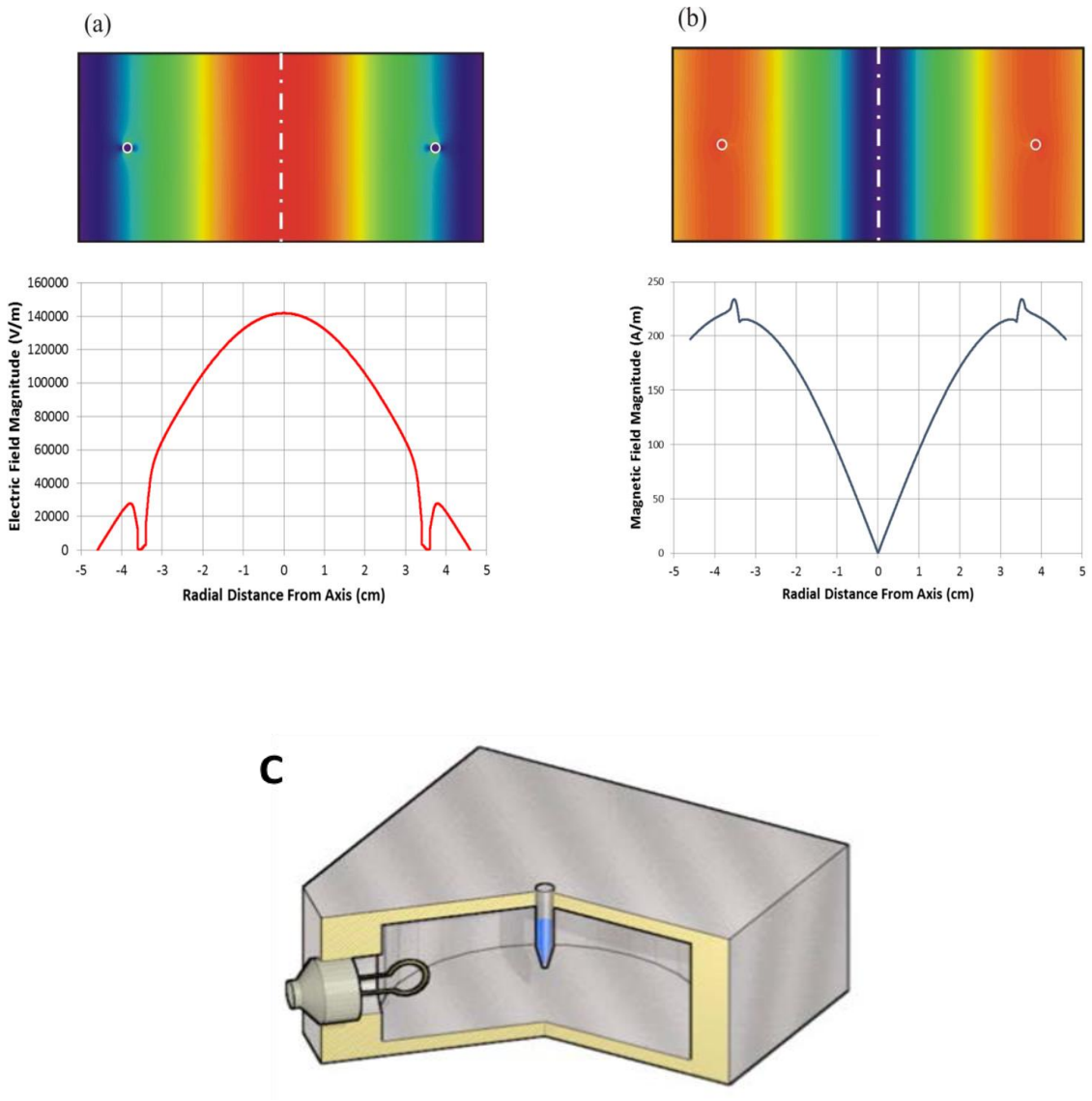

Figure 5.4 Modelling (COMSOL) of the E field (A) and H field (B) distribution at the centre of the one-hole TM010 cavity. Maximum E and H fields were obtained at 140 kV/m (1.4 kV/cm) and 0 A/m respectively. Picture reproduced with permission from (Williams *et al*. 2016). (B) A picture of the TM_{010} resonant cavity indicating sample location in the middle. This cavity was designed to study MW E field alone.

5.9 Methods

5.9.1 Culture and preparation of bacterial and yeast cells

The following microorganisms with differences in membrane structure were used in this study: *Escherichia coli* (NCTC 1093), *Staphylococcus aureus* (NCTC 13373), *Mycobacterium smegmatis* (NCTC 8159) and *Candida albicans* (NCPF 3179). *E. coli*, *S. aureus*, *C. albicans* and *M. smegmatis* were cultured as described earlier (section 2.3.2). Bacterial suspensions were also prepared to a concentration of 1 $x10^8$ CFU/mL as described in section 2.3.4.

5.9.2 DNA extraction

DNA was extracted from *M. abscessus* (ATCC 19977^T) following the method discussed in section 3.8.3.

5.10 MW irradiation

Two separate MW excitation conditions were applied. To examine pulsed MW effects of biological cells, a 1% duty cycle for 60 seconds was applied to cells as this reduces global heating in sample solution. For the speedy release of DNA from bacterial cells to support the development of the detection assay, a higher duty cycle was investigated. The duty cycle refers to the ratio of pulse duration or pulse width to the total period of the waveform and is expressed in ratio or as a percentage.

5.10.1 Effects of MW radiation on *M. abscessus* DNA

To investigate the effect of MWs on purified *M. abscessus* DNA (3.5 ng/μL) where there is minimal global heating, 2.45 GHz MWs were applied at 1% duty cycle for 60 seconds.

The pulse period and the ON time were kept constant at 1000 ms and 10 ms, respectively. Post microwaved DNA were quantified for dsDNA and ssDNA to determine whether there is any decrease in the dsDNA and ssDNA concentrations. The concentrations were determined using the Qubit BR assay kit and Qubit 3.0 fluorometer. Untreated DNA was included as a control.

5.10.2 Effect of 2.45 GHz MW on the cell density of *M. smegmatis*

Cells of *M. abscessus* (170 μL; 1 x10^8 CFU/mL) were treated with MW E field alone at 1% for 60 seconds, using the same pulse parameters as above (section 5.10.1). As a positive control, cells were treated with 1% Triton X-100 for 60 min at 37 °C. Triton X-100 is a chemical known to disrupt bacterial cell wall. Untreated cells were included as a negative control.

5.10.3 Determination of cell viability in MW treated samples

The viability of cells (*S. aureus*, *E. coli*, *C. albicans* and *M. smegmatis*) was determined following exposure to E, H and E+H fields. MW power was pulsed at 1% duty cycle for 60 sec. This time frame was used to minimise global heating while exposing samples to MW pulses. The pulse period was the same as above (section 5.10.1). Sample excitation was performed at room temperature and repeated 5 more times with a 2 min interval between each excitation cycle. Cell viability was determined immediately after MW exposure using the drop count method (Miles and Misra 1938). Cells were incubated overnight at 37 ºC and the dilution containing countable bacterial colonies (between 30 and 300) were used to determine viability. *M. smegmatis*, *E. coli* and *S. aureus* were plated

on LB agar and *C. albicans* was plated on yeast extract agar. Cells without MW treatment were included as negative controls.

5.10.4 Quantification of dsDNA released following MW treatment

Using similar MW exposure conditions, sample volume and concentration, 170 µL aliquots of test microorganism (*M. smegmatis*) in a 0.2 mL mini-micro tube (Alpha laboratories, UK) were placed in the different radial positions of the TM_{010} mode resonant cavity to determine the effect of exposure to E, H and E+H fields on DNA release. Sample exposure was performed for 5 times. DNA concentration of the bacterial suspension was determined immediately following exposure to E, H and E+H fields using the Qubit dsDNA BR Assay Kit (Invitrogen) and Qubit 3.0 fluorometer (Invitrogen). Suspensions of MW treated cells (20 µL) were mixed with 180 µL of dsDNA BR Qubit assay reagent and vortexed. The concentration of dsDNA was then quantified using the Qubit 3.0 fluorometer (Invitrogen). Untreated bacterial suspension was used as a negative control.

5.10.5 MW induced membrane disruption

To determine the effect of MW (E, H and E+H) field exposure on cell wall permeability the entry of fluorescently labelled dextran particles into micro-organisms of structural diversity was examined. Suspensions of the following size particles were prepared in water and tested; 3 kDa (Cat. No. D3308) and 70 kDa (Cat. No. D1818) both tetramethyl rhodamine (TMR) and 10 kDa Alexa 488 (Cat. No. D22910), all purchased from Fisher Scientific, UK. Cells were treated with MW power pulsed at 1% duty cycle for 60 sec. Sample excitation was repeated 5 more times with a 2 min interval between each

irradiation cycle to minimise sample heating. MW treated samples were centrifuged at 10000 g for 5 min, washed twice with distilled water and then resuspended in 100 µL of distilled water. An aliquot (10 µL) of this suspension was spotted on a microscope slide, mounted with glass cover slip (diameter = 0.1-0.17 mm) (Fisher Scientific, UK) and observed with a fluorescent microscope (Leica DM IRB, Germany) using ×63 objective lens under oil immersion. TMR dextran particles (3 and 70 kDa) and 10 kDa Alexa 488 were excited using the green (530-550 nm) and blue (460-490 nm) excitation filter blocks, respectively. Ten images from different fields of view were captured under phase contrast and fluorescent views, and subsequently analysed. The percentage of fluorescent cells after separate exposures to E, H and E+H fields were calculated as the ratio of the total number of cells under phase contrast to the number of fluorescent cells. Cell suspensions containing fluorescent dextran particles without MW treatment was used as controls. All experiments were performed in triplicate and the percentage of fluorescent and non-fluorescent cells calculated as mean ± standard deviation (SD). To determine if MW exposure caused permanent damage to the cell wall, permeability to 10 kDa fluorescent dextran particles was assessed in *M. smegmatis* at 5, 10, 60, 120 and 300 seconds following MW E field exposure.

5.11 Theoretical and experimental calculation of bulk sample heating

To predict the rate of bulk heat generation following MW exposure of cell suspensions under the conditions used in this study, we employed a formula based on the definition of the specific heat capacity of the cell suspension, close to that of water C_w, of approximate value of 4.2 J/g/K. The initial rate of temperature rise in a sample during MW exposure is then defined as: $dT/dt = P/(mC_w)$, where m is the mass of the sample and P is the MW

rms power dissipated. The total sample volume is 170 µL (i.e. a mass of approximately 0.17 g). Since the MW cavity is critically coupled and also, since the water sample provides the main load, the rms MW power dissipated is approximately the rms input power (P_{in}) generated by the MW circuitry, i.e. 12 W, which is reduced to an effective value of 0.12 W when taking into account the standard 1 % duty cycle. This yields an initial heating rate of approximately 0.17 ^{0}C/s over the standard 60 s exposure time, even if this initial heating rate were to be maintained the maximum possible temperature rise would be about 10 ^{0}C; in practice, heat transfer to the surroundings will limit this temperature rise to only a fraction of this maximum value, so we expect a temperature rise of a few ^{0}C at most. To validate this calculation, the temperature of samples during MW excitation was measured using a Luxtron fibre optic temperature sensor (LumaSense Technologies, Santa Clara, CA, USA). Using this temperature sensor probe, the bulk temperature increases of the cell suspension placed at the E field position was measured to be 2.6 ± 0.4 ºC over 60 seconds exposure time at 1 % duty cycle with 12 W rms power input and this is entirely consistent with the calculation above.

5.12 Theoretical calculation of MW power generated in one-hole and three-hole MW cavities

The total power generated within the MW cavity was calculated using the formula below

$$P_{diss} = \pi\varepsilon_0\varepsilon_2 f E_1^2 V \quad \text{……. Eqn. 5.2}$$

where:

P_{diss} = rms MW power dissipated into the cavity (around 12 W)

ε_0 = permittivity in vacuum, 8.85×10^{-12} F/m

ε_2 = dielectric loss factor of water, approximately 9.2 at 2.45 GHz

f = microwave frequency, 2.45 GHz

E_1 = the spatially averaged electric field amplitude generated within the sample

V = the sample volume placed in the MW cavity, 170 µL

To determine the E field value, Eqn. 5.2 can be rearranged as;

$$E_1 \approx \sqrt{\frac{P_{diss}}{\pi \varepsilon_2 \varepsilon_0 f V}} \quad \ldots\ldots \quad \text{Eqn. 5.3}$$

Thus, the calculated E field value is estimated at **10.2 kV/m** for the one-hole TM_{010} mode cavity. Using the 3-hole cavity designed for combined E, H and E+H fields excitation, the power dissipated in the cavity is readjusted to accommodate the two additional holes that have been created. The total power dissipated in the 3-hole cavity (fig 5.3, right) becomes;

$$P_{diss} = P_A + P_B + P_C \quad \ldots\ldots\ldots\ldots\ldots \text{Eqn. 5.4}$$

where:

P_A = power dissipated at port A

P_B = power dissipated at port B, which is approximately half of that in P_A (i.e. P_B = ½ P_A)

P_C = power dissipated in port C, which is approximately zero since there is almost zero E field at this position (rather, a maximum H field).

Thus, for the cavity displayed in Fig 5.3, with three samples at each of the ports A, B and C, Eqn. 5.3 now becomes

$$E_1 \approx \sqrt{\frac{4P_{\text{diss}}}{5\pi\varepsilon_2\varepsilon_0 f V}} \quad \text{……. Eqn. 5.5}$$

Thus, the calculated E field amplitudes within the samples at for ports A, B and C is 9.2 kV/m, 4.6 kV/m and 0 kV/m**,** respectively. To determine the magnitude of the H field at the perimeter of the cavity, the formula (below) was applied.

$$H_1 = E_1 \frac{J_1(2.405)}{377}/\eta_0 \text{……... Eqn. 5.6}$$

where:

$J_1(x)$ is a first order Bessel function of the first kind

η_0 is the free space wave impedance, approximately 377 η.

Since $J_1(2.405) = 0.519$, the amplitude of the azimuthal magnetic field at port C is determined to be 12.6 A/m.

5.13 Data Analysis

Results were analysed with SPSS (v.23). Significant differences within groups were determined using one-way analysis of variance (ANOVA) followed by a multiple comparison analysis using Tukey and Bonferroni tests. Graphs were plotted in Microsoft

excel 2016. All simulations were performed using COMSOL Multiphysics software (version 5.3a). Schematic drawing of the bench-top microwave was performed using 3D SolidWorks.

5.14 Results

5.14.1 Estimating the global heat generated in a microwaved sample using COMSOL

The maximum E field and H field intensity at the central position of the one-hole TM_{010} mode cavity (Fig 5.4) was calculated at 10.24 kV/m and 0 A/m respectively. Similarly, E and H field intensity at the central and circumferential sample positions within the three-hole TM_{010} mode cavity (Fig. 5.3) were calculated to be approximately 9.16 kV/m and 12.6 A/m (corresponding to a magnetic flux density of 15.80 µT), respectively. Based on the design of the cavity, the E field is halved at port B of the three-hole cavity and this was calculated to be 4.58 kV/m.

By placing the sample tube into the three-hole TM_{010} mode cavity, the field intensity is perturbed. For this reason, the Q value (representing the amount power dissipated into the sample) at the three sample positions were measured by determining the Q value (power dissipated into sample) in each sample tube containing similar sample volumes of 170 µL. The Q values when cavity is loaded with sample and without sample at the E, E+H and H positions are presented in Table 5.1 below.

Table 5.1 Mean F_o, Q and loss (dB) measured at E, E+H and H field positions with loaded sample (water)

	E field	E+H field	H field
Mean F_o (MHz)	2353.32 ± 2.92	2392.3 ± 1.23	2406.28 ± 0.05
Mean Q_L	644 ± 10.98	1798.725 ± 143.20	7459.05 ± 458.52
Mean Loss (dB)	-43.595 ± 0.13	-34.4425 ± 0.63	-23.1275 ± 0.38

The Q value for the empty tube (Q_E) was measured at 7429

With the measured Q values, the power dissipated (P_{diss}) and mean E field in the sample tube can be related by the formulae below;

$$P_{diss} \propto \Delta\left(\frac{1}{Q}\right) \quad \text{..... Eqn. 5.7}$$

$$P_{diss} \propto E_{in}{}^{2}$$

Therefore;

$$E_{in} \propto \sqrt{\Delta\left(\frac{1}{Q}\right)} \quad \text{..... Eqn. 5.8}$$

The inverse of the change in Q (ΔQ) is determined using the formulae below;

$$\Delta\left(\frac{1}{Q}\right) = \frac{1}{Q_L} - \frac{1}{Q_E}$$

Where Q_L represent the Q value when the cavity is loaded with water at E field position and Q_E is when the cavity is empty. Therefore,

$$\Delta\left(\frac{1}{Q}\right) = \frac{1}{644} - \frac{1}{7429}$$

$$= 0.001418$$

Based on Eqn 5.8, mean E field at E field position is 0.03765 V/m. Similarly, inverse of ΔQ and mean E field dissipated at position E+H are determined below;

$$\Delta\left(\frac{1}{Q}\right) = \frac{1}{Q_L} - \frac{1}{Q_E}$$

Where Q_L represent the Q value when the cavity is loaded with water at E+H field position and Q_E is when the cavity is empty.

$$\Delta\left(\frac{1}{Q}\right) = \frac{1}{1799} - \frac{1}{7429}$$

$$\Delta\left(\frac{1}{Q}\right) = 0.000421$$

$$E_{in} = 0.\ 02051 \text{ V/m}$$

Finally, inverse of ΔQ and mean E field dissipated at the H field position is also determined below

$$\Delta\left(\frac{1}{Q}\right) = \frac{1}{Q_L} - \frac{1}{Q_E}$$

Where Q_L represent the Q value when the cavity is loaded with water at H field position and Q_E is when the cavity is empty.

$$\Delta\left(\frac{1}{Q}\right) = \frac{1}{7459} - \frac{1}{7429}$$

$$\Delta\left(\frac{1}{Q}\right) \propto 0$$

Therefore, $E_{in} \propto 0$ V/m

Based on the above formula, the fractional E field dissipated into the sample at the E, E+H and H field positions are 1, 0.544 and zero respectively. This further explains that there is E field reduction in the E+H positions.

5.14.2 Effect of MW E field exposure on the cell morphology and viability of *M. smegmatis*

The effect of MW energy (1% duty cycle for 60 seconds) on cellular morphology and cell viability of *M. smegmatis* was determined. Gross cellular morphology was not affected following MW treatment, as no significant difference in optical density was observed ($p > 0.05$). However, there was a significant decrease in cell density following chemical treatment ($p < 0.001$) (Fig 5.5).

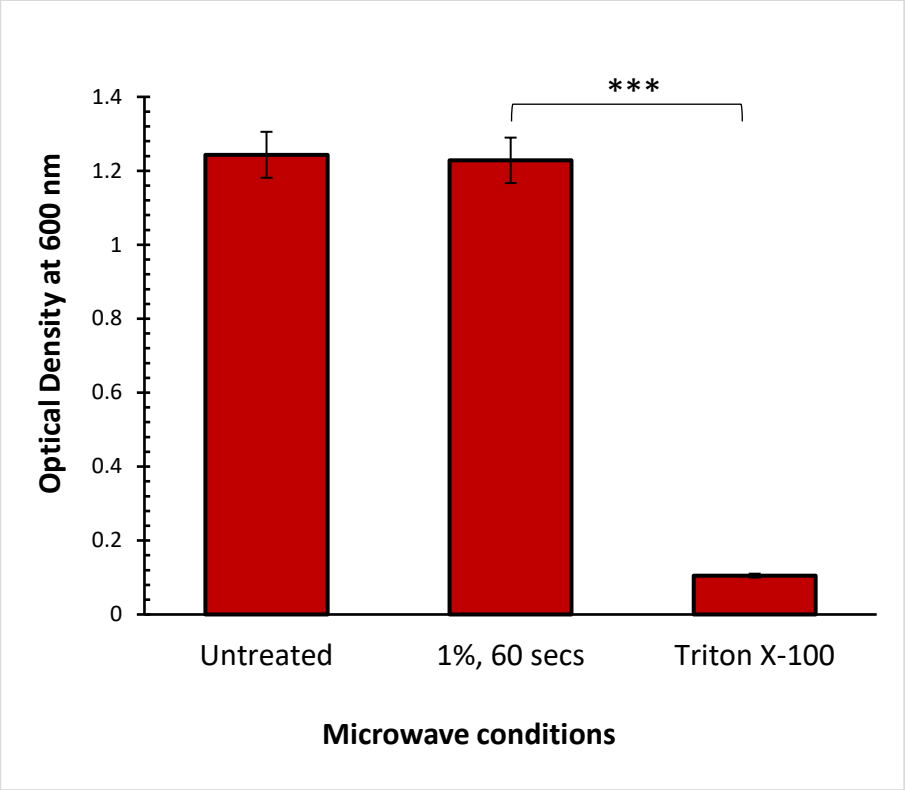

Figure 5.5 Effect of MWs on the cell morphology of *M. smegmatis*. The optical density of cells of *M. smegmatis* were measured following MW treatment (1% duty cycle for 60 seconds). Untreated and chemical (1% Triton X-100) treated cells were included as negative and positive controls respectively. *M. smegmatis* cells density were not affected following MW treatment ($p > 0.05$). Cells density was significantly reduced following chemical treatment ($p < 0.001$). Data represent mean of triplicate experiment ± standard deviation.

Cell membranes of microorganism act as a permeability barrier, protecting cells from the hostile environment and sustain viability. Any breach in membrane permeability will increase the influx and efflux of chemicals and may adversely affect viability. To determine the effect of MW exposure on the viability of *M. smegmatis* we counted the number of viable cells (CFU/mL) immediately following exposure to the E, H, and E+H fields. The effects of exposure to E field radiation can be seen in figure 5.6. At 1% MW pulsing, there was no significant loss ($p > 0.05$) of viability after 60 seconds. A higher

MW duty cycle (30%) was also tested to determine cells viability and when this was investigated, there was a significant loss of cells viability ($p < 0.001$) after 30 seconds. At this duty cycle, the temperature of cells suspension reached approximately 79°C. Thus, it possible that extreme heating could have resulted in the loss of cells viability (Fig 5.6).

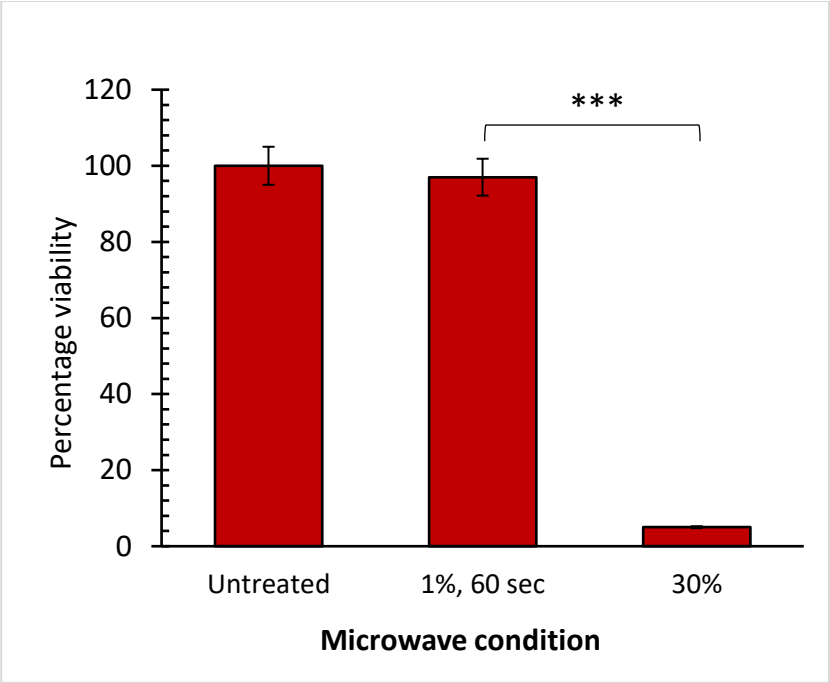

Figure 5.6 Effect of MW E field on *M. smegmatis* viability. Suspension of *M. smegmatis* were treated with pulse MWs at 1% duty cycle for 60 secs and 30% duty cycles for 30 seconds. Cells viability (expressed as percentage) was determined using the drop count method. Pulse MW treatment of cells at 30% duty cycle reduced the viability significantly ($p < 0001$). Data represent mean of 3 independent experiment ± standard deviation.

The effect of the H field and the E+H fields combined at the same 1% duty cycle on the viability of *M. smegmatis* was investigated. As can be seen from fig 5.7, exposure had no significant effect ($p>0.05$) on viability.

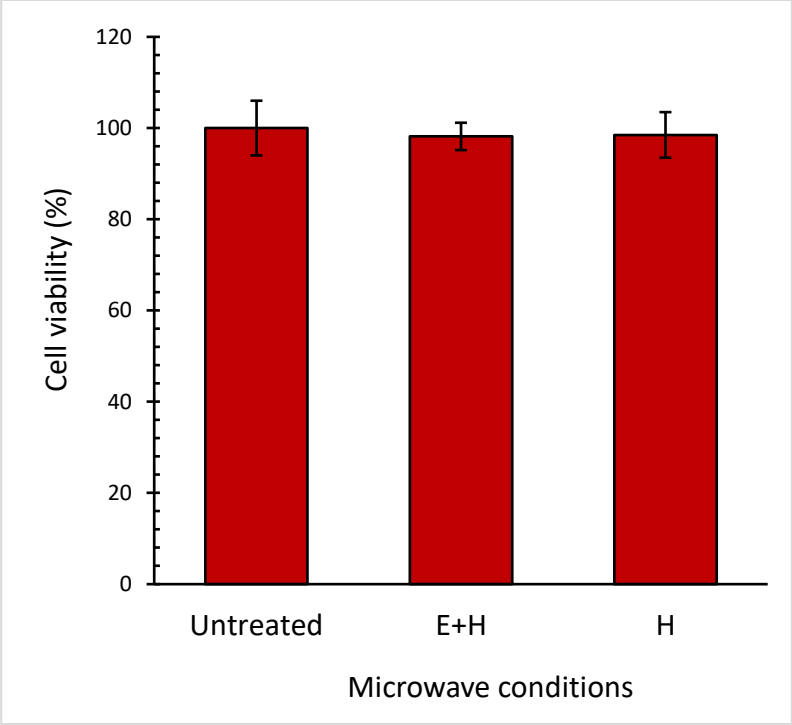

Figure 5.7 The effect of E and E+H MW fields on the viability of *M. smegmatis*. Suspension of *M. smegmatis* were treated with E and E+H fields at 1% duty cycle for 1 min. MW treatment were repeated for 5 times. Cells viability was determined and expressed as a percentage. The E and E+H fields did not significantly affect cells viability ($p > 0.05$). Data represent mean of 3 independent experiment ± standard deviation.

Since cells belonging to different taxa have different membrane compositions and cell wall structures, the effect of exposure of these cell types to the various MW fields were determined. The viability of *E. coli*, *S. aureus* and *C. albicans* under the same test condition (1% duty cycle for 60 seconds) and to eliminate global heating was investigated. Exposure to E, H and E+H fields at a 1% duty cycle for 60 seconds had no significant effect ($p>0.05$) on the viability of any of the test microorganisms (fig. 5.8).

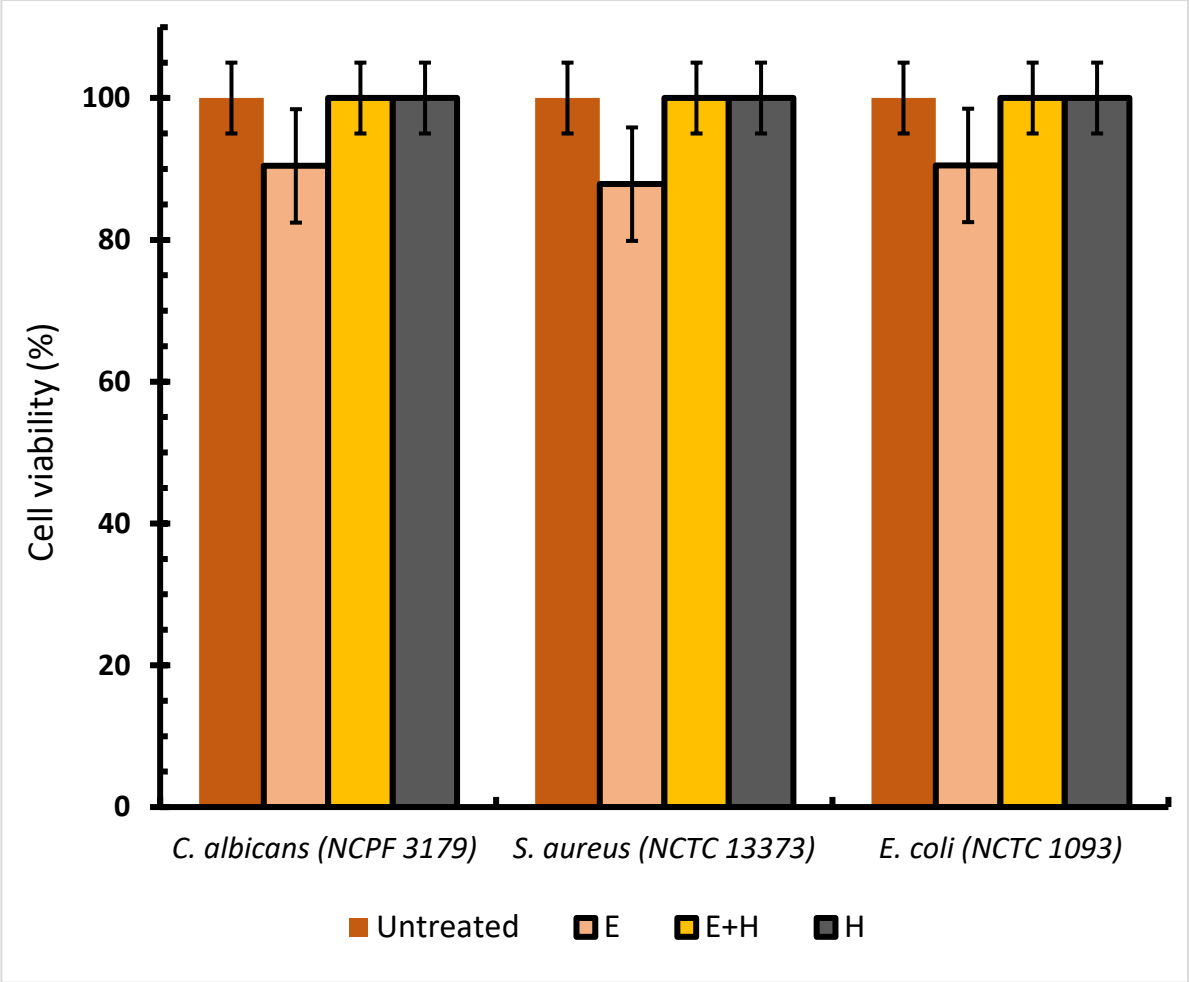

Figure 5.8 The effects of E, H and E+H fields on cell viability. MW power was pulsed at 1% duty cycle for 60 seconds. Sample excitation was repeated 5 more times with a 2 min interval between each excitation cycle. Cell viability after exposure to E, H and E+H fields was determined and expressed as percentage. Viability reduced (but not significantly) in cells treated with E fields alone (p>0.05), while cells treated with H and E+H fields remained unaffected as untreated. Data are mean ± SD of three independent experiments.

5.14.3 Effect of MW E, H and E+H fields on membrane permeability

Fluorescent dextran particles have been used to determine membrane integrity (Shamis *et al*. 2011). Infiltration of dextran particles into MW exposed cells would suggest some form of cell wall disruption. To determine if this was the case, cells *E. coli*, *M. smegmatis*,

S. aureus and *C. albicans* were exposed to MW E, H and E+H fields at 1% duty cycle for 60 seconds in the presence of 3 kDa fluorescent dextran particles. While exposure to the H field and a combination of E+H fields did not result in the internalisation of 3 kDa dextran particles (fig. 5.9), all microorganisms exposed to the E field alone exhibited a significant uptake of 3 kDa fluorescent dextran particles ($p<0.05$) (fig. 5.9 - 5.11).

To determine if cell wall composition of a microorganism affected its ability to internalise dextran particles following exposure to E field radiation, the relative ability of the cells to internalise 3kDa dextran particles was compared (Fig 5.11). Cells of *M. smegmatis* (50.4 ± 2.5%) demonstrated a significantly higher ($p < 0.05$) level of particle uptake compared to the other isolates. The fluorescence of *C. albicans* (30.5 ± 2.1%) was significantly higher than those of *E. coli* (17.5 ± 1.9%) ($p=0.01$) but not in *S. aureus* (23.6 ± 4.6%) ($p = 0.096$).

Variation in the degree of MW-mediated disruption in the test organisms was further assessed by comparing their ability to internalise 10 and 70 kDa fluorescent dextran particles. All micro-organisms except for *S. aureus* internalised 10 kDa dextran particles while none of the organisms appeared to internalise 70 kDa dextran particles (Fig 5.11). The low proportion of untreated fluorescent cells in each population are likely to represent dead or damaged cells which have non-specifically bound the fluorescent dextran particles (Shi *et al.* 2007; Peterson *et al.* 2012).

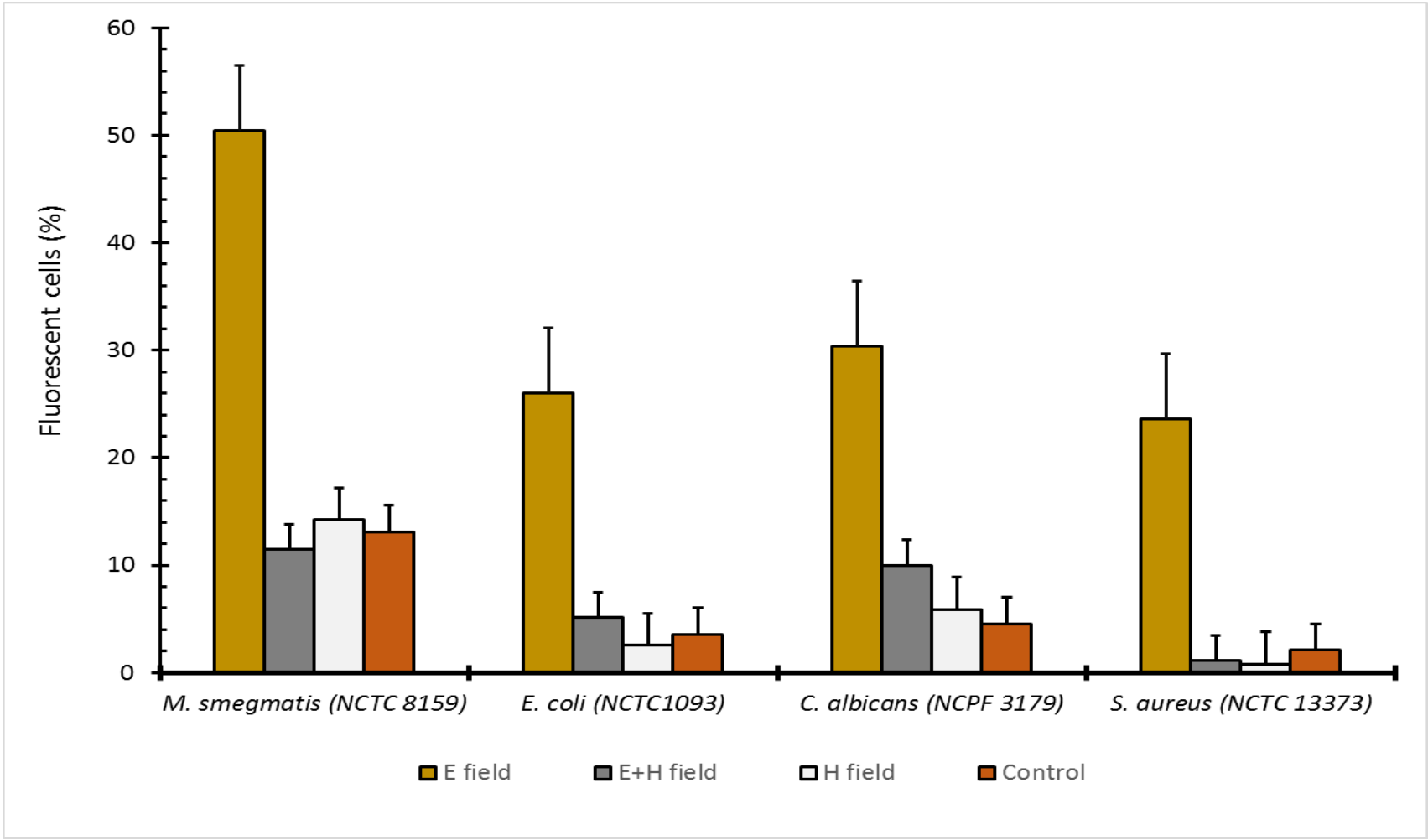

Figure 5.9 Quantification of fluorescent cells after separate exposure to MW E, H and E+H fields at 1% duty cycle for 60 seconds. Sample excitation was repeated 5 more times with a 2 min interval between each excitation cycle. Cells exposed to E+H-field (grey bars) and H-field (white bars) did not result in significant uptake of 3 kDa dextran particle in all cells tested as compared to the control group (orange bar) ($p>0.05$). Cells exposed to E field alone (dark bars) resulted in a significant uptake of 3 kDa fluorescent dextran particle ($p<0.05$). Values represent mean ± SD of three independent experiments.

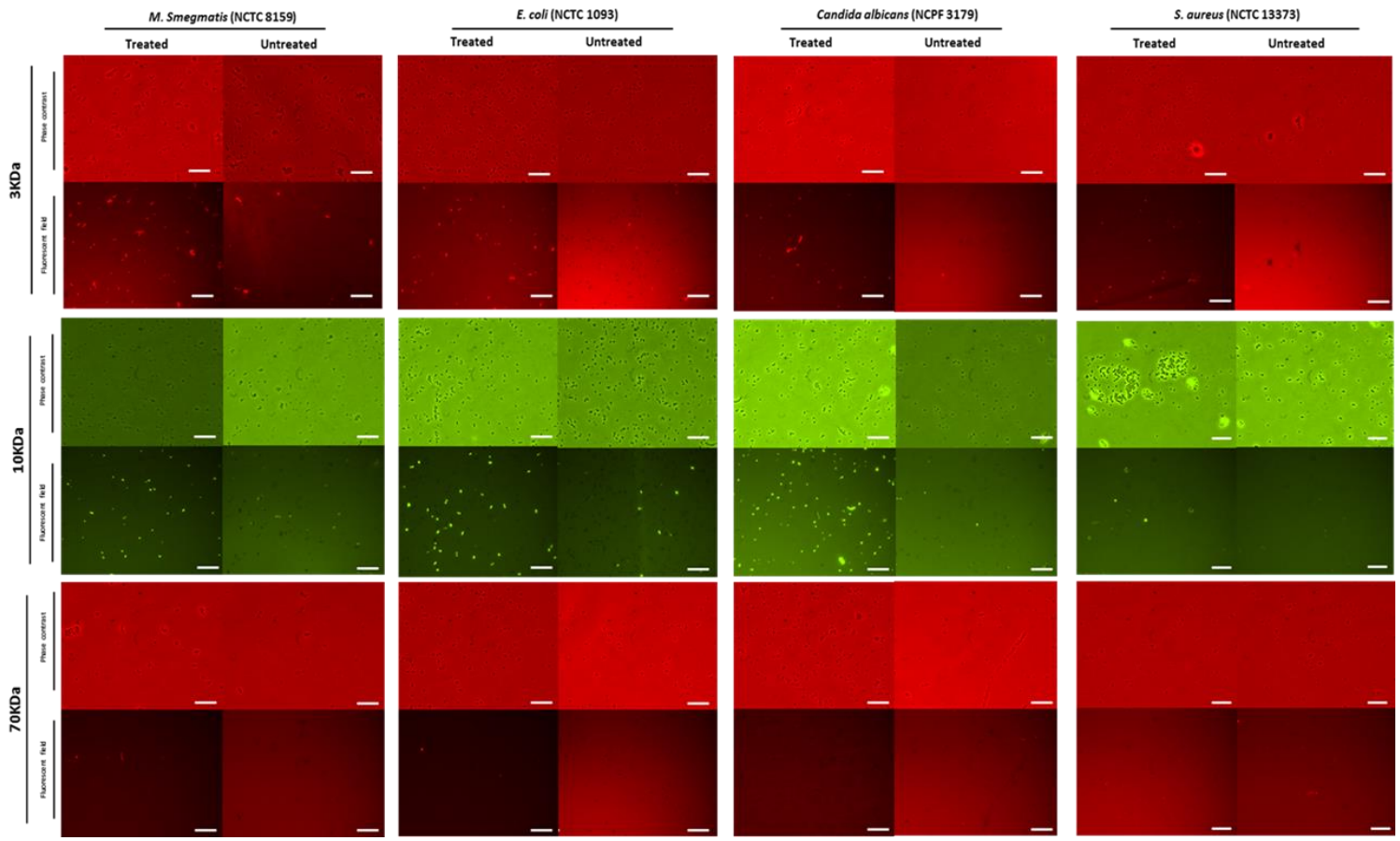

Figure 5.10 Uptake of varying sizes of fluorescent dextran particles into cells after MW E-field exposure at 1% duty cycle for 60 seconds. Sample excitation was repeated 5 more times with a 2 min interval between each excitation cycle. Images captured under phase contrast and fluorescent fields following 3 kDa, 10 kDa and 70 kDa dextran application to MW treated cell suspensions of *M. smegmatis* (NCTC 8159), *E. coli* (NCTC 1093), *C. albicans* (NCPF 3179) and *S. aureus* (NCTC 13373) with corresponding controls (MW untreated). Images in phase contrast are of the same field as fluorescent view. Mostly 3 kDa and 10 kDa dextran were internalised in *M. smegmatis*, *E. coli*, *C. albicans* but not 70 kDa. Only 3 kDa was internalised in *S. aureus*. Scale bars correspond to 20µm.

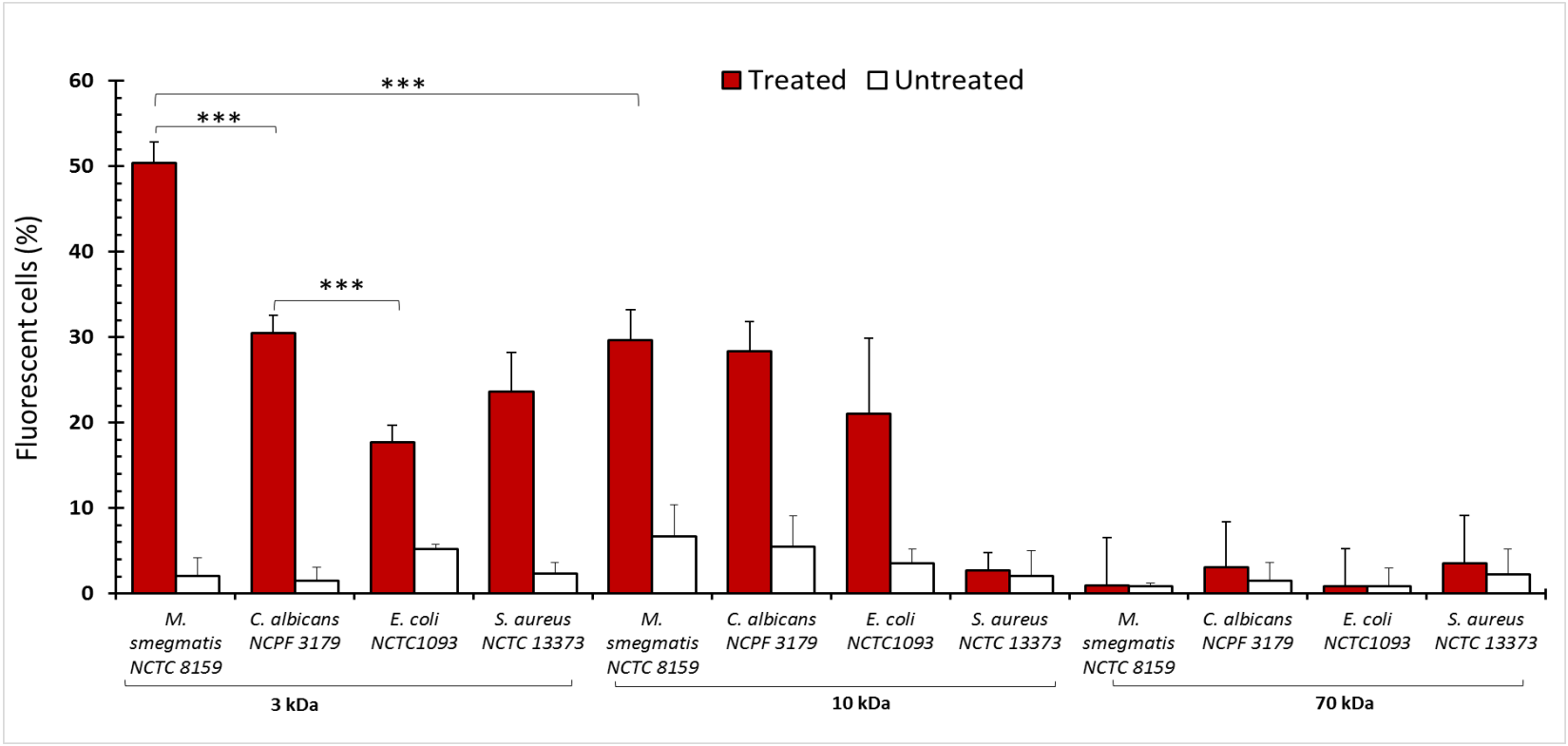

Figure 5.11 Quantification of fluorescent cells after MW E-field exposure at 1% duty cycle for 60 seconds. Sample excitation was repeated 5 more times with a 2 min interval between each excitation cycle. The percentage of fluorescent cells after MW treatment (grey bars) and the corresponding untreated cells (white bars) was determined for each dextran particle size. Percentage of fluorescent cells was calculated as a ratio of the number of cells in fluorescent view to the total number counted under phase contrast. The percentage of fluorescent cells with 3 kDa dextran uptake was significantly high in *M. smegmatis* than in all cells (p<0.05) and in *C. albicans* in comparison to *E. coli* (p=0.01). Fluorescent cells of *M. smegmatis* and *S. aureus* decreased significantly when dextran size was increased to 10 kDa (p<0.05). None of the cells internalised the 70 kDa dextran particle. The label (*) and (***) represents (p<0.05) and (p<0.0001) respectively between groups compared and are statistically significant. Values represent mean ± SD of three independent experiments.

Studies suggest that, different types of phospholipids and fatty acids interact differently with MWs and hence could contribute to their varying level of sensitivity to MWs (Nguyen *et al*., 2016). Owing to the observed difference in the uptake of dextran particles across the different types of microorganisms, we sought to determine whether differences in fatty acid and phospholipids did contribute to this. The percentage of fatty acids (saturated and unsaturated) and phospholipids present in all cells reported in previous studies were analysed and are presented in Table 5.2. Comparing Table 5.2 and Figure 5.11, differences in fatty acids composition (saturated and unsaturated) does not explain why uptake of dextran particles across microorganisms differ, and thus other factors could be responsible.

Table 5.2. Compositions of fatty acids (saturated and unsaturated) and phospholipids in cell membranes of *S. aureus, E. coli, C. albicans and M. smegmatis*.

Biomolecule	*S. aureus*	*E. coli*	*C. albicans*	*M. smegmatis*
Saturated fatty acid (%)	96.7	77.5	35.8	89
Unsaturated fatty acid (%)	<1	22.5	64.2	11
Phospholipid	PG, LPG	PE	PC, PE	PE, PI, CL

PG = Phosphatidyl glycerol
LPG = Lysyl phosphatidyl glycerol
PE = Phosphatidyl ethanolamine
PC = Phosphatidyl choline
PI = Phosphatidyl inositol
CL = Cardiolipin

5.14.4 Duration of cell wall disruption

To determine the time frame of cell wall disruption *M. smegmatis* cells were exposed to MW E fields 1% duty cycle for 60s and 10 kDa dextran particles were added at different time periods post exposure after which intracellular fluorescent was determined. The shortest time to be investigated was 5 seconds post exposure which resulted in a 75.6% reduction ($p<0.05$) compared to when cells are microwaved in the presence of dextran particles (positive control). There was no significant difference in dextran particle uptake at periods longer than 5 seconds suggesting that disruption is transient (Fig 5.12).

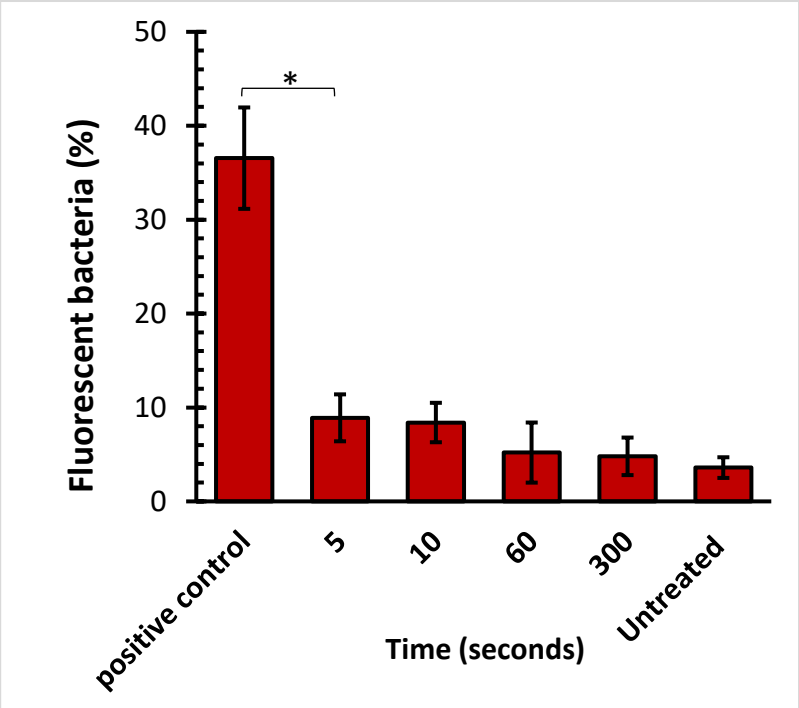

Figure 5.12 Time taken to regain structural integrity following MW exposure at 1% duty cycle. Addition of dextran particle (10 kDa) to MW E field treated bacterial suspension was delayed for 5s, 10s, 60 and 300 seconds. The percentage of fluorescent bacteria was significantly high ($p<0.05$) in MW treated suspension containing dextran particle (positive control) than when the addition of dextran particle was delayed (5, 10, 60 and 300 seconds) and in untreated. Values represent mean ± SD of two independent experiments.

5.14.5 Effect of MW E field exposure on the release of DNA from *M. smegmatis*

To determine if exposure to the level of MW radiation which disrupted membrane permeability did result in the release of intracellular material, the concentration of dsDNA in cultures of *M. smegmatis* before and after exposures to 1% pulse of E, H and E+H MW fields was determined. While there was no significant increase in the concentration of dsDNA following five sequential exposures to E+H and H field radiation, there was a significant increase ($p<0.05$) in dsDNA concentration following five E field exposures (fig. 5.13). A release of nucleic acids from the cells without significant loss of viability (Fig 5.8) was observed. This could be attributed to a myriad of factors. For instance, increased cells population could reduce the local E field distribution in sample suspension in comparison to low cell suspensions and subsequently decrease the transmembrane voltage on the cell membrane (Pucihar *et al*., 2007). In a high cell population other cells could be shielded from MW interaction. Thus, the amount of dsDNA released could not be released from the entire cell population. The orientation of cells in the suspension could also affect transmembrane potential as cells at the poles have maximal transmembrane potential than and are easily electroporated (Kanduser and Miklavcic, 2008).

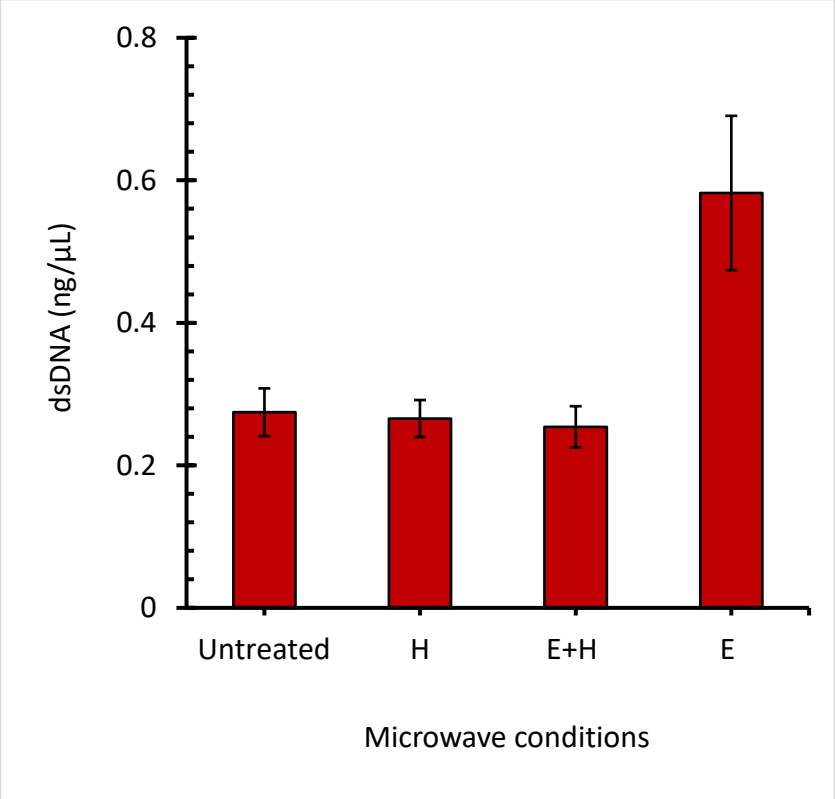

Figure 5.13 Release of double stranded DNA (dsDNA) following MW exposure. A suspension of *M. smegmatis* was treated (5 times) with MW E, H and E+H fields. MW pulsing was kept at 1% duty cycle for 60 seconds. A 2 min interval was allowed between exposures to avoid sample heating. The concentration of dsDNA release was significantly higher ($p<0.05$) in suspensions treated with MW E field alone. Data are mean ± SD of three independent experiments.

5.14.6 Effect of MW E field exposure on purified DNA

The effect of MW exposure on the structural integrity of genomic DNA isolated from *M. smegmatis* was determined to assess if the energy levels employed had a detrimental effect on DNA recovery. Nucleic acid concentration was measured immediately following MW exposure. The concentration of ssDNA and dsDNA following MW treatment at a 1% duty cycle for 60 seconds was significantly reduced ($p < 0.001$) (Fig 5.14). 30% duty cycle was applied to test its effect on DNA integrity as significant heating (79°C) is produced with higher MW pulses.

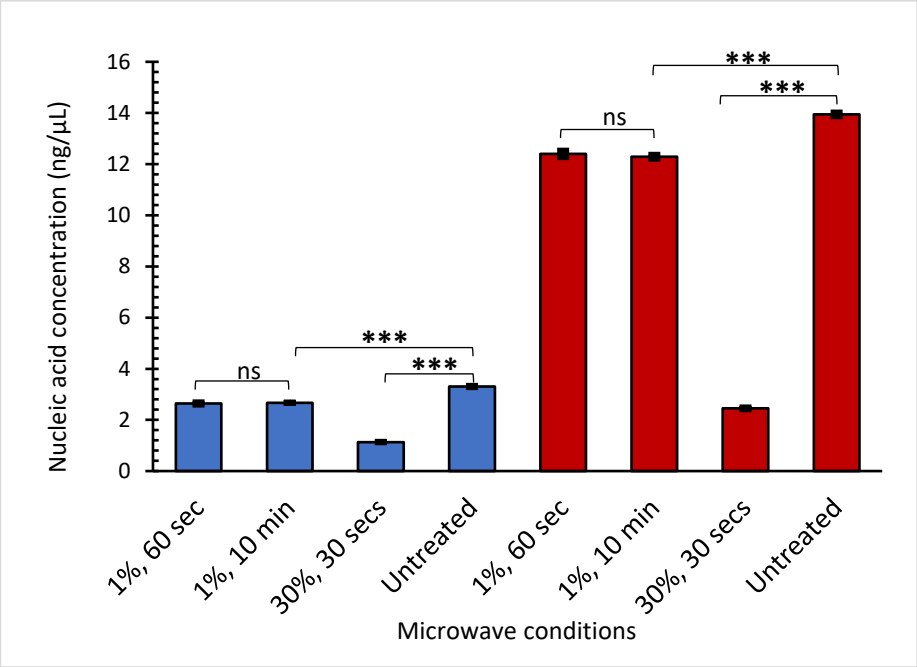

Figure 5.14 Effect of MW exposure on the structural integrity of *M. smegmatis* genomic DNA. The concentration of dsDNA (blue bar) and ssDNA (red bar) were quantified using the Qubit assay reagent following MW treatment at 1% duty cycle for 60 seconds and 10 minutes and at 30% duty cycle for 30 seconds. Untreated DNA was used as a control and the concentration of dsDNA and ssDNA were also quantified. MWs significantly reduced ($p < 0.001$) the concentration of dsDNA and ssDNA following MW treatment at 1% and 30% duty cycle for 60 seconds and 30 seconds respectively. The concentration in nucleic acid concentration was not significant (ns) after multiple exposures (10 times) at 1% duty cycle for 60 seconds. Data represent mean of triplicate experiment ± standard deviation.

5.15 Discussion

The biological effects of MWs are associated with thermal and non-thermal mechanisms. The former is attributed to temperature change while the latter is temperature independent and is thought to be due to the action of E and/ or H field effects (Challis 2005). The present study focused on characterising the effect of nonthermal MWs (E, H and E+H) on cell morphology, viability and the cell wall permeability of a range of structurally diverse microorganisms.

To examine the existence of nonthermal MW effects, maintaining the temperature change at a level that is not detrimental to the cell is vital. To minimise the bulk temperature change during exposure to 1% duty cycle of MW energy was maintained at approximately 2.6 °C. Under these conditions, exposure to E, H and E+H fields did not result in a significant change in cell morphology or in cell viability, however, when a higher duty cycle (30%) was applied to the cells the viability of the cells decreased significantly and this could be attributed to the heat generated by MWs. *M. smegmatis* was the most sensitive microorganism while *S. aureus* was the least. These results are likely to reflect differences in cell wall, polarity and membrane composition of lipids, fatty acids, cholesterol and phospholipids (Nguyen *et al*. 2015; Nguyen *et al*. 2016).

The degree of MW induced cell wall disruption varied with the type and proportion of membrane phospholipids (Leontiadou *et al.* 2004 ; van Uitert *et al*. 2010a; Piggot *et al*. 2011). Based on the percentages of phospholipids and fatty acids present in the cells studied, *S. aureus* membranes contain a significant proportion of unusual lipids (phosphatidyl glycerol (PG) and lysyl phosphatidyl glycerol (LPG)) which have been

predicted to enhance membrane disruption (Haest *et al*. 1972; Piggot *et al*. 2011). Experimentally, this was not the case in this study as there was lower dextran infiltration into *S. aureus* compared to the other microorganisms. A similar experimental observation has been reported by Nguyen and colleagues (Nguyen *et al*. 2015; Nguyen *et al*. 2016).

Saturated fatty acids are known to reduce membrane fluidity and increase stability and as a consequence may increase resistance to an externally applied E field (Israelachvili and Mitchell 1975; Cullis and De Kruijff 1979; Smaby *et al*. 1994; Veatch and Keller 2005; van Uitert *et al*. 2010a; van Uitert *et al*. 2010b). The predominant fatty acids present in *S. aureus* are saturated, estimated to be more than 90% (Atilano *et al*. 2011; Brown *et al*. 2013), hence they could have contributed to a reduction of infiltration by 10 kDa dextran.

Phosphatidyl choline, phosphatidyl inositol and phosphatidyl ethanolamine are the major phospholipids in *E. coli* and *C. albicans* (Haest *et al*. 1969; Georgopapadakou *et al*. 1987), in addition to cardiolipin which is present in *M. smegmatis* (Crellin *et al*. 2013). Cardiolipin increases membrane fluidity and reduces mechanical stability (Unsay *et al*. 2013b). The composition of saturated fatty acids in *E. coli* and *C. albicans* were below 50% (Haest *et al*. 1969; Georgopapadakou *et al*. 1987) suggesting a less compact membrane. It is likely that the presence of these lipids and the high proportions of unsaturated fatty acids could have influenced infiltration of 3 and 10 kDa dextran particles. In the case of *M. smegmatis*, mycolic acid is the major fatty acids constituting about 30-60% and these are predominantly saturated (89%) (Taneja *et al*. 1979). The

expectation therefore is that, cell membranes in *M. smegmatis* will be compact and less permeable, but this was the most sensitive to MW and dextran infiltration.

These results suggest that differences in fatty acids and phospholipids content cannot not provide a satisfactory explanation for the varying uptake of dextran particles and thus other membrane factors e.g. proteins, cytoskeleton and inherent physical factors (e.g. dielectric properties, microthermal heating) could be contributing factors.

Cells in suspension are surrounded by water molecules normally referred to as bulk or free water. Water molecules can also be tightly coupled to cell membranes (i.e. bound water) and have different dielectric properties compared to bulk water (Robinson 1931). Electrical conductivity is higher in bound water than in bulk water (Robinson 1931; Kaatze 1990). Secondly, the intermolecular interaction between bound water and cell membrane surface is stronger than between bulk water molecules. Due to the strong molecular bonding, bound water molecules will have to surpass a higher potential barrier in order to align to an applied E field (Dawkins *et al.* 1979b), suggesting a higher MW absorption resulting in localised/microthermal heating effects. Measuring localised heating can be experimentally challenging if not impossible (Rougier *et al*. 2014). Thus, the effects observed may still reflect a combination of thermal and non-thermal effects as the bulk temperature measured (2.6°C) is unlikely to be a true reflection of the temperature at the cell membrane surface.

While no significant effect on cell viability and morphology was observed, there was a significant release of dsDNA from cells and the results suggest that once released this DNA may be subject to degradation but only following E field exposure. E field exposure realised a significant reduction in the concentration of ssDNA and dsDNA. This could possibly have occurred via DNA fragmentation and according to MW theory could not have been achieved via covalent bond disruption as MW energy are non-ionising and are not able to generate the required threshold energy (1 eV) to induce such bond disruption (Beavers 2001; Geddes *et al*. 2017). Reactive oxygen species (ROS) are generated in samples following MW treatment (Geddes *et al*. 2017). ROS generated are believed to launch a nucleophilic attack on phosphodiester bonds and this could have led to DNA fragmentation (Scholes *et al*. 1960; von sonntag 2007).

The mechanism by which the E field interacts with biological cells remains unclear. High frequency vibration of cell membranes (mechanical cell stimulation), enhanced diffusion across membranes, abnormal gating of voltage channels, increased membrane conductance and pore formation have all been cited as possible mechanisms (Benz and Zimmermann 1980; Chernomordik *et al.* 1987; Dower *et al.* 1988; Hibino *et al.* 1993; Krassowska and Filev 2007; Bockmann *et al.* 2008; Marrink *et al*. 2009; Pall 2013, 2014, 2015). Pore formation has been likened to the process of electroporation (Kinosita and Tsong 1977; Teissie and Tsong 1981; Tieleman 2004; van Uitert *et al*. 2010a; Shamis *et al*. 2011).

The result of this study confirmed the findings of Shamis and colleagues which reported that the observed biological effects are due to the E field (Shamis *et al*. 2011). Biological membranes act as electrical insulators. For influx/efflux mechanism to occur, their membrane must be destabilised, and this can be achieved via the application of an external E field higher than the membrane potential. The field causes membrane instability, transforming if from its stable impermeable state to one in which it is more permeable facilitating the efflux and influx of molecules.

The effects of H and E+H fields on cell membranes at the power levels used in this study were non-existent. The reason being that, the port of the TM_{010} mode cavity for combined E and H field exposure has the E field intensity halved. Since the observed effects are E field dependent, halving the magnitude is likely to diminish any biological effect as a critical E field value is usually required to induce electroporation.

In a study by Kardos and colleagues, the application of static H fields at field strength of 4 Tesla did cause pore formation in the skin of guinea pig (Kardos and Rabussay 2012). Also, the combined effect of E+H fields on yeast cells has been reported by Novickij and colleagues which saw the permeabilization of yeast cells to exogenous particles (Novickij *et al.* 2016). Certainly, these results cannot be compared to the present study as the experimental design and the MW parameters are not the same. Static H field was used which is different from MW H field levels. Based on the result obtained, a critical H field value higher than what is reported in this study (H = 15.80 µ Tesla) if applied to cells

would have induced membrane disruption and enhanced permeabilization to dextran particles.

In conclusion, this study has shown that MW generated E fields can temporarily disrupt cell wall permeability resulting in the uptake of dextran particles and the release of DNA. The study does not completely rule out thermal effects as the temperature measured is global and does not reflect localised heating. Further work is required to distinguish the contribution of these two forms of energy (i.e. thermal and electric). By optimising this approach, it may be possible to enhance the efficiency of influx and minimizing the detrimental target cell damage as mostly encountered in electroporation. Further studies are required to determine if this is indeed the case. The rapid release of DNA from cells following MW treatment is also an improvement on the current DNA extraction methodologies. The released DNA may be employed for downstream applications (e.g. PCR, DNA hybridisation) and to support the development of point-of-care applicators. The applicability of this is discussed in the next chapter.

Chapter 6

Rapid method of detecting *Mycobacterium abscessus* and *Mycobacterium smegmatis* using microwave assisted Enzyme Linked oligonucleotide sandwiched hybridization assay (ELOSHA)

6.0 Introduction

6.1 Technologies for diagnostics

The increasing demand for technologies capable of rapidly detecting the presence of substances has received much attention in areas of clinical diagnosis, agriculture, defence and security and environmental monitoring (Luka *et al.* 2015; Vigneshvar *et al.* 2016). Examples of these technologies include; Gas chromatography - mass spectrometry (GC-MS), high pressure liquid chromatography (HPLC) and biosensors (Wang and Kricka 2018). The ability of these tools to detect proteins, metabolites, whole cell bacteria and DNA has been demonstrated across numerous studies (Shi *et al*. 2007). DNA based diagnostic tools are the most specific in clinical (Choe *et al.* 2015). Although they have proven to be sensitive and specific, current approaches are time consuming due to the requirement for sample processing i.e. DNA extraction and amplification step making them unsuitable for near patients' bedside use (Ng *et al*. 2015; Sajid *et al.* 2015). These limitations have driven the development of alternate detection technologies.

Lateral flow assays (LFA) are a promising technology for the development of low-cost, rapid, easy to use diagnostic assays. They require minimal labour, generate results rapidly and can be read visually (Sajid *et al*. 2015). LFA are mostly built on the principle of ELISAs to detect proteins and DNA from clinical samples, the former being the most commonly detected (Hsieh *et al.* 2017). Detecting the latter is very sensitive and informative in disease diagnosis, as DNA is biochemically more stable than RNA, proteins and cells (Yang *et al.* 2017). Although LFA are promising, their sensitivity and signal intensity are affected by the concentration of DNA in the sample, especially when the test procedure does not include a DNA amplification step. To overcome this limitation, magnetic particles (MP's) have been frequently used to enrich the recovery of target DNA from samples (Pankhurst *et al.* 2003; Chen *et al.* 2017b; Modh *et al.*

2018). The characteristic properties of MPs and their applications in diagnostic assays are discussed below.

6.2 Magnetic particles (MPs) and applications in biosensing

MPs (as shown in figure 6.1) are usually of the nano- and micrometre sizes, consisting of iron oxide (Fe_2O_3) embedded inside a non-magnetic matrix (Thielbeer *et al.* 2011; Giouroudi and Keplinger 2013). MPs are usually smaller than the biological molecules the seek to detect e.g. viruses (20-450 nm), proteins (5-50 nm), genes (2 nm wide and 10-100 nm long), (Giouroudi and Keplinger 2013). The applicability of MPs in biosensing is enhanced by their high density, hydrophilicity, uniform dispersion in suspension, colloidal stability and super-paramagnetism (Pankhurst *et al*. 2003). Super-paramagnetism is the property of magnetic materials which provides a super-fast response to an external magnetic field (Annink and Gill 2014).

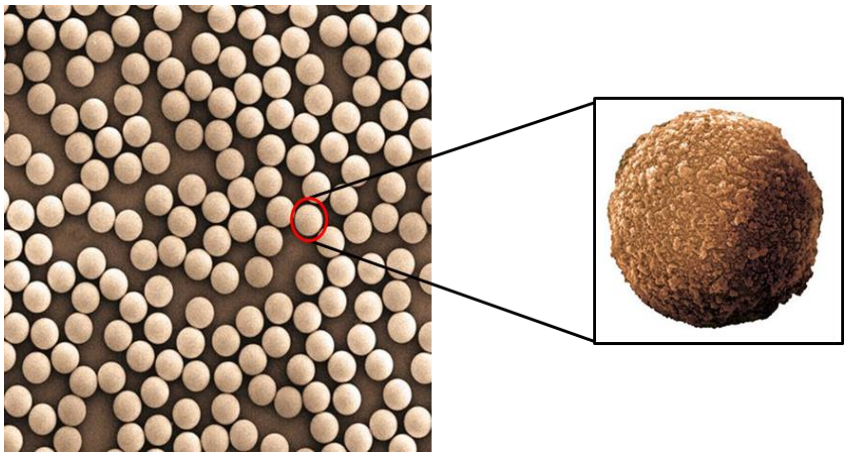

Fig 6.1. Photograph of streptavidin coated magnetite particle (MPs). The particle presented are of 1 µm size (Adapted from: https://www.fishersci.ie/shop/products/sera-mag-speedbeads-streptavidin-magnetic-beads-2/11869912) [Date accessed: 08.03.2018].

For MPs to interact with biological markers, their surfaces have to be modified with functional groups e.g. carboxylate (-COOH), amine (-NH_2) or proteins e.g. streptavidin or neutravidin (Salata 2004). In this study, streptavidin coated magnetic microparticles of commercial origin and with a size of about 1 µm were used to develop a hybridization assay for the detection of *M. abscessus* and *M. smegmatis*. Streptavidin MPs were opted to enable binding with the biotin functionalized probes designed in section 3.2. Biotin-streptavidin interaction is one of the strongest non-covalent interaction and demonstrates resistance to heat and extreme pH conditions (Chung *et al.* 2013; Annink and Gill 2014). Using this approach, DNA targets can be concentrated from diverse samples and hybridized to their complementary probes (Edelstein *et al.* 2000). The principle of the detection assay is discussed in the next section.

6.3 Principle of Enzyme linked oligonucleotide sandwich hybridization assay

Enzyme linked oligonucleotide sandwich hybridization assay **(**ELOSHA) is simple to perform and provides the best sensitivity compared to other DNA based methods (Bahadır and Sezgintürk 2016; Mak *et al.* 2016). In principle, this assay involves the capture of a target gene, herein ssDNA, between two complementary probes (capture and detector) to form a 3-strand DNA complex. The capture probe has biotin attached at the 5' end which anchors the ssDNA and the reporter probe to the surface of MP (fig 6.2). Preceding the anchor probe at the 5' end is a sequence of five thymidine residues to allow probe flexibility when bound to the MP via biotin-streptavidin interaction. The robustness and reproducibility of ELOSHA assays depends on several factors such as the flexibility and length of the capture probe (Parham *et al.* 2007; Patel *et al.* 2011). Probe sequences greater than 20 base pairs provide stability for target-probe binding (Wang 2011). The presence of the target gene is determined indirectly via a signal generated from the detector probe upon reaction with substrates such as 3,3,5,5-tetramethylbenzidine (TMB) or alkaline phosphatase

(AP) (fig. 6.3) (Thieme *et al.* 2008). TMB reacts with horse radish peroxidase (HRP) to form a blue color with maximum absorbance at 370 and 652 nm. This enzyme substrate reaction is terminated by the addition of 0.1 M hydrochloric acid which gives a yellow color with absorption maxima at 450 nm (Eickhoff and Malik 2013).

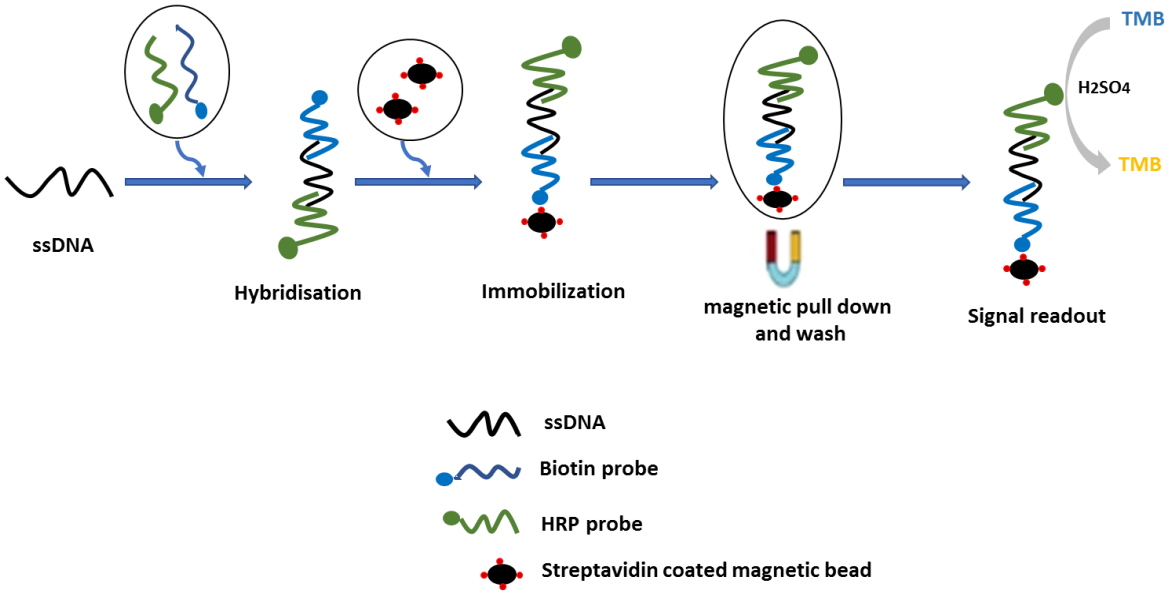

Figure 6.2 Principle of sandwich hybridization assay. The three-strand hybrid complex (anchor probe-target ssDNA-detector probe) are immobilized unto MPs. The three-strand hybrid complex can be separated by the application of a magnetic field and the target gene is indirectly detected by the signal intensity generated by the detector (HRP) probe. The enzyme substrate reaction is then terminated by the addition of HCl (stopping solution).

Any DNA based test capable of delivering speedy results will depend on the sample preparatory step i.e. DNA extraction. The current methods of DNA extraction, as discussed in section 1.20, are expensive and time consuming. The next section discusses the applications of MW technology to rapidly release nucleic acids to support the hybridization assay.

6.4 Microwave (MW) induced DNA release

The applications of MWs in releasing nucleic acids from bacterial cells have been studied extensively. Joshi and colleagues have demonstrated the use of MW energy in disrupting vegetative and sporulating *C. difficile* to release ssDNA and facilitate the detection of *C. difficile* toxins using specific DNA probes (Joshi *et al.* 2014). A similar approach has also been used to recover DNA from *Bacillus anthracis* spores (Aslan *et al.* 2008) and *Chlamydia trachomatis* (Zhang *et al*. 2010). In chapter 5, it was observed that DNA release from cells was as a result of membrane disruption (Jankovic *et al*. 2014). In this chapter, the optimum MW condition for the release of ssDNA from *M. abscessus* and other microorganisms was investigated as it is key step in the development of a MP based detection assay.

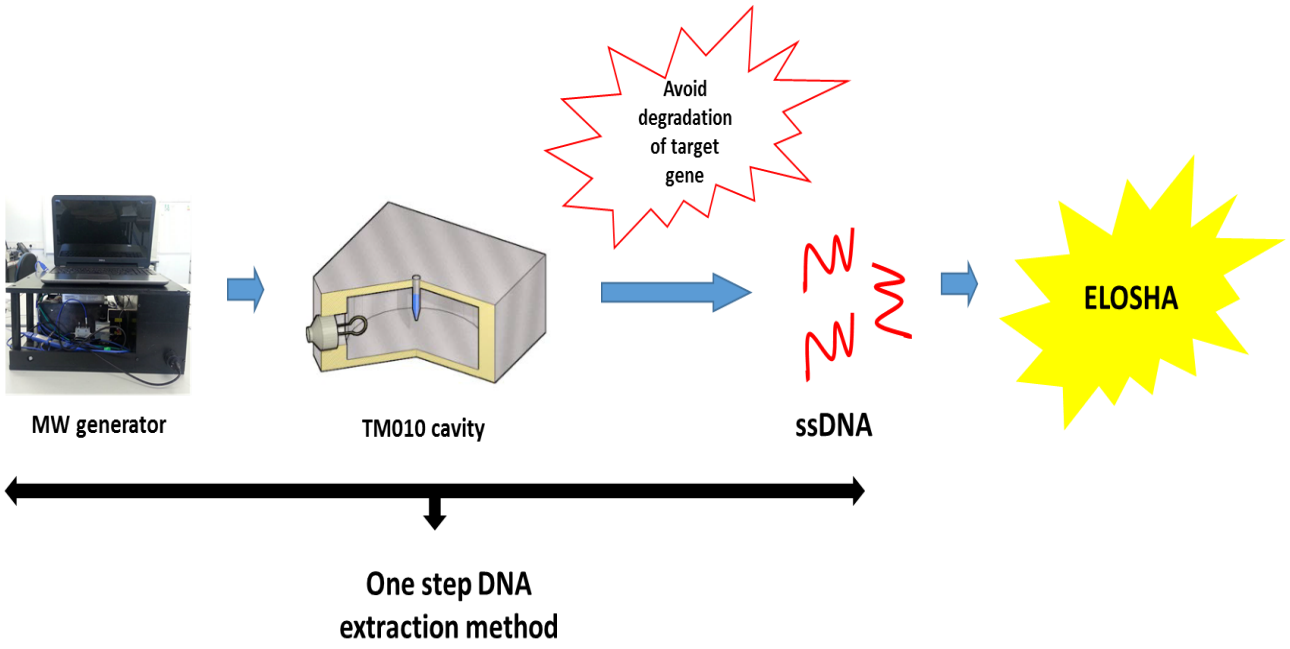

Figure 6.3 Flow chart of sample processing and detection of targeted bacteria. ssDNA released from MW treated bacterial suspensions will be applied to an ELISA assay using specific probes to determine the presence or absence of target gene.

6.5 Bacterial-macrophage infection model

Preparation of target DNA can present several challenges depending on the composition and complexity of the sample. In diagnosing *M. abscessus* from cystic fibrosis (CF) patients, sputum is the sample of choice. Sputum is a complex mixture of pus, cell debris, dead tissues and could contain common bacterial pathogens e.g. *Pseudomonas aeruginosa* which is also frequently isolated from CF patients (Birmes *et al*. 2017). During infection, macrophages are produced, and these engulf and destroy invading pathogenic microorganisms. Paradoxically, some intracellular microorganisms have the preference to multiply within macrophages and escape killing (Price and Vance 2014). Thus, clinical sputum samples may include not only macrophages but *M. abscessus* trapped within macrophages. The ability of MW's to interact with *M. abscessus* trapped within macrophages and to release bacterial nucleic acids is a key first step in the development of the detection assay described in section 6.3.

In the absence of clinical samples, a bacteria-macrophage infection model was developed to mimic. bacterial cells trapped inside a macrophage. The ability of the MWs to disrupt both macrophage and bacterial membrane to release unfragmented target DNA, and to be detected in the hybridization assay will be investigated. *M. smegmatis* instead of *M. abscessus* was used as a surrogate to infect macrophages as we were unable to obtain *M. abscessus* green fluorescent protein (GFP) expressing variant.

6.6 Aim

The **aim** of this chapter is to develop a sandwich hybridization assay capable of detecting *M. abscessus* using specifically designed probes. The speed and sensitivity of the assay is enhanced by the application of MWs to liberate ssDNA from bacteria and from macrophages infected with bacteria which is subsequently captured by MPs. In future applications, this assay can be applied for the detection of *M. tuberculosis*.

6.7 Objectives

The **objectives** are;

1. To determine the optimum MW conditions for the release of bacteria specific nucleic acid from bacteria and macrophages infected with bacteria
2. To optimize the assay parameters for the specific detection of *M. abscessus*
3. To determine the specificity and sensitivity of the assay in detecting *M. abscessus*
4. To develop a bacterial infection model for the detection of *M. smegmatis* (surrogate for *M. abscessus*)
5. To determine sensitivity of the assay in *M. smegmatis*-macrophage infected cultures

6.8 Materials

6.8.1 Hybridization assay

Magnetite particles (MPs) - Dynabeads MyOne streptavidin coated beads C1 were purchased from Invitrogen, Thermofisher. Tween 20, Triton X-100, Bovine Serum Albumin (BSA), 1M H_2SO_4 (stopping solution) and 1-StepTM Ultra TMB-ELISA solution were all purchased from Thermofisher Scientific. A MagRack 6 for the separation of magnetic beads was purchased from (Sigma Aldrich).

6.8.2 Developing macrophage-infection model

Mouse BALB/c monocyte macrophage; J774A.1, were purchased from the European Collection of Authenticated Cell Cultures (ECACC 91051511) as it is a very effective phagocytic cell line (Anes *et al*. 2006; Jordao *et al.* 2008). Dubelco Minimum Essential Media (DMEM), L-Glutamine, Pen-Strep, Fetal bovine serum (FBS) and 1 X PBS (Gibco™) were purchased from ThermoFisher Scientific, UK. Gentamicin sulphate was purchased from Sigma Aldrich.

6.8.3 Fluorescent labelling and confocal microscopy

Transferrin Alexa Fluor™ 546, Mounting oil solution (Dako) and para-formaldehyde (PFA) were purchased from Thermofisher Scientific.

6.9 Methodology

6.9.1 Determining the optimum MW power for the release of nucleic acids

To identify the optimum MW condition for the release of dsDNA and ssDNA from M. abscessus and from J774A.1 macrophage cells, 170 µL of each cell type;

M. abscessus suspension (3.4 x 10^7 CFU/mL) and J774A.1 (1 x 10^6 cells/mL) were irradiated separately with MWs pulsed at varying duty cycles (30%, 40% and 50%) for 10 and 20 seconds. MW pulsing was kept at a width of 1000 ms while the ON period was varied at 300 ms, 400 ms and 500 ms corresponding to 30% and 40% and 50% duty cycles respectively. *M. abscessus* and macrophage cells without MW treatment were included as negative controls. MW treated samples were quantified for dsDNA and ssDNA using the Qubit BR assay kit and Qubit 3.0 fluorometer (Life Technologies). The integrity of the released DNA following MW treatment of bacterial cells were determined on a 1.5% agarose gel as described in section (3.8.5.1)

6.9.2. Capture of biotin labelled probes by streptavidin coated MPs

MPs (100 µL) were washed three times with 1 X PBS to remove the storage buffer which contained azide and can inhibit the hybridization assay. To immobilize biotin probes on to MPs, 10 µL of 20 µM biotin modified probes were immobilized on 100 µL of MPs at room temperature for 1 hour in an orbital shaker (170 rpm). Unbound probes were removed from the MPs by the application of a magnet (MagRack 6, GE Healthcare) followed by washing with 1X PBS. To determine whether biotin probes had bound to the MPs, the concentration of probe before and after addition to MPs was determined. The difference in probe concentration before and after addition to beads was determined to estimate the amount of probe bound to bead. The Qubit 3.0 fluorometer was used to determine probe concentration. The possibility of probes leeching from MPs after several washes was also determined by measuring the probe concentration in the wash buffers after three washing steps.

6.9.3 Blocking unbound and free sites on surfaces of MPs

Reducing background signal generated by the non- specific binding of HRP labelled DNA probes was important in developing this assay. Three different blocking solutions were tested to determine their effectiveness at blocking non-specific binding to the surfaces of the MPs. MPs were incubated with 200 µL of one of the following blocking solutions: (i) 1% BSA + 1% Triton X-100+ 1% Tween 20, (ii) 2X casein and (iii) 1% BSA solution, at room temperature and shaking at 170 rpm for 1 hour. Following blocking, MPs were collected from the suspension using a magnet and washed three times with hybridization buffer (PBS-Tween 20 (0.05%)). To determine the success of the blocking process, MPs were incubated with probe modified with horse radish peroxidase (HRP) (5 µL, 10 µM) in 195 µL of hybridization buffer for 1 hour. MPs were then washed thrice with hybridization buffer and the presence of HRP, if any, was detected by the addition of TMB substrate followed by the addition of 0.1 M HCl.

6.9.4 The detection of *M. abscessus* ssDNA using ELOSHA

The presence of purified and crude (released from microwaved bacteria) ssDNA were determined using probes targeting either the *rpoB* or the *erm*-41gene. In a typical experiment, ssDNA obtained from *M. abscessus* cells i.e. purified = 10 ng/µL or microwaved = 20 ng/µL were incubated with biotin probe functionalized MPs (10 µL), HRP probe (5 µL, 10 µM) and 150 µL of hybridization buffer. The mixture contained in a microcentrifuge tube was incubated at 50°C in an orbital incubator shaker at 200 rpm for 1 hour. After 1 hour of hybridization, the hybrid complex was separated from the solution via the application of a magnet and the supernatant which includes unbound probes were removed. The MPs were washed thrice with hybridization buffer and the presence of target gene was indirectly detected by addition of 100 µL TMB substrate for 10 min which would generate a blue color for a positive test. The enzyme substrate reaction was then stopped by the addition of 100 µL of 0.1 M HCl yielding a yellow color. As a control, non-specific

bacteria (*E. coli, S. aureus*, *C. albicans* and *Enterococcus faecalis*) were included to determine the specificity of the assay. A no template control (NTC) was also included in the assay.

6.9.5 Determining the sensitivity and specificity of the detection assay

The sensitivity of the ELOSHA was determined using the *erm-41* probes with purified ssDNA as a template. Serial dilutions of the following purified ssDNA; 10 ng/ µL, 1 ng/µL, 100 pg/µL, 10 pg/µL and 1 pg/µL were prepared and tested in the assay as described in section 6.9.4. The specificity of the assay was also determined using a cocktail of ssDNA obtained from non-*M. abscessus* isolates (*C. albicans, E. coli*, MRSA, *M. smegmatis* and *E. faecalis*). ssDNA from these bacterial cells with (positive DNA mix) or without (negative DNA mix) *M. abscessus* ssDNA were mixed to a final concentration of 10 ng/µL. Twenty microliters of these solutions were tested in the assay as described in section 6.9.4.

6.9.6 Developing bacterial-macrophage infection model

6.9.6.1 Cell Line culture and bacterial infection

J774A.1 macrophage was cultured in Dubleco Modified Eagle media (DMEM) supplemented with 10% FBS, 1% L-glutamine and 1% Pen-Strep (complete culture media). Macrophages were incubated at 37ºC in 5% CO_2 to 80% confluency, harvested and seeded onto 16 mm diameter cover slips in an 8-well tissue culture plate to a concentration of 1.0 x 10^6 cells/mL and incubated overnight in a fresh culture media. Cells were then washed with warm culture media and replaced with culture media without 1% Pen-Strep (antibiotic-free medium) for bacterial infection. To allow optimum infection of macrophage cells, bacterial cells (GFP *M. smegmatis*) at varying concentrations of 1 x 10^6 CFU/mL, 5 x 10^6 CFU/mL and 1 x 10^7 CFU/mL were added to macrophage cells to achieve a multiplicity of infection (MOI) of 1, 5 and 10 respectively.

Macrophage infected with bacterial cells were incubated for 3 hours at 37 ºC in 5% CO_2. The optimum bacterial concentration to infect bacterial cells identified by this method was used in subsequent assays.

6.9.6.2 Estimating the percentage of viable intracellular bacteria

Infected macrophage cells were incubated for 3 hours to allow phagocytosis. To estimate the percentage of viable intracellular GFP *M. smegmatis*, macrophage infected cells were treated with (Gen +) or without (Gen -) gentamicin 50 µg/mL and incubated at 37 °C for 1 hour to kill extracellular bacteria. Their previous incubation times after addition of bacterial cells were 2 hours followed by 1 hour with gentamicin. Cells were then washed three times with warm PBS and further lysed with 500 µL of distilled water at 37°C for 1 hour. Cell lysates were serially diluted, plated on LB agar and incubated at 37 °C overnight. Visible colonies were counted and calculated in log cfu/mL as described in chapter 2. The percentage of intracellular bacteria was estimated using the formula below.

$$\text{Viable intracellular bacteria} = \frac{\text{Bacterial concentration after gentamicin treatment (Gen +)}}{\text{Bacterial concentration without gentamicin treatment (Gen -)}} \times 100$$

6.9.6.3 Fluorescent labelling and confocal microscopy

Macrophages infected with GFP *M. smegmatis* were washed three times with ice cold 1X PBS (Gibco™) to remove extracellular bacteria and stained with cold transferrin 546 (10 µg/mL) for 15 min in the dark. After staining, cells were washed with 1X PBS and fixed with 3% para-formaldehyde for 15 min in the dark. Fixed cells were then washed with warm 1X PBS, blotted

dry and mounted on a microscope slide and covered with 20 µL mounting oil immersion. Images were captured on a Leica SP5 confocal laser scanning microscope (Leica, Germany) under a X63 objective lens. GFP and transferrin 546 were excited at 488 nm and 543 nm respectively and emissions were collected sequentially at 510 nm and 573 nm respectively. Z-stack images were generated with a z-step of 0.49 µm. Images were captured from 10 different fields and analysed using Fiji imaging software (Schindelin *et al.* 2012).

6.9.6.4 Identification of *M. smegmatis* in macrophage cells

Following the successful development of the macrophage-bacterial infection, cell suspension was treated with MWs at 40% duty cycle for 20 seconds to release ssDNA of *M. smegmatis,* which will include ssDNA of that of macrophage cells. Their concentration was determined with Qubit BR assay kit. The ssDNA released (20 ng/µL), quantified with the Qubit 3.0 fluorometer were tested in the detection assay (described in section 6.9.4) using *M. smegmatis* specific probes (designed in chapter 3).

6.9.6.5 Sensitivity of assay in macrophage infected bacterial cells

Macrophage infected bacterial cells were diluted 5, 25, 125 and 625 times in PBS. Sample dilutions were treated with MWs pulsed at 40% duty cycle for 20 seconds and the amount of ssDNA quantified using the Qubit BR assay kit. The ssDNA released (20 ng/µL) were then subjected to the detection assay as described in section 6.9.4.

6.10 Statistical Analysis

Analysis of data for the hybridisation assay were normalised against the *E. coli* control. In the absence of an *E. coli* control, the results were normalised against the negative control (No template control).

6.11 Results

6.11.1 Determining optimum MW condition for the release of dsDNA and ssDNA

The concentration of single stranded DNA (ssDNA) and double stranded DNA (dsDNA) released following MW treatment at varying duty cycles were quantified using the Qubit BR assay kit. After 20 seconds, maximum concentration of dsDNA was released at 30 % and 40% duty cycles in *M. abscessus* and at 50% duty cycle from 774A.1 macrophage (fig.6.4). There was no significant difference in dsDNA concentrations released from *M. abscessus* at 30 % and 40% duty cycles. Similarly, the maximum release of ssDNA was observed at 30% and 40% duty cycle from *M. abscessus* and at 30% from macrophage cells all after 20 seconds of MW treatment (fig.6.5). Again, there was no significant difference in ssDNA concentration at 30% and 40% duty cycles. The results in fig. 6.4 and fig. 6.5 indicates that increasing MW duty cycles to 50% decreases the concentration of ssDNA and dsDNA. It is likely that the decrease in dsDNA and ssDNA concentration be as a result of fragmentation induced by MWs. Temperature generation during MW excitation is inevitable. Thus, a combination of temperature and MW specific effect could be responsible for this decrease. Microwaved bacteria were electrophoresed in duplicate on agarose gel for all conditions tested. DNA released was observed at approximately 100 bp after 20 seconds of microwave irradiation at 30%, 40% and 50% duty cycles. Except at 50% duty cycle, DNA was not visible after 10 seconds at 30% and 40% duty cycles. The reason for this observation could be attributed to the higher MW intensity and longer time duration, herein 20 seconds for which bacterial cells were exposed. On the contrary, low intensity MWs when applied for a short period of time (10 seconds) was not enough to cause DNA release (fig. 6.6). In comparison to the untreated cells, it is likely that DNA released following MW irradiation were predominantly ssDNA which were observed mainly at 100 bp. High molecular weight DNA (<3000 bp) and extracellular DNA attached to bacterial cells were observed trapped in the wells in the untreated

samples. The movement of these extracellular DNA could have been restricted owing to their overall size and attachment to bacterial cells (fig. 6.6).

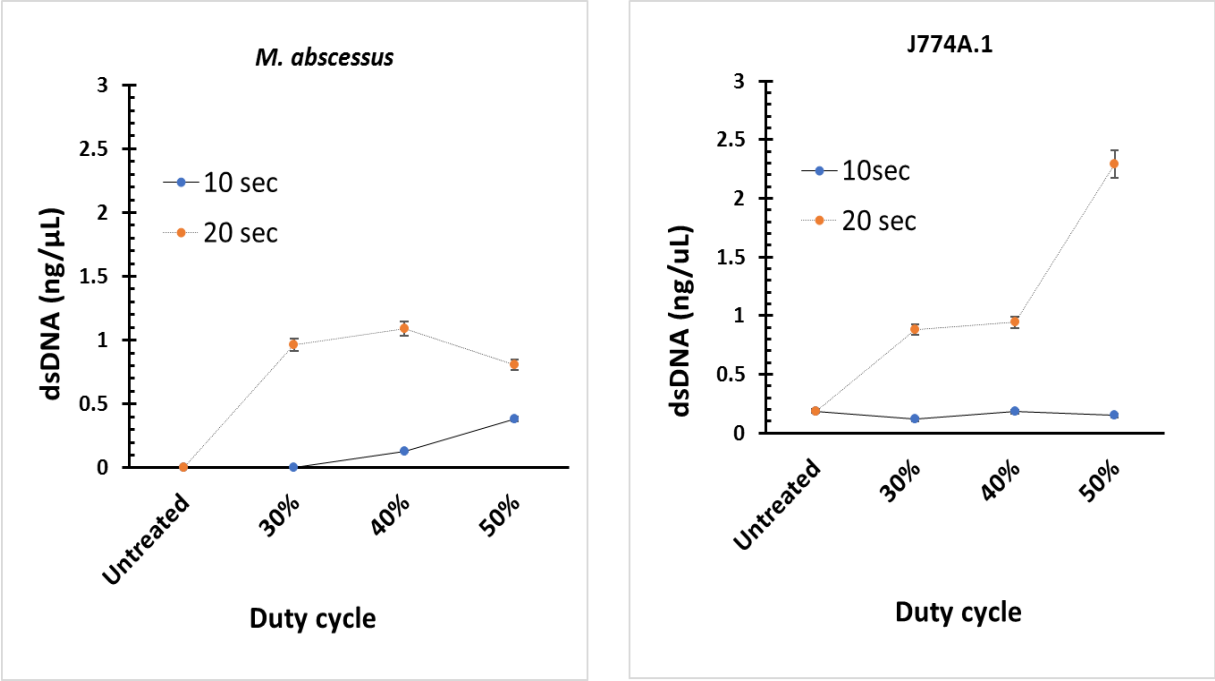

Figure 6.4. MW induced release of dsDNA from *M. abscessus* and from J774A.1 cells. *M. abscesssus* (3.4 x 10^7 CFU/mL) and J774A.1 macrophage (1.0 x 10^6 cells/mL) were treated with 12 W MW energy pulsed at 30%, 40% and 50% duty cycles for 10 (blue dots) and 20 (red dots) seconds. The concentration of dsDNA released were determined using the Qubit dsDNA BR assay kit (Invitrogen) and Qubit 3.0 fluorometer. Data represent mean of triplicate experiment ± standard deviation.

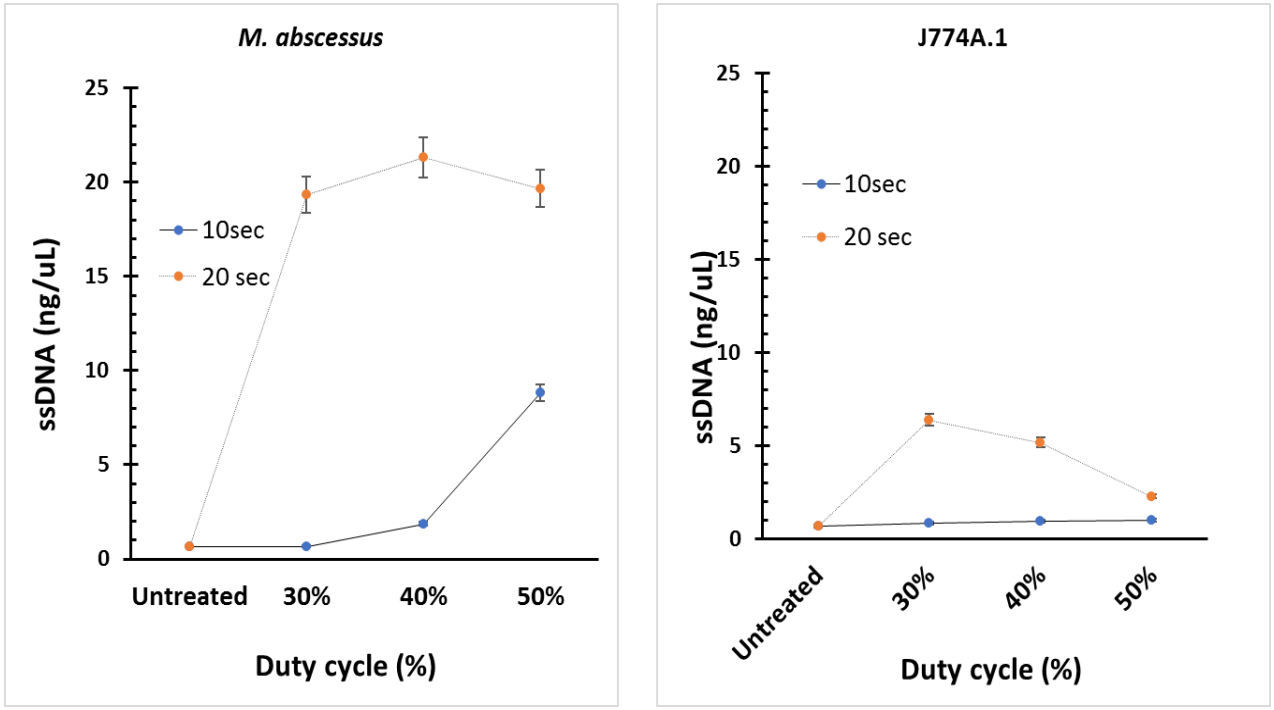

Figure 6.5. MW induced release of ssDNA from *M. abscessus* and J774A.1 cells. *M. abscesssus* (3.4 x 10^7 CFU/mL) and J774A.1 macrophage (1.0 x 10^6 cells/mL) were treated with 12 W MW energy pulsed at 30%, 40% and 50% duty cycles for 10 (blue dots) and 20 (red dots) seconds. The concentration of dsDNA released were determined using the Qubit dsDNA BR assay kit (Invitrogen) and Qubit 3.0 fluorometer. Data represent mean of triplicate experiment ± standard deviation.

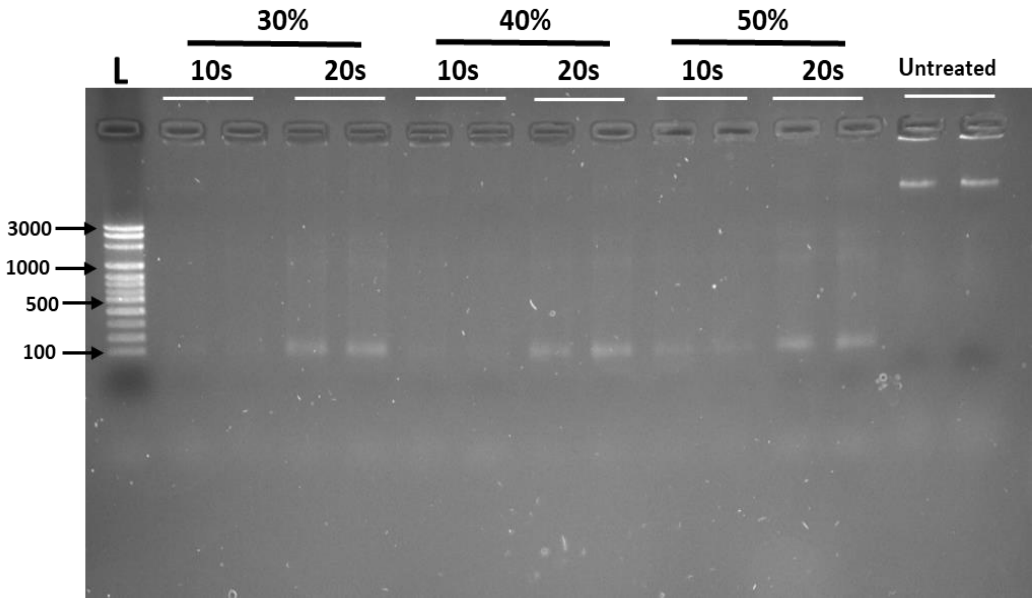

Figure 6.6. Release of nucleic acids in post microwave irradiated *M. abscessus* cells. Suspensions of *M. abscessus* ($1x10^8$ CFU/mL) were treated with microwave energy at 30%, 40% and 50% duty cycles for 10 and 20 seconds time intervals. Microwaved samples were loaded in duplicate for each microwave condition and compared with untreated samples. Lane L= molecular weight ladder

6.11.2 Determining binding capacity of magnetite particles and the effect of blocking buffers to reduce background signals

To confirm that biotin probes had bound to the MPs whose surface is modified with streptavidin, the two were mixed and incubated together. The concentration of biotin probe before and after addition of MPs was determined and the percentage of probe bound estimated. There was significant decrease ($p < 0.001$) in the concentration of biotin probe following the addition to MPs (orange bar), indicating that the probes were bound to MPs possibly via biotin-streptavidin interaction (fig 6.7). The binding capacity of the MPs was determined at 89.82% based on the ratio of bound and free biotin probe in the solution. Repeated washing of the biotin labelled probes did not result in the removal of the probes from the MP surface (fig. 6.8). When HRP labelled DNA probes lacking biotin modification was added to the MPs, there was no obvious decrease in their free concentration suggesting that minimal non-specific binding to surface of the MPs had occurred (fig 6.7).

To determine if low level, non-specific DNA binding had occurred, HRP labelled DNA probes were mixed with MP, washed and then suspended in TMB solution. The results indicate that the HRP labelled probe does attach to the MPs resulting in a background signal (fig 6.9). To minimize the background signal, MPs immobilized with biotin probe were incubated with varying blocking solutions prior to incubation with the HRP probe. The background signal was effectively removed when MPs were blocked with a solution comprising 1% Tween 20, 1% Triton X-100 and 1% BSA (fig 6.10). In contrast, casein (2x) and 1% BSA were not effective in preventing HRP from binding to the MP (fig. 6.10).

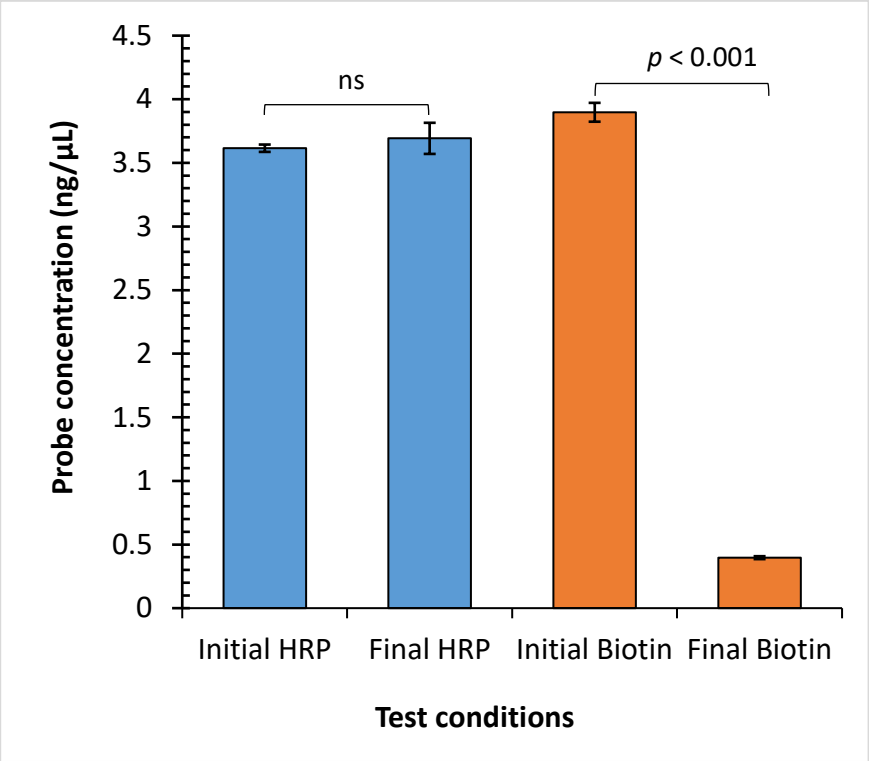

Figure 6.7 Characterization of the binding of biotin labelled probes to MPs. Biotin (10 µL, 20 µM) and HRP labelled probe (5 µL, 10 µM) were added separately to MPs (1.3 x 10^8 particles/mL) and incubated at RT for 1 hour. The concentration of HRP and biotin probes in the supernatant after addition to MPs were quantified using the Qubit BR assay kit and Qubit 3.0 fluorometer. Data represents the average of four separate experiments ± standard deviation. **ns** represent no significance.

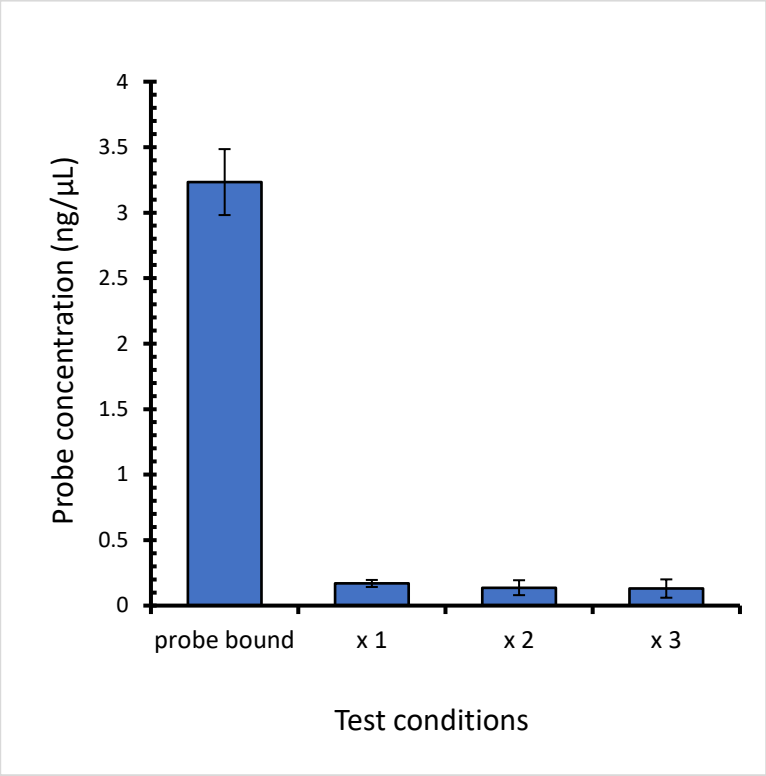

Figure 6.8 Determining the ability of biotin probes to leech from MPs following repeated washing. Biotin probes bound to MPs (probe bound) were subjected to three washing steps and the supernatants were collected after the first (x1), second (X2) and third (X3) wash with hybridization buffer and the concentration of free probes, if any, in the washing buffers were quantified using the Qubit 3.0 fluorometer. Data represent mean of triplicate experiment ± standard deviation.

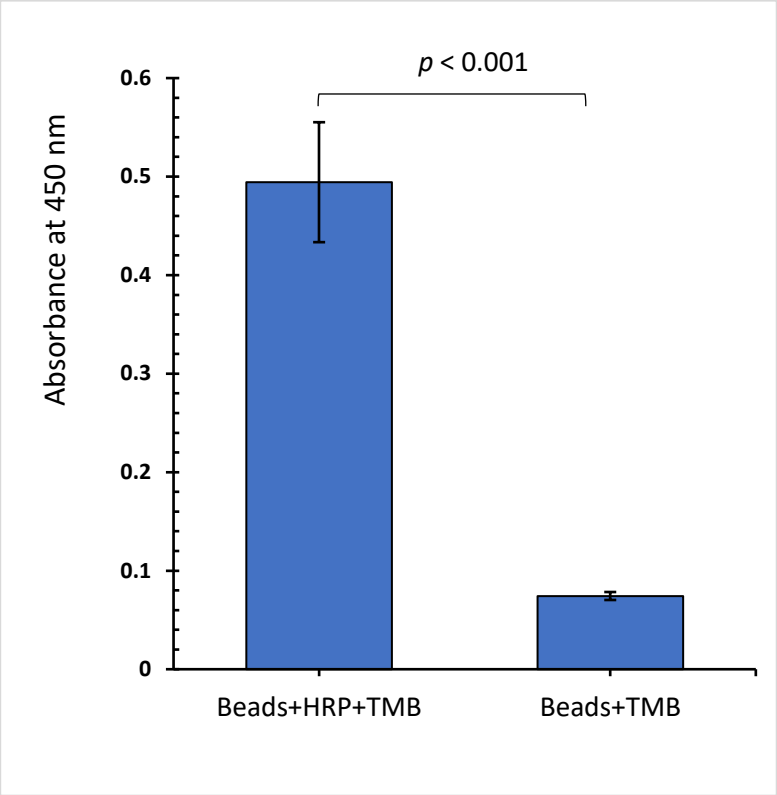

Figure 6.9 Signal generated by mixing MPs with HRP labelled DNA probe. MPs (1.3×10^8 particles/mL) incubated with HRP probes (5 µL, 10 µM) were washed thrice with hybridization buffer followed by the addition of TMB substrate for 10 min and stopping solution. A background signal was measured even after three washing step with hybridization buffer. Data represent mean of duplicate experiment ± standard deviation.

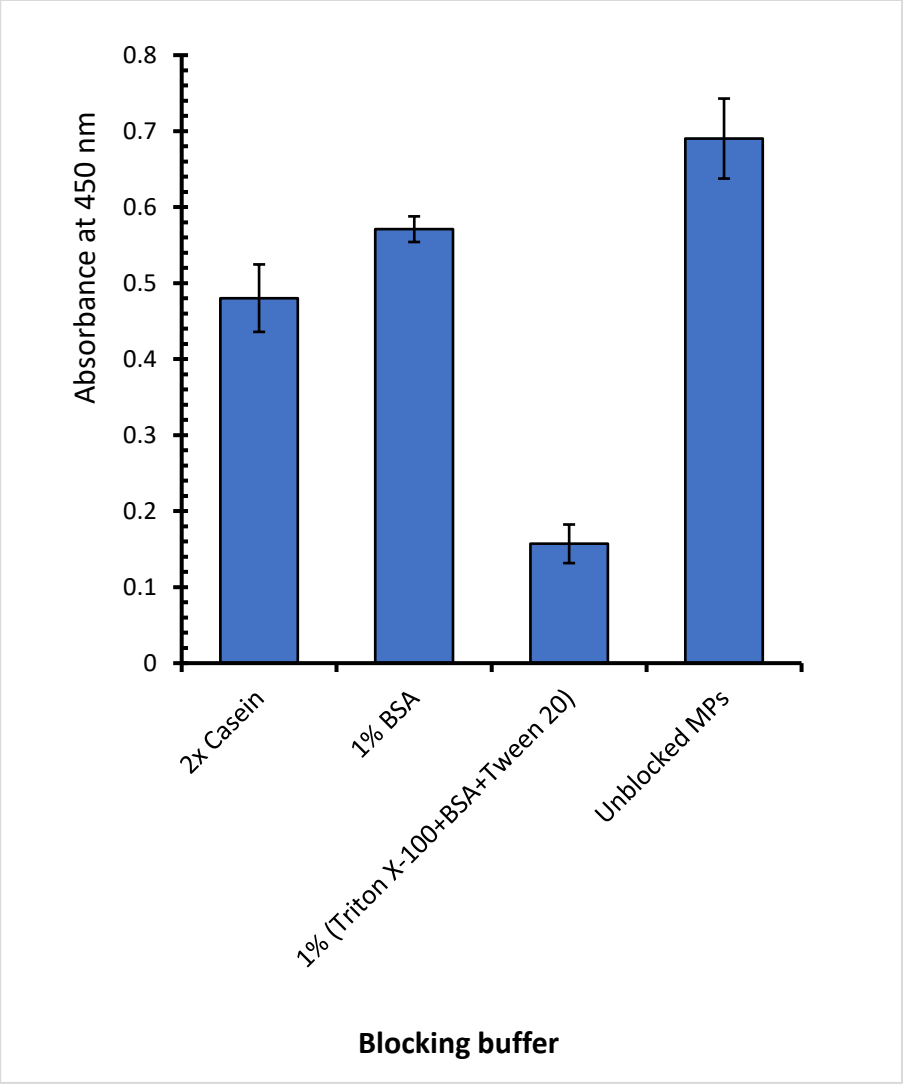

Figure 6.10 The ability of blocking buffers to reduce the background signal. The ability of different blocking solutions to reduce background signal were determined. HRP probe (5 µL, 10 µM) was added to blocked MPs (1.3 x 10^8 particles/mL) and incubated for 1 hour. The presence of HRP probe was determined by the addition of TMB. Background signal was effectively reduced below cut-off value when blocking solution comprising 1% Tween 20+1% Triton X-100+1% BSA was used. Data represent mean of triplicate experiment ± standard deviation. Data represent mean of duplicate experiment ± standard deviation.

6.11.3 Detection of purified *M. abscessus* DNA using ELOSHA

The principle of the ELOSHA is based on the hybridization of target ssDNA to corresponding anchor and the detector probes, with the formation of a 3-strand DNA complex. This assay was developed to detect 50-nucleotide sequences within the *rpoB* and *erm*-41 genes of *M. abscessus*. The complex is anchored to streptavidin coated MPs via biotin interaction. The target ssDNA is indirectly detected by the signal generated from the detector probe (HRP) following the addition of TMB substrate (fig 6.2). We first looked at the ability of the *erm*-41 (fig. 6.11) and *rpoB* (fig. 6.12) probes to distinguished *M. abscessus* from non-*M. abscessus* isolates (*M. smegmatis*, *E. coli*, MRSA, *E. faecalis* and *C. albicans*) using purified DNA to determine the specificity of the assay. Data were normalised against *E. coli* or against reaction mixture without DNA template i.e. no template controls (NTC). Following normalisation of all data, the assay distinguished *M. abscessus* from non-*M. abscessus* isolates using the *erm*-41 (fig. 6.11) and the *rpoB* probe (fig. 6.12). The *rpo*B probe was discontinued because it produced large variations between isolates.

When the *erm*-41 was tested against impure ssDNA released from microwaved bacteria, it was able to distinguish *M. abscessus* isolates from non-*M. abscessus* isolates (fig. 6.13). Next, the ability of the assay to detect target *M. abscessus* DNA in the presence of DNA derived from a cocktail of non-*M. abscessus* isolates (*C. albicans*, *E. coli*, MRSA, *M. smegmatis* and *E. faecalis*) was determined. An aliquot of *M. abscessus* ssDNA was mixed with a cocktail of non-*M. abscessus* DNA (positive mix). The negative mix consisted of a cocktail of ssDNA isolated from non-*M. abscessus* isolates. All ssDNA was mixed at a concentration of 10 ng/µL. As can be seen from figure 6.14, the assay was able to detect *M. abscessus* in the presence of unrelated bacterial DNA (fig. 6.14).

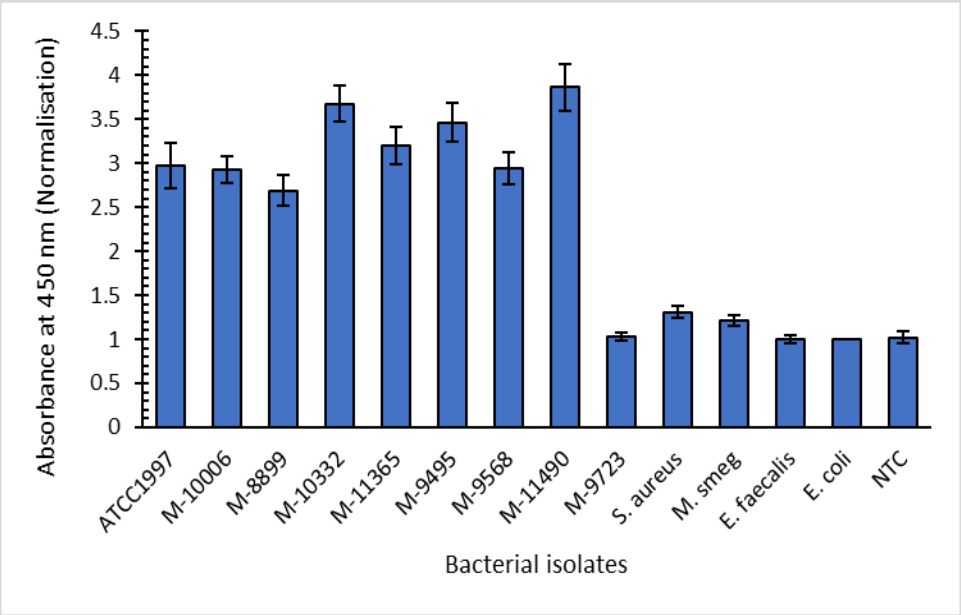

Figure 6.11 Colorimetric detection of purified *M. abscessus* ssDNA using *erm*-41 probe. ssDNA (10 ng/µL) obtained from 7 *M. abscessus* isolates and non-*M. abscessus* isolates were tested in the detection assay. M-9723 previously identified as *M. smegmatis* did not give any significant signal in comparison to the test isolates. A no template control (NTC) was also included. Data represent mean of triplicate experiment ± standard deviation.

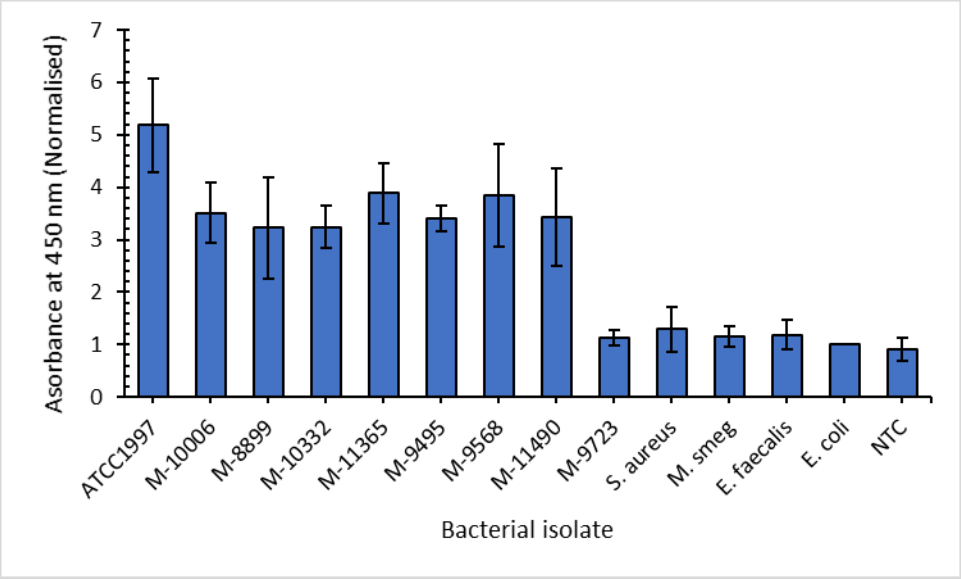

Figure 6.12 Colorimetric detection of purified *M. abscessus* DNA using *rpo*B probe. ssDNA (10 ng/µL) obtained from 7 *M. abscessus* isolates and non-*M. abscessus* isolates were tested in the detection assay. A no template control (NTC) was also included. Data represent mean of triplicate experiment ± standard deviation.

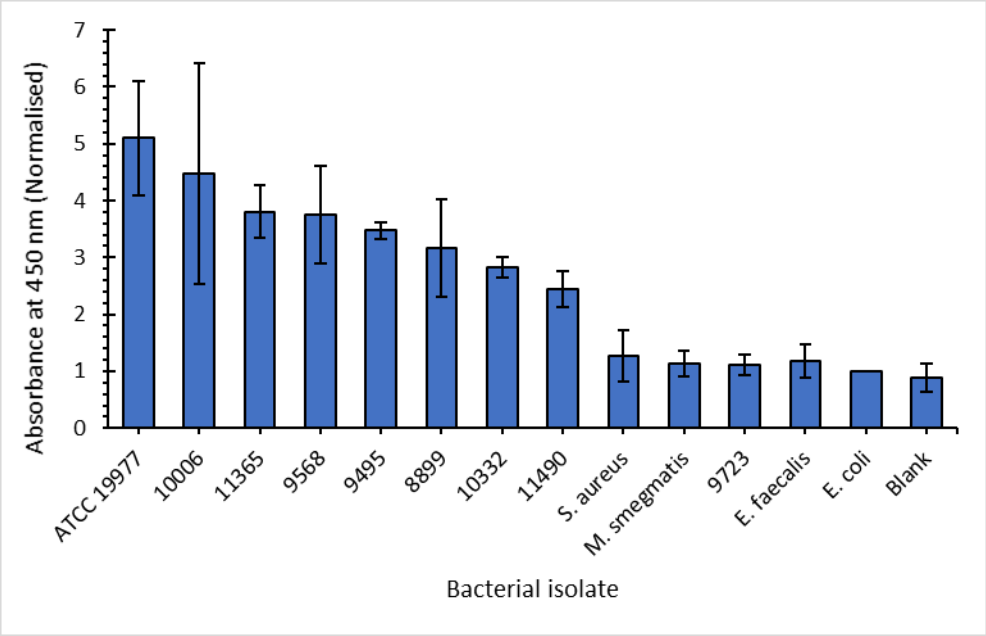

Figure 6.13 Colorimetric detection of microwaved *M. abscessus* DNA using *erm*-41 probe. ssDNA (20 ng/µL) obtained following MW treatment of bacterial suspensions ($1x10^8$ CFU/mL) were subjected to the detection assay. *M. abscessus* ssDNA were detected from non. *M. abscessus* DNA. Positive control (ATCC 19977) and a NTC were also included. Data represent mean of triplicate experiment ± standard deviation.

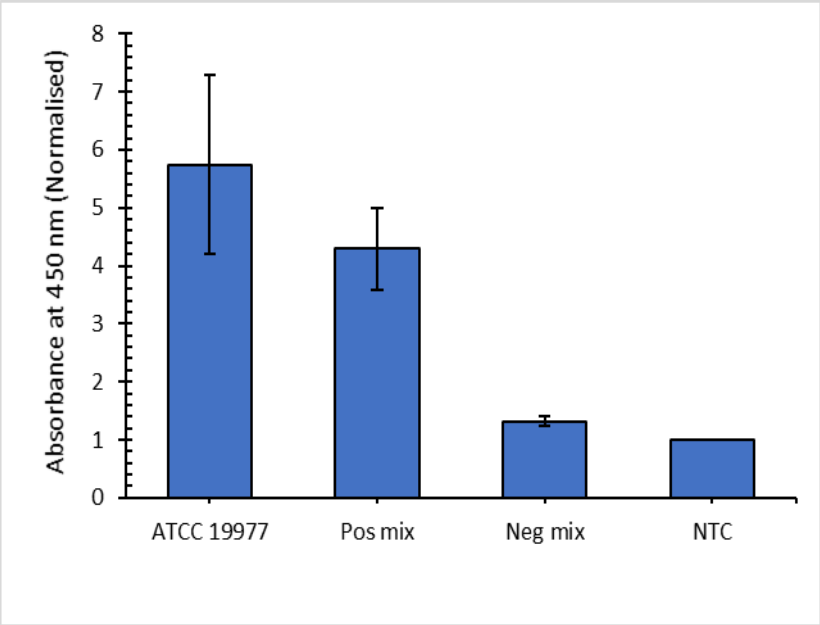

Figure 6.14 Specificity of *erm*-41 gene assay for *M. abscessus* in the presence of ssDNA cocktail derived from unrelated bacteria. The signal generated from pure *M. abscessus* ssDNA (ATCC 19977) and a positive mix (*M. abscessus* ssDNA was mixed with a cocktail of non-*M. abscessus* ssDNA) were significantly higher than that of the negative mix (cocktail of ssDNA isolated from non-*M. abscessus* isolates) and NTC ($p < 0.05$). The data represent mean of triplicate experiment ± standard deviation.

6.11.4 Determining the limit of detection of the assay

The sensitivity of the assay was determined using a range of concentrations of purified ssDNA: 10 ng/µL, 1 ng/µL, 100 pg/µL and 10 pg/µL, 1 pg/µL, 0.1 pg/µL, 10 fg/µL and 1 fg/µL. As can be seen from fig 6.15 the limit of detection was 1 pg/µL.

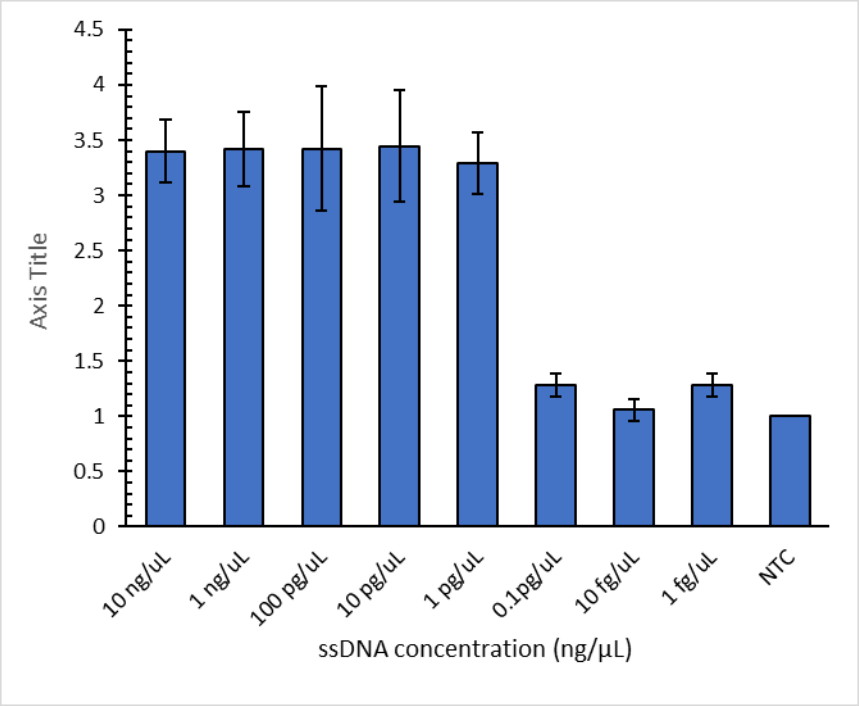

Figure 6.15 Sensitivity of the assay using *erm*-41 probe. The limit of detection using purified ssDNA was 1 pg/µL. The difference in absorbance between 1 pg/µL and 0.1 pg/µL was significant ($p < 0.05$). Data are shown as mean of triplicate experiment ± standard deviation

6.11.5 Development of macrophage-infection model

The results above confirm the ability of the assay to detect *M. abscessus* when suspended in solution. While encouraging the next step would be to determine the ability of the approach to detect the presence of the pathogen in clinically relevant samples such as infected macrophages. Unfortunately, we lacked access to fully validated *M. abscessus* infected macrophage model. While the creation of such a model was feasible the amount of time required to optimize this approach was beyond the scope of this project. For this reason, we switched to an *M. smegmatis* infected macrophage model which had been developed as part of another project. This approached

offered the additional advantage that we could employ a GFP expressing *M. smegmatis* and thus visualize the location of the bacteria within the infected cells.

To optimize the uptake of GFP *M. smegmatis* into macrophage cells, varying concentrations of the bacteria were incubated with macrophages to achieve an MOI of 1, 5 and 10 bacteria per macrophage. To determine the number of viable intracellular bacteria, cells sticking to the external surfaces of the macrophages (extracellular bacteria) were killed by exposure to gentamicin after which the cells were lysed in water. Gentamicin does not penetrate macrophage cell membranes hence does not interfere with the viability of intracellular bacteria. To determine the appropriate level of gentamicin to use in this assay a time-kill experiment using 50 and 100 µg/mL of gentamicin was performed. As can be seen from figure 6.16, treatment with 50 µg/mL resulted in bacterial killing after 60 min of treatment of macrophage exposed cells and was the level used in subsequent studies.

The optimum MOI by exposing the macrophages to a range of bacterial concentrations was determined. Using an MOI of 1, uptake of bacteria was sparse, leaving most of the macrophages empty without bacilli. At MOI of 10, macrophages had high numbers of both intracellular and extracellular bacilli. When macrophages were infected with bacterial cells at MOI of 5, the number of bacilli in macrophages were almost even, resulting in an average of 2-3 bacilli per macrophage (fig 6.18). Overall the concentration of viable intracellular bacteria was estimated at 2.8 $x10^5$ CFU/mL (fig 6.16) representing about 86.81±8.47% of the total bacteria being phagocytosed. For this reason, subsequent macrophage infection was carried out at a MOI of 5.

In addition to measuring the recovery of viable bacteria from infected macrophages, the ability of this bacterium to express GFP meant that it was possible to visualize the location within infected macrophages using a fluorescent microscope (fig 6.17). While a useful tool to determine bacterial uptake, it is unable to distinguish between live and dead cells as dead cells retain the ability to fluoresce.

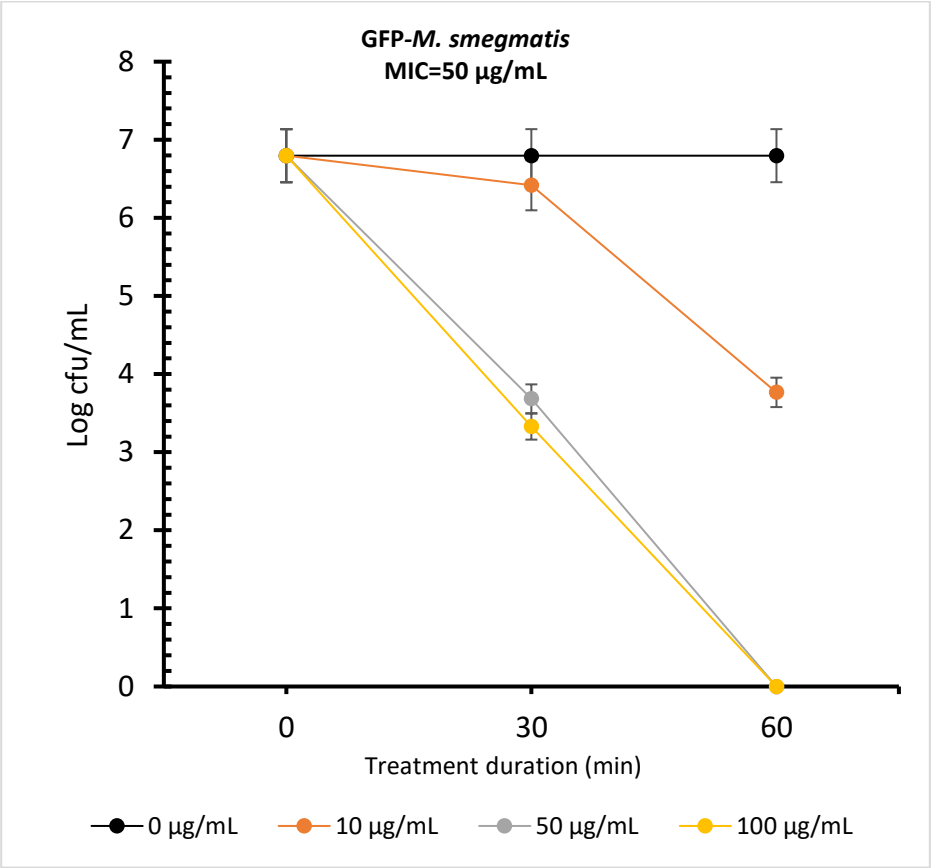

Figure 6.16 Time-kill kinetics of gentamicin against GFP-*M. smegmatis*. GFP *M. smegmatis* (1 x 10^6 CFU/mL) was treated with varying concentration of gentamicin (10, 50 and 100 µg/mL) and incubated at 37 °C for 30 min and 60 min. Cells without gentamicin treatment were set as controls and the concentration of viable cells determined using the Miles and Misra method. The results are expressed as log CFU/mL. After 60 min, cells viability was completely lost after gentamicin treatment at 50 and 100 µg/mL. Data represent mean of triplicate experiment ± standard deviation.

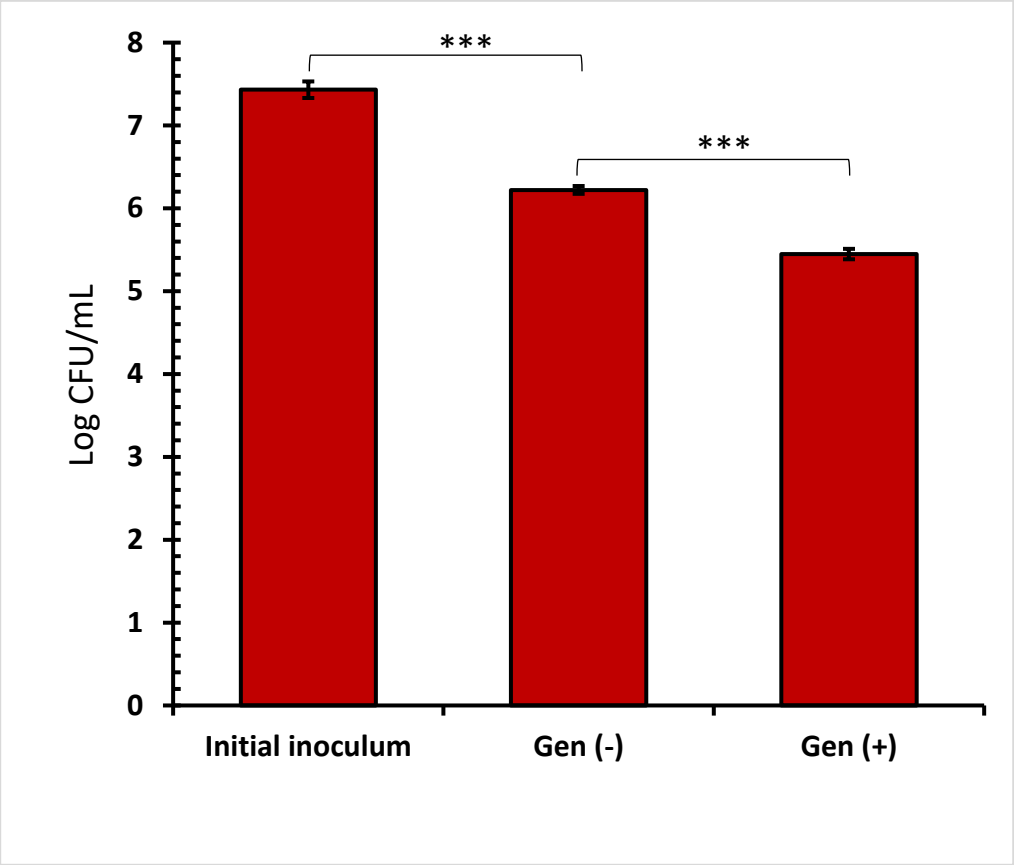

Figure 6.17 Estimating the concentration of viable intracellular bacteria. J774A.1 macrophage was infected with GFP *M. smegmatis* at MOI = 5 for 3 hours including 1 hour gentamicin treatment. Post infected cells were treated with (+) or without (-) gentamicin (50 µg/mL) for 1 hour to kill extracellular bacteria. Macrophage cells were washed thrice with warm PBS and lysed with distilled water for 1 hour at 37 °C. Bacterial concentration in cell lysate was determined using the Miles and Misra method. The concentration of bacterial cells used to infect macrophages were also quantified (initial inoculum). The percentage of viable internalized bacteria was estimated at 86.81±8.47%**.** Data represent mean of triplicate experiment. (***) represent $p < 0.001$.

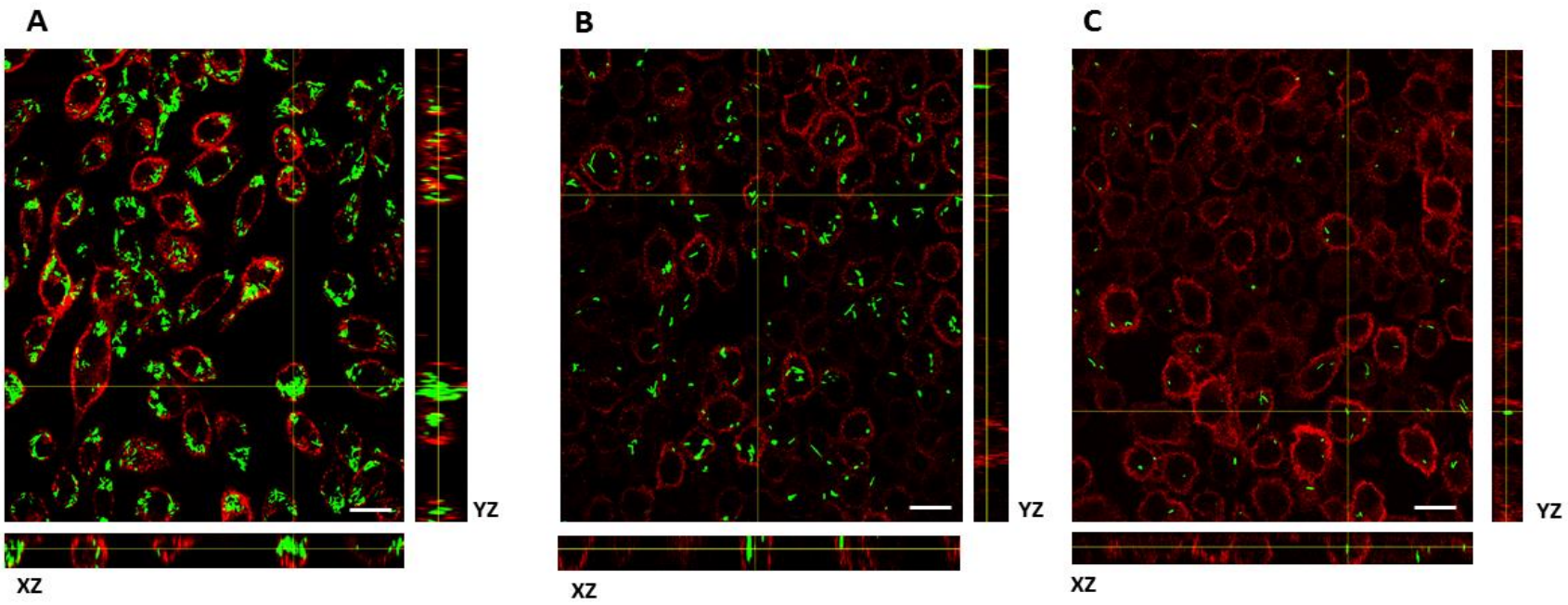

Figure 6.18 Determining the optimum bacterial concentration for macrophage infection. J774A.1 macrophage (1.0 x 10^6 cells/mL) were infected with varying concentrations of GFP-*M. smegmatis* (1 x 10^6 CFU/mL, 5 x 10^6 CFU/mL and 1 x 10^7 CFU/mL) resulting in a MOI of 1 (A), 5 (B) and 10 (C) respectively. Infected macrophages were incubated for 3 hours and the macrophage membrane stained with Transferrin Alexa 546 (red). Stained cells were observed on a confocal microscope under x63 objective lens. Internalized GFP-*M. smegmatis* was confirmed by capturing Z-stack images and analysed with Image J. Captured images are presented in orthogonal views (XZ and YZ) to confirm phagocytic activity. Scale bar in each image correspond to 10 µm.

6.11.6 Detection of *M. smegmatis* in macrophage cells

Following the successful development of the macrophage-*M. smegmatis* infection model, the next step was to determine the ability of the assay to detect the presence of *M. smegmatis* engulfed by macrophage cells. Infected macrophages were treated with MWs at 40% duty cycle for 20 seconds and the released ssDNA was detected using the hybridization assay developed in this study. Using the *rpo*B probe (designed in chapter 3) specific for *M. smegmatis*, the specificity of the assay was determined using purified *M. smegmatis* ssDNA, macrophages infected with *M. smegmatis*, lysed non-infected macrophages, lysed macrophages spiked with 10 ng/µL of *E. coli* DNA (control DNA) and a no template control (NTC). With the cut-off value determined at 0.314, a positive signal was obtained from purified *M. smegmatis* ssDNA and from *M. smegmatis* infected macrophages but not in non-infected macrophages or from lysed non-infected macrophages spiked with *E. coli* DNA (control DNA) or from the NTC (fig. 6.18). For this particular assay, the *rpoB* probe was used rather than the *erm*-41 since the *erm*-41 gene was specific to *M. abscessus* only. The *M. smegmatis* specific *rpo*B probe that was designed in section 3.10.3 was able to distinguish *M. smegmatis* from *M. abscessus*. For this reason, the same probe sequences (anchor and detector) were modified with biotin and HRP respectively and synthesized to be used in this detection assay.

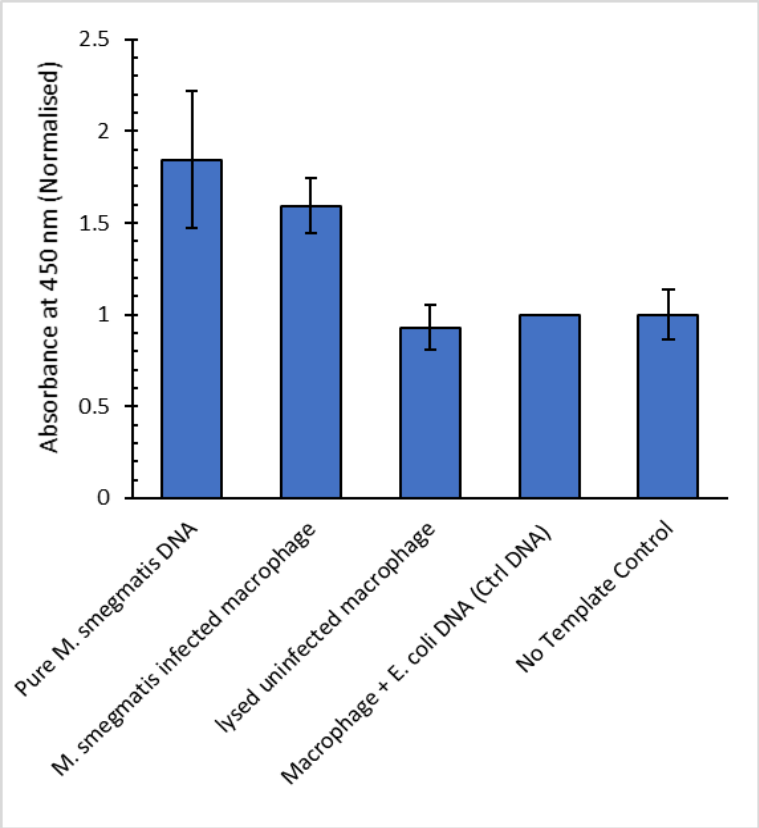

Figure 6.19 Detection of *M. smegmatis* DNA in macrophage infected cells. Purified ssDNA was obtained from *M. smegmatis*, microwaved *M. smegmatis* infected macrophages (20 ng/uL), lysed non-infected macrophages spiked with *E. coli* DNA (20 ng/uL), lysed non-infected macrophages (20 ng/uL) and a NTC were tested in the detection assay using the *rpo*B gene. The presence of target gene was determined by measuring the signal generated by HRP. Data represent mean of triplicate experiment ± standard deviation.

6.11.7 Determining the limit of detection of assay in macrophage-bacterial suspensions

In section 6.10.5, the concentration of viable intracellular *M. smegmatis* released upon macrophage lysis was estimated at 2.85 x 10^5 CFU/mL. The following range of dilutions, 5, 25, 625 and 3125-fold of this lysate were prepared to determine the limit of detection of the ELOSHA. The concentration of ssDNA in sample dilutions before and after MW treatment were quantified using the Qubit 3.0 fluorometer. Sample dilutions were treated with MW at 40% duty cycle for 20 seconds. The concentration of ssDNA (from macrophages and *M. smegmatis*) was significantly increased after MW treatment in samples diluted to a factor of 5, 25, 125 and 625, but not in the sample diluted by a factor of 3125 (fig 6.20). The initial ssDNA concentration measured before MW exposure is likely to be extracellular nucleic acids present in the cell suspension (fig. 6.19). Cells treated with MWs saw a gradual reduction in the concentration of ssDNA (fig 6.20). The number of viable bacteria present in each sample dilution was determined using the Miles and Misra method and the results displayed in figure 6. 21. As can be seen, there was about a one log reduction (from the first to the last dilution) in the concentration of viable bacterial with increasing sample dilutions. On the basis of the results presented in figure 6.22 the minimum number of intracellular *M. smegmatis* that could be detected using the assay in its current configuration was approximately 7.8 x 10^4 CFU/mL.

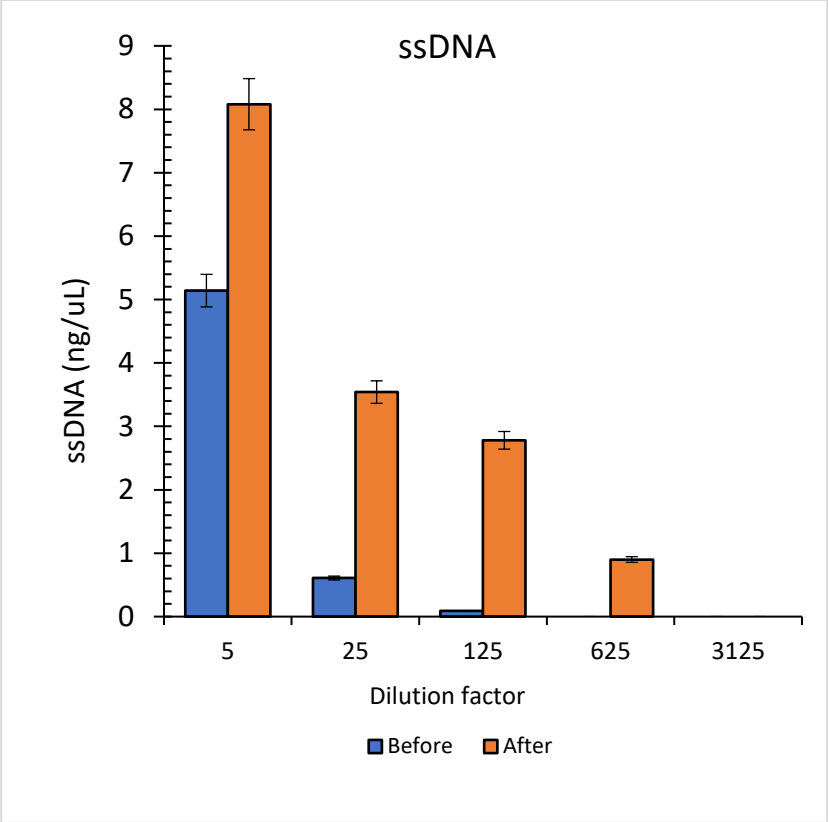

Figure 6.20 Quantification of ssDNA in sample dilutions following MW treatment. Macrophage infected with bacterial cells at MOI of 5(section 6.10.5) were diluted in water to yield the following dilution range 5, 25, 125, 625 and 3125. Diluted cells were treated with MWs at 40% duty cycle for 20 seconds and the concentration of ssDNA released after MW excitation was quantified using the Qubit 3.0 fluorometer. Blue and orange bars indicate samples before and after microwave treatment respectively. The concentration of ssDNA decreases gradually in samples from dilution factor of 5 to 625 but was not detected at a dilution of 3125. Data represent mean of triplicate experiment ± standard deviation.

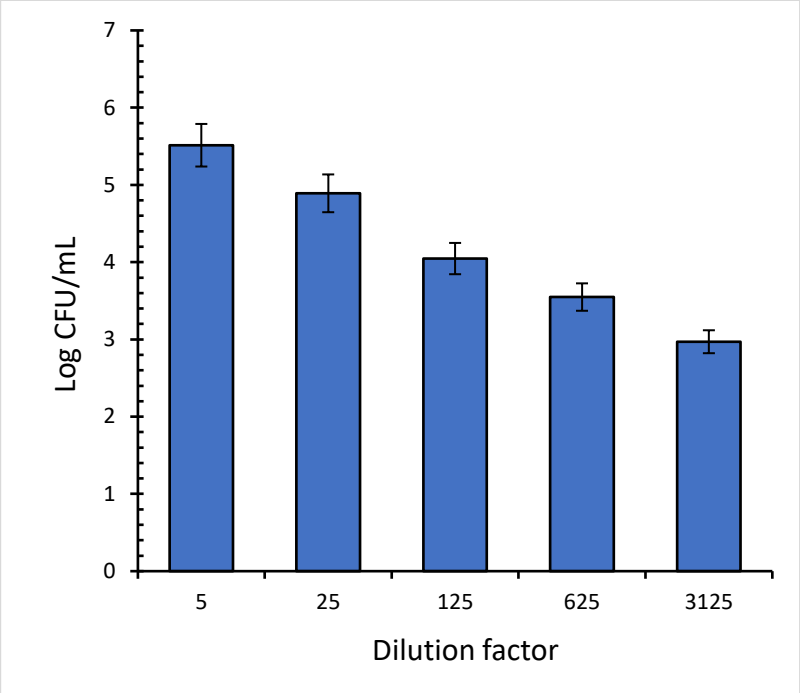

Figure 6.21 Concentration of viable bacteria in lysed macrophage infected cells. Macrophage cells (1.0 x 10^6 cells/mL) were infected with GFP *M. smegmatis* (5.0 x 10^6 cfu/mL) representing a MOI of 5 and incubated for 2 hours and treated with gentamicin for additional 1 hour to kill extracellular bacteria. Post infected macrophages are lysed in water to release intracellular bacteria and diluted to the factors of 5, 25, 125, 625 and 3125. The concentration of viable bacteria in each of the dilutions were enumerated and the concentration calculated as log CFU/mL. Data represent mean of triplicate experiment ± standard deviation.

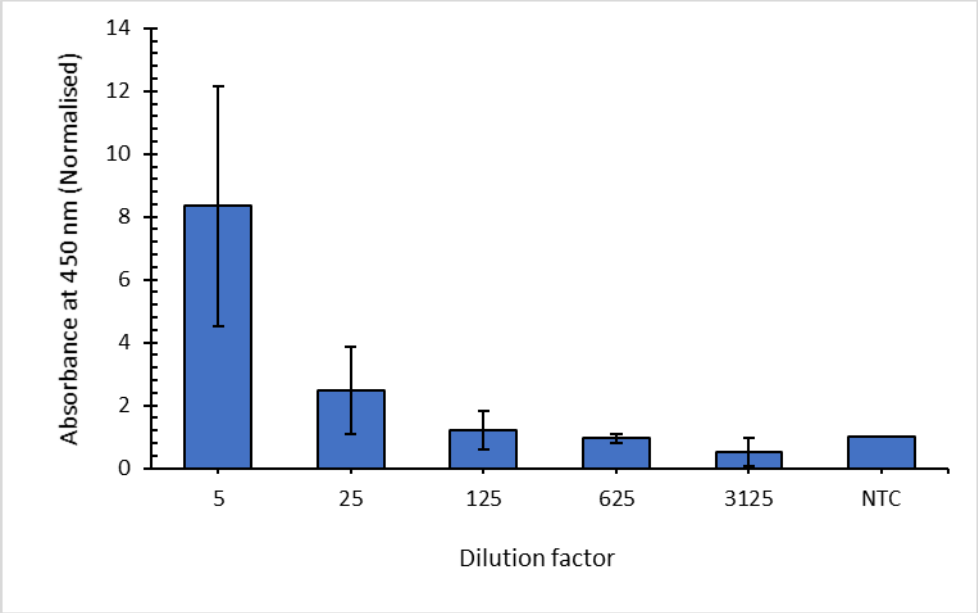

Figure 6.22 Detection of *M. smegmatis* in sample dilutions using ELOSHA. Sample dilutions diluted were treated with MWs at 40% duty cycle for 20 seconds. ssDNA released from sample dilutions were analysed in the detection assay targeting the *rpo*B gene of *M. abscessus*. The limit of detection was obtained at a dilution factor of 25, corresponding to 4.89 log CFU/mL. NTC was included in the assay. Data represent mean of triplicate experiment ± standard deviation.

6.12 Discussion

Diseases associated with *M. abscessus* e.g. cystic fibrosis are of public health importance and requires attention. More worrying is their possibility of being transmitted from one person to another via aerosol generation (Birmes *et al*. 2017). The current DNA based diagnostic tests for *M. abscessus* e.g. Cobas Amplicor, INNO-LiPA, GenoType NTM-DR kit are sensitive and specific but are costly, have long turnaround time and are not easily integrated into the medical workflow. They are also only as good as the quality and quantity of DNA they must work with. The above challenge necessitates the need to develop simple and low-cost technologies for DNA extraction which can be integrated into POC assays. The release of DNA from bacteria such as members of the mycobacteria family is particularly challenging due to the rigidity of the mycobacterial cell wall. Commercial DNA extraction tools struggle with speed and are costly, hence cannot be easily integrated into current diagnostic approaches (Kaser *et al*. 2009; Käser *et al*. 2010).

In this proof-of-concept study, an assay capable to detect the presence of *M. abscessus* has been developed. This prototype assay employs MW technology to release ssDNA from microorganisms in under 20 seconds, followed by detection of these targets using a colorimetric sandwich hybridization assay using target specific DNA probes. To enhance the development of the assay, MPs modified with probes were used to enrich targets via their complementary sequence. The target was then identified indirectly by the signal generated from the HRP modified detector probe following a catalytic oxidation with TMB substrate solution. Using this principle, the assay was able to distinguish *M. abscessus* from non-*M. abscessus* using the *erm*-41 probe. Based on the inconsistency of the *rpo*B probe, i.e. generating variability in signal intensity in two of the isolates (8899 and 10006) and having a higher cut-off value than the *erm*-41 probe, further application of the probe was discontinued. This observation further establishes the need for experimental testing

of probes designed using bioinformatic tools and brings to light the limitation in using bioinformatic approaches which mostly employ heuristic approaches. Additionally, the genome sequences obtained from NCBI only represent a fraction of the diversity that exist in the real world, hence the possibility of detecting non-specific bacteria. The assay demonstrated specificity in detecting *M. abscessus* in the presence of other non-*M. abscessus* ssDNA and in complex mixture of macrophages and *M. smegmatis*, pointing to the robustness of the prototype assay. The sensitivity of the assay with regards to the detection of purified M. *abscessus* DNA was 1.0 pg/µL and in the presence of macrophages a positive signal was generated with as few as 7.8 x 10^4 CFU/mL of *M. smegmatis*.

Diagnostic assays (displayed in appendix 4) currently employed for *M. abscessus* detection requires between 4-6 hours to generate results (Peter-Getzlaff *et al.* 2008; Ngan *et al.* 2011; Qvist *et al.* 2015; Shenai *et al.* 2016; Rocchetti *et al.* 2017). The prototype assay cannot yet be compared to these assays as it requires optimization (outlined in section 7.3) and is yet to be evaluated using clinical samples. The relative rapidity of the assay is due to the application of MWs to release DNA for detection. The ability of microwaves to mediate the rapid release of DNA from bacteria has previously been reported (Vaid and Bishop 1998; Joshi *et al*. 2014). The mechanism by which MWs release nucleic acids from cells is unclear. Membrane disruption via thermal or athermal means has been frequently reported (Copty *et al.* 2006). When higher MW power is used, this could induce dsDNA and ssDNA fragmentation (Vaid and Bishop 1998) and this could compromise the sensitivity of the assay. For this reason, the optimum MW conditions i.e. MW power, MW pulse rate and duration of exposure needed to be determined. In our study MW power (12W) pulsed at 40% duty cycle was optimal for the release of unfragmented ssDNA targets. A major advantage in MW mediated DNA isolation is that it is rapid and does not require the use of expensive or toxic reagents. In addition, the MW technology can be incorporated into microfluidic

devices (Breadmore *et al.* 2003) facilitating the development of POC devices. To improve on the sensitivity of the assay, the MW conditions required to liberate ssDNA from low concentrations of bacterial cells need to be identified. Also, the concentration of probes displayed on the surface of MPs, the concentration of MPs themselves and DNA probes design needs further optimization.

In conclusion, a simple ELOSHA for the detection of *M. abscessus* and of *M. smegmatis* ssDNA in macrophage cells have been developed. The assay has the potential to be developed into a rapid POC which could be used to screen patients upon admission to hospital to enable appropriate treatment regimens and clinical management decisions to be made. In the future, the assay can be developed to detect other common pathogens of public health importance, particularly *M. tuberculosis.*

Chapter 7

General Discussion

7.1 General Discussion

The aim of this project was to develop a rapid and simple assay capable of detecting *M. abscessus* and which could ultimately be adapted to detect *M. tb*. Chapter 3 describes the development of a novel chemical-based DNA extraction method for the recovery of high yield, pure DNA from rigid *M. abscessus* cells. Lysis buffer A proved to be the most effective, when compared to commercial systems, at recovering DNA from cells of *M. abscessus*. Using this method, sufficient DNA template was isolated to support VNTR and PCR based characterisation of the collection of suspected clinical isolates of *M. abscessus.* In combination with clarithromycin sensitivity testing, 7 of the 8 bacterial isolates were identified as *M. abscessus* and one as *M. smegmatis*.

In chapter 4, a bioinformatic approach was employed to design probes and primers which recognised the *erm*-41 and *rpo*B genes of *M. abscessus* and *M. smegmatis.* The specificity and sensitivity of these probes was determined against the panel of 7 *M. abscessus* clinical isolates and a collection of non-*M. abscessus* isolates using PCR assay. The probes which performed the best in terms of specificity and sensitivity test were then used to form the basis of the detection assay.

In Chapter 5 the interaction of pulsed nonthermal 2.45 GHz MWs with cell viability and membrane integrity of structurally diverse microorganisms was explored. The results showed that exposure to sub-lethal MW power levels disrupted cell membrane integrity and resulted in the uptake of dextran particles and the release of nucleic acids. The effect appeared to be due to the actions of the E field as the H field alone did not cause any membrane disruption. The results also showed that a critical E field intensity is required

to cause membrane disruption as halving the E field intensity diminished this effect. Although the effects seen occurred within approximately 2°C change in bulk temperature, there could be some microthermal influence. Thus, cells membrane disruption may be a combination of both thermal and MW specific effects.

The development of the detection assay is discussed in chapter 6. The main accelerating component of the hybridisation assay is the use of MWs to release nucleic acids from microorganisms within 20 seconds. Nucleic acids are mainly locked within the cell's nucleus which is then surrounded by layers of cell membranes and a cell wall (Tortoli 2014). Using the *erm*-41 probe designed in chapter 4 and magnetite particles, a detection assay capable of distinguishing *M. abscessus* from non-*M. abscessus* was developed. The assay recorded a sensitivity to the level of 1 pg/uL in detecting purified *M. abscessus* ssDNA and 7.8 $x10^4$ CFU/mL in macrophage infected *M. smegmatis* cells.

In our recent publication, we report the development of a novel split ring MW resonator capable of releasing single stranded DNA from *C. difficile* spores. The split ring resonator MW applicator was designed so that so that it could be incorporated into a portable handheld diagnostic device. With this approach, different strains of *C. difficle* were distinguished using specific probes (Hayder *et al*., 2019). Based on our published data, the current detection assay has the potential of being built into a handheld lateral flow assay for the detection of *M. abscessus* and other pathogens of public health importance.

7.2 Final conclusions

Overall, this study has successfully achieved the principal aim of developing a rapid assay which can detect *M. abscessus*. The study further proves it is robust and can detect *M. abscessus* in the presence of non-*M. abscessus* ssDNA and in detecting *M. smegmatis* in the presence of macrophage cells. The speed of the current assay was enhanced using MWs to disrupt bacterial cells and release ssDNA within 20 seconds. The mechanism by which nucleic acids were released from cells was dependent on the MW E fields plus possible thermal temperature effect.

7.3 Future work

1. Develop a macrophage infection model using *M. abscessus*
2. Optimising assay parameters such as probe design, magnetic particle concentrations and the concentration of biotin probes loaded on the magnetite particles surface to increase sensitivity and reduce the time required to generate a result
3. Optimise the various components of the hybridisation buffer as this contributes to hybridisation efficiency and could also reduce the assay time
4. Testing the robustness of the current prototype assay using clinical samples
5. Adapt the technology to detect *M. tuberculosis*

8.0 References

Abston, E. and Farber, H. (2018). Pulmonary Cavity From Mycobacterium malmoense in an HIV-Infected Patient: Complicated by Bronchopleural Fistula. *Open Forum Infect Dis* **5**.

Achkar, J. M. and Ziegenbalg, A. (2012). Antibody responses to mycobacterial antigens in children with tuberculosis: challenges and potential diagnostic value. *Clin Vaccine Immunol* **19:**1898-1906.

Adekambi, T., Berger, P., Raoult, D. and Drancourt, M. (2006). rpoB gene sequence-based characterization of emerging non-tuberculous mycobacteria with descriptions of Mycobacterium bolletii sp. nov., Mycobacterium phocaicum sp. nov. and Mycobacterium aubagnense sp. nov. *Int J Syst Evol Microbiol* **56:**133-143.

Adékambi, T., Colson, P. and Drancourt, M. (2003). rpoB-Based Identification of Nonpigmented and Late-Pigmenting Rapidly Growing Mycobacteria. *J. Clin. Microbiol* **41:**5699–5708.

Adekambi, T. and Drancourt, M. (2004). Dissection of phylogenetic relationships among 19 rapidly growing Mycobacterium species by 16S rRNA, hsp65, sodA, recA and rpoB gene sequencing. *Int J Syst Evol Microbiol* **54:**2095-2105.

Ahmad, S. (2010). New approaches in the diagnosis and treatment of latent tuberculosis infection. *Respir Res* **11:**169.

Ahmed, A., Rushworth, J. V., Hirst, N. A. and Millner, P. A. (2014). Biosensors for whole-cell bacterial detection. *Clin Microbiol Rev* **27:**631-646.

AIDSinfo. (2018). Guidelines for the prevention and treatment of opportunistic infections among HIV-exposed and HIV-infected children [Online]. AIDSinfo. Available at: https://aidsinfo.nih.gov/guidelines [Accessed: 24/10/2018].

Almeida Da Silva, P. E. and Palomino, J. C. (2011). Molecular basis and mechanisms of drug resistance in Mycobacterium tuberculosis: classical and new drugs. *J Antimicrob Chemother* **66:**1417-1430.

Altschul, S. F., Gish, W., Miller, W., Myers, E. W. and Lipman, D. J. (1990). Basic local allignment search tool. *Journal of Molecular Biology* **215:**403-410.

Altschul, S. F., Madden, T. L., Schäffer, A. A., Zhang, J., Zhang, Z., Miller, W. and Lipman, D. J. (1997). Gapped BLAST and PSI-BLAST- a new generation of protein database search programs. *Nucleic Acids Research* **25 (17):**3389–3402.

Ando, T., Xuan, W., Xu, T., Dai, T., Sharma, S. K., Kharkwa, G. B., Huang, Y.-Y. *et al.* (2011). Comparison of Therapeutic Effects between Pulsed and Continuous Wave 810-nm Wavelength Laser Irradiation for Traumatic Brain Injury in Mice. *PLoS One* **6**.

Anes, E., Peyron, P., Staali, L., Jordao, L., Gutierrez, M. G., Kress, H., Hagedorn, M. *et al.* (2006). Dynamic life and death interactions between Mycobacterium smegmatis and J774 macrophages. *Cell Microbiol* **8:**939-960.

Annink, C. and Gill, R. (2014). Nanoparticle Aggregate-Based Fluorescence Enhancement for Highly Sensitive and Reproducible Detection of DNA. *Particle & Particle Systems Characterization* **31:**943-947.

Aryan, E., Makvandi, M., Farajzadeh, A., Huygen, K., Bifani, P., Mousavi, S. L., Fateh, A. *et al.* (2010). A novel and more sensitive loop-mediated isothermal amplification assay targeting IS6110 for detection of Mycobacterium tuberculosis complex. *Microbiol Res* **165:**211-220.

Aslan, K., Previte, M. J. R., Zhang, Y., Gallagher, T., Baillie, L. and Geddes, C. D. (2008). Extraction and Detection of DNA from Bacillus anthracis spores and the vegetative cells within 1 min. *Anal. Chem* **80:**4125–4132.

Astarie-Dequeker, C., Le Guyader, L., Malaga, W., Seaphanh, F. K., Chalut, C., Lopez, A. and Guilhot, C. (2009). Phthiocerol dimycocerosates of M. tuberculosis participate in macrophage invasion by inducing changes in the organization of plasma membrane lipids. *PLoS Pathog* **5:**e1000289.

Atilano, M. L., Yates, J., Glittenberg, M., Filipe, S. R. and Ligoxygakis, P. (2011). Wall teichoic acids of Staphylococcus aureus limit recognition by the drosophila peptidoglycan recognition protein-SA to promote pathogenicity. *PLoS Pathog* **7:**e1002421.

Awasthy, D., Ambady, A., Narayana, A., Morayya, S. and Sharma, U. (2014). Roles of the two type II NADH dehydrogenases in the survival of Mycobacterium tuberculosis in vitro. *Gene* **550:**110-116.

Bach, H., Papavinasasundaram, K. G., Wong, D., Hmama, Z. and Av-Gay, Y. (2008). Mycobacterium tuberculosis virulence is mediated by PtpA dephosphorylation of human vacuolar protein sorting 33B. *Cell Host Microbe* **3:**316-322.

Bahadır, E. B. and Sezgintürk, M. K. (2016). Lateral flow assays: Principles, designs and labels. *TrAC Trends in Analytical Chemistry* **82:**286-306.

Banik, S., Bandyopadhyay, S. and Ganguly, S. (2003). Bioeffects of microwave - a brief review. *Bioresource Technology* **87:**155–159.

Barnard, M., Albert, H., Coetzee, G., O'Brien, R. and Bosman, M. E. (2008). Rapid molecular screening for multidrug-resistant tuberculosis in a high-volume public health laboratory in South Africa. *Am J Respir Crit Care Med* **177:**787-792.

Bastian, S., Veziris, N., Roux, A. L., Brossier, F., Gaillard, J. L., Jarlier, V. and Cambau, E. (2011). Assessment of clarithromycin susceptibility in strains belonging to the Mycobacterium abscessus group by erm(41) and rrl sequencing. *Antimicrob Agents Chemother* **55:**775-781.

Batista Napotnik, T. and Miklavcic, D. (2018). In vitro electroporation detection methods - An overview. *Bioelectrochemistry* **120:**166-182.

Battaglioli1, T., Rintiswati, N., Martin, A., Palupi, K. R., Bernaerts, G., Dwihardiani, B., Ahmad, R. A. *et al.* (2013). Comparative performance of Thin Layer Agar and Lowenstein–Jensen culture for diagnosis of tuberculosis. *Clin Microbiol Infect* **19:**502-510.

Beavers, R. (2001). DNA and The Microwave Effect [Online]. http://www.engr.psu.edu/ae/wjk/mwaves.html: Available at: [Accessed: 13th September, 2016].

Behling, C. A., Bennet, B., Takayama, K. and Hunter, R. L. (1993). Development of a Trehalose 6,6'-Dimycolate Model Which Explains Cord Formation by Mycobacterium tuberculosis. *Infection and Immunity* **61:**2296-2303.

Belisle, J. T. and Sonnenberg, M. G. (1998). Isolation of Genomic DNA from Mycobacteria. In: Parish T., Stoker N.G. (eds) Mycobacteria Protocols. Methods in Molecular Biology™. USA: Humana Press Inc.

Benz, R. and Zimmermann, U. (1980). Pulse-length dependence of the electrical breakdown in lipid bilayer membranes. *Biochimica et Biophysica Acta* **597:** 637-642.

Bernut, A., Herrmann, J. L., Kissa, K., Dubremetz, J. F., Gaillard, J. L., Lutfalla, G. and Kremer, L. (2014). Mycobacterium abscessus cording prevents phagocytosis and promotes abscess formation. *Proc Natl Acad Sci U S A* **111:**E943-952.

Best, C. A. and Best, T. J. (2009). Mycobacterium smegmatis Infection of the Hand. *HAND* **4:**165–166.

Bhalla, M., Sidiq, Z., Sharma, P. P., Singhal, R., Myneedu, V. P. and Sarin, R. (2013). Performance of light-emitting diode fluorescence microscope for diagnosis of tuberculosis. *Int J Mycobacteriol* **2:**174-178.

Bhuachalla, D. N., Corner, L. A. L., More, S. J. and Gormley, E. (2015). The role of badgers in the epidemiology of Mycobacterium bovis infection (tuberculosis) in cattle in the United Kingdom and the Republic of Ireland: current perspectives on control strategies. *Veterinary Medicine: Research and Reports* **6:**27-38.

Biehle, J. and Cavalieri, S. J. (1992). In Vitro Susceptibility of Mycobacterium kansasii to Clarithromycin. *Antimicrobial agents and Chemotherapy* **36:**2039-2041.

Birmes, F. S., Wolf, T., Kohl, T. A., Ruger, K., Bange, F., Kalinowski, J. and Fetzner, S. (2017). Mycobacterium abscessus subsp. abscessus Is Capable of Degrading Pseudomonas aeruginosa Quinolone Signals. *Front Microbiol* **8:**339.

Blaas, S. H., Mutterlein, R., Weig, J., Neher, A., Salzberger, B., Lehn, N. and Naumann, L. (2008). Extensively drug resistant tuberculosis in a high income country: a report of four unrelated cases. *BMC Infect Dis* **8:**60.

Bockmann, R. A., de Groot, B. L., Kakorin, S., Neumann, E. and Grubmuller, H. (2008). Kinetics, statistics, and energetics of lipid membrane electroporation studied by molecular dynamics simulations. *Biophys J* **95:**1837-1850.

Boehme, C. C., Nabeta, P., Hillemann, D., Nicol, M. P., Shenai, S., Krapp, F., Allen, J. *et al.* (2010). Rapid molecular detection of tuberculosis and rifampin resistance. *N Engl J Med* **363:**1005-1015.

Bohsali, A., Abdalla, H., Velmurugan, K. and Briken, V. (2010). The non-pathogenic mycobacteria M. smegmatis and M. fortuitum induce rapid host cell apoptosis via a caspase-3 and TNF dependent pathway. *BMC Microbiology* **10**.

Boom, R., Sol, C. J. A., Salimans, M. M. M., Jansen, C. L., Dillen, P. M. E. W.-V. and Noordaa, J. V. D. (1990). Rapid and Simple Method for Purification of Nucleic Acids. *Journal of Clinical Microbiology* **28:**495-503.

Breadmore, M. C., Wolfe, K. A., Arcibal, I. G., Leung, W. K., Dickson, D., Giordano, B. C., Power, M. E. *et al.* (2003). Microchip-based purification of DNA from biological samples. *Anal Chem* **75:**1880-1886.

Brown-Elliott, B. A., Nash, K. A. and Wallace, R. J., Jr. (2012). Antimicrobial susceptibility testing, drug resistance mechanisms, and therapy of infections with nontuberculous mycobacteria. *Clin Microbiol Rev* **25:**545-582.

Brown-Elliott, B. A., Vasireddy, S., Vasireddy, R., Iakhiaeva, E., Howard, S. T., Nash, K., Parodi, N. *et al.* (2015). Utility of sequencing the erm(41) gene in isolates of Mycobacterium abscessus subsp. abscessus with low and intermediate clarithromycin MICs. *J Clin Microbiol* **53:**1211-1215.

Brown-Elliott, B. A. and Wallace, R. J. (2002). Clinical and Taxonomic Status of Pathogenic Nonpigmented or Late-Pigmenting Rapidly Growing Mycobacteria. *Clinical Microbiology Reviews* **15:**716-746.

Brown, L., Wolf, J. M., Prados-Rosales, R. and Casadevall, A. (2015). Through the wall: extracellular vesicles in Gram-positive bacteria, mycobacteria and fungi. *Nat Rev Microbiol* **13:**620-630.

Brown, S., Santa Maria, J. P., Jr. and Walker, S. (2013). Wall teichoic acids of gram-positive bacteria. *Annu Rev Microbiol* **67:**313-336.

Bryant, J. M., Grogono, D. M., Greaves, D., Foweraker, J., Roddick, I., Inns, T., Reacher, M. *et al.* (2013). Whole-genome sequencing to identify transmission of Mycobacterium abscessus between patients with cystic fibrosis: a retrospective cohort study. *The Lancet* **381:**1551-1560.

Buddle, B. M., Livingstone, P. G. and de Lisle, G. W. (2009). Advances in ante-mortem diagnosis of tuberculosis in cattle. *N Z Vet J* **57:**173-180.

Butler, W. R., Jost, K. C. and Kilburn, J. (1991). Identification of Mycobacteria by High-Performance Liquid Chromatography. *Journal of Clinical Microbilogy* **29 (11):**2468-2472.

Buxton, G. V., Greenstock, C. L., Helman, W. P. and Ross, A. B. (1988). Critical review of rate constants for reactions of hydrated electrons, hydrogen atoms, and hydroxyl radicals (•OH/•O−) in aqueous solution. *J. Phys. Chem.* **17:**513–886.

Byrd, T. F. and Lyons, C. R. (1999). Preliminary Characterization of a Mycobacterium abscessus Mutant in Human and Murine Models of Infection. *Infection and Immunity* **67:**4700-4707.

Cade, C. E., Dlouhy, A. C., Medzihradszky, K. F., Salas-Castillo, S. P. and Ghiladi, R. A. (2010). Isoniazid-resistance conferring mutations in Mycobacterium tuberculosis KatG: catalase, peroxidase, and INH-NADH adduct formation activities. *Protein Sci* **19:**458-474.

Canatella, P. J., Karr, J. F., Petros, J. A. and Prausnitz, M. R. (2001). Quantitative study of electroporation-mediated molecular uptake and cell viability. *Biophysical Journal* **80:**755–764.

Carl, B. (2015). Bovine TB statistics: Great Britain [Online]. Available at: http://researchbriefings.parliament.uk/ResearchBriefing/Summary/SN06081 [Accessed: 5th July 2016].

Castellana, G., Grimaldi, A., Castellana, M., Farina, C. and Castellana, G. (2016). Pulmonary nocardiosis in Chronic Obstructive Pulmonary Disease: Anew clinical challenge. *Respiratory Medicine Case Reports* **18:**14-21.

Castro-Escarpulli, G., Alonso-Aguilar, N. M., Sánchez, G. R., Bocanegra-Garcia, V., Guo, X., Juárez-Enríquez, S. R., Luna-Herrera, J. *et al.* (2015). Identification and Typing Methods for the Study of Bacterial Infections: a Brief Review and Mycobacterial as Case of Study. *Arch Clin Microbiol* **7**.

Cécile Rousseau, Y. B., Michel Huerre, Nathalie Winter, Olivier Neyrolles, Brigitte Gicquel, Elisabeth Pivert, Patrick Avé, Mary Jackson. (2004). Production of phthiocerol dimycocerosates protects Mycobacterium tuberculosis from the cidal activity of reactive nitrogen intermediates produced bymacrophages and modulates the early immune response to infection. *Cellular Microbiology* **6:**11.

Celandroni, F., Longo, I., Tosoratti, N., Giannessi, F., Ghelardi, E., Salvetti, S., Baggiani, A. *et al.* (2004). Effect of microwave radiation on Bacillus subtilis spores. *J Appl Microbiol* **97:**1220-1227.

Challis, L. J. (2005). Mechanisms for interaction between RF fields and biological tissue. *Bioelectromagnetics* **7:**98-106.

Chamani, J., Dehghan-Naeri, N. and Saleh-Moghadam, M. (2010). Anionic Surfactant Binding to Lysozyme and Hydrophobic Interactions Effect to the Binding: A Novel Binding Model. *Asian Journal of Chemistry* **22:**4347-4355.

Chan, J., Fan, X., Hunter, S. W., Brennan, P. J. and Bloom, B. R. (1991). Lipoarabinomannan, a Possible Virulence Factor Involved in Persistence of Mycobacterium tuberculosis within Macrophages. *Infection and Immunity* **59:**1755-1761.

Chang, J. C., Miner, M. D., Pandey, A. K., Gill, W. P., Harik, N. S., Sassetti, C. M. and Sherman, D. R. (2009). igr Genes and Mycobacterium tuberculosis cholesterol metabolism. *J Bacteriol* **191:**5232-5239.

Chaturvedi, V., Dwivedi, N., Tripathi, R. P. and Sinha, S. (2007). Evaluation of Mycobacterium smegmatis as a possible surrogate screen for selecting molecules active against multi-drug resistant Mycobacterium tuberculosis. *J. Gen. Appl. Microbiol.* **53:**333–337.

Chen, K., Zhang, Y. and Peng, Y. (2017a). Variable-number tandem repeat markers for Mycobacterium intracellulare genotyping: comparison to the 16S rRNA gene sequencing. *J Infect Dev Ctries* **11:**158-165.

Chen, Y. T., Kolhatkar, A. G., Zenasni, O., Xu, S. and Lee, T. R. (2017b). Biosensing Using Magnetic Particle Detection Techniques. *Sensors (Basel)* **17**.

Chernomordik, L. V., Sukharev, S. I., Popov, S. V., Pastushenko, V. F., Sokirko, A. V., I.G., A. and Chizmadzhev, Y. A. (1987). The electrical breakdown of cell and lipid membranes: the similarity of phenomenologies. *Biochemica Biophysica Acta* **902:**360-373.

Cho, S. N. (2007). Current Issues on Molecular and Immunological Diagnosis of Tuberculosis. *Yonsei Medical Journal* **48:**347-359.

Choe, H., Deirmengian, C. A., Hickok, N. J., Morrison, T. N. and Tuan, R. S. (2015). Molecular Diagnostics. *J Am Acad Orthop Surg.* **23:**26-31.

Choi, G. E., Chang, C. L., Whang, J., Kim, H. J., Kwon, O. J., Koh, W. J. and Shin, S. J. (2011). Efficient differentiation of Mycobacterium abscessus complex isolates to the species level by a novel PCR-based variable-number tandem-repeat assay. *J Clin Microbiol* **49:**1107-1109.

Chung, H. J., Castro, C. M., Im, H., Lee, H. and Weissleder, R. (2013). A magneto-DNA nanoparticle system for rapid detection and phenotyping of bacteria. *Nat Nanotechnol* **8:**369-375.

Classen, D. C., Morningstar, J. M. and Shanley, J. D. (1987). Detection of antibody to murine cytomegalovirus by enzyme-linked immunosorbent and indirect immunofluorescence assays. . *J Clin Microbiol.* **25:**600–604.

CLSI. (2012). Methods for Dilution Antimicrobial Susceptibility Tests f or Bacteria That Grow Aerobically; Approved St andard—Ninth Edition. 9th ed. CLSI document M07-A9. Wayne, PA: Clinical and Laboratory, Standards Institute, USA p. 68.

Conville, P. S. and Witebsky, F. G. (1998). Variables Affecting Results of Sodium Chloride Tolerance Test for identification of rapidly growing mycobacteria. *Journal of clinical microbiology* **36:**1555–1559.

Cook, G. M., Berney, M., Gebhard, S., Heinemann, M., Cox, R. A., Danilchanka, O. and Niederweis, M. (2009). Physiology of Mycobacteria. **55:**81-319.

Copty, A. B., Neve-Oz, Y., Barak, I., Golosovsky, M. and Davidov, D. (2006). Evidence for a specific microwave radiation effect on the green fluorescent protein. *Biophys J* **91:**1413-1423.

Cortes, M. A., Nessar, R. and Singh, A. K. (2010). Laboratory maintenance of Mycobacterium abscessus. *Curr Protoc Microbiol* **Chapter 10:**Unit 10D 11.

Cousins, D. V., Bastida, R., Cataldi, A., Quse, V., Redrobe, S., Dow, S., Duignan, P. *et al.* (2003). Tuberculosis in seals caused by a novel member of the Mycobacterium tuberculosis complex: Mycobacterium pinnipedii sp. nov. *Int J Syst Evol Microbiol* **53:**1305-1314.

Craw, P. and Balachandran, W. (2012). Isothermal nucleic acid amplification technologies for point-of-care diagnostics: a critical review. *Lab Chip* **12:**2469-2486.

Crellin, P. K., Luo, C.-Y. and Morita, Y. S. (2013). Metabolism of Plasma Membrane Lipids in Mycobacteria and Corynebacteria, Lipid Metabolism. In: Baez, R.V. (ed.) *Lipid Metabolism*. InTechOpen, pp. 119-148.

Cullis, P. R. and De Kruijff, B. (1979). Lipid polymorphism and the functional roles of lipids in biological membranes. *Biochimica et Biophysica Acta* **559:**399 420.

da Costa, C., Walker, B. and Bonavia, A. (2015). Tuberculosis vaccines--state of the art, and novel approaches to vaccine development. *Int J Infect Dis* **32:**5-12.

Danilevich, V. N., Petrovskaya, L. E. and Grishin, E. V. (2008). A Highly Efficient Procedure for the Extraction of Soluble Proteins from Bacterial Cells with Mild Chaotropic Solutions. *Chemical Engineering & Technology* **31:**904-910.

Daugelaite, J., O' Driscoll, A. and Sleator, R. D. (2013). An Overview of Multiple Sequence Alignments and Cloud Computing in Bioinformatics. *ISRN Biomathematics* 14.

Davidson, R. M., Hasan, N. A., de Moura, V. C., Duarte, R. S., Jackson, M. and Strong, M. (2013). Phylogenomics of Brazilian epidemic isolates of Mycobacterium abscessus subsp. bolletii reveals relationships of global outbreak strains. *Infect Genet Evol* **20:**292-297.

Dawkins, A. W. J., Nightingale, N. R. V., South, G. P., Sheppard, R. J. and Grant, E. H. (1979a). The role of water in microwave absorption by biological material with particular reference to microwave hazards. *Phys. Med. Biol.* **24:**1168-1176.

Dawkins, A. W. J., Nightingale, N. R. V., South, G. P., Sheppard, R. J. and Grant, E. H. (1979b). The role of water in microwave absorption by biological materials with particular reference to microwave hazards. *PHYS. MED. BIOL.* **24:**1168-1176.

de la Hoz, A., Díaz-Ortiz, A. and Moreno, A. (2007). Review on Non-Thermal Effects of Microwave Irradiation in Organic Synthesis. *Journal of Microwave Power & Electromagnetic Energy* **41:**41-66

de la Rua-Domenech, R., Goodchild, A. T., Vordermeier, H. M., Hewinson, R. G., Christiansen, K. H. and Clifton-Hadley, R. S. (2006). Ante mortem diagnosis of tuberculosis in cattle: a review of the tuberculin tests, gamma-interferon assay and other ancillary diagnostic techniques. *Res Vet Sci* **81:**190-210.

de Zwaan, R., van Ingen, J. and van Soolingen, D. (2014). Utility of rpoB gene sequencing for identification of nontuberculous mycobacteria in the Netherlands. *J Clin Microbiol* **52:**2544-2551.

Deng, X. and Cheng, J. (2011). MSACompro: protein multiple sequence alignment using predicted secondary structure, solvent accessibility, and residue-residue contacts. *BMC Bioinformatics* **12:**472.

Dheda, K., Ruhwald, M., Theron, G., Peter, J. and Yam, W. C. (2013). Point-of-care diagnosis of tuberculosis: past, present and future. *Respirology* **18:**217-232.

Döffinger, R., Jouanguy, E., Dupuis, S., Fondanèche, M., Stephan, J., Emile, J., Lamhamedi-Cherradi, S. *et al.* (2000). Partial Interferon-g Receptor Signaling Chain Deficiency in a Patient with Bacille Calmette-Gue´rin and Mycobacterium abscessus Infection. *The Journal of Infectious Diseases* **181:**379–384.

Dower, W. J., Miller, J. F. and Ragsdale, C. W. (1988). High efficiency transformation of E.coli by high voltage electroporation. *Nucleic Acids Research* **16** 6127-6145.

Duarte, R. S., Lourenco, M. C., Fonseca Lde, S., Leao, S. C., Amorim Ede, L., Rocha, I. L., Coelho, F. S. *et al.* (2009). Epidemic of postsurgical infections caused by Mycobacterium massiliense. *J Clin Microbiol* **47:**2149-2155.

Dubnau, E. (2002). Mycobacterium tuberculosis Genes Induced during Infection of Human Macrophagesdagger. *Infection and Immunity* **70:**2787-2795.

Duffey, P. S., Guthertz, L. S. and Evans, G. C. (1996). Improved Rapid Identification of Mycobacteria by Combining Solid-Phase Extraction with High-Performance Liquid Chromatography Analysis of BACTEC Cultures. *Journal of Clinical Microbilogy* **34 (8):**1939–1943.

Edelstein, R. L., Tamanaha, C. R., Sheehan, P. E., Miller, M. M., Baselt, D. R., Whitman, L. J. and Colton, R. J. (2000). The BARC biosensor applied to the detection of biological warfare agents. *Biosensors & Bioelectronics* **14:**805–813.

Edwards, Y. J. and Cottage, A. (2003). Bioinformatics methods to predict protein structure and function. A practical approach. *Mol Biotechnol.* **2:**39-66.

Eickhoff, H. and Malik, A. (2013). Planar Protein Arrays in Microtiter Plates: Development of a New Format Towards Accurate, Automation-Friendly and Affordable (A3) Diagnostics. *Adv Biochem Eng Biotechnol* **133:**149–165.

Eisenberg, E. and Levanon, E. Y. (2013). Human housekeeping genes, revisited. *Trends Genet* **29:**569-574.

El-Hajj, H. H., Marras, S. A., Tyagi, S., Kramer, F. R. and Alland, D. (2001). Detection of rifampin resistance in Mycobacterium tuberculosis in a single tube with molecular beacons. *J Clin Microbiol* **39:**4131-4137.

El Helou, G., Viola, G. M., Hachem, R., Han, X. Y. and Raad, I. I. (2013). Rapidly growing mycobacterial bloodstream infections. *The Lancet Infectious Diseases* **13:**166-174.

Enarsona, D. A. and Billo, N. E. (2007). Critical evaluation of the Global DOTS Expansion Plan. *85* **5:**395–398.

Engstrom, A., Morcillo, N., Imperiale, B., Hoffner, S. E. and Jureen, P. (2012). Detection of first- and second-line drug resistance in Mycobacterium tuberculosis clinical isolates by pyrosequencing. *J Clin Microbiol* **50:**2026-2033.

Esteban, J. and Ortiz-Pe´rez, A. (2009). Current treatment of atypical mycobacteriosis. *Expert Opin. Pharmacother* **10:**2787-2799.

Esther, C. R., Jr., Esserman, D. A., Gilligan, P., Kerr, A. and Noone, P. G. (2010). Chronic Mycobacterium abscessus infection and lung function decline in cystic fibrosis. *J Cyst Fibros* **9:**117-123.

Fletcher, H. A. and Schrager, L. (2016). TB vaccine development and the End TB Strategy: importance and current status. *Trans R Soc Trop Med Hyg* **110:**212-218.

Fletcher, L. A., Chen, Y., Whitaker, P., Denton, M., Peckham, D. G. and Clifton, I. J. (2016). Survival of Mycobacterium abscessus isolated from people with cystic fibrosis in artificially generated aerosols. *European Respiratory Journal* **48:**1789-1791.

Floto, R. A., Olivier, K. N., Saiman, L., Daley, C. L., Herrmann, J. L., Nick, J. A., Noone, P. G. *et al.* (2016). US Cystic Fibrosis Foundation and European Cystic Fibrosis Society consensus recommendations for the management of non-tuberculous mycobacteria in individuals with cystic fibrosis. *Thorax* **71 Suppl 1:**i1-22.

Floyd, M. M., Silcox, V. A., W D Jones, J., Butler, W. R. and Kilburn, J. O. (1992). Separation of Mycobacterium bovis BCG from Mycobacterium tuberculosis and Mycobacterium bovis by Using High-Performance Liquid Chromatography of Mycolic Acids. *Journal of Clinical Microbilogy* **30:**1327-1330.

Forrellad, M. A., Klepp, L. I., Gioffre, A., Sabio y Garcia, J., Morbidoni, H. R., de la Paz Santangelo, M., Cataldi, A. A. *et al.* (2013). Virulence factors of the Mycobacterium tuberculosis complex. *Virulence* **4:**3-66.

Franco-Paredes, C., Rouphael, N., del Rio, C. and Santos-Preciado, J. I. (2006). Vaccination strategies to prevent tuberculosis in the new millennium: from BCG to new vaccine candidates. *Int J Infect Dis* **10:**93-102.

Frick, M. (2015). The Tuberculosis Vaccines Pipeline: A New Path to the Same Destination?

García-Agudo, L., Jesús, I., Rodríguez-Iglesias, M. and García-Martos, P. (2011). Evaluation of INNO-LIPA mycobacteria v2 assay for identification of rapidly growing mycobacteria. *Brazilian Journal of Microbiology* **42:**1220-1226.

Geddes, C. D., Yoshimura, T., Verschaeve, L., Panagopoulos, D. J., Kostoff, R. N., Imaizumi, K., Furtado-Filho, O. V. *et al.* (2017). Microwave Effects on DNA and Proteins. Springer International Publishing.

Georgopapadakou, N. H., Dix, B. A., Smith, S. A., Freudenberger, J. and Funke, P. T. (1987). Effect of Antifungal Agents on Lipid Biosynthesis and Membrane Integrity in Candida albicans. *Antimicrobial Agents and Chemotherapy* **31:**46-51.

Giouroudi, I. and Keplinger, F. (2013). Microfluidic biosensing systems using magnetic nanoparticles. *Int J Mol Sci* **14:**18535-18556.

Godzik, A., Jambon, M. and Friedberg, I. (2007). Computational protein function prediction: Are we making progress? . *Cell Mol Life Sci*

64:2505–2511.

Gomez, M. P., Donkor, S., Adetifa, I. M., Ota, M. O. C. and Sutherland, J. S. (2012). Analysis of LAM and 38 kDa Antibody Levels for Diagnosis of TB in a Case-Control Study in West Africa. *ISRN Immunology* **2012:**1-6.

Grandjean, L., Martin, L., Gilman, R. H., Valencia, T., Herrera, B., Quino, W., Ramos, E. *et al.* (2008). Tuberculosis diagnosis and multidrug resistance testing by direct sputum culture in selective broth without decontamination or centrifugation. *J Clin Microbiol* **46:**2339-2344.

Granger, K., Moore, R. J., Davies, J. K., Vaughan, J. A., Stiles, P. L., Stewart, D. J. and Tizard, M. L. (2004). Recovery of Mycobacterium avium subspecies paratuberculosis from the natural host for the extraction and analysis in vivo-derived RNA. *J Microbiol Methods* **57:**241-249.

Griffith, D. E., Aksamit, T., Brown-Elliott, B. A., Catanzaro, A., Daley, C., Gordin, F., Holland, S. M. *et al.* (2007). An official ATS/IDSA statement: diagnosis, treatment, and prevention of nontuberculous mycobacterial diseases. *Am J Respir Crit Care Med* **175:**367-416.

Griffith, D. E., Brown-Elliott, Barbara. A. , Benwill, J. L. and Wallace, R. J. J. (2015). Mycobacterium abscessus “Pleased to Meet You, Hope You Guess My Name...”. *AnnalsATS* **12**.

Guerrero, D., Bautista, R., Villalobos, D. P., Canton, F. R. and Claros, M. G. (2010). AlignMiner: a Web-based tool for detection of divergent regions in multiple sequence alignments of conserved sequences. *Algorithms Mol Biol* **5:**24.

Günther, G. (2014). Multidrug-resistant and extensively drug-resistant tuberculosis: a review of current concepts and future challenges. *Clinical Medicine* **14:**279–285.

Haest, C. W. M., De Gier, J., OP DEN Kamp, J. A. F., Bartels, P. and VAN DEENEN, L. L. M. (1972). Changes in permeability of staphylococcus aureus and derived liposomes with varying lipid composition. *Biochimica et Biophysica Acta* **255:**720-733.

Haest, C. W. M., De Gier, J. and Van Deenen, L. L. M. (1969). Changes in the chemical and the barrier properties of the membrane lipids of E. coli by variation of the temperature of growth. *Chem. Phys. Lipids* **3:**413-417.

Han, X. Y., De, I. and Jacobson, K. L. (2007). Rapidly growing mycobacteria: clinical and microbiologic studies of 115 cases. *Am J Clin Pathol* **128:**612-621.

Harland, C. W., Rabuka, D., Bertozzi, C. R. and Parthasarathy, R. (2008). The Mycobacterium tuberculosis virulence factor trehalose dimycolate imparts desiccation resistance to model mycobacterial membranes. *Biophys J* **94:**4718-4724.

Harris, K. A. and Kenna, D. T. (2014). Mycobacterium abscessus infection in cystic fibrosis: molecular typing and clinical outcomes. *J Med Microbiol* **63:**1241-1246.

Harris, K. A., Kenna, D. T., Blauwendraat, C., Hartley, J. C., Turton, J. F., Aurora, P. and Dixon, G. L. (2012). Molecular fingerprinting of Mycobacterium abscessus strains in a cohort of pediatric cystic fibrosis patients. *J Clin Microbiol* **50:**1758-1761.

Henkle, E. and Winthrop, K. (2014). Nontuberculous Mycobacteria Infections in Immunosuppressed Hosts. *Clin Chest Med* **36:**91–99.

Hett, E. C. and Rubin, E. J. (2008). Bacterial growth and cell division: a mycobacterial perspective. *Microbiol Mol Biol Rev* **72:**126-156, table of contents.

Hibino, M., Itoh, H. and Kinosita, K. J. (1993). Time courses of cell electroporation as revealed by submicrosecond imaging of transmembrane potential. *Biophysica Joumal* **64:**1789-1800.

Hill, R., Masui, K. W. and Scott, D. (2018). The Spectrum of the Universe.

Hol, W. G. J., Halie, L. M. and Sander, C. (1981). Dipoles of the a-helix and (J-sheet: their role in protein folding *Nature* **294:**532-536.

Honda, J. R., Hasan, N. A., Davidson, R. M., Williams, M. D., Epperson, L. E., Reynolds, P. R., Smith, T. *et al.* (2016). Environmental Nontuberculous Mycobacteria in the Hawaiian Islands. *PLoS Negl Trop Dis* **10:**e0005068.

Howard, S. T., Rhoades, E., Recht, J., Pang, X., Alsup, A., Kolter, R., Lyons, C. R. *et al.* (2006). Spontaneous reversion of Mycobacterium abscessus from a smooth to a rough morphotype is associated with reduced expression of glycopeptidolipid and reacquisition of an invasive phenotype. *Microbiology* **152:**1581-1590.

Hsieh, H. V., Dantzler, J. L. and Weigl, B. H. (2017). Analytical Tools to Improve Optimization Procedures for Lateral Flow Assays. *Diagnostics (Basel)* **7**.

Huanga, K. C., Mukhopadhyay, R., Wena, B., Gitaia, Z. and Wingreen, N. S. (2008). Cell shape and cell-wall organization in Gram-negative bacteria. *PNAS* **105:**19282–19287.

Huebner, R. E., Schein, M. F. and John B. Bass, J. (1993). The Tuberculin Skin Test. *Clinical Infectious Diseases* **17:**968-975.

Hunter, R. L., Olsen, M. R., Jagannath, C., and Actor, J. K. (2006). "Multiple roles of cord factor in the pathogenesis of primary, secondary, and cavitary tuberculosis, including a revised description of the pathology of secondary disease," *Annals of Clinical and Laboratory Science*, **36 (4):** 371–386.

Hysom, D. A., Naraghi-Arani, P., Elsheikh, M., Carrillo, A. C., Williams, P. L. and Gardner, S. N. (2012). Skip the Alignment: Degenerate, Multiplex Primer and Probe Design Using K-mer Matching Instead of Alignments. *PLoS ONE* **7:**e34560.

Iakhiaeva, E., McNulty, S., Elliott, B. A. B., Falkinham, J. O., Williams, M. D., Vasireddy, R., Wilson, R. W. *et al.* (2012). Mycobacterial Interspersed Repetitive-Unit–Variable-Number Tandem-Repeat (MIRU-VNTR) Genotyping of Mycobacterium intracellulare for Strain Comparison with Establishment of a PCR-Based Database. *Journal of Clinical Microbiology* **51:**409–416.

IDT. (2011). The Polymerase Chain Reaction [Online]. IDT. Available at: http://sfvideo.blob.core.windows.net/sitefinity/docs/default-source/biotech-basics/the-polymerase-chain-reaction.pdf?sfvrsn=7493407_4 [Accessed: 27.04.2019].

Islam, M. S., Aryasomayajula, A. and Selvaganapathy, P. R. (2017). A Review on Macroscale and Microscale Cell Lysis Methods. *Micromachines* **8**.

Israelachvili, J. N. and Mitchell, D. J. (1975). A model for the packing of lipids in bilayer membranes. *Biochim Biophys Acta* **389** 13-19.

Iwamoto, T., Sonobe, T. and Hayashi, K. (2003). Loop-Mediated Isothermal Amplification for Direct Detection of Mycobacterium tuberculosis Complex, M. avium, and M. intracellulare in Sputum Samples. *Journal of Clinical Microbiology* **41:**2616-2622.

Jacobson, K. R., Theron, D., Kendall, E. A., Franke, M. F., Barnard, M., van Helden, P. D., Victor, T. C. *et al.* (2013). Implementation of genotype MTBDRplus reduces time to multidrug-resistant tuberculosis therapy initiation in South Africa. *Clin Infect Dis* **56:**503-508.

Jagielski, T., van Ingen, J., Rastogi, N., Dziadek, J., Mazur, P. K. and Bielecki, J. (2014). Current methods in the molecular typing of Mycobacterium tuberculosis and other mycobacteria. *Biomed Res Int* **2014:**645802.

Jankovic, S., Milosev, M. and Novakovic, M. (2014). The Effects of Microwave Radiation on microbial cultures. *International Multidisciplinary Journal* **1:**102-108.

Jarand, J., Levin, A., Zhang, L., Huitt, G., Mitchell, J. D. and Daley, C. L. (2011). Clinical and microbiologic outcomes in patients receiving treatment for Mycobacterium abscessus pulmonary disease. *Clin Infect Dis* **52:**565-571.

Jeong, J., Kim, S. R., Lee, S. H., Lim, J. H., Choi, J. I., Park, J. S., Chang, C. L. *et al.* (2011). The Use of High Performance Liquid Chromatography to Speciate and Characterize the Epidemiology of Mycobacteria. *Lab Med* **42:**612-617.

Johnson, M. M. and Odell, J. A. (2014). Nontuberculous mycobacterial pulmonary infections. *J Thorac Dis* **6:**210-220.

Jordao, L., Bleck, C. K., Mayorga, L., Griffiths, G. and Anes, E. (2008). On the killing of mycobacteria by macrophages. *Cell Microbiol* **10:**529-548.

Joshi, L. T., Mali, B. L., Geddes, C. D. and Baillie, L. (2014). Extraction and sensitive detection of toxins A and B from the human pathogen Clostridium difficile in 40 seconds using microwave-accelerated metal-enhanced fluorescence. *PLoS One* **9:**e104334.

Joshi, S. M., Pandey, A. K., Capite, N., Fortune, S. M., Rubin, E. J. and Sassetti, C. M. (2006). Characterization of mycobacterial virulence genes through genetic interaction mapping. *Proc Natl Acad Sci U S A* **103:**11760-11765.

Kaatze, U. (1990). On the existence of bound water in biological systems as probed by dielectric spectroscopy. *Phys. Med. Biol.* **35:**1663-1681.

Kalendar, R., Khassenov, B., Ramankulov, Y., Samuilova, O. and Ivanov, K. I. (2017). FastPCR: An in silico tool for fast primer and probe design and advanced sequence analysis. *Genomics* **109:**312–319.

Kamphee, H., Chaiprasert, A., Prammananan, T., Wiriyachaiporn, N., Kanchanatavee, A. and Dharakul, T. (2015). Rapid Molecular Detection of Multidrug-Resistant Tuberculosis by PCR-Nucleic Acid Lateral Flow Immunoassay. *PLoS One* **10:**e0137791.

Kanduser, M. and Miklavcic, D. (2008). "Electroporation in biological cell and tissue: an overview," Electrotechnologies for Extraction from Food Plants and Biomaterials, E. Vorobiev and N. Lebovka, eds., pp. 1-37, New York: Springer Science.

Kardos, T. J. and Rabussay, D. P. (2012). Contactless magneto-permeabilization for intracellular plasmid DNA delivery in-vivo. *Hum Vaccin Immunother* **8:**1707-1713.

Karlin, S. and Altschul, S. F. (1990). Methods for assessing the statistical significance of molecular sequences features by using general scoring schemes. *Proc Natl Acad Sci* **87:**2264-2268.

Karlin, S., Bucher, P. and Brendel, V. (1991). Statistical methods and insights for protein and DNA sequences. *Annu. Rev. Biophys. Biophys. Chem.* **20:**175-203.

Kaser, M., Ruf, M. T., Hauser, J., Marsollier, L. and Pluschke, G. (2009). Optimized method for preparation of DNA from pathogenic and environmental mycobacteria. *Appl Environ Microbiol* **75:**414-418.

Käser, M., T., R. M., Hauser, J. and Pluschke, G. (2010). Optimized DNA preparation from mycobacteria. *Cold Spring Harb Protoc*.

Kasprowicz, V. O., Churchyard, G., Lawn, S. D., Squire, S. B. and Lalvani, A. (2011). Diagnosing latent tuberculosis in high-risk individuals: rising to the challenge in high-burden areas. *J Infect Dis* **204 Suppl 4:**S1168-1178.

Katial, R. K., Hershey, J., Purohit-Seth, T., Belisle, J. T., Brennan, P. J., Spencer, J. S. and Engler, R. J. (2001). Cell-mediated immune response to tuberculosis antigens: comparison of skin testing and measurement of in vitro gamma interferon production in whole-blood culture. *Clin Diagn Lab Immunol* **8:**339-345.

Kaufmann, S. (2001). How can immunology contribute to the control of tuberculosis? *Nature Reviews Immunology* **1:**20-30.

Kaufmann, S. H., Weiner, J. and von Reyn, C. F. (2017). Novel approaches to tuberculosis vaccine development. *Int J Infect Dis* **56:**263-267.

Kim, H. Y., Kim, B. J., Kook, Y., Yun, Y. J., Shin, J. H., Kim, B. J. and Kook, Y. H. (2010). Mycobacterium massiliense is differentiated from Mycobacterium abscessus and Mycobacterium bolletii by erythromycin ribosome methyltransferase gene (erm) and clarithromycin susceptibility patterns. *Microbiol Immunol* **54:**347-353.

Kim, K., Hong, S. H., Kim, B. J., Kim, B. R., Lee, S. Y., Kim, G. N., Shim, T. S. *et al.* (2015). Separation of Mycobacterium abscessus into subspecies or genotype level by direct application of peptide nucleic acid multi-probe- real-time PCR method into sputa samples. *BMC Infect Dis* **15:**325.

Kim, T., Lee, J. and Lee, K.-H. (2014). Microwave heating of carbon-based solid materials. *Carbon Letters* **15:**15-24.

Kinosita, K. J. and Tsong, T. Y. (1977). Voltage-Induced Pore Formation and Hemolysis of Human Erythrocytes. *Biochimica et Biophysica Acta* **471:**227-242.

Kipiani, M., Mirtskhulava, V., Tukvadze, N., Magee, M., Blumberg, H. M. and Kempker, R. R. (2014). Significant clinical impact of a rapid molecular diagnostic test (Genotype MTBDRplus assay) to detect multidrug-resistant tuberculosis. *Clin Infect Dis* **59:**1559-1566.

Klenchin, V. A., Sukharev, S., Serov, S. M., Chernomordik, L. V. and Chizmadzhev, Y. A. (1991). Electrically induced DNA uptake by cells is a fast process involving DNA electrophoresis. *Biophys. J. Biophysical Society* **60:**804-811.

Koga, D. and Kramer, K., J. (1983). Hydrolysis of Glycol chitin by chitinolytic enzymes. *Comp. Biochem. Physiol.* **76B:**291-293.

Koh, S. J., Song, T., Kang, Y. A., Choi, J. W., Chang, K. J., Chu, C. S., Jeong, J. G. *et al.* (2010). An outbreak of skin and soft tissue infection caused by Mycobacterium abscessus following acupuncture. *Clin Microbiol Infect* **16:**895-901.

Konno, K., Feldmann, F. M. and McDermott, W. (1967). Pyrazinamide susceptibility and amidase activity of tubercle bacilli. *Am Rev Respir Dis* **95:**461-469.

Kotlowski, R., Martin, A., Ablordey, A., Chemlal, K., Fonteyne, P. A. and Portaels, F. (2004). One-tube cell lysis and DNA extraction procedure for PCR-based detection of Mycobacterium ulcerans in aquatic insects, molluscs and fish. *J Med Microbiol* **53:**927-933.

Krane, D. E. and Raymer, M. L. (2002). Fundamental Concepts of Bioinformatics. San Francisco, USA: Pearson Education, Inc., p. 303.

Krassowska, W. and Filev, P. D. (2007). Modeling electroporation in a single cell. *Biophys J* **92:**404-417.

Kulandai, L. T., Lakshmipathy, D., Ramasubban, G. and Rao, M. H. N. (2014). Isolation of Mycobacterium massiliense from a corneal biopsy in India. *JMM Case Reports* **1**.

Kumar, A. and Kaur, J. (2014). Primer Based Approach for PCR Amplification of High GC Content Gene: Mycobacterium Gene as a Model. *Molecular Biology International*.

Kumbhar, A. (2017). Overview of ISM Bands and Software-Defined Radio Experimentation. *Wireless Pers Commun* **97:**3743–3756.

Kwon, Y. H., Lee, G.-Y., Kim, W.-S. and Kim, K. J. (2009). A Case of Skin and Soft Tissue Infection Caused by Mycobacterium abscessus. *Ann Dermatol* **21:**84-87.

Laboratory Info. (2018). Ziehl-Neelsen Stain (ZN-Stain): Principle, Procedure, Reporting and Modifications [Online]. Available at: https://laboratoryinfo.com/zn-stain/ [Accessed: 02.10.2018].

Lalvani, A. and Pareek, M. (2010). A 100 year update on diagnosis of tuberculosis infection. *Br Med Bull* **93:**69-84.

Lardeux, F., Torrico, G. and Aliaga, C. (2016). Calculation of the ELISA's cut-off based on the change-point analysis method for detection of Trypanosoma cruzi infection in Bolivian dogs in the absence of controls. *Mem Inst Oswaldo Cruz* **111:**501–504.

Larkin, M. A., Blackshields, G., Brown, N. P., Chenna, R., McGettigan, P. A., McWilliam, H., Valentin, F. *et al.* (2007). Clustal W and Clustal X version 2.0. *Bioinformatics* **23:**2947-2948.

Larsen, M. H., Vilchèze, C., Kremer, L., Besra, G. S., Parsons, L., Salfinger, M., Heifets, L. *et al.* (2002). Overexpression of inhA, but not kasA, confers resistance to isoniazid and ethionamide in Mycobacterium smegmatis, M. bovis BCG and M. tuberculosis. *Molecular Microbiology* **2:**453–466.

Leão, S., Viana-Niero, C., Matsumoto, C., Lima, K., Lopes, M., Palaci, M., Hadad, D. *et al.* (2010). Epidemic of surgical-site infections by a single clone of rapidly growing mycobacteria in Brazil. *Future Microbiol* **5(6):**971-980.

Leao, S. C., Tortoli, E., Euzeby, J. P. and Garcia, M. J. (2011). Proposal that Mycobacterium massiliense and Mycobacterium bolletii be united and reclassified as Mycobacterium abscessus subsp. bolletii comb. nov., designation of Mycobacterium abscessus subsp. abscessus subsp. nov. and emended description of Mycobacterium abscessus. *Int J Syst Evol Microbiol* **61:**2311-2313.

Lee, M.-R., Sheng, W.-H., Hung, C.-C., Yu, C.-J., Lee, L.-N. and Hsueh, P.-R. (2015). Mycobacterium abscessus Complex Infections in Humans. *Emerging Infectious Diseases* **21 (9):**1638-1646.

Lee, M. U., Lee, J. K. and Yun, G. S. (2018). Generation of energetic electrons in pulsed microwave plasmas. *Plasma Process Polym* **15**.

Lee, S. H. (2016a). Tuberculosis Infection and Latent Tuberculosis. *Tuberc Respir Dis (Seoul)* **79:**201-206.

Lee, S. H. (2016b). Tuberculosis Infection and Latent Tuberculosis. *Tuberc Respir Dis* **79:**201-206.

Lee, S. H., Yoo, H. K., Kim, S. H., Koh, W. J., Kim, C. K., Park, Y. K. and Kim, H. J. (2014). Detection and assessment of clarithromycin inducible resistant strains among Korean Mycobacterium abscessus clinical strains: PCR methods. *J Clin Lab Anal* **28:**409-414.

Leontiadou, H., Mark, A. E. and Marrink, S. J. (2004). Molecular Dynamics Simulations of Hydrophilic Pores in Lipid Bilayers. *Biophysical Journal* **86:**2156–2164.

Lever, M. A., Torti, A., Eickenbusch, P., Michaud, A. B., Šantl-Temkiv, T. and Jørgensen, B. B. (2015). A modular method for the extraction of DNA and RNA, and the separation of DNA pools from diverse environmental sample types. *Front. Microbiol* **6**.

Lilenmaum, W., Ribeiro, E. R. and Souza, G. N. (1999). Evaluation of an ELISA-PPD for the diagnosis of bovine tuberculosis in field trials in Brazil. *Research in Veterinary Science* **66:** 191–195.

Lomzov, A. A., Vorobjev, Y. N. and Pyshnyi, D. V. (2015). Evaluation of the Gibbs Free Energy Changes and Melting Temperatures of DNA/DNA Duplexes Using Hybridization Enthalpy Calculated by Molecular Dynamics Simulation. *J. Phys. Chem.* **119:**15221−15234.

Loy, A., Arnold, R., Tischler, P., Rattei, T., Wagner, M. and Horn, M. (2008). probeCheck – a central resource for evaluating oligonucleotide probe coverage and specificity. *Environmental Microbiology* **10:**2894–2898.

Luka, G., Ahmadi, A., Najjaran, H., Alocilja, E., DeRosa, M., Wolthers, K., Malki, A. *et al.* (2015). Microfluidics Integrated Biosensors: A Leading Technology towards Lab-on-a-Chip and Sensing Applications. *Sensors* **15:**30011–30031.

Luo, H., Gao, F. and Lin, Y. (2015). Evolutionary conservation analysis between the essential and nonessential genes in bacterial genomes. *Sci. Rep.* **5**.

Maček-Lebar, A. and Miklavčič, D. (2001). Cell electropermeabilization to small molecules in vitro: control by pulse parameters. *Radiol Oncol* **35:**193-202.

Machado, G. E., Matsumoto, C. K., Chimara, E., Duarte, R. d. S., Freitas, D. d., Palaci, M., Hadad, D. J. *et al.* (2014). Multilocus Sequence Typing Scheme versus Pulsed-Field Gel Electrophoresis for Typing Mycobacterium abscessus Isolates. *Journal of Clinical Microbiology* **52 (8):** 2881–2891.

Macheras, E., Roux, A. L., Bastian, S., Leao, S. C., Palaci, M., Sivadon-Tardy, V., Gutierrez, C. *et al.* (2011). Multilocus sequence analysis and rpoB sequencing of Mycobacterium abscessus (sensu lato) strains. *J Clin Microbiol* **49:**491-499.

Maciel, H., Mathis, H., Lopes Ferreira, N., Lyew, D., Guiot, S., Monot, F., Greer, C. W. *et al.* (2008). Use of Mycobacterium austroafricanum IFP 2012 in a MTBE-degrading bioreactor. *J Mol Microbiol Biotechnol* **15:**190-198.

Madden, T. (2013). The BLAST Sequence Analysis Tool.*The NCBI Handbook [Internet]*. 2nd ed., Vol. 2019. USA: Bethesda (MD): National Center for Biotechnology Information (US).

Maiga, M., Abaza, A. and Bishai, W. R. (2012). Current tuberculosis diagnostic tools & role of urease breath test. *Indian J Med Res* **135:**731-736.

Mak, W. C., Beni, V. and Turner, A. P. F. (2016). Lateral-flow technology: From visual to instrumental. *TrAC Trends in Analytical Chemistry* **79:**297-305.

Marrink, S. J., de Vries, A. H. and Tieleman, D. P. (2009). Lipids on the move: simulations of membrane pores, domains, stalks and curves. *Biochim Biophys Acta* **1788:**149-168.

Matsumoto, C. K., Chimara, E., Bombarda, S., Duarte, R. S. and Leao, S. C. (2011). Diversity of pulsed-field gel electrophoresis patterns of Mycobacterium abscessus type 2 clinical isolates. *J Clin Microbiol* **49:**62-68.

McKenzie, C. G. J., Koser, U., Lewis, L. E., Bain, J. M., Mora-Montes, H. M., Barker, R. N., Gow, N. A. R. *et al.* (2010). Contribution of Candida albicans Cell Wall Components to Recognition by and Escape from Murine Macrophages. *Infection and Immunity* **78:**1650–1658

McKinney, J. D., Bentrup, K. H., Munoz-Eliaz, E. J., Miczak, A., Chen, B., Chan, W.-T., Swenson, D. *et al.* (2000). Persistence of Mycobacterium tuberculosis in macrophages and mice requires glyxylate shunt enzymes isocitrate lyase. *Nature* **406:**735-738.

McNerney, R., Maeurer, M., Abubakar, I., Marais, B., McHugh, T. D., Ford, N., Weyer, K. *et al.* (2012). Tuberculosis diagnostics and biomarkers: needs, challenges, recent advances, and opportunities. *J Infect Dis* **205 Suppl 2:**S147-158.

McRee, D. I. (1974). Biological Effects of Microwave Radiation. *Journal of the Air Pollution Control Association* **24:**122-127.

Medjahed, H., Gaillard, J. L. and Reyrat, J. M. (2010). Mycobacterium abscessus: a new player in the mycobacterial field. *Trends Microbiol* **18:**117-123.

Meena, L. S. and Rajni. (2010). Survival mechanisms of pathogenic Mycobacterium tuberculosis H37Rv. *FEBS J* **277:**2416-2427.

Melendez, J. H., Santaus, T. M., Brinsley, G., Kiang, D., Mali, B., Hardick, J., Gaydos, C. A. *et al.* (2016). Microwave-accelerated method for ultra-rapid extraction of Neisseria gonorrhoeae DNA for downstream detection. *Anal Biochem* **510:**33-40.

Michel, A. L., Muller, B. and van Helden, P. D. (2010). Mycobacterium bovis at the animal-human interface: a problem, or not? *Vet Microbiol* **140:**371-381.

Migliori, G. B., Ortmann, J., Girardi, E., Besozzi, G., Lange, C., Cirillo, D. M., Ferrarese, M. *et al.* (2007). Extensively drug resistant TB in italy and germany. *Emerging Infectious Diseases* **13:**780-781.

Miller, N., Infante, S. and Cleary, T. (2000). Evaluation of the LiPA MYCOBACTERIA Assay for Identification of Mycobacterial Species from BACTEC 12B Bottles. *Journal of Clinical Microbilogy* **38 (5):**1915–1919.

Mini Physics. (2018). The Electromagetic spectrum [Online]. Available at: https://www.miniphysics.com/electromagnetic-spectrum_25.html [Accessed: 18.12.2018].

Mitchell, G. J., Wiesenfeld, K., Nelson, D. C. and Weitz, J. S. (2012). Critical cell wall hole size for lysis in Gram-positive bacteria. *Journal of the Royal Society Interface*.

Modh, H., Scheper, T. and Walter, J. G. (2018). Aptamer-Modified Magnetic Beads in Biosensing. *Sensors (Basel)* **18**.

Molicotti, P., Bua, A. and Zanetti, S. (2014). Cost-effectiveness in the diagnosis of tuberculosis: choices in developing countries. *J Infect Dev Ctries* **8:**24-38.

Moreno-Altamirano, M. M. B., Paredes-González, I. S., Espitia, C., Santiago-Maldonado, M., Hernández-Pando, R. and Sánchez-García, F. J. (2012). Bioinformatic identification of Mycobacterium tuberculosis proteins likely to target host cell mitochondria: virulence factors? *Microbial Informatics and Experimentation* **2:**9.

Morgulis, A., Coulouris, G., Raytselis, Y., Madden, T. L., Agarwala, R. and Schäffer, A. A. (2008). Database indexing for production MegaBLAST searches. *Bioinformatics* **24:**1757–1764.

Mortaz, E., Masjedi, M. R., Matroodi, S., Abedini, A., Kiani, A., Soroush, D. and Adcock, I. M. (2013). Concomitant Patterns of Tuberculosis and Sarcoidosis *National Research Institute of Tuberculosis and Lung Disease* **12:**6-9

Mostowy, S., Inwald, J., Gordon, S., Martin, C., Warren, R., Kremer, K., Cousins, D. *et al.* (2005). Revisiting the evolution of Mycobacterium bovis. *J Bacteriol* **187:**6386-6395.

Mostowy, S., Onipede, A., Gagneux, S., Niemann, S., Kremer, K., Desmond, E. P., Kato-Maeda, M. *et al.* (2004). Genomic analysis distinguishes Mycobacterium africanum. *J Clin Microbiol* **42:**3594-3599.

Mougaria, F., Bouzianeb, F., Crockettb, F., Nessar, R., Chaub, F., Veziris, N., Saprielf, G. *et al.* (2017). Selection of Resistance to Clarithromycin in Mycobacterium abscessus Subspecies. *Antimicrobial Agents and Chemotherapy* **61**.

Murray, S. J., Barrett, A., Magee, J. G. and Freeman, R. (2003). Optimisation of acid fast smears for the direct detection of mycobacteria in clinical samples. *J. Clin. Pathol* **56:**613–615.

N'Goma, J. C. B., Moigne, V. L., Soismier, N., Laencina, L., Chevalier, F. L., Roux, A.-L., Poncin, I. *et al.* (2015). Mycobacterium abscessus Phospholipase C Expression Is Induced during Coculture within Amoebae and Enhances M. abscessus Virulence in Mice. *Infection and Immunity* **83:**780-791.

Nachiappan, A. C., Rahbar, K., Shi, X., Guy, E. S., Barbosa, E. J. M. J., Shroff, G. S., Ocazionez, D. *et al.* (2017). Pulmonary Tuberculosis- Role of radiology in Diagnosis and management. *Radiology Society of North America* **37:**52–72.

Nagar, A. and Hahsler, M. (2013). Fast discovery and visualization of conserved regions in DNA sequences using quasi-alignment. *BMC Bioinformatics* **14:**S2.

Nash, K. A. (2003). Intrinsic Macrolide Resistance in Mycobacterium smegmatis Is Conferred by a Novel erm Gene, erm(38). *Antimicrobial Agents and Chemotherapy* **47:**3053-3060.

Nash, K. A., Brown-Elliott, B. A. and Wallace, R. J., Jr. (2009). A novel gene, erm(41), confers inducible macrolide resistance to clinical isolates of Mycobacterium abscessus but is absent from Mycobacterium chelonae. *Antimicrob Agents Chemother* **53:**1367-1376.

Nash, K. A., Zhang, Y., Brown-Elliott, B. A. and Wallace, R. J., Jr. (2005). Molecular basis of intrinsic macrolide resistance in clinical isolates of Mycobacterium fortuitum. *J Antimicrob Chemother* **55:**170-177.

Nasiri, M. J., Shahraki, A. H., Fooladi, A. A. I., Dabiri, H. and Feizabadi, M. M. (2017). rpoB Gene Sequencing for Identification of Rapidly Growing Mycobacteria *Arch Pediatr Infect Dis* **5:**e40001.

National Institute of Allergy and Infectious Diseases. (2016). Tuberculosis Drugs and Mechanisms of Action [Online]. NIAID. Available at: https://www.niaid.nih.gov/diseases-conditions/tbdrugs [Accessed: 23/08/2018].

Nature Research. (2019). What 5G means for our health. https://www.nature.com/articles/d42473-019-00009-7. Date accessed:01/10/2019

Nessar, R., Cambau, E., Reyrat, J. M., Murray, A. and Gicquel, B. (2012). Mycobacterium abscessus: a new antibiotic nightmare. *J Antimicrob Chemother* **67:**810-818.

Ng, B. Y. C., Wee, E. J. H., West, N. P. and Trau, M. (2015). Naked-Eye Colorimetric and Electrochemical Detection of Mycobacterium tuberculosis—toward Rapid Screening for Active Case Finding. *ACS Sensors* **1:**173-178.

Ngan, G. J., Ng, L. M., Jureen, R., Lin, R. T. and Teo, J. W. (2011). Development of multiplex PCR assays based on the 16S-23S rRNA internal transcribed spacer for the detection of clinically relevant nontuberculous mycobacteria. *Lett Appl Microbiol* **52:**546-554.

Nguyen, T. H., Pham, V. T., Nguyen, S. H., Baulin, V., Croft, R. J., Phillips, B., Crawford, R. J. *et al.* (2016). The Bioeffects Resulting from Prokaryotic Cells and Yeast Being Exposed to an 18 GHz Electromagnetic Field. *PLoS One* **11:**e0158135.

Nguyen, T. H., Shamis, Y., Croft, R. J., Wood, A., McIntosh, R. L., Crawford, R. J. and Ivanova, E. P. (2015). 18 GHz electromagnetic field induces permeability of Gram-positive cocci. *Sci Rep* **5:**10980.

Nie, W., Duan, H., Huang, H., Lu, Y., Bi, D. and Chu, N. (2014). Species identification of Mycobacterium abscessus subsp. abscessus and Mycobacterium abscessus subsp. bolletii using rpoB and hsp65, and susceptibility testing to eight antibiotics. *Int J Infect Dis* **25:**170-174.

Nishiuchi, Y., Iwamoto, T. and Maruyama, F. (2017). Infection Sources of a Common Non-tuberculous Mycobacterial Pathogen, Mycobacterium avium Complex. *Frontiers in Medicine* **4**.

Notredame, C., Higgins, D. and Heringa, J. (2000). T-Coffee: A novel method for fast and accurate multiple sequence alignment. *J Mol Biol* **302(1):**205-217.

Novickij, V., Grainys, A., Lastauskiene, E., Kananaviciute, R., Pamedytyte, D., Kalediene, L., Novickij, J. *et al.* (2016). Pulsed Electromagnetic Field Assisted in vitro Electroporation: A Pilot Study. *Sci Rep* **6:**335-337.

Nunes-Costa, D., Alarico, S., Dalcolmo, M. P., Correia-Neves, M. and Empadinhas, N. (2016). The looming tide of nontuberculous mycobacterial infections in Portugal and Brazil. *Tuberculosis (Edinb)* **96:**107-119.

Odumeru, J., Gao, A., Chen, S., Raymond, M. and Mutharia, L. (2001). Use of the bead beater for preparation of Mycobacterium paratuberculosis template DNA in milk. *The Canadian Journal ot Veterinary Research* **65:**201-205.

Oh, N. and Park, J.-H. (2014). Endocytosis and exocytosis of nanoparticles in mammalian cells. *International Journal of nanomedicine* **9:**51–63.

Omar, B. A., Atif, H. A. and Mogahid, M. E. (2014). Comparison of three DNA extraction methods for polymerase chain reaction (PCR) analysis of bacterial genomic DNA. *African Journal of Microbiology Research* **8:**598-602.

Oncul, S., Cuce, E. M., Aksu, B. and Inhan Garip, A. (2016). Effect of extremely low frequency electromagnetic fields on bacterial membrane. *Int J Radiat Biol* **92:**42-49.

Ormerod, L. P. (2005). Multidrug-resistant tuberculosis (MDR-TB): epidemiology, prevention and treatment. *Br Med Bull* **73-74:**17-24.

Otu, A. A. (2013). Is the directly observed therapy short course (DOTS) an effective strategy for tuberculosis control in a developing country? *Asian Pac J Trop. Dis* **3:**227-231.

Ou, X., Li, Q., Xia, H., Pang, Y., Wang, S., Zhao, B., Song, Y. *et al.* (2014). Diagnostic accuracy of the PURE-LAMP test for pulmonary tuberculosis at the county-level laboratory in China. *PLoS One* **9:**e94544.

Padilla, E., Gonzalez, V., Manterola, J. M., Perez, A., Quesada, M. D., Gordillo, S., Vilaplana, C. *et al.* (2004). Comparative evaluation of the new version of the INNO-LiPA Mycobacteria and genotype Mycobacterium assays for identification of Mycobacterium species from MB/BacT liquid cultures artificially inoculated with Mycobacterial strains. *J Clin Microbiol* **42:**3083-3088.

Pai, M., Behr, M. A., Dowdy, D., Dheda, K., Divangahi, M., Boehme, C. C., Ginsberg, A. *et al.* (2016). Tuberculosis. *Nat Rev Dis Primers* **2:**16076.

Pall, M. L. (2013). Electromagnetic fields act via activation of voltage-gated calcium channels to produce beneficial or adverse effects. *J Cell Mol Med* **17:**958-965.

Pall, M. L. (2014). Electromagnetic field activation of voltage-gated calcium channels: role in therapeutic effects. *Electromagn Biol Med* **33:**251.

Pall, M. L. (2015). Scientific evidence contradicts findings and assumptions of Canadian Safety Panel 6: microwaves act through voltage-gated calcium channel activation to induce biological impacts at non-thermal levels, supporting a paradigm shift for microwave/lower frequency electromagnetic field action. *Rev Environ Health* **30:**99-116.

Palomino, J. C. and Martin, A. (2014). Drug Resistance Mechanisms in Mycobacterium tuberculosis. *Antibiotics (Basel)* **3:**317-340.

Panagopoulos, D. J., Johansson, O. and Carlo, G. L. (2015). Polarization: A Key Difference between Man-made and Natural Electromagnetic Fields, in regard to Biological Activity. *Sci Rep* **5:**14914.

Pandey, B. D., Poudel, A., Yoda, T., Tamaru, A., Oda, N., Fukushima, Y., Lekhak, B. *et al.* (2008). Development of an in-house loop-mediated isothermal amplification (LAMP) assay for detection of Mycobacterium tuberculosis and evaluation in sputum samples of Nepalese patients. *J Med Microbiol* **57:**439-443.

Pankhurst, Q. A., Connolly, J., Jones, S. K. and Dobson, J. (2003). Applications of magnetic nanoparticles in biomedicine. *J. Phys. D: Appl. Phys.* **36:**167–181.

Parham, N. J., Picard, F. J., Peytavi, R., Gagnon, M., Seyrig, G., Gagne, P. A., Boissinot, M. *et al.* (2007). Specific magnetic bead based capture of genomic DNA from clinical samples: application to the detection of group B streptococci in vaginal/anal swabs. *Clin Chem* **53:**1570-1576.

Park, K. T., Allen, A. J. and Davis, W. C. (2014). Development of a novel DNA extraction method for identification and quantification of Mycobacterium avium subsp. paratuberculosis from tissue samples by real-time PCR. *J Microbiol Methods* **99:**58-65.

Patel, M., Gonzalez, R., Halford, C., Lewinski, M. A., Landaw, E. M., Churchill, B. M. and Haake, D. A. (2011). Target-specific capture enhances sensitivity of electrochemical detection of bacterial pathogens. *J Clin Microbiol* **49:**4293-4296.

Pavlin, M., Kanduser, M., Rebersˇek, M., Pucihar, G., Hart, F. X., Magjarevic, R. and Miklavc, D. (2005). Effect of Cell Electroporation on the Conductivity of a Cell Suspension. *Biophysical Journal* **88:**4378–4390.

Pavlin, M., Pavselj, N. and Miklavcic, D. (2002). Dependence of Induced Transmembrane Potential on Cell Density, Arrangement, and Cell Position Inside a Cell System. *IEEE TRANSACTIONS ON BIOMEDICAL ENGINEERING* **49:**605-612.

Pawlik, A., Garnier, G., Orgeur, M., Tong, P., Lohan, A., Le Chevalier, F., Sapriel, G. *et al.* (2013). Identification and characterization of the genetic changes responsible for the characteristic smooth-to-rough morphotype alterations of clinically persistent Mycobacterium abscessus. *Mol Microbiol* **90:**612-629.

Pearson, W. R. (2013). An introduction to sequence similarity ("homology") searching. *Curr Protoc Bioinformatics* **Chapter 3:**Unit3 1.

Pearson, W. R. and Lipman, D. J. (1998). Improved tools for biological sequence comparison. *Proc. Natl. Acad. Sci* **85:**2444-2448.

Perkins, M. D., Roscigno, G. and Zumla, A. (2006). Progress towards improved tuberculosis diagnostics for developing countries. *The Lancet* **367:**942-943.

Peter-Getzlaff, S., Luthy, J., Boddinghaus, B., Bottger, E. C. and Springer, B. (2008). Development and evaluation of a molecular assay for detection of nontuberculous mycobacteria by use of the cobas amplicor platform. *J Clin Microbiol* **46:**4023-4028.

Peter, J. G., Theron, G., van Zyl-Smit, R., Haripersad, A., Mottay, L., Kraus, S., Binder, A. *et al.* (2012). Diagnostic accuracy of a urine lipoarabinomannan strip-test for TB detection in HIV-infected hospitalised patients. *Eur Respir J* **40:**1211-1220.

Peterson, B. W., Sharma, P. K., van der Mei, H. C. and Busscher, H. J. (2012). Bacterial cell surface damage due to centrifugal compaction. *Appl Environ Microbiol* **78:**120-125.

Petrini, B. (2006). Mycobacterium abscessus: an emerging rapid-growing potential pathogen. *APMIS* **114:** 319–328.

Phillipsa, M. S. and von Reyn, C. F. (2001). Nosocomial Infections Due to Nontuberculous mycobacteria. *Clin Infect Dis* **33:**1363–1374.

Piccazzo, R., Paparo, F. and Garlaschi, G. (2014). Diagnostic accuracy of chest radiography for the diagnosis of tuberculosis (TB) and its role in the detection of latent TB infection: a systematic review. *J Rheumatol Suppl* **91:**32-40.

Piggot, T. J., Holdbrook, D. A. and Khalid, S. (2011). Electroporation of the E. coli and S. Aureus membranes: molecular dynamics simulations of complex bacterial membranes. *J Phys Chem B* **115:**13381-13388.

Pliquett, U., Joshi, R. P., Sridhara, V. and Schoenbach, K. H. (2007). High electrical field effects on cell membranes. *Bioelectrochemistry* **70:**275-282.

Pouchot, J., Grasland, A., Collet, C., Coste, J., Esdaile, J. M. and Vinceneux, P. (1997). Reliability of tuberculin skin test measurement. *Ann. Int. Med* **126:**210-214.

Price, J. V. and Vance, R. E. (2014). The Macrophage Paradox. *Immunity* **41:**685-693.

Pucihar, G., Kotnik, T., Valic, B. and Miklavcic, D. (2006). Numerical Determination of Transmembrane Voltage Induced on Irregularly Shaped Cells. *Annals of Biomedical Engineering* **34:**642–652.

Pucihar, G., Kotnik, T., Teissié, J. et al. Eur Biophys J (2007) 36: 173. https://doi.org/10.1007/s00249-006-0115-1

Qazi, O., Rahman, H., Tahir, Z., Qasim, M., Khan, S., Ahmad Anjum, A., Yaqub, T. *et al.* (2014). Mutation pattern in rifampicin resistance determining region of rpoB gene in multidrug-resistant Mycobacterium tuberculosis isolates from Pakistan. *Int J Mycobacteriol* **3:**173-177.

Quainoo, S., Coolen, J. P. M., van Hijum, S. A. F. T., Huynen, M. A., Melchers, W. J. G., van Schaik, W. and Wertheim, H. F. L. (2017). Whole-Genome Sequencing of Bacterial Pathogens: the Future of Nosocomial Outbreak Analysis. *Clin. Microbiol. Rev.* **30:**1015–1063.

Qvist, T., Pressler, T., Taylor-Robinson, D., Katzenstein, T. L. and Hoiby, N. (2015). Serodiagnosis of Mycobacterium abscessus complex infection in cystic fibrosis. *Eur Respir J* **46:**707-716.

Radomski, N., Kreitmann, L., McIntosh, F. and Behr, M. A. (2013). The critical role of DNA extraction for detection of mycobacteria in tissues. *PLoS One* **8:**e78749.

Raetz, C. R. and Dowhan, W. (1990). Biosynthesis and function of phospholipids in Escherichia coli. *J. Biol Chem* **265:**1235–1238.

Raetz, C. R. and Whitfield, C. (2002). Lipopolysaccharide endotoxins. *Annu Rev Biochem* **71:**635–700.

Ramaswamy, S. and Musser, J. M. (1998). Molecular genetic basis of antimicrbial agent resistance in Mycobacterium tuberculosis: 1998 update. *Tubercle and Lung Disease* **79:**3-29.

Ravn, P., Pinxteren, L. A. H. V., Andersen, A. P., Agger, E. M. and Pollock, J. (2000). Diagnosis of TB based on two specific antigens ESAT-6 ans CFP-10. *Clinical and Diagnostic Laboratory Immunology*

7:155–160.

Renna, M., Schaffner, C., Brown, K., Shang, S., Tamayo, M. H., Hegyi, K., Grimsey, N. J. *et al.* (2011). Azithromycin blocks autophagy and may predispose cystic fibrosis patients to mycobacterial infection. *J Clin Invest* **121:**3554-3563.

Ridell, M. (2015). Mycobacterium abscessus: An environmental mycobacteria being a human pathogen. *International Journal of Mycobacteriology* **4:**41.

Ripoll, F., Pasek, S., Schenowitz, C., Dossat, C., Barbe, V., Rottman, M., Macheras, E. *et al.* (2009). Non mycobacterial virulence genes in the genome of the emerging pathogen Mycobacterium abscessus. *PLoS One* **4:**e5660.

Robinson, W. (1931). Free and bound water determinations by the heat of fusion of ice method. *J. Biol. Chem* **92:**699-709.

Rocchetti, T. T., Silbert, S., Gostnell, A., Kubasek, C., Campos Pignatari, A. C. and Widen, R. (2017). Detection of Mycobacterium chelonae, Mycobacterium abscessus Group, and Mycobacterium fortuitum Complex by a Multiplex Real-Time PCR Directly from Clinical Samples Using the BD MAX System. *J Mol Diagn* **19:**295-302.

Rols, M.-P. (2006). Electropermeabilization, a physical method for the delivery of therapeutic molecules into cells. *Biochimica et Biophysica Acta* **1758:**423–428.

Rossato Silva, D., Muller, A. M. and Dalcin Pde, T. (2012). Factors associated with delayed diagnosis of tuberculosis in hospitalized patients in a high TB and HIV burden setting: a cross-sectional study. *BMC Infect Dis* **12:**57.

Rougier, C., Prorot, A., Chazal, P., Leveque, P. and Leprat, P. (2014). Thermal and nonthermal effects of discontinuous microwave exposure (2.45 gigahertz) on the cell membrane of Escherichia coli. *Appl Environ Microbiol* **80:**4832-4841.

Roux, A. L., Catherinot, E., Ripoll, F., Soismier, N., Macheras, E., Ravilly, S., Bellis, G. *et al.* (2009). Multicenter study of prevalence of nontuberculous mycobacteria in patients with cystic fibrosis in france. *J Clin Microbiol* **47:**4124-4128.

Rubio, M., March, F., Garrigo, M., Moreno, C., Espanol, M. and Coll, P. (2015). Inducible and Acquired Clarithromycin Resistance in the Mycobacterium abscessus Complex. *PLoS One* **10:**e0140166.

Ruger, K., Hampel, A., Billig, S., Rucker, N., Suerbaum, S. and Bange, F. C. (2014). Characterization of rough and smooth morphotypes of Mycobacterium abscessus isolates from clinical specimens. *J Clin Microbiol* **52:**244-250.

Ruiz-Herrera, J., Elorza, M. V., Valent´ın, E. and Sentandreu, R. (2006). Molecular organization of the cellwall ofCandida albicans and its relation to pathogenicity. *FEMS Yeast Res* **6:**14–29.

Russell, D. G. (2001). Mycobacterium tuberculosis: Here today, and here tomorrow. *Nature Reviews molceular Cell Biology* **2**.

Ryu, Y. J. (2015). Diagnosis of pulmonary tuberculosis: recent advances and diagnostic algorithms. *Tuberc Respir Dis (Seoul)* **78:**64-71.

Sa´nchez-Chardi, A., Olivares, F., Byrd, T. F., Julia´n, E., Brambilla, C. and Luquin, M. (2011). Demonstration of Cord Formation by Rough Mycobacterium abscessus Variants: Implications for the Clinical Microbiology Laboratory. *Journal of Clinical Microbiology* **49:**2293–2295.

Sajid, M., Kawde, A.-N. and Daud, M. (2015). Designs, formats and applications of lateral flow assay: A literature review. *Journal of Saudi Chemical Society* **19:**689-705.

Salata, O. V. (2004). Applications of nanoparticles in biology and medicine. *Journal of Nanobiotechnology* **2**.

Saleh, M. T. and Belisle, J. T. (2000). Secretion of an Acid Phosphatase (SapM) by Mycobacterium tuberculosis That Is Similar to Eukaryotic Acid Phosphatases. *Journal of Bacteriology* **182:**6850–6853.

Salton, M. R. J. (1958). The Lysis of Micro-organisms by Lysozyme and Related Enzymes. *J . Gen. Microbial.* **18:**481-490.

Sapriel, G., Konjek, J., Orgeur, M., Bouri, L., Frezal, L., Roux, A. L., Dumas, E. *et al.* (2016). Genome-wide mosaicism within Mycobacterium abscessus: evolutionary and epidemiological implications. *BMC Genomics* **17:**118.

Sassi, M., Ben Kahla, I. and Drancourt, M. (2013). Mycobacterium abscessus multispacer sequence typing. *BMC Microbiol* **13:**3.

Satkauskas, S., Bureau, M. F., Puc, M., Mahfoudi, A., Scherman, D., Miklavcic, D. and Mir, L. M. (2002). Mechanisms of in Vivo DNA Electrotransfer: Respective Contributions of Cell Electropermeabilization and DNA Electrophoresis. *Molecular therapy* **5:**133-140.

Schiller, I., Oesch, B., Vordermeier, H. M., Palmer, M. V., Harris, B. N., Orloski, K. A., Buddle, B. M. *et al.* (2010). Bovine tuberculosis: a review of current and emerging diagnostic techniques in view of their relevance for disease control and eradication. *Transbound Emerg Dis* **57:**205-220.

Schindelin, J., Arganda-Carreras, I., Frise, E., Kaynig, V., Longair, M., Pietzsch, T., Preibisch, S. *et al.* (2012). Fiji - an Open Source platform for biological image analysis. *Nat Methods* **9**.

Scholes, G., Ward, J. F. and Weiss, J. (1960). Mechanism of the radiation-induced degradation of nucleic acids. *J. Mol. Biol.* **2:**379–391.

Schorey, J. S. and Sweet, L. (2008). The mycobacterial glycopeptidolipids: structure, function, and their role in pathogenesis. *Glycobiology* **18:**832-841.

Scorpio, A. and Zhang, Y. (1996). Mutations in pncA, a gene causing pyrazinamide/nicotinamidase, cause resistance to the anti TB drug pyrazinamide in tuberculous bacilli. *Nature Medicine* **2:**662-667.

Segal, W. and Hubert, B. (1955). Biochemical differentiation of Mycobacterium tuberculosis grown in vivo and in vitro. *J. Bacteriol* **72:**132-145.

Shah, N. S., Wright, A., Bai, G.-H., Barrera, L., Boulahbal, F., Martín-Casabona, N., Drobniewski, F. *et al.* (2007). Worldwide Emergence of Extensively Drug-resistant Tuberculosis. *Emerging Infectious Diseases* **13:**380-387.

Shahin, S., Singh, V. P., Shukla, R. K., Dhawan, A., Gangwar, R. K., Singh, S. P. and Chaturvedi, C. M. (2013). 2.45 GHz microwave irradiation-induced oxidative stress affects implantation or pregnancy in mice, Mus musculus. *Appl Biochem Biotechnol* **169:**1727-1751.

Shamis, Y., Taube, A., Mitik-Dineva, N., Croft, R., Crawford, R. J. and Ivanova, E. P. (2011). Specific electromagnetic effects of microwave radiation on Escherichia coli. *Appl Environ Microbiol* **77:**3017-3022.

Shenai, S., Armstrong, D. T., Valli, E., Dolinger, D. L., Nakiyingi, L., Dietze, R., Dalcolmo, M. P. *et al.* (2016). Analytical and Clinical Evaluation of the Epistem Genedrive Assay for Detection of Mycobacterium tuberculosis. *J Clin Microbiol* **54:**1051-1057.

Shenai, S., Rodrigues, C., Almeida, A. and Mehta, A. (2001). Rapid diagnosis of Tuberculosis using transcription mediated amplification. *Indian Journal of Medical Microbiology* **19:**184-189.

Shi, L., Gunther, S., Hubschmann, T., Wick, L. Y., Harms, H. and Muller, S. (2007). Limits of propidium iodide as a cell viability indicator for environmental bacteria. *Cytometry A* **71:**592-598.

Shi, L., Jung, Y. J., Tyagi, S., Gennaro, M. L. and North, R. J. (2003). Expression of Th1-mediated immunity in mouse lungs induces a Mycobacterium tuberculosis transcription pattern characteristic of nonreplicating persistence. *Proc Natl Acad Sci U S A* **100:**241-246.

Shingadia, D. and Novelli, V. (2003). Diagnosis and treatment of tuberculosis in children. *The Lancet Infectious Diseases* **3:**624-632.

Silcox, V. A., Good, R. C. and Floyd, M. M. (1981). Identification of Clinically Significant Mycobacterium fortuitum complex isolates. *Journal of Clinical Microbilogy* **14 (6):**686-691.

Silhavy, T. J., Kahne, D. and Walker, S. (2010). The Bacterial Cell Envelope. *Cold Spring Harb Perspect Biol* **2**.

Singh, A. and Kashyap, V. K. (2012). Specific and Rapid Detection of Mycobacterium tuberculosis Complex in Clinical Samples by Polymerase Chain Reaction. *Interdiscip Perspect Infect Dis* **2012:**654694.

Singhal, R. and Myneedu, V. P. (2015). Microscopy as a diagnostic tool in pulmonary tuberculosis. *Int J Mycobacteriol* **4:**1-6.

Skoura, E., Zumla, A. and Bomanji, J. (2015). Imaging in tuberculosis. *Int J Infect Dis* **32:**87-93.

Smaby, J. M., Brockman, H. L. and Brown, R. E. (1994). Cholesterol's Interfacial Interactions with Sphingomyelins and Phosphatidylcholines: Hydrocarbon Chain Structure Determines the Magnitude of Condensation. *Biochemistry* **33:**9135–9142.

Smith, I. (2003). Mycobacterium tuberculosis Pathogenesis and Molecular Determinants of Virulence. *Clinical Microbiology Reviews* **16:**463-496.

Sobhy, H. and Colson, P. (2012). Gemi: PCR Primers Prediction fromMultiple Alignments. *Comparative and Functional Genomics*.

Sohlenkamp, C. and Geiger, O. (2016). Bacterial membrane lipids: diversity in structures and pathways. *FEMS Microbiol Rev* **40:**133-159.

Sreevatsan, S., Stockbauer, K. E., Pan, X., Kreiswirth, B. N., Moghazeh, S. L., Jacobs, W. R., Telenti, A. *et al.* (1997). Ethambutol Resistance in Mycobacterium tuberculosis critical role of embB mutations. *Antimicrobial agents and Chemotherapy* **41:**1677–1681.

Stevenson, K., McVey, A. F., Clark, I. B. N., Swain, P. S. and Pilizota, T. (2016). General calibration of microbial growth in microplate readers. *Sci. Rep. 6, 38828* **6**.

Stout, J. E. and Floto, R. A. (2012). Treatment of Mycobacterium abscessus: all macrolides are equal, but perhaps some are more equal than others. *Am J Respir Crit Care Med* **186:**822-823.

Suffys, P. N., da Silva Rocha, A., de Oliveira, M., Campos, C. E., Barreto, A. M., Portaels, F., Rigouts, L. *et al.* (2001). Rapid identification of Mycobacteria to the species level using INNO-LiPA Mycobacteria, a reverse hybridization assay. *J Clin Microbiol* **39:**4477-4482.

Sukharev, S., Klenchin, V. A., Serov, S. M., Chernomordik, L. V. and Chizmadzhev, Y. A. (1992). Electroporation and electrophoretic DNA transfer into cells-the effect of DNA interaction with electropores. *Biophys. J* **63:**1320-1327.

Sun, J., Wang, W., Yue, Q. (2016). Review on Microwave-Matter Interaction Fundamentals and Efficient Microwave-Associated Heating Strategies. *Materials 9*, 231.

Sunder, S., Lanotte, P., Godreuil, S., Martin, C., Boschiroli, M. L. and Besnier, J. M. (2009). Human-to-human transmission of tuberculosis caused by Mycobacterium bovis in immunocompetent patients. *J Clin Microbiol* **47:**1249-1251.

Talati, N. J., Rouphael, N., Kuppalli, K. and Franco-Paredes, C. (2008). Spectrum of CNS disease caused by rapidly growing mycobacteria. *The Lancet Infectious Diseases* **8:**390-398.

Taneja, R., Malik, U. and Khuller, G. K. (1979). Effect of Growth Temperature on the Lipid Composition of Mycobacterium smegmatis ATCC 607. *Journal of General Microbiology* **113:**413-416.

Teissie, J. and Tsong, T. Y. (1981). Electric Field Induced Transient Pores in Phospholipid Bilayer Vesicles. *Biochemistry* **20:**1548–1554.

Tettelin, H., Davidson, R. M., Agrawal, S., Aitken, M. L., Shallom, S., Hasan, N. A., Strong, M. *et al.* (2014). High-level relatedness among Mycobacterium abscessus subsp. massiliense strains from widely separated outbreaks. *Emerg Infect Dis* **20:**364-371.

The Stop TB Strategy. (2018).

Theron, G., Peter, J., Richardson, M., Barnard, M., Donegan, S., Warren, R., Steingart, K. *et al.* (2014). The diagnostic accuracy of the GenoType® MTBDRsl assay for the detection of resistance to second-line anti-tuberculosis drugs. *Cochrane Database of Systematic Reviews*.

Thibert, L. and Lapierre, S. (1993). Routine Application of High-Performance Liquid chromatography for identification of mycobacteria. *Journal of Clinical Microbilogy* **31 (7):**1759-1763.

Thielbeer, F., Donaldson, K. and Bradley, M. (2011). Zeta potential mediated reaction monitoring on nano and microparticles. *Bioconjug Chem* **22:**144-150.

Thieme, D., Neubauer, P., Nies, D. H. and Grass, G. (2008). Sandwich hybridization assay for sensitive detection of dynamic changes in mRNA transcript levels in crude Escherichia coli cell extracts in response to copper ions. *Appl Environ Microbiol* **74:**7463-7470.

Thompson, J. D., Higgins, D. G. and Gibson, T. J. (1994). CLUSTAL W: improving the sensitivity of progressive multiple sequence alignment through sequence weighting, position-specific gap penalties and weight matrix choice. *Nucleic Acids Research* **22 (22):**4673-4680.

Tieleman, D. P. (2004). The molecular basis of electroporation. *BMC Biochem* **5:**10.

Timms, V. J., Mitchell, H. M. and Neilan, B. A. (2015). Optimisation of DNA extraction and validation of PCR assays to detect Mycobacterium avium subsp. paratuberculosis. *J Microbiol Methods* **112:**99-103.

Torres-Gonzalez, P., Soberanis-Ramos, O., Martinez-Gamboa, A., Chavez-Mazari, B., Barrios-Herrera, M. T., Torres-Rojas, M., Cruz-Hervert, L. P. *et al.* (2013). Prevalence of latent and active tuberculosis among dairy farm workers exposed to cattle infected by Mycobacterium bovis. *PLoS Negl Trop Dis* **7:**e2177.

Tortoli, E. (2014). Microbiological features and clinical relevance of new species of the genus Mycobacterium. *Clin Microbiol Rev* **27:**727-752.

Tortoli, E., Pecorari, M., Fabio, G., Messino, M. and Fabio, A. (2010). Commercial DNA probes for mycobacteria incorrectly identify a number of less frequently encountered species. *J Clin Microbiol* **48:**307-310.

Trajman, A., Steffen, R. E. and Menzies, D. (2013). Interferon-Gamma Release Assays versus Tuberculin Skin Testing for the Diagnosis of Latent Tuberculosis Infection: An Overview of the Evidence. *Pulm Med* **2013:**601737.

Trovato, A., Baldan, R., Costa, D., Simonetti, T. M., Cirillo, D. M. and Tortoli, E. (2017). Molecular Typing of Mycobacterium Abscessus Isolated from Cystic Fibrosis Patients. *Int. J. Mycobacteriol* **6:**138-141.

Udwadia, Z. F., Amale, R. A., Ajbani, K. K. and Rodrigues, C. (2012). Totally Drug-Resistant Tuberculosis in India. *Clinical Infectious Diseases* **54:**579–581.

Unsay, J. D., Cosentino, K., Subburaj, Y. and Garcia-Saez, A. J. (2013a). Cardiolipin effects on membrane structure and dynamics. *Langmuir* **29:**15878-15887.

Unsay, J. D., Cosentino, K., Subburaj, Y. and García-Saez, A. J. (2013b). Cardiolipin Effects on Membrane Structure and Dynamics. *Langmuir* **29:**15878−15887.

Urdea, M., Penny, L. A., Olmsted, S. S., Giovanni, M. Y., Kaspar, P., Shepherd, A., Wilson, P. *et al.* (2006). Requirements for high impact diagnostics in the developing world *Nature* 73-79.

Vaid, H. and Bishop, A. (1998). The destruction by microwave radiation of bacterial endospores and amplification of the released DNA. *Journal of Applied Microbiology* **85:**115-122.

van Uitert, I., Le Gac, S. and van den Berg, A. (2010a). Determination of the electroporation onset of bilayer lipid membranes as a novel approach to establish ternary phase diagrams: example of the l-α-PC/SM/cholesterol system. *Soft Matter* **6:**4420.

van Uitert, I., Le Gac, S. and van den Berg, A. (2010b). The influence of different membrane components on the electrical stability of bilayer lipid membranes. *Biochim Biophys Acta* **1798:**21-31.

Vandeventer, P. E., Weigel, K. M., Salazar, J., Erwin, B., Irvine, B., Doebler, R., Nadim, A. *et al.* (2011). Mechanical disruption of lysis-resistant bacterial cells by use of a miniature, low-power, disposable device. *J Clin Microbiol* **49:**2533-2539.

Veatch, S. L. and Keller, S. L. (2005). Miscibility phase diagrams of giant vesicles containing sphingomyelin. *Phys Rev Lett* **94:**148101.

Velayati, A. A., Masjedi, M. R., Farnia, P., Tabarsi, P., Ghanavi, J., ZiaZarifi, A. H. and Hoffner, S. E. (2009). Emergence of new forms of totally drug-resistant tuberculosis bacilli: super extensively drug-resistant tuberculosis or totally drug-resistant strains in iran. *Chest* **136:**420-425.

Venturini, E., Turkova, A., Chiappini, E., Galli, L., Martino, M. d. and Thorne, C. (2014). Tuberculosis and HIV co-infection in children. *BMC Infectious Diseases* **14**.

Vergne, I., Chua, J. and Deretic, V. (2003). Tuberculosis toxin blocking phagosome maturation inhibits a novel Ca2+/calmodulin-PI3K hVPS34 cascade. *J Exp Med* **198:**653-659.

Vigneshvar, S., Sudhakumari, C. C., Senthilkumaran, B. and Prakash, H. (2016). Recent Advances in Biosensor Technology for Potential Applications – An Overview. *Front Bioeng Biotechnol* **4**.

Vilcheze, C., Iwamoto, H., Morbidoni, H. R., Kuo, M., Weisbrod, T. R., Sacchettini, J. C. and Jacobs, W. R. J. (2000). Inactivation of the inhA-Encoded Fatty Acid Synthase II (FASII) Enoyl-Acyl Carrier Protein Reductase Induces Accumulation of the FASI End Products and Cell Lysis of Mycobacterium smegmatis. *Journal of Bacteriology* **182:**4059–4067.

Viveiros, M., Leandro, C., Rodrigues, L., Almeida, J., Bettencourt, R., Couto, I., Carrilho, L. *et al.* (2005). Direct application of the INNO-LiPA Rif.TB line-probe assay for rapid identification of Mycobacterium tuberculosis complex strains and detection of rifampin resistance in 360 smear-positive respiratory specimens from an area of high incidence of multidrug-resistant tuberculosis. *J Clin Microbiol* **43:**4880-4884.

von sonntag, C. (2007). Free-radical induced DNA damage and its repair; A chemical perspective. *Free Radical Research* **41:**376-377.

Vorst, A. V., Rosen, A. and Kotsuka, Y. (2006). RF/microwave interaction with biological tissues. New Jersey, Hoboken: John Wiley & Sons, Inc., p. 346.

Wadhwa, A., Hickling, G. J. and Eda, S. (2012). Opportunities for improved serodiagnosis of human tuberculosis, bovine tuberculosis, and paratuberculosis. *Vet Med Int* **2012:**674238.

Walburger, A., Koul, A., Ferrari, G., Nguyen, L., Prescianotto-Baschong, C., Huygen, K., Klebl, B. *et al.* (2004). Protein Kinase G from Pathogenic Mycobacteria Promotes Survival Within Macrophages. *Science* **304:**1800.

Wallace, R. J., Glassroth, J., Griffith, D. E., Olivier, K. N., Cook, J. L. and Gordin, F. (1997). Diagnosis and Treatment of Disease Caused by Nontuberculous Mycobacteria. *Am J Respir Crit Care Med Vol.. pp. ,* **156:**S1–S25.

Wallace, R. J., Zhang, Y., Brown, B. A., Fraser, V., Mazurek, G. H. and Maloney, S. (1993). DNA Large Restriction Fragment Patterns of Sporadic and epidemic nosocomial strains of M. chelonae and M. abscessus. *Journal of Clinical Microbilogy* **31 (10):**2697-2701.

Wang, L. (2011). Oligonucleotide bioanalysis: sensitivity versus specificity. *Bioanalysis* **3:**1299–1303.

Wang, H., and Zhang, X. (2017). Magnetic Fields and Reactive Oxygen Species. *Int. J. Mol Sci.* **18**, 2175.
http: https://pdfs.semanticscholar.org/2576/04cca6c91440e54dab498c47f070239821ac.pdf

Wang, P. and Kricka, L. J. (2018). Current and Emerging Trends in Point-of-Care Technology and Strategies for Clinical Validation and Implementation. *Clinical Chemistry* **64**.

Wachtel, H., Beblo, D., Vargas, C., Bassen, H., and D. Brown, "Comparison of the efficacy of pulsed versus CW microwave fields in evoking body movements," *Images of the Twenty-First Century. Proceedings of the Annual International Engineering in Medicine and Biology Society,*, Seattle, WA, USA, 1989, pp. 1136-1137 vol.4. doi: 10.1109/IEMBS.1989.96124. URL: http://ieeexplore.ieee.org/stamp/stamp.jsp?tp=&arnumber=96124&isnumber=3080

Wertz, J. E., Goldstone, C., Gordon, D. M. and Riley, M. A. (2003). A molecular phylogeny of enteric bacteria and implications for a bacterial species concept. *J. of Evol. Biol.* **16:**1236–1248.

Weyer, K., Carai, S. and Nunn, P. (2011). Viewpoint TB diagnostics: what does the world really need? *J Infect Dis* **204 Suppl 4:**S1196-1202.

Whitfield, M. G., Soeters, H. M., Warren, R. M., York, T., Sampson, S. L., Streicher, E. M., van Helden, P. D. *et al.* (2015). A Global Perspective on Pyrazinamide Resistance: Systematic Review and Meta-Analysis. *PLoS One* **10:**e0133869.

WHO. (2010). Multidrug and extensively drug-resistant TB (M/XDR-TB) 2010 GLOBAL REPORT ON SURVEILLANCE AND RESPONSE [Online]. Available at: http://apps.who.int/iris/bitstream/10665/44286/1/9789241599191_eng.pdf [Accessed: 03-09-2016].

WHO. (2013). Global Tuberculosis report, 2013 [Online]. Available at: http://apps.who.int/iris/bitstream/10665/91355/1/9789241564656_eng.pdf [Accessed: 30-05-2016].

WHO. (2015). Global Tuberculosis report, 2015 [Online]. Available at: http://apps.who.int/iris/bitstream/10665/191102/1/9789241565059_eng.pdf [Accessed: 17-02-2016].

Williams, C. F., Geroni, G. M., Pirog, A., Lloyd, D., Lees, J. and Porch, A. (2016). The separated electric and magnetic field responses of luminescent bacteria exposed to pulsed microwave irradiation. *Applied Physics Letters* **109:**093701.

Wolf, H., Rols, M. P., Boldt, E., Neumann, E. and Teissiet, J. (1994). Control by pulse parameters of electric field-mediated gene transfer in mammalian cells. *Biophysical Journal* **66:**524–531.

Wong, Y. L., Ong, C. S. and Ngeow, Y. F. (2012). Molecular typing of Mycobacterium abscessus based on tandem-repeat polymorphism. *J Clin Microbiol* **50:**3084-3088.

Wu, T., Rappaport, T. S. and Collins, C. M. (2015). The Human Body and Millimeter-Wave Wireless comm systems-interactions and implications. In: *IEEE International Conference on Communications.*

Xiong, J. (2006). Essential Bioinformatics. Cambridge University Press, p. 331.

Xu, J. N., Chen, J. P. and Chen, D. L. (2012). Serodiagnosis efficacy and immunogenicity of the fusion protein of Mycobacterium tuberculosis composed of the 10-kilodalton culture filtrate protein, ESAT-6, and the extracellular domain fragment of PPE68. *Clin Vaccine Immunol* **19:**536-544.

Yadav, R. N., Singh, B. K., Sharma, S. K., Sharma, R., Soneja, M., Sreenivas, V., Myneedu, V. P. *et al.* (2013). Comparative Evaluation of GenoType MTBDRplus Line Probe Assay with Solid Culture Method in Early Diagnosis of Multidrug Resistant Tuberculosis (MDR-TB) at a Tertiary Care Centre in India. *PLoS ONE* **8**.

Yang, W.-J. and Wang, J. H. (1979). Shortwave and microwave diathermy for deep-tissue heating *Med. & Biol. Eng. & Comput.* **17:**518-523

Yang, X., Wen, Y., Wang, L., Zhou, C., Li, Q., Xu, L., Li, L. *et al.* (2017). PCR-Free Colorimetric DNA Hybridization Detection Using a 3D DNA Nanostructured Reporter Probe. *ACS Appl Mater Interfaces* **9:**38281-38287.

Yang, Y., Gao, J., Wang, J., Heffernan, R., Hanson, J., Paliwal, K. and Zhou, Y. (2016). Sixty-five years of the long march in protein secondary structure prediction: the final stretch? *Briefings in Bioinformatics* **19:**482–494.

Yoshida, S., Tsuyuguchi, K., Suzuki, K., Tomita, M., Okada, M., Shimada, R. and Hayashi, S. (2014). Rapid identification of strains belonging to the Mycobacterium abscessus group through erm(41) gene pyrosequencing. *Diagn Microbiol Infect Dis* **79:**331-336.

Zaczek, A., Brzostek, A., Augustynowicz-Kopec, E., Zwolska, Z. and Dziadek, J. (2009). Genetic evaluation of relationship between mutations in rpoB and resistance of Mycobacterium tuberculosis to rifampin. *BMC Microbiol* **9:**10.

Zeigler, D. R. (2003). Gene sequences useful for predicting relatedness of whole genomes in bacteria. *Int J Syst Evol Microbiol* **53:**1893–1900.

Zelazny, A. M., Root, J. M., Shea, Y. R., Colombo, R. E., Shamputa, I. C., Stock, F., Conlan, S. *et al.* (2009). Cohort study of molecular identification and typing of Mycobacterium abscessus, Mycobacterium massiliense, and Mycobacterium bolletii. *J Clin Microbiol* **47:**1985-1995.

Zhang, H., Li, D., Zhao, L., Fleming, J., Lin, N., Wang, T., Liu, Z. *et al.* (2013). Genome sequencing of 161 Mycobacterium tuberculosis isolates from China identifies genes and intergenic regions associated with drug resistance. *Nat Genet* **45:**1255-1260.

Zhang, Y., Agreda, P., Kelley, S., Gaydos, C. and Geddes, C. D. (2010). Development of a microwave-accelerated metal-enhanced fluorescence 40 second, 100 cfu.mL point of care assay for the detection of Chlamydia trachomatis. *IEEE*.

Zhen, H., Han, T., Fennell, D. E. and Mainelis, G. (2013). Release of Free DNA by Membrane-Impaired Bacterial Aerosols Due to Aerosolization and Air Sampling. *Applied and Environmental Microbiology* **79:**7780–7789.

Zhou, H. Y. and Zhou, Y. Q. (2005). SPEM: improving multiple sequence alignment with sequence profiles and predicted secondary structures. *Bioinformatics* **21:**3615–3621.

Zuker, M. (2003). Mfold web server for nucleic acid folding and hybridization prediction. *Nucleic Acids Res.* **31:**3406–3415.

9.0 Appendices

Appendix 1, 2, 3 and 4 are contained in the attached CD.